Differential Proteolysis of the Amyloid Precursor Protein Isoforms: The Role of Cellular Location and Protein-Protein Interactions

A thesis submitted to the University of Manchester for the degree of

Doctor of Philosophy (PhD)

In Faculty of Medical and Human Sciences

School of Medicine

Institute for Brain, Behaviour and Mental Health

2015

Robert John Andrew

Contents

Contents 2
List of Figures 7
List of Tables 8
List of Abbreviations 9
Abstract 11
Declaration 12
Copyright statement 12
Dedication and acknowledgements 13
Chapter 1. Introduction 14
1.1 Dementia and Alzheimer's disease 14
1.1.1 Social and economic impact of Alzheimer's disease 14
1.1.2 Alzheimer's disease hallmarks and symptoms 14
1.1.3 Diagnosis of disease 16
1.1.4 Current therapies for Alzheimer's disease 17
1.2 Current understanding of Alzheimer's disease 17
1.2.1 The Amyloid Cascade Hypothesis 17
1.2.2 Proteolytic cleavage of APP 19
1.2.3 Familial Alzheimer's disease 21
1.2.4 Sporadic Alzheimer's disease 23
1.3 The molecular players in Alzheimer's disease 24
1.3.1 The amyloid precursor protein 24
1.3.2 APP isoforms 26
1.3.3 α-secretase 30
1.3.4 β-secretase 30
1.3.5 γ-secretase 31
1.3.6 APP trafficking affects its proteolysis 33
1.3.7 Role of Tau 37
1.4 APP metabolites 38
1.4.1 Aβ 38
1.4.2 sAPPα 41
1.4.3 sAPPβ 42
1.4.4 AICD 43
1.4.5 p3 43
1.4.6 CTFs 44

1.5 Targeting Aβ therapeutically 44
1.5.1 BACE1 inhibitors 44
1.5.2 γ-secretase inhibitors and modulators 45
1.5.3 α-secretase enhancers 46
1.5.4 Promoting Aβ clearance 46
1.5.5 Preventing Aβ aggregation 48
1.6 The APP interactome 48
1.6.1 Studies of the APP interactome 48
1.6.2 APP interactors can alter its proteolysis 50
1.7 Aims 51
Chapter 2. Materials and methods 56
2.1 Materials 56
2.1.1 Molecular biology reagents 56
2.1.2 Cell culture reagents 56
2.1.3 Antibodies, ELISAs and Meso Scale Discovery assays 57
2.1.4 General laboratory reagents 57
2.2 Methods 57
2.2.1 Cloning of APP695-FLAG 57
2.2.2 Cloning of APP751-GFP 59
2.2.3 Site directed mutagenesis 59
2.2.4 DNA sequencing 60
2.2.5 Ethanol precipitation of DNA for stable transfection 60
2.2.6 Cell culture 61
2.2.7 Stable transfection of SH-SY5Y cells 61
2.2.8 Transient transfection of SH-SY5Y cells 61
2.2.9 Stable isotope labelling of amino acids in cell culture 62
2.2.10 Pharmacological cell treatments 62
2.2.11 siRNA mediated protein knockdown 62
2.2.12 Protein degradation assay 62
2.2.13 Cell lysate and media preparation 63
2.2.14 Bicinchoninic acid (BCA) assay 63
2.2.15 Lipid raft preparations 63
2.2.16 Cell surface biotinylation 64
2.2.17 Protein co-immunoprecipitations 64
2.2.18 Human brain samples 65
2.2.19 Sodium dodecyl sulphate polyacrylamide gel electrophoresis (SDS-PAGE) 65
2.2.20 Immunoblotting 65

2.2.21 sAPP and Aβ quantification 66
2.2.22 pGlu-Aβ3-40 ELISA....66
2.2.23 Immunofluorescence microscopy 68
2.2.24 Liquid chromatography – tandem mass spectrometry (LC MS/MS) 68
2.2.25 Bioinformatic analysis 70
2.2.26 Statistical analysis....71
Chapter 3. APP isoforms show differential subcellular localisation contributing to differential proteolysis 72
3.1 Introduction....72
3.1.1 The APP isoforms show differential proteolysis....72
3.1.2 Does subcellular location contribute to the differential proteolysis of APP isoforms?72
3.1.3 Aims 73
3.2 Results 74
3.2.1 FLAG-tagged APP isoforms, but not GFP-tagged APP isoforms show the expected differences in proteolysis 74
3.2.2 The subcellular location of the APP isoforms varies and contributes to differential proteolysis 81
3.2.3 APP isoforms show no significant differences in protein degradation rate....99
3.2.4 Various proteolytic fragments of APP are present in the conditioned medium, and vary between the isoforms....99
3.3 Discussion 103
3.3.1 Does differential subcellular localisation contribute to differential proteolysis of the APP isoforms? 103
3.3.2 Does retention within the early secretory pathway attenuate amyloidogenic APP proteolysis? 110
3.3.3 Do the APP isoforms undergo differential proteolysis at other sites?....111
Chapter 4. Investigating the APP isoform interactomes and their implications for APP proteolysis 114
4.1 Introduction....114
4.1.1 Proteomic analysis and its application to neurodegenerative diseases 114
4.1.2 Can interactome studies imply novel molecular functions for APP? 114
4.1.3 Can interactomic studies identify novel modulators of APP proteolysis? 115
4.1.4 Aims 115
4.2 Results 116
4.2.1 APP-FLAG immunoprecipitation optimisation and SILAC....116
4.2.2 APP isoforms show differences in interactomes which indicate differential functions 119
4.2.3 Validation of the APP interactome data....122

4.2.4 The APP interactome yields modulators of APP proteolysis 129
4.2.5 Ataxin-10, but not GAP43, is altered in the AD brain 143
4.3 Discussion 145
4.3.1 Application of SILAC to APP interactomic analysis 145
4.3.2 Functional clues from the APP interactome 146
4.3.3 The APP interactome identifies isoform specific modulators of Aβ production 149
Chapter 5. Investigating the effect of a familial and a protective APP mutation on APP proteolysis 153
5.1 Introduction 153
5.1.1 The Icelandic mutation protects carriers from AD and age related cognitive decline and reduces Aβ production in a non-neuronal cell model 153
5.1.2 N-terminally truncated Aβ displays enhanced toxicity and aggregation 154
5.1.3 Aims 154
5.2 Results 155
5.2.1 APP_{ICE} undergoes less, and APP_{ITA} undergoes more, amyloidogenic proteolysis than APP_{WT} 155
5.2.2 APP isoforms with the Italian mutation undergo differential proteolysis 161
5.2.3 BACE1 and cathepsin B inhibitors both reduce amyloidogenic proteolysis of APP 161
5.2.4 SH-SY5Y cells expressing WT and mutant APP do not produce detectable levels of pGlu-Aβ3-40 168
5.3 Discussion 169
5.3.1 Familial mutations have the same effect on proteolysis in the APP isoforms 169
5.3.2 BACE1 and cathepsin B inhibition both reduce APP proteolysis 171
5.3.3 SH-SY5Y cells expressing APP695 do not produce detectable pGlu-Aβ3-40 174
Chapter 6. Discussion 176
6.1 Introduction 176
6.2 The APP isoforms undergo differential proteolysis and show differences in subcellular location and interactomes 176
6.3 The case for targeting Aβ 177
6.4 Trafficking as a determinant of APP proteolysis and a potential therapeutic target 178
6.5 APP interactions as an alternative target in Aβ generation 180
6.5.1 The caveats of BACE1 and γ-secretase as therapeutic targets 180
6.5.2 Do modulators of APP proteolysis overcome the inherent difficulties of direct inhibition of the secretases? 181
6.5.3 The effect of protein-protein interactions on Aβ production is not limited to the interactome of APP 182
6.6 Alternative pathways of APP proteolysis 183

6.7 Outstanding questions on the causes and consequences of differences in the APP isoforms 186
6.7.1 The causes of changes in APP expression profile remain enigmatic 186
6.7.2 Specific functions for APP isoforms have not been determined 187
6.7.3 The spatial and temporal expression of APP isoforms remains poorly understood 189
6.8 Concluding remarks 191
References 192

Final word count: 45,874

List of Figures

Figure 1.1 Typical brain atrophy and histopathological hallmark accumulation in an Alzheimer's disease patient brain 15
Figure 1.2 Two proteolysis pathways for APP release distinct soluble fragments 20
Figure 1.3 Genetic mutations can cause AD or protect against its development 22
Figure 1.4 Structural domains within the amyloid precursor protein 25
Figure 1.5 APP proteolysis is intrinsically linked to its trafficking 34
Figure 1.6 APP and fragments produced by its proteolysis have distinct and overlapping functions 39
Figure 3.1 Production of APP-FLAG constructs 75
Figure 3.2 Expression and proteolysis of FLAG-tagged APP constructs 77
Figure 3.3 APP isoform proteolysis analysis by Meso Scale Discovery 78
Figure 3.4 Expression of fluorescent APP constructs 80
Figure 3.5 Expression and proteolysis of fluorescent APP 82
Figure 3.6 The APP isoforms show subtle variations in subcellular distribution 83
Figure 3.7 The APP isoforms bearing the Swedish mutation maintain their differential amyloidogenic proteolysis 87
Figure 3.8 Rab11a knockdown decreases Aβ in APP695-FLAG, but not APP751-FLAG, expressing cells 88
Figure 3.9 More APP695 is present at the cell surface than APP751 91
Figure 3.10 Inhibition of endocytosis decreases APP proteolysis but is not isoform specific 92
Figure 3.11 A pool of endogenous and over-expressed APP localises to lipid rafts 95
Figure 3.12 APP695-FLAG and APP751-FLAG show no difference in lipid raft distribution 96
Figure 3.13 Flotillin-1 and flotillin-2 knockdown decreases Aβ in APP751-FLAG, but not APP695-FLAG, expressing cells 97
Figure 3.14 Degradation rates of the APP isoforms show no significant differences 100
Figure 3.15 APP soluble fragments of various lengths are present in conditioned media from APP expressing cell lines 101
Figure 3.16 APP trafficking complexities and proposed targets 112
Figure 4.1 FLAG-tag affinity gel efficiently immunoprecipitates FLAG tagged APP 117
Figure 4.2 Cell lysis in IP buffer results in higher co-immunoprecipitation of Fe65 with APP than lysis with CHAPSO buffer 118
Figure 4.3 SILAC and LC-MS/MS used to identify proteins differentially interacting with FLAG-tagged APP695 and APP751 isoforms 120
Figure 4.4 Identification of enriched data from mass spectrometry analysis 121
Figure 4.5 Co-immunoprecipitation for the confirmation of APP interactors 127
Figure 4.6 Immunoprecipitation of Ataxin-10 or GAP43 results in co-immunoprecipitation of APP 128
Figure 4.7 Fe65 knockdown increases amyloidogenic proteolysis in APP695-FLAG, but not APP751-FLAG, expressing cells 131
Figure 4.8 The amount of phosphorylated APP does not differ significantly between the APP isoforms 133
Figure 4.9 Ataxin-10 knockdown reduces Aβ in APP695-FLAG, but not APP751-FLAG expressing cells 135
Figure 4.10 GAP43 knockdown reduces Aβ in APP751-FLAG, but not APP695-FLAG expressing cells 137

Figure 4.11 ABCB1 and peroxiredoxin-1 knockdown do not consistently alter APP proteolysis in APP695-FLAG or APP751-FLAG expressing cells 140
Figure 4.12 ITM2C and DPP7 could not be significantly knocked down in SH-SY5Y cells 142
Figure 4.13 Ataxin-10 is significantly reduced, and GAP43 is unchanged, in the temporal cortex of AD patients 144
Figure 5.1 Immunoblot analysis shows $APP695_{ICE}$ undergoes less, and $APP695_{ITA}$ undergoes more, amyloidogenic proteolysis than $APP695_{WT}$ 156
Figure 5.2 Meso Scale Discovery analysis confirms $APP695_{ICE}$ undergoes less, and $APP695_{ITA}$ undergoes more, amyloidogenic proteolysis than $APP695_{WT}$ 157
Figure 5.3 Mutations at the β-secretase site in APP can alter γ-secretase proteolysis 159
Figure 5.4 Immunoblot analysis shows $APP751_{ICE}$ undergoes less, and $APP751_{ITA}$ mutation undergoes more, amyloidogenic proteolysis than $APP751_{WT}$ 160
Figure 5.5 The Italian mutation does not over-ride the protective effect of the KPI-domain to the same extent as the Swedish mutation 162
Figure 5.6 BACE1 inhibition alters APP profiles in cells expressing $APP695_{WT}$ and $APP695_{ITA}$ but not those expressing $APP695_{ICE}$ 163
Figure 5.7 BACE1 inhibition reduces amyloidogenic APP proteolysis of $APP695_{WT}$, $APP695_{ICE}$ and $APP695_{ITA}$ 164
Figure 5.8 Cathepsin B inhibition does not alter mature to immature APP ratios but significantly increases $APP695_{ICE}$ levels 166
Figure 5.9 Cathepsin B inhibition reduces amyloidogenic APP proteolysis of $APP695_{WT}$ and $APP695_{ITA}$ 167

List of Tables

Table 1.1 APP isoform expression alterations in AD 28
Table 1.2 APP interactors which affect proteolysis 52
Table 2.1 Primary and secondary antibody sources 58
Table 2.2 Primary antibody dilutions and secondary antibodies for immunoblot analysis 67
Table 2.3 Primary antibody dilutions and secondary antibodies for immunofluorescence microscopy 69
Table 4.1 The APP695 and APP751 interactome 123
Table 4.2 Gene ontology analysis of APP interacting proteins 125
Table 4.3 Mitochondrial and nuclear proteins are enriched in the APP695 interactome 126
Table 5.1 The effect of the APP A673T and A673V mutations on Aβ generation and properties 172
Table 6.1 The complexities of APP proteolysis 184
Table 6.2 The potential isoform specific APP fragments produced by tryptic digestion 190

List of Abbreviations

Aβ – Amyloid-β

AD – Alzheimer's Disease

ADAM – A disintegrin and metalloproteinase

AICD – APP intracellular domain

AMPA – α-amino-3-hydroxy-5-methyl-4-isoxazolepropionic acid

APH1 – Anterior pharynx-defective 1

APLP (1/2) – Amyloid precursor protein-like protein (1/2)

APOE4 – Apolipoprotein E ε4

APP – Amyloid precursor protein

$APP_{WT/SWE/ICE/ITA}$ – APP wild-type/Swedish (K670N/M671L)/Icelandic (A673T)/Italian (A673V)

AP4 – Adaptor related protein 4

ARF6 – ADP ribosylation factor 6

ARIA – Amyloid related imaging abnormalities

BACE1 – β-site amyloid precursor protein cleaving enzyme 1

BCA – Bicinchoninic acid

BSA – Bovine serum albumin

CSF – Cerebrospinal fluid

CTF – C-terminal fragment

CJD – Creutzfeldt-Jakob disease

DMEM – Dulbecco's modified Eagle's medium

DMSO – Dimethyl sulfoxide

EGFP – Enhanced green fluorescent protein

EGCG – Epigallocatechin-3-gallate

ELISA – Enzyme-linked immunosorbent assay

ER – Endoplasmic reticulum

FSG – Fish skin gelatin

GAP43 – Growth-associated protein 43

GGA – Golgi-localised γ-adaptin ear-containing ADP ribosylation factor binding protein

GPI – glycophosphatidylinositol

GRP78 – 78 kDa glucose-related protein

GSI – γ-secretase inhibitor

GSM – γ-secretase modulator

HEK – human embryonic kidney

HSPA8 – Heat shock cognate 78 kDa protein 8

IDE – Insulin degrading enzyme

iPSC – Induced pluripotent stem cells

iTRAQ – Isobaric tags for absolute and relative quantification

KPI – Kunitz protease inhibitor

LC-MS/MS – Liquid chromatography – tandem mass spectrometry

LINGO-1 – Leucine-rich repeat and immunoglobulin-like domain-containing protein 1

LRPPRC – Leucine-rich PPR motif-containing protein

LRP (1/1B/10) – Low-density lipoprotein receptor-related protein (1/1B/10)

LTD – Long term depression

LTP – Long term potentiation

MSD – Meso Scale Discovery

MT5-MMP – Membrane-type-5 matrix metalloproteinase

NEP – Neprilysin

NCT - Nicastrin

NFT – Neurofibrillary tangle

NMDA – N-methyl-D-aspartate

PBS – Phosphate buffered saline

PCR – Polymerase Chain reaction

PEN2 – Presenilin enhancer 2

PET – Positron emission tomography

pGlu-Aβ –Pyroglutamate amyloid-β

PiB – Pittsburgh compound B

PS(1/2) – Presenilin (1/2)

PSP – Progressive supranuclear palsy

PTM – Post-translational modification

QC – Glutaminyl cyclase

sAPPα/β/η – Soluble APP α/β/η

SDS-PAGE – Sodium dodecyl sulfate polyacrylamide gel electrophoresis

SILAC – Stable isotope labelling of amino acids in cell culture

TfR – Transferrin receptor

TGN – trans-Golgi network

VDAC (1/3) – Voltage-dependent anion-selective channel protein (1/3)

VPS – Vacuolar protein sorting

Abstract

The University of Manchester

Robert John Andrew

Doctor of Philosophy (PhD)

Differential Proteolysis of the Amyloid Precursor Protein Isoforms: The Role of Cellular Location and Protein-Protein Interactions

2015

Dementia, the most common cause of which is Alzheimer's disease (AD), currently affects 850,000 people in the UK, a figure set to rise to over 1 million by 2025. There is currently no disease modifying therapy available to slow or halt this progressive disease. Current understanding of AD implicates the neurotoxic amyloid-β (Aβ) peptide as the primary initiator in a cascade of events leading to the neuronal cell death and brain atrophy associated with the disease. Therefore, inhibiting the production or enhancing the clearance of Aβ within the brain has become a major target for the production of disease modifying therapeutics. Aβ is produced by brain cells through the sequential proteolytic cleavage of a larger transmembrane protein known as the amyloid precursor protein (APP) by β- and γ-secretases. Several aspects of APP physiology can influence its proteolysis, and thus Aβ production, including the isoform of APP which is expressed, its trafficking and subcellular location and its physical interactions with other proteins in the cellular environment. Here we have investigated the influence of subcellular trafficking and location and protein-protein interactions on the differential proteolysis of two APP isoforms, APP695 and APP751 in a neuroblastoma cell line. We have shown that APP751 undergoes less amyloidogenic proteolysis than APP695 and that retention within the early secretory pathway may contribute to this difference. APP751 shows higher co-localisation to the trans-Golgi network than APP695 in immunofluorescence microscopy studies, while addition of a mutation which causes APP proteolysis in the secretory pathway reduces the large difference in amyloidogenic proteolysis of these two isoforms. Targeting APP endocytosis from the cell surface, thought to be a key determinant in Aβ generation, effects APP isoform proteolysis and Aβ production to a similar extent in both the APP isoforms suggesting differences in proteolysis occur before this trafficking event. We also show by immunoblot analysis that the APP isoforms may be differentially cleaved by proteases other than β- and γ-secretase to produce recently identified proteolytic fragments. Using a liquid chromatography – tandem mass spectrometry approach coupled to prior stable isotope labelling of amino acids in cell culture (SILAC), we have identified the interactomes of the two APP isoforms in our model system. Gene ontology analysis identified enrichment of nuclear and mitochondrial proteins specifically in the APP695 interactome. Using siRNA mediated protein knockdown, we have shown interactions with Fe65 and ataxin-10 specifically influence Aβ generation from the APP695 isoform. Fe65 alters proteolysis at the rate limiting β-secretase cleavage step, while ataxin-10 alters proteolysis by γ-secretase. Interaction with growth-associated protein 43 specifically influences Aβ generation from the APP751 isoform, altering proteolysis at the γ-secretase step. Finally we have shown that recently discovered familial AD-linked mutation and protective mutation within the Aβ region of the APP protein have consistent effects on APP proteolysis in both the APP isoforms.

Declaration

No portion of the work referred to in this thesis has been submitted in support of an application for another degree or qualification of this or any other University or other institute of learning.

Copyright statement

I) The author of this thesis (including any appendices and/or schedules to this thesis) owns certain copyright or related rights in it (the "Copyright") and he has given The University of Manchester certain rights to use such copyright, including for administrative purposes.

II) Copies of this thesis, either in full or in extracts and whether in hard or electronic copy, may be made **only** in accordance with the Copyright, Designs and Patents Act 1988 (as amended) and regulations issued under it or, where appropriate, in accordance with licencing agreements which the University has from time to time. This page must form part of any such copies made.

III) The ownership of certain Copyright, patents, designs, trade marks and other intellectual property (the "Intellectual Property") and any reproductions of copyright works in the thesis, for example graphs and tables ("Reproductions"), which may be described in this thesis, may not be owned by the author and may be owned by third parties. Such Intellectual Property and Reproductions cannot and must not be made available for use without the prior written permission of the owner(s) of the relevant Intellectual Property and/or Reproductions.

IV) Further information on the conditions under which disclosure, publication and commercialisation of this thesis, the Copyright and any Intellectual Property and/or Reproductions described in it may take place is available in the University IP Policy (see http://documents.manchester.ac.uk/DocuInfo.aspx?DocID=487), in any relevant Thesis restriction declarations deposited in the University Library, The University Library's regulations (see http://www.manchester.ac.uk/library/aboutus/regulations) and in The University's policy on Presentation of Theses.

Dedication and acknowledgements

I would like to dedicate the contents of this thesis to the memory of John Malcolm Young Andrew and to John Barrie Brearley, whose past, and ongoing battles with dementia have inspired and motivated me through my 3 year philosophical doctorate research program.

Firstly, I would like to thank Professor Nigel Hooper for giving me the opportunity to undertake a fulfilling and interesting research project in his lab. His invaluable insight, support and experience have been a greatly appreciated guiding hand over the last three years. I would also like to thank members of the Hooper lab past and present for technical support, critical analysis, and above all, their friendship. Thanks to Ben Allsop, Dr Sreemoti Banerjee, Dr Nicola Corbett, Carmel Edwards, Dr Carolyn Jackson, Alys Jones, Beth Noble, Dr Nicole Watt and Dr Izzy Whitehouse. Special thanks must go to Dr Kate Kellett and Dr Heledd Jarosz-Griffiths who have been a huge support since I began life in the Hooper lab over 3 years ago and Dr Kate Fisher whose technical and moral support has helped me in the final push to the finish line. I must also thank the various academic, post-doctoral and support staff that have helped me over the last three years. Thanks to people who have helped during my time at the University of Leeds; Prof Anthony Turner, Prof Adrian Whitehouse, Prof Mike McPherson, Dr James Duce, Dr Gareth Howell, Dr Sally Boxhall and members of the Duce, Milner and Ponambalam labs. Thanks also to those who have helped and advised since our move across the Pennines; Prof Stuart Allan, Dr Richard Unwin, Dr Steve Marsden, Dr Peter March and members of the Pickering-Brown lab. Thanks also to our proteomics collaborator at the University of Bristol, Dr Kate Heesom for sample analysis and advice on elements of this project that were completely new to our lab. Thanks also to Alzheimer's Research UK for funding this project.

I would like to thank my parents and my sisters for their unwavering support, not only over the last three years, but throughout my whole life. My parents have played a huge part in everything I have achieved, providing me with the guidance and support I have needed to get here.

Finally, I would like to thank my long suffering fiancé, Fiona. No matter how badly a day, week, month or year at work seems to have gone, she is always there to pick me up at the end of the day and encourage me to persevere. She has put up with my weekends and late nights spent in the lab or bent over my computer, my inability to arrive home in time to cook and my desire to take her half way across the world, only ever complaining that she doesn't see me enough. I couldn't have asked for more from her.

Chapter 1. Introduction

1.1 Dementia and Alzheimer's disease

1.1.1 Social and economic impact of Alzheimer's disease

Dementia, the most common form of which is Alzheimer's disease (AD), represents one of the greatest challenges facing the scientific and medical communities, with over 850,000 people in the UK living with dementia, a figure set to rise to over 1 million by 2025 (http://www.alzheimersresearchuk.org/). The economic cost of dementia in the UK is currently estimated at £24 billion per year, set to rise to £32.5 billion per year by 2025 (http://www.alzheimersresearchuk.org/). Significantly, almost 50% of the economic burden of dementia is borne by unpaid carers, be they spouses, family members or friends of those living with dementia (http://www.alzheimersresearchuk.org/). This means the social and economic impact of the disease does not begin and end with the patient, but extends to every person they rely on for care and companionship. The greatest risk factor for the development of AD is ageing, a factor which, combined with an ageing worldwide population and increased life span in both developed and developing countries, suggests the severity of the problem is yet to reach its peak. As life expectancy across the world continues to rise, so does the desperate need for research into AD, improving both fundamental understanding of the disease and increasing the likelihood of producing therapies.

1.1.2 Alzheimer's disease hallmarks and symptoms

The link between AD pathology and the symptoms associated with the disease date back to 1906, when Dr Alois Alzheimer first documented the behavioural symptoms of 51 year old Auguste Deter and, following her death, linked them to what is now referred to as AD pathology. The pathology of AD has been studied intensively, with the aggregations of amyloid-β (Aβ) peptide into extracellular amyloid plaques, and intracellular neurofibrillary tangles (NFTs) consisting of hyperphosphorylated forms of the microtubule associated protein tau, present post-mortem in the brain of patients (Querfurth and LaFerla 2010) (**Figure 1.1**). However, it has become apparent more recently that other pathological features are present in the AD brain, and often patients present with mixed pathology post-mortem (Jack and Holtzman 2013). AD is also characterised by marked synaptic and neuronal loss, particularly in specific areas of the brain which play an important role in memory including the hippocampus and entorhinal cortex (Karran and Hardy 2014b) (**Figure 1.1**). Indeed, atrophy within the brain of AD patients is

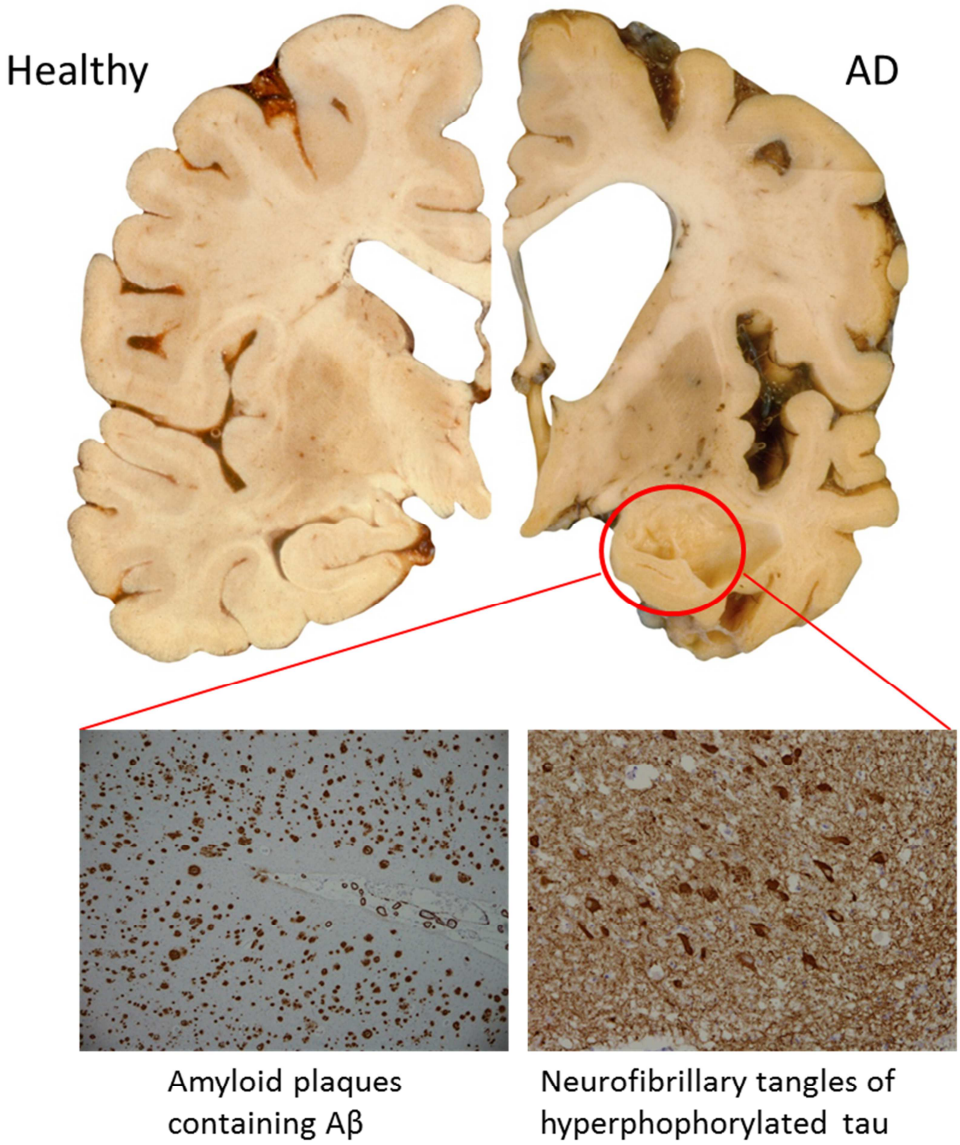

Figure 1.1 Typical brain atrophy and histopathological hallmark accumulation in an Alzheimer's disease patient brain

Alzheimer's disease (AD) is characterised by severe brain atrophy, particularly in the cortex and hippocampus when compared to healthy brains. Accumulation of the pathological hallmarks may occur in distinct patterns, but both can be observed in the hippocampal regions (circled) as shown by amyloid plaque immunostaining with Aβ antibodies (left) and phospho-tau antibodies. The healthy and AD brain image is courtesy of Professor Seth Love (University of Bristol, UK) and the amyloid plaque and neurofibrilllary tangle images are courtesy of Dr Tammaryn Lashley (University College London, UK). Permission was sought from both the image owners to reproduce the images.

possibly the most reliable correlate with disease severity across a wide range of onset ages, while the histopathological features appear to correlate at younger ages of onset (Savva et al. 2009).

In their updated review on Alzheimer's disease, the Alzheimer's Association (2015) define the symptoms of AD as beginning with confusion, difficulties with short term memory, problem solving and day to day tasks, often leading to behavioural changes and mood swings. Eventually, as neuronal damage spreads through the brain, patients are left without control of various functions including the capacity to walk, speak or swallow.

1.1.3 Diagnosis of disease

A lack of reliable biochemical biomarkers for AD, particularly those indicative of prodromal AD, make identification of at risk patients extremely difficult. Indeed, one of the main issues cited as the reason for failure of some recent AD drug clinical trials, is the inability to diagnose the disease with absolute certainty (Hardy 2012).

Clinical diagnosis of AD often relies upon the use of generalised cognition tests including the Mini-Mental State Examination and imaging techniques including magnetic resonance imaging and which can contribute to diagnosis but require longitudinal examination of patients (Hardy 2012), and thus may lead to delays in diagnosis and treatment. Improved imaging techniques including amyloid Pittsburgh compound B (PiB) positron emission tomography (PET) can now provide pathological insight in living patients, allowing the separation of vascular and mixed pathology dementias from pure AD forms (Johnson et al. 2012). While amyloid PET can allow diagnosis of disease in a subset of patients who are amyloid positive, not all AD patients have significant amyloid deposition, while some of the cognitively normal aged population can display significant amyloid deposition (Hyman et al. 2012). Hypometabolism identified via fluorodeoxyglucose PET imaging can also indicate neurodegeneration within the brain (Jack and Holtzman 2013). Cerebrospinal fluid (CSF) levels of Aβ (decreased in AD) and tau (increased in AD) act as useful markers of brain pathology and neurodegeneration, respectively, and can predict disease progression (Toledo et al. 2015). However, the cost of PET imaging is prohibitively expensive for widespread application, while the lumber puncture required for CSF sampling is considered an invasive technique (Henriksen et al. 2014).

Therefore the search for an effective and cheap diagnostic tool continues. A recent research output indicated a new method of cognitive testing combining various tests of memory and function could identify those at risk of progression to AD 18 years prior to diagnosis (Rajan et al. 2015). In addition, the identification of a blood biomarker to provide a cheap and accessible test

for AD remains a priority for some (Henriksen et al. 2014). While AD may have some specific symptoms and markers, the only method for absolute diagnosis of AD remains through post-mortem examination and identification of the histopathological hallmarks previously described (Karran and Hardy 2014b).

1.1.4 Current therapies for Alzheimer's disease

There are currently no disease-modifying drugs available for AD meaning that progression of disease, though often unpredictable, is inevitable. Current therapies available for AD are for the treatment of symptoms rather than the underlying aetiology. These include NMDA (*N*-methyl-D-aspartate) receptor antagonists such as memantine and acetylcholinesterase inhibitors such as donepezil and rivastigmine (Aisen et al. 2012). NMDA receptor antagonists work by reducing the entry of calcium ions into neurons which, when dysregulated, can result in excitotoxicity and associated neuronal death (Aisen et al. 2012). Acetylcholinesterase inhibitors on the other hand reduce acetylcholine breakdown in the synaptic cleft, enhancing inter-neuronal communication (Aisen et al. 2012). Though shown to modestly improve cognition and function in patients (Roberson and Mucke 2006), these drugs do not target the underlying pathology of AD. Clinical trials for disease modifying AD therapeutics are on-going and difficulties in translating pre-clinical data into successful human trials have been attributed to poor patient stratification, poor drug target engagement and insufficient dosing strategies (Romero et al. 2015).

1.2 Current understanding of Alzheimer's disease

1.2.1 The Amyloid Cascade Hypothesis

Over the last three decades much research in the area of AD has focused on the theory that AD is primarily caused by the accumulation of Aβ in the brain. The 'amyloid cascade hypothesis' posits that production of the neurotoxic Aβ fragment of varying length (but most often 40 or 42 amino acids long (Aβ40 or Aβ42)), through sequential proteolytic cleavage of the amyloid precursor protein (APP) in the brain, causes various abnormalities in the brain which lead to neuronal death and progressive neurodegeneration (Hardy and Allsop 1991;Reitz 2012). Support for this theory came from identification of Aβ as the main constituent of amyloid plaques (Masters et al. 1985;Glenner and Wong 1984) and genetic links between early onset forms of the disease and mutations in either APP itself (Citron et al. 1992), or in one of the two genes encoding the presenilins (PS) (part of the γ-secretase complex responsible for APP proteolysis) (Scheuner et al. 1996) and a large number of current AD therapeutic strategies still focus on modulating Aβ levels by targeting its production or clearance. Critically though, failure

to successfully reverse or reduce any AD symptoms by targeting any of the proteins involved in the amyloidogenic proteolysis of neuronal APP and subsequent Aβ accumulation with drug compounds, has placed increased scrutiny on the hypothesis leading to an array of critical reviews (Herrup 2015;Pimplikar 2009;Pimplikar et al. 2010;Reitz 2012) and reappraisals (Hardy 2006;Hardy 2009;Hardy and Selkoe 2002;Selkoe 1991;Selkoe 2000) of the current evidence. Aβ sceptics have fingered the lack of spatial and temporal correlation between plaque pathology (which begins in cortical brain regions) and neuronal cell death (which begins in the entorhinal cortex and hippocampus) as fundamental evidence that Aβ is not the primary driver of AD (Musiek and Holtzman 2015). NFTs on the other hand correlate better with regions in which neurodegeneration occurs and progresses in a consistent manner (Serrano-Pozo et al. 2011). However, the presence of Aβ appears to be necessary for the NFTs to spread through the brain, a prerequisite for the development of AD (Musiek and Holtzman 2015). In reappraisals of the amyloid cascade hypothesis, a shift from blaming Aβ plaque pathology to blaming the aggregation prone nature and accumulation of soluble forms of Aβ for AD can be observed (Hardy and Selkoe 2002), with a distinct focus on the Aβ42 form (Selkoe 2000). The focus on the Aβ42 form came from the proposal that the additional amino acids at the C-terminus of the peptide enhanced its aggregation propensity (Benilova et al. 2012). In fact it is now becoming apparent that soluble, specifically conformed oligomeric forms of Aβ correlate better with neuronal loss and AD than do plaques (Tomic et al. 2009;McLean et al. 1999) and can induce behavioural deficits in rats (Cleary et al. 2005), suggesting a crucial role in initiating the neurodegeneration. That is not to say however that there is no pathology associated with plaques, which are often surrounded by dystrophic neurites and microglial activation (Spires-Jones and Hyman 2014). While the complex pathological path from Aβ generation to AD is still being determined, there is substantial evidence for a role for Aβ in inducing synaptic loss and dysfunction, a subtle but key alteration in the brain of AD patients (Mucke and Selkoe 2012). Indeed, Aβ oligomers derived from several sources can induce long term depression (Li et al. 2009) and prevent long term potentiation (Li et al. 2011). As Aβ is produced throughout life, one important gap in understanding of the amyloid cascade is comprehension of which causes a shift in 'normal' Aβ production to its pathological accumulation (Musiek and Holtzman 2015). Furthermore, defining how the accumulation of Aβ leads to the dysregulation and loss of synapses and eventually neuronal cells would aid in the corroboration of the amyloid cascade hypothesis (Spires-Jones and Hyman 2014).

1.2.2 Proteolytic cleavage of APP

In order to appreciate the role of Aβ in AD it is important to consider the proteolytic events which lead to its liberation. The proteolytic cleavage of APP can follow two major routes (**Figure 1.2A**). The production of Aβ relies upon sequential proteolysis by β- and γ-secretase in the amyloidogenic pathway, while non-amyloidogenic proteolysis by α- and γ-secretase precludes the formation of Aβ. While both pathways are constitutively active in the brain throughout life, physiological imbalances in either the production or clearance of their metabolites contributes to the progression of AD (Querfurth and LaFerla 2010).

In the non-amyloidogenic pathway, cleavage by the α-secretases occurs within the Aβ region of APP, thus precluding its formation. This liberates an N-terminal fragment known as soluble APPα (sAPPα) which is released into the extracellular space and leaves a short membrane bound C-terminal fragment (CTF) known as C83 or CTFα. In the amyloidogenic pathway the initial proteolytic cleavage by the β-site APP cleaving enzyme 1 (BACE1) is the rate limiting step in the production of Aβ (Cole and Vassar 2007). Proteolysis occurs in the extracellular domain at the N-terminus of the Aβ region liberating the slightly shorter soluble fragment, soluble APPβ (sAPPβ), and leaving a slightly longer membrane bound stub known as C99 or CTFβ. Both amyloidogenic and non-amyloidogenic pathways follow the same secondary cleavage event, where the γ-secretase complex cleaves at an intramembrane site at the C-terminus of the Aβ region liberating an Aβ peptide varying from 38-43 amino acids in length in the amyloidogenic pathway, and the fragment p3 in the non-amyloidogenic pathway. γ-secretase appears to cleave APP at several sites in the transmembrane domain, resulting in the production of Aβ species with various C-terminal truncations (Takami and Funamoto 2012;Takami et al. 2009). Indeed, the preliminary γ-secretase cleavage of APP may determine the final C-terminal length of the Aβ peptide through this C-terminal 'nibbling' activity of the complex (**Figure 1.2B**). More than 90% of APP is thought to undergo proteolysis down the non-amyloidogenic pathway, while only 10% undergoes amyloidogenic proteolysis (Nalivaeva and Turner 2013). While both Aβ40 and Aβ42, along with other C- and N-terminally truncated Aβ species are constitutively produced through the proteolysis of APP, Aβ40 is thought to account for 90% of Aβ production (Thinakaran and Koo 2008). The remaining APP intracellular domain (AICD), can then be rapidly degraded by insulin degrading enzyme (IDE) in the cytosol, or can be transported to the nucleus where it has a role in transcriptional regulation (Beckett et al. 2012). Direct competition between the two processing pathways has been widely debated and the reciprocal nature of the pathways may depend on the cell line being examined (Colombo et al. 2013).

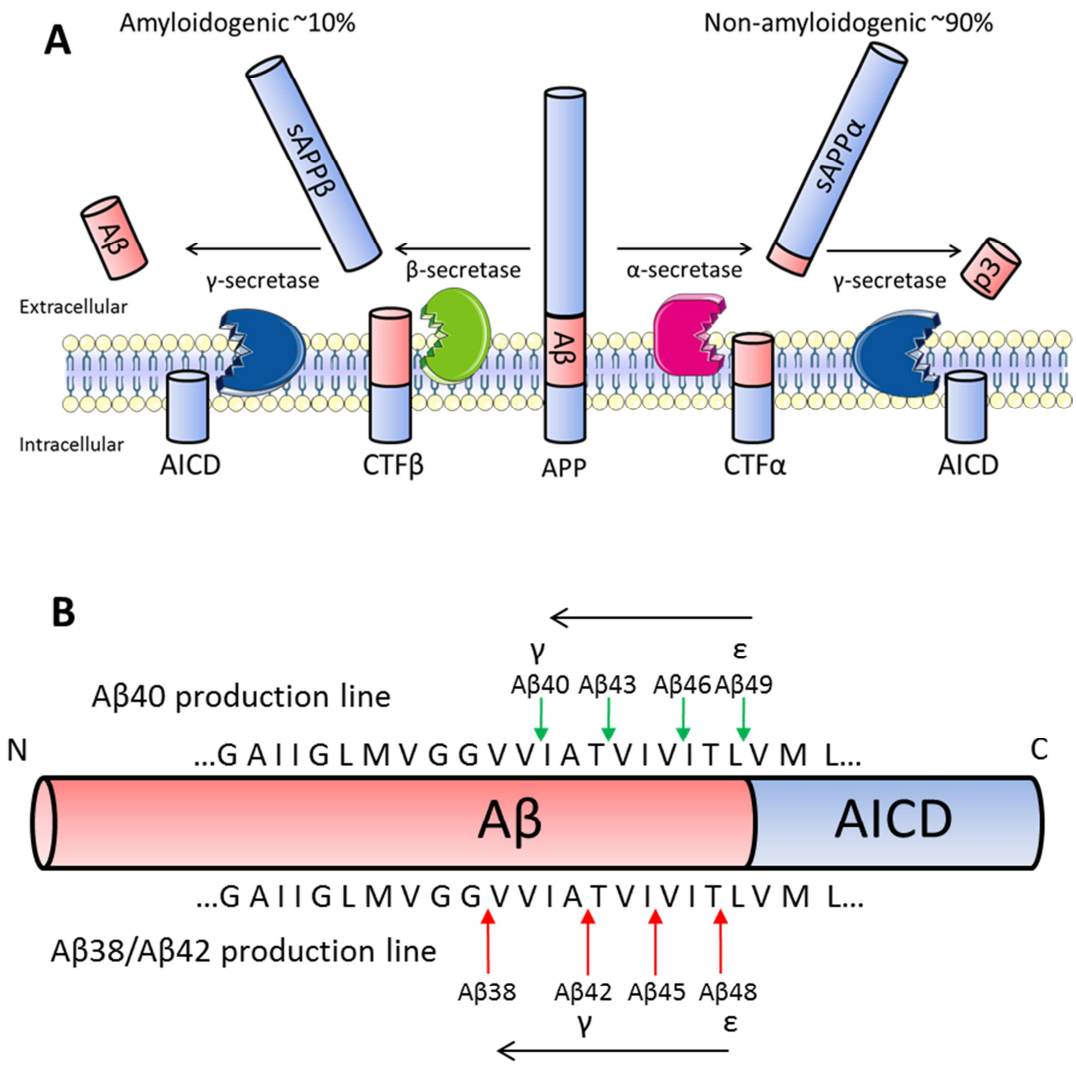

Figure 1.2 Two proteolysis pathways for APP release distinct soluble fragments

A) APP can follow two major proteolysis pathways; the amyloidogenic pathway and the non-amyloidogenic pathway. In the amyloidogenic pathway cleavage by β- and γ-secretase liberates sAPPβ and Aβ and is thought to account for 10% of APP proteolysis. In the non-amyloidogenic proteolysis pathway cleavage by α- and γ-secretase liberates sAPPα and p3 and accounts for 90% of APP proteolysis. Both pathways leave AICD which can be proteolytically degraded or translocated to the nucleus where it has roles in transcriptional regulation. **B)** Cleavage of APP CTFs by γ-secretase follows a 'nibbling' pattern in the direction indicated by the arrows, where the initial (ε) cleavage dictates the final (γ) cleavage. Importantly, the initial cleavage can dictate the C-terminal length of Aβ and thus its amyloidogenic potential. N= N-terminus, C = C-terminus.

1.2.3 Familial Alzheimer's disease

Familial AD cases have provided substantial evidence for the argument for APP proteolysis, and ultimately Aβ production, being the primary contributor to AD development. Mutations in the coding region of APP have been discovered in cohorts of patients with early onset AD from various ethnic backgrounds, all of which lie in, and immediately surround, the Aβ region (**Figure 1.3**) (Diagram adapted from information available at www.alzforum.org/mutations). These have been shown to have varying effects on APP processing including increasing β-secretase cleavage and increasing production of aggregation prone Aβ42 and some have also been shown to increase propensity of the Aβ to aggregate.

One well studied APP mutant, discovered in a Swedish family with familial AD and thus referred to as $APP_{SWE,}$ has been widely studied due to the 3-6 fold increased production of Aβ associated with the double point mutation (K670N/M671L) immediately preceding the BACE1 cleavage site (Citron et al. 1992). Note that here, and in all further references to an amino acid residue in the APP protein sequence within this thesis, the position refers to the position of that amino acid in the APP770 isoform. This double point mutation increases the efficiency of BACE1 cleavage (Haass et al. 2012;Citron et al. 1992) resulting in APP cleavage in the secretory pathway (Haass et al. 1995) and a reduction in mature APP reaching the cell surface (Yamakawa et al. 2010). A second mutation in APP, immediately following the β-secretase cleavage site (A673V), was discovered in an Italian family (APP_{ITA}) was also shown to increase sAPPβ, Aβ40 and Aβ42, and to reduce sAPPα, as well as enhancing the aggregation prone nature of the Aβ molecule (Di Fede et al. 2009). Though the biochemical mechanism resulting in the up-regulation of Aβ production in APP_{ITA} has not been elucidated, studies have shown that people that are heterozygous for the mutation do not exhibit AD symptoms (Di Fede et al. 2009). Further investigation showed that the heterogeneous mixture of mutated and wild-type APP (APP_{WT}) reduced the propensity for the mutant Aβ to form fibrils *in vitro* (Di Fede et al. 2009). Other familial mutations in the middle of the Aβ region have been shown to increase the aggregation propensity of the Aβ molecule suggesting the aggregation step is of crucial importance in the development of AD (Hardy and Selkoe 2002). A recent publication discovered a potential neuroprotective mutation in APP, the presence of which in a small Icelandic population appeared to contribute to reduced age-related cognitive decline and reduced the risk of developing AD (Jonsson et al. 2012). Interestingly the mutation, A673T (APP_{ICE}), is at the same amino acid residue as the previously described Italian mutation, but the mutation has been shown to reduce the levels of sAPPβ, Aβ40 and Aβ42 produced significantly below that seen for APP_{WT} in cell culture models (Jonsson et al. 2012).

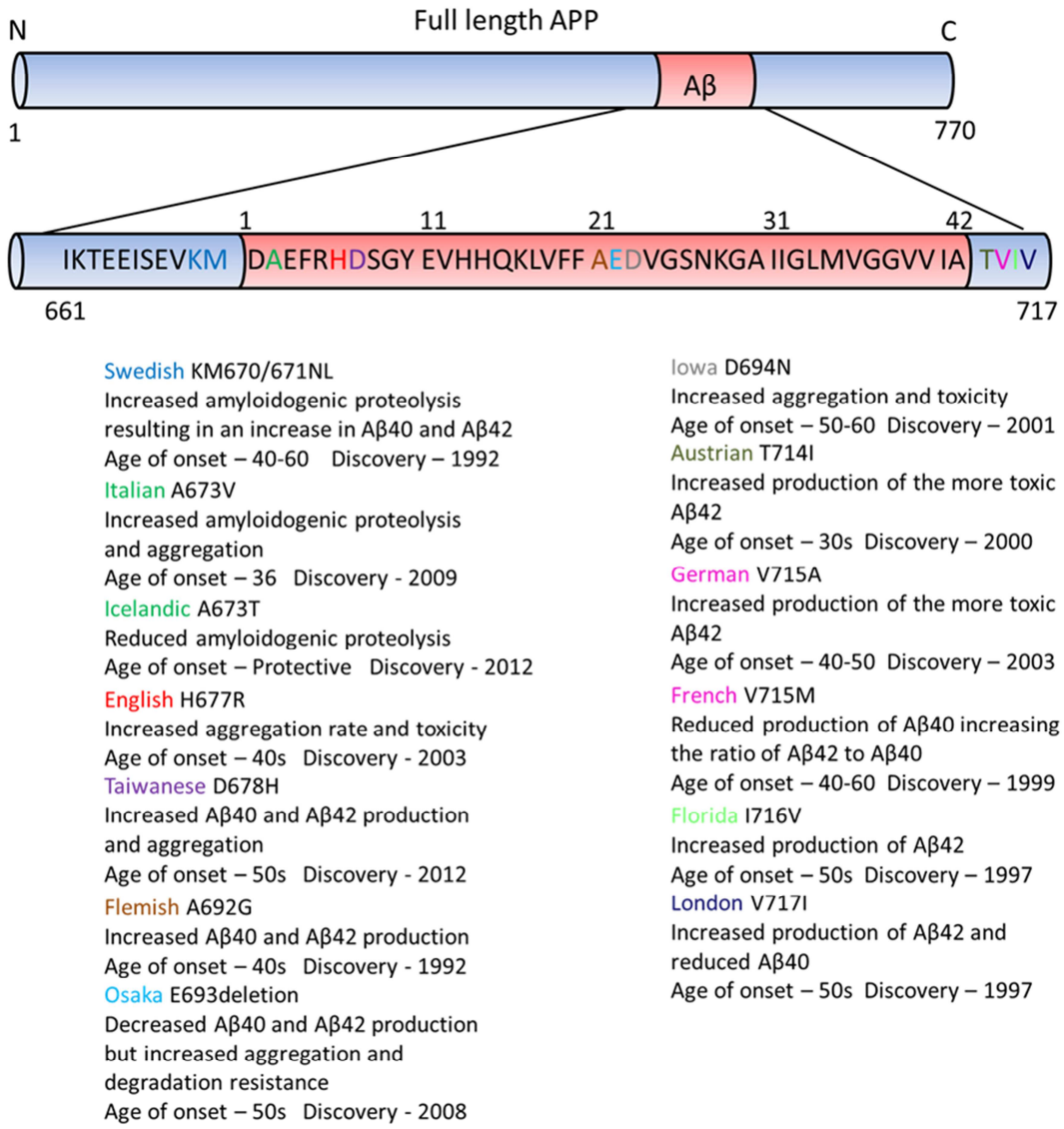

Figure 1.3 Genetic mutations can cause AD or protect against its development

Support for the amyloid cascade hypothesis comes from the discovery of a large number of mutations within APP, concentrated in or immediately surrounding the Aβ region. The majority of mutations increase Aβ production, aggregation propensity of the molecule or the ratio of Aβ42:Aβ40 produced from its amyloidogenic proteolysis. A single mutation in APP adjacent to the β-secretase cleavage site protects carriers against AD and age-related cognitive decline (A673T). Numbers below the APP image and the enlarged Aβ region indicated their position in the APP amino acid sequence (APP770 numbering) and the numbers above the enlarged Aβ region indicate the amino acid position in the Aβ sequence. N= N-terminus, C = C-terminus.

In addition to mutations in APP, mutations in the proteolytic PS subunit of the γ-secretase complex responsible for the liberation of the Aβ peptide have also been shown to result in familial AD. Many of the mutations in PS associated with AD alter the ratio of the production of Aβ40:Aβ42 from APP, increasing the relative proportion of the more aggregation prone Aβ42 molecule (De Strooper et al. 2012). The pathogenicity of familial AD caused by PS mutations is perhaps less clear cut than that for APP mutations, as they have been shown to have various effects on Aβ production, in some cases actually reducing it (Bentahir et al. 2006). This had led to the suggestion that the mutations in PS result in the loss of essential functions of the γ-secretase complex resulting in neurodegeneration (Shen and Kelleher 2007). However, given that no mutations in other γ-secretase substrates have been linked to AD, it seems likely that alterations in APP metabolism cause the disease in these cases (De Strooper et al. 2012). Remarkably, no mutations in BACE1 have ever been linked to familial AD.

1.2.4 Sporadic Alzheimer's disease

Though familial AD cases initiated and have shaped our current understanding of AD, they account for a small proportion of the large number of cases. Late onset or sporadic AD cases occur later in life than the familial forms and are not caused by pathological mutations in APP or the enzymes directly involved in the generation of Aβ. The aetiology of this form of AD is therefore more complex, but it is possible that genetic risk factors play a role in up to 80% of these cases (Tanzi 2012). Large scale genetic studies have identified a range of risk factors associated with sporadic AD which vary in their association with disease. The *APOE* ε4 allele represents the strongest of these genetic risk factors, increasing risk of disease 3-fold and 12-fold in heterozygous and homozygous carriers, respectively (Verghese et al. 2011). Evidence implicates the apolipoprotein E ε4 (ApoE4) protein in the development of amyloid plaque pathology, both through influencing the aggregation of Aβ molecules and influencing its clearance from the brain through microglial and proteolytic degradation and transport across the blood brain barrier (Yu et al. 2014). Other genetic risk factors have been identified by genome wide association studies (GWAS) and have been broadly grouped into genes for proteins involved in the endosomal cycling systems (includes *SORL1*, *BIN1*, *PICALM* and *CD2AP*), lipid and cholesterol metabolism (including *CLU* and *ABCA7*) and immune and inflammatory responses (including *CD33*, *CR1* and *INPP5D*) and several have been linked to alterations in Aβ and tau pathologies (See (Van Cauwenberghe et al. 2015)). Interestingly, the association between cholesterol metabolism and inflammatory responses in AD suggests there may be some benefit to targeting these pathways through the prescription of already available

cholesterol lowering and anti-inflammatory drugs for AD patients (Jones et al. 2010). Aside from the contribution of genetic risk factors, understanding the causes of sporadic AD has remained challenging. Epidemiological influence on AD risk is complex and a range of environmental factors have been linked to AD including diet, exercise and body mass index, while co-morbidities such as cardiovascular disease and diabetes may also contribute (Mayeux and Stern 2012). Understanding how genetic and epidemiological factors confer risk remains a major challenge for the AD research community.

1.3 The molecular players in Alzheimer's disease

1.3.1 The amyloid precursor protein

The APP family of genes comprises *APP* and the two APP-like proteins *APLP1* and *APLP2* in humans, *Appl* in flies and *apl-1* in worms, all of which show striking evolutionary conservation and similarities in proteolytic processing (Shariati and De Strooper 2013;Thinakaran and Koo 2008). Of the proteins produced from these genes, only APP contains the Aβ peptide implicated in AD (Nalivaeva and Turner 2013;Shariati and De Strooper 2013). Over 25 years ago, the complimentary DNA (cDNA) encoding APP was isolated by Kang et al. (1987) and its locus mapped to chromosome 21. APP, a type I transmembrane protein, has a large extracellular domain and a short intracellular domain (Kang et al. 1987). Though the exact function of APP is still to be fully elucidated (Rajendran and Annaert 2012), various studies have identified distinct domains and motifs within the protein which appear to have functional significance (**Figure 1.4**). The ectodomain contains metal binding domains, a growth factor like domain, an extracellular matrix binding domain, a protease inhibitory domains in the case of the APP751 and APP770 isoforms (see **Section 1.3.2**), several regions linked to trophic properties of the protein (Thinakaran and Koo 2008). Though relatively unstructured, the C-terminal, cytosolic region of APP has several phosphorylation sites and is thought to be responsible for interactions with proteins involved in transport and neuronal migration (van der Kant and Goldstein 2015). This domain also contains the YENPTY motif which has essential roles in APP trafficking, particularly endocytosis (Nhan et al. 2015). Within the soluble ectodomain is the five amino acid RERMS sequence, which has been linked to the trophic capabilities of APP (Pawlik et al. 2007).

Some functional clues for APP have come from knockout studies in mice. Though viable, APP-null mice display several phenotypes including increased reactive gliosis, some deficits in long term potentiation (LTP) and learning and reductions in dendrite formation (Dawson et al. 1999;Seabrook et al. 1999). Though heterozygous knockout mice for any of the *APP*, *APLP1* or

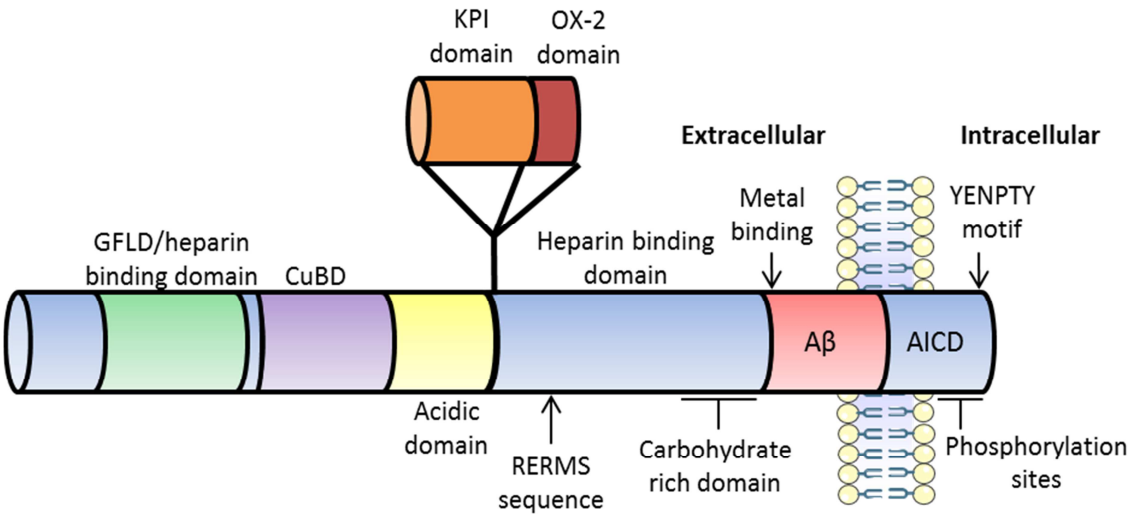

Figure 1.4 Structural domains within the amyloid precursor protein

APP is a type one transmembrane protein with a large extracellular ectodomain and a short intracellular domain. The soluble ectodomain contains domains including a Growth factor like domain (GFLD), cooper/zinc binding domain (CuBD), acidic domain, extracellular matrix/heparin binding domains and a carbohydrate rich domain containing N- and O-glycosylation sites. Alterative splicing of the APP mRNA determines the incorporation of the Kunitz protease inhibitor (KPI) domain and the OX-2 domain. The cytosolic domain contains seven reported phosphorylation sites. Important amino acid motifs within the protein have been identified including the RERMS sequence, thought to be involved in the trophic properties of the protein, and the YENPTY endocytosis motif.

APLP2 genes are viable, combined knock-out of *APLP2* and *APP* or *APLP2* and *APLP1* is embryonically lethal, suggesting a limited amount of functional redundancy and interchangeability between the related family members (Heber et al. 2000). Though all three family members are proteolytically cleaved by the same enzymes, only the intracellular domain (ICD) from APP and APLP2 are proposed to undergo nuclear translocation, suggesting distinct roles for these family members (Gersbacher et al. 2013). These related family members have also been shown to display subtle differences in subcellular location and their capacity to dimerise, indicating differential sorting and functional roles (Kaden et al. 2009).

It has been suggested APP has roles in cell-cell adhesion (Schubert et al. 1989;Soba et al. 2005), synaptogenesis (Wang et al. 2009), neurite outgrowth (Hoe et al. 2009;Spillantini et al. 1989), cell proliferation (Saitoh et al. 1989), neuronal migration during development (Nikolaev et al. 2009;Young-Pearse et al. 2007;Rice et al. 2012), roles as a cell surface receptor (Rice et al. 2013;Reinhard et al. 2005) and involvement in iron (Duce et al. 2010) and cholesterol (Pierrot et al. 2013) homeostasis to name just a few. The trophic properties of APP are often attributed to the extracellular domain of APP and may be mediated through interactions with extracellular matrix proteins (Musardo et al. 2013). Though there is evidence for the presence of APP at the synapse (Wang et al. 2009), its role there has remained controversial, with conflicting reports on the effect of its expression on dendritic spines. Both increases (Priller et al. 2006) and decreases (Lee et al. 2010) in spine density have been show as a result of APP down-regulation in mice. Particularly interesting in the context of the enrichment of proteins involved in lipid metabolism in GWAS studies, is the fact that APP has been shown to interact with several members of the low-density lipoprotein receptor family (van der Kant and Goldstein 2015). In addition the APP C-terminal fragment C99 has been shown to bind cholesterol (though cholesterol is also likely to bind full length APP) (Barrett et al. 2012).

1.3.2 APP isoforms

Alternative splicing of APP mRNA produces isoforms of varying length. Due to their expression within the brain, the main isoforms of interest in the Alzheimer's field are APP695, APP751 and APP770, comprising 695, 751 and 770 amino acids respectively. Exon 7 of the *APP* gene codes for a 56 amino acid Kunitz-type protease inhibitor (KPI) domain found in both APP751 and APP770 with 50% sequence homology with the Kunitz family of serine protease inhibitors (Kitaguchi et al. 1988;Sandbrink et al. 1996). An additional 19 amino acid domain with sequence homology to the OX-2 antigen of thymus derived lymphoid cells is coded for by exon 8 of the *APP* gene and is only present in the APP770 isoform (Muller-Hill and Beyreuther 1989). Neither of these two domains are present in the APP695 isoform. The expression level of APP695 in the

brain has been reported to be 20- and 2- fold higher than that of APP770 and APP751, respectively, on the basis of mRNA quantification (Tanaka et al. 1989), while analysis of protein levels in the human brain cortex suggested almost equivalent levels of KPI domain-containing isoforms and non-KPI containing isoforms (Moir et al. 1998). However, within the brain there is variation in isoform expression between cell type, with APP695 being expressed more abundantly in neurons, while glial cells express more APP751 (Bordji et al. 2010;Rohan de Silva et al. 1997). Despite this, it has been suggested, based on the presence of mRNA transcripts in the hippocampal granule and pyramidal cells, that neurons still express APP isoforms containing the KPI-domain (Spillantini et al. 1989;Johnson et al. 1990). In the foetal brain APP695 mRNA has been shown to account for ~90% of total APP transcripts, while in middle to old age levels of APP695 mRNA may drop below 50% (Beyreuther et al. 1993). Furthermore, increases in the expression of the KPI domain containing isoforms has been shown in response to damaging stimuli such as trauma in the mouse brain (Lesne et al. 2005) and sustained glutamate mediated NMDA receptor activation in cortical neurons (Willoughby et al. 1995). Importantly in the context of AD, various molecular and biochemical techniques have indicated alteration in the expression profile of APP isoforms in the AD brain (See **Table 1.1**). The mechanisms which control the alternative splicing of APP mRNA transcripts have remained enigmatic, and thus the cause and effect of the changes is unresolved.

Differences in APP isoform proteolysis have been observed previously, with more amyloidogenic APP processing of the APP695 isoform compared to KPI domain-containing APP isoforms previously reported in neuronal cells (Belyaev et al. 2010), though the cause of these differences remains unresolved. Ben Khalifa et al. (2012) proposed dimerisation induced by the presence of the KPI domain increased its trafficking to the cell surface, leading to a reduction in amyloidogenic proteolysis. In another study, the addition of a glycophosphatidylinositol (GPI) -anchor to BACE1 to direct its targeting to membrane lipid raft microdomains was also shown to enhance APP695 proteolysis to a much greater extent than APP751, suggesting differences in subcellular trafficking and location of these isoforms (Cordy et al. 2003). Linked to the identification of differences in APP proteolysis, Belyaev et al. (2010) also showed transcriptional regulation of the gene encoding the Aβ degrading enzyme neprilysin (NEP) was specific to AICD produced from the APP695 isoform, with no apparent gene regulatory activity observed for cells expressing the APP751 or APP770 isoforms. Previous research has also identified differences in proteolytic cleavage of APP isoforms lacking exon 15 (Hartmann et al. 1996).

Study	Number	Method	Brain region	Result
(Palmert et al. 1988)	Control (C) = 7 Alzheimer's disease (AD) = 11	**mRNA** In situ hybridisation	Nucleus basalis, locus ceruleus, hippocampal subiculus, basis pontis, occipital cortex	• Neurons of nucleus basalis and locus ceruleus showed increased APP-KPI in AD • No change observed in other regions
(Spillantini et al. 1989)	C = 5 AD = 5	**mRNA** Northern blot In situ hybridisation	Frontal cortex	• Increased APP695:APP751 ratio • Caused by decreased APP695 mRNA
(Koo et al. 1990)	C = 5 AD = 7	**mRNA** PCR	Frontal, temporal and occipital cortices	• No change in ratio between AD and control • Increase in 751/770:695 ratio in ageing
(Golde et al. 1990)	C = 5 AD = 5	**mRNA** PCR	Temporal cortex, cerebellum, frontal grey/white matter, Hippocampus	• Increase in all APP isoforms in white matter • Increased APP695 in regions of high amyloid deposition in AD • Increased APP-KPI in regions of low amyloid deposition in AD
(Johnson et al. 1990)	C = 4 AD = 7	**mRNA** In situ hybridisation	Hippocampus	• Elevated APP751:695 ratio in AD • Caused by increased APP751 transcript (no change in 695)

Table 1.1 APP isoform expression alterations in AD

Table continued overleaf.

Study	Number	Method	Brain region	Result
(Rockenstein et al. 1995)	C = 5 AD = 4	**mRNA** RNA hybridisation	Frontal cortex	• Increase in ratio of APP751:695
(Johnston et al. 1996)	C = 9 AD = 14	**mRNA** RNA hybridisation	Mid-temporal cortex, Superior frontal cortex	• Reduced total APP mRNA • Increase in APPKPI:695 ratio
(Moir et al. 1998)	C = 7 AD = 10	**Protein** Immunoblot	Cortex	• Elevated soluble APP-KPI in AD
(Barrachina et al. 2005)	C = 6 AD (Braak I-II) = 3 AD (Braak V) = 4	**mRNA** PCR	Frontal cortex	• 4.28 fold increase in APP751/770 :APP695 ratio • Seen at Braak stage V, not at stage I-II • Lower total mRNA for all isoforms
(Matsui et al. 2007)	C = 21 AD = 27	**mRNA** PCR	Temporal neocortex	• Increase in KPI domain containing isoforms
(Tharp et al. 2012)	C = 12 AD = 10	**mRNA** PCR	Superior frontal gyrus, cerebellum	• Reduced APP and APP695 mRNA • Increased APP770 mRNA

Table 1.1 cont. APP isoform expression alterations in AD

1.3.3 α-secretase

α-secretase proteolysis of APP and other membrane bound proteins including receptors and growth factors is a constitutive process regulated by zinc metalloproteinases from the family of "a disintegrin and metalloproteinases" or ADAM enzymes (De Strooper et al. 2010;Musardo et al. 2013). The family includes ADAM9, ADAM10, ADAM17 (also known as tumour necrosis factor cleaving enzyme 1) and ADAM19, all of which possess α-secretase properties (Allinson et al. 2003), though ADAM10 is thought to be the primary α-secretase in neurons (Jorissen et al. 2010;Kuhn et al. 2010). ADAM10 is synthesised as a pro-protein, with a pro-domain which is proteolytically cleaved by furin during its maturation (Jiang et al. 2014), and mutations within its pro-domain have been linked to reduced maturation and late-onset AD (Suh et al. 2013). Relatively little is known about ADAM10 trafficking but it is known to undergo N-glycosylation during transit through the secretory pathway (Musardo et al. 2013) and interactions with tetraspanin12 and synapse-associated protein 97 (SAP97) have been reported to influence its subcellular location (Lichtenthaler 2011). In fact, the capacity for ADAM10 to reach the synapse may be compromised in AD through reduced interaction with SAP97, suggesting an important functional role for α-secretase at the synapse (Marcello et al. 2012). In addition to APP, various membrane bound proteins, including proteins with relevance to AD such as the cellular prion protein (Vincent et al. 2001) and notch receptors (Brou et al. 2000), undergo ectodomain shedding by α-secretases suggesting conformation, rather than sequence, specificity (Haass et al. 2012). ADAM10 has also been shown to proteolytically cleave a range of cell surface adhesion proteins including neuroligin-1, N-cadherin, and nectin-1 (Musardo et al. 2013) and indeed the majority of its activity is thought to occur at the cell membrane (Parvathy et al. 1999). α-secretase activity, contrary to that of β-secretase, is reduced in the brains of AD patients (Tyler et al. 2002).

1.3.4 β-secretase

The discovery of the BACE1 occurred following the identification of Aβ as the primary constituent of amyloid plaques. In a series of experiments, including gene expression analysis, database analysis and isolation of the protease from the human brain, BACE1 was identified by several groups as the protease responsible for amyloidogenic APP proteolysis (Vassar et al. 2014). BACE1 belongs to the aspartyl protease family of enzymes, and is a type I membrane protein with a large extracellular domain, and short cytoplasmic tail (Vassar 2004) that is highly expressed in neurons (Vassar et al. 2009). BACE1 is produced as a zymogen, maturing following cleavage of the pro-peptide by furin or other proprotein convertases in the trans-Golgi network (TGN), in a similar manner to α-secretase (Creemers et al. 2001). BACE1 undergoes various

post-translational modifications (PTMs) including *N*-linked glycosylation, acetylation, phosphorylation, ubiquitination and palmitoylation (Tan and Evin 2012) and is trafficked either to the cell surface where it can become enriched in lipid raft domains (Hattori et al. 2006;Riddell et al. 2001) or directly to the endosomal system depending on its phosphorylation status and interaction with specific adaptor proteins (Rajendran and Annaert 2012;Tan and Evin 2012). Internalisation of BACE1 is mediated by a dileucine motif in its cytosolic region and requires the action of the GTPase Arf6 (Sannerud et al. 2011). The protease can subsequently be recycled back to the cell surface (Udayar et al. 2013), recycled to the TGN (Wahle et al. 2005) or trafficked to lysosomes where it is degraded (Haass et al. 2012). Trafficking of BACE1 is strongly regulated by several members of the Golgi-localised γ-adaptin ear-containing ADP ribosylation factor binding proteins (GGAs). GGA1 enhances recycling of phosphorylated BACE1 from the endosomal system back to the TGN (Wahle et al. 2005), and thus can influence the production of Aβ, while GGA3 traffics ubiquitinated BACE1 to the lysosomes where its proteosomal degradation occurs (Tan and Evin 2012). The amount of GGA3 in the AD brain is reduced and correlates with an increase in BACE1, highlighting its importance in BACE1 turnover (Tesco et al. 2007). A recent report also highlighted a role for the protein snapin in BACE1 trafficking to the lysosome for degradation (Ye and Cai 2014). The majority of BACE1 mediated proteolysis is thought to occur in the early endosomes where their enzymatic activity is optimised due to the acidic nature of the luminal environment (Vassar et al. 1999).

Conflicting results have been reported on the effect of BACE1 knockout in mice with early reports claiming viability and little morphological alteration (Luo et al. 2001). However, further investigation identified shortened life span, subtle behavioural variations and altered sodium channel inactivation (Dominguez et al. 2005). BACE1 has been shown to have an important role in nerve myelination through its capacity to cleave neuregulin 1 (Hu et al. 2006;Willem et al. 2006) and a large number of other BACE1 substrates have been identified (for a recent list see (Vassar 2014)). Its involvement in AD pathogenesis is supported by a wealth of evidence for increased BACE1 protein and activity in AD brains (Tan and Evin 2012). Though BACE1 was originally proposed to be the sole β-secretase responsible for proteolysis of APP (Haass et al. 2012), recent work has proposed cathepsin B (Hook et al. 2014) and meprin β (Bien et al. 2012) as alternative β-secretases.

1.3.5 γ-secretase

The functional γ-secretase complex comprises four proteins thought to be necessary for catalytic activity: nicastrin (NCT), anterior pharynx defective-1 (APH1), presenilin-1 (PS1) or presenilin-2 (PS2) and presenilin enhancer-2 (PEN2), and is responsible for the proteolysis of various

membrane bound proteins including APP (De Strooper et al. 2012). Many elements of γ-secretase remain controversial, including the subcellular site of its action, the function of its subunits and the requirement of these subunits for its activity. Similar to APP, the role of γ-secretase in AD was identified and supported by evidence from familial mutations in the *PS1* and *PS2* genes, over 150 of which have now been identified (Zhang et al. 2014). Conserved aspartate residues within two of the trans-membrane domains of PS (D257 in transmembrane domain 6 and D385 in transmembrane domain 7) possess proteolytic capabilities (Wolfe et al. 1999). PS is proteolytically cleaved *in vivo* to generate an N- and a C-terminal fragment (Thinakaran et al. 1996a), which is thought to be required for its activity, and while the PEN2 subunit has been shown to catalyse this endoproteolysis in cells (Prokop et al. 2004) and in an *in vitro* cell free system (Ahn et al. 2010), PS has also been suggested to autocatalyse its own proteolysis (Fukumori et al. 2010). NCT may contribute to substrate recognition by binding the nascent amino terminal region of γ-secretase substrates following a preceding proteolytic cleavage (Shah et al. 2005), though this function has also been questioned, with suggestions the NCT subunit affects complex maturation rather than substrate recognition (Chavez-Gutierrez et al. 2008). Though prior ectodomain shedding of γ-secretase substrates by an alternative protease was originally thought to be required for its activity, γ-secretase was recently shown to shed the B cell maturation antigen from the surface of plasma cells without its prior cleavage (Laurent et al. 2015). A specific function for APH-1 remains elusive, but it may act as a scaffold for complex formation through interactions with NCT (Pardossi-Piquard et al. 2009;Shirotani et al. 2004). The order in which these subunits assemble to form the active complex has also been described on the basis of a large number of studies on individual interactions of the subunits (see (De Strooper et al. 2012;Zhang et al. 2014)). Differences in the incorporation of the two PS proteins, as well as two splice variants of APH-1, means that the γ-secretase complex can be formed in six different ways, potentially attenuating or enhancing substrate specificity and proteolysis, though distinct activity and subcellular localisation of different complexes is not fully understood (Rajendran and Annaert 2012). Though a large amount of PS1 is localised in the endoplasmic reticulum (ER) and the Golgi apparatus, several lines of evidence suggest proteolytic activity occurs in the plasma membrane or, following endocytosis, in the endosomal system (Haass et al. 2012;Rajendran and Annaert 2012). Two of the components of the γ-secretase complex, NCT and APH1 can be palmitoylated, resulting in association with lipid raft microdomains within the cell membrane (Cheng et al. 2009).

Genetic deletion of APH-1, PS1 and NCT have all been shown to be embryonically lethal, indicating the vital role of the γ-secretase complex in development (Zhang et al. 2014). The γ-secretase complex is involved in the proteolytic cleavage of a large number of protein substrates

(Haapasalo and Kovacs 2011). Perhaps the best studied of these outside of APP proteolysis is its role in notch signalling through its capacity to cleave notch itself, as well as its ligands, delta and jagged (De Strooper et al. 1999;Ikeuchi and Sisodia 2003;LaVoie and Selkoe 2003). Its role in notch signalling is essential in the control of cell differentiation, making γ-secretase a difficult therapeutic target (De Strooper et al. 2012).

1.3.6 APP trafficking affects its proteolysis

The subcellular location and trafficking of APP is an important factor in the regulation of its proteolysis (Rajendran and Annaert 2012). As has just been described, the molecular mechanisms involved in trafficking of the secretases are complex, and the same is true of APP. The proteolytic cleavage of APP is inherently linked to its trafficking, as the subcellular location it resides within will determine the likelihood of encountering the proteases responsible for its cleavage. Understanding how APP trafficking contributes to proteolysis has remained a major target in understanding Aβ generation. Though APP synthesis and trafficking are undoubtedly complex, particularly in polarised cells such as neurons, a generalised picture of APP synthesis and trafficking has emerged (**Figure 1.5**). APP is synthesised in the ER and is subsequently trafficked to the Golgi apparatus where it undergoes several PTMs including N- and O-linked glycosylation, phosphorylation, palmitoylation and tyrosine sulphation (Caster and Kahn 2013;Haass et al. 2012). The Golgi acts as the preliminary checkpoint at which membrane bound proteins such as APP undergo sorting to determine their distinct destinations within the cell (Caster and Kahn 2013). While the majority of APP remains localised to the Golgi apparatus (Jiang et al. 2014) and the TGN, a subset of APP, estimated at approximately 10%, is then trafficked to the cell surface via the secretory pathway (Thinakaran and Koo 2008). Upon reaching the cell surface APP is either proteolytically cleaved by α-secretase or re-internalised into endosomes due to the presence of the YENPTY motif in its cytosolic domain (Koo and Squazzo 1994). Internalisation can be clathrin mediated or lipid raft dependent, depending on membrane microdomain sorting of the APP protein (Rajendran and Annaert 2012). Following internalisation APP can be recycled to the cell surface or be sorted to late endosomes and lysosomes where proteosomal degradation occurs (Haass et al. 2012). The importance of cell membrane microdomain sorting of APP, and its effect on APP processing has been widely debated. Clustering of APP to lipid raft microdomains within the cell membrane, possibly through palmitoylation (Bhattacharyya et al. 2013), may lead to increased spatial proximity to BACE1, which can also be palmitoylated at four different cysteine residues (Vetrivel et al. 2009), resulting in proteolysis within these domains (Rajendran and Annaert 2012). In addition, depleting cellular cholesterol has been shown to significantly reduce amyloidogenic proteolysis

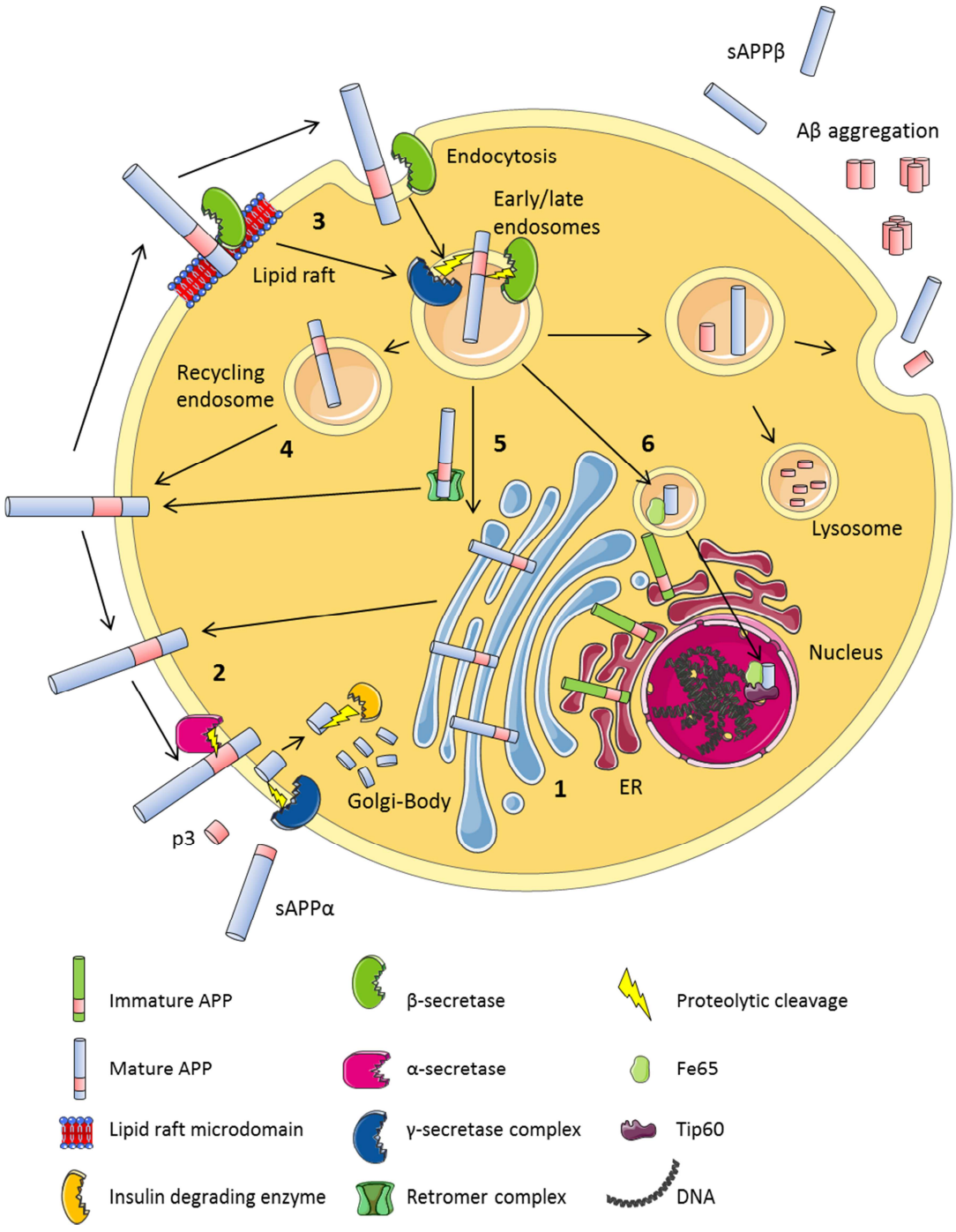

Figure 1.5 APP proteolysis is intrinsically linked to its trafficking

Figure legend overleaf.

Figure 1.5 cont. APP proteolysis is intrinsically linked to its trafficking

1) APP is synthesised in the ER and undergoes various PTMs in the Golgi apparatus, where the majority of APP is thought to reside. 2) APP can be transported to the cell surface where it can undergo non-amyloidogenic proteolysis. 3) Alternatively partitioning into lipid rafts or endocytosis to the endosomal system can result in amyloidogenic proteolysis by β-secretase. The site of APP proteolysis by γ-secretase is a contentious issue, but evidence suggests it can occur at the plasma membrane or in the endosomal system. 4) The recycling endosomal system can traffic APP back to the cell surface. 5) Retromer mediated transport can recycle APP from the early endosomes back to the TGN or to the cell surface. 6) Following amyloidogenic proteolysis , AICD can be transported to the nucleus, possibly aided by Fe65, where it can form a complex involved in transcriptional regulation of several genes. ER = endoplasmic reticulum.

of APP (Rushworth and Hooper 2010). APP and BACE1 are also thought to converge in early endosomes, proposed as the main site of APP proteolysis due to the acidic optimal pH of BACE1 (Vassar 2004). APP may also be trafficked from early endosomes back to the TGN or the cell surface in multi-protein complexes called retromers, which can alter APP proteolysis and is thought to be dependent on phosphorylation of the cytoplasmic S730 residue (Mecozzi et al. 2014;Vieira et al. 2010). The exact site of γ-secretase proteolysis has remained contentious, though consensus suggests its activity at the plasma membrane or within the endosomal system (Haass et al. 2012). Alternatively, others have proposed γ-secretase cleavage of CTFs in the TGN (Choy et al. 2012). Interestingly, the subcellular location in which γ-secretase proteolysis occurs has been shown to influence the amino acid residue at which APP CTFs are cleaved, indicating the relative pH of the subcellular environment can also influence γ-secretase proteolysis (Fukumori et al. 2006). Following amyloidogenic proteolysis, AICD can be transported to the nucleus where it has roles in transcriptional regulation, though the cause(s) of the differential fate of AICD from the two APP processing pathways remains an enigma (Beckett et al. 2012).

In neurons, APP transport relies upon kinesin-1 as the main motor protein facilitating its axonal transport (Kaether et al. 2000). It has been suggested that the JNK-interacting protein 1, through interactions with kinesin heavy chain, regulates the trafficking of APP in neurons by acting as a switch between retrograde and anterograde transport (Fu and Holzbaur 2013). The sequence YKFFE in the C-terminal region of APP appears to promote interaction with adaptor related protein complex 4 (AP-4), aiding in its recruitment to the specific vehicles required for its anterograde axonal transport (Musardo et al. 2013). During its trafficking through neuronal axons, APP can undergo proteolysis (Thinakaran and Koo 2008) and it has been suggested that large amounts of proteolysis occur in the neuronal soma, after which APP C-terminal and N-terminal fragments are trafficked via distinct pathways, possibility contributing to their disparate functional roles (see S**ection 1.4**) or cellular consequences (Villegas et al. 2014). APP is targeted to both pre- and post-synaptic regions in neurons where it is reportedly involved in synaptogenesis, again possibly through involvement in adhesion between synapses (Musardo et al. 2013).

The study of APP trafficking has provided invaluable insight into the subcellular site in which APP proteolysis occurs and has implicated endosomal dysfunction as a key early driver in AD pathology (Rajendran and Annaert 2012). Differences observed in the proteolysis of APP isoforms previously identified (Belyaev et al. 2010), could be due to differences in trafficking and further investigating this could identify trafficking mechanisms or subcellular sites that result in reduced APP proteolysis. Indeed, despite broadly similar structure, large differences have been

observed in the subcellular distribution of APP and its homologs APLP1 and APLP2 (Kaden et al. 2009), suggesting distinct trafficking mechanisms for these closely related proteins.

1.3.7 Role of Tau

As discussed previously, NFTs of hyperphosphorylated tau are the second histopathological hallmark of AD. Though mutations in tau are not specifically linked to AD, they are causative of other forms of dementia such as frontotemporal dementia (Querfurth and LaFerla 2010). The normal function of tau is to stabilise microtubules within the axons of neurons (Spires-Jones and Hyman 2014). However, in the disease state tau becomes hyperphosphorylated resulting in its dissociation from the microtubules and what was initially considered to be mis-localisation to the somato-dendritic compartment of neurons (Mandelkow and Mandelkow 2012). However, it has been suggested that tau may have a role in the dendrites, and that it is accumulation of hyperphosphorylated oligomeric forms of tau in the synapse that is linked to the disease (Tai et al. 2012). Indeed, it has been shown that tau translocates to the post-synaptic density in response to synaptic activity, implicating it in normal synaptic function (Frandemiche et al. 2014). In the disease state, dysregulation of a number of kinases and phosphatases that control the phosphorylation state of tau may be responsible for its hyperphosphorylation (Noble et al. 2013). In addition to phosphorylation, a wide range of other PTMs have been observed in wild-type and human APP-expressing mouse models (Morris et al. 2015), though their relevance to the disease state remains to be determined. Furthermore, tau can be proteolytically cleaved by caspases, increasing its tendency to aggregate, though the interrelationship between cleavage and phosphorylation is not clear (Noble et al. 2013). Tau can also be expressed as 6 isoforms in the brain, and the maintenance of the correct ratio of isoform expression has been proposed to be of importance in preventing neurodegeneration (Goedert and Spillantini 2006). Though the prevailing hypothesis is that Aβ accumulation precedes tau hyperphosphorylation and cell death, it is thought that the toxicity of Aβ may actually be mediated through tau (Ittner et al. 2010;Roberson et al. 2011;Roberson et al. 2007). However, the exact mechanism through which Aβ accumulation results in tau hyperphosphorylation remains enigmatic. (Noble et al. 2013). While mutations in tau can cause tauopathies including frontotemporal dementia and progressive supranuclear palsy (PSP), none have been linked to AD (Mandelkow and Mandelkow 2012). Though various tau targeting therapeutic interventions are currently being developed for AD (Wisniewski and Goni 2015), the position of Aβ upstream of tau in the neurodegenerative cascade makes it a prime target for preventative medicines. Interestingly though, one recent study showed tau removal from the brain of a transgenic AD mouse model by passive

immunisation with anti-tau oligomer antibodies could also alleviate Aβ pathology by allowing the removal of oligomeric Aβ (Castillo-Carranza et al. 2015).

1.4 APP metabolites

As previously eluded to, the APP holo-protein has numerous proposed functions within the cell. The role of Aβ in the amyloid cascade hypothesis has focused the attention of the majority of the AD research community on its production and its toxic mechanisms. However, a number of other studies have focused on other proteolytic fragments of APP and identified roles in the neurodegenerative process and intriguingly, also identified neuroprotective properties for some fragments (**Figure 1.6**).

1.4.1 Aβ

The toxic species

Aβ has garnered the most interest of the APP soluble products due to its proposed role as the AD 'neurotoxin'. Clearly the aggregation of the monomeric form of Aβ is the crucial step in the conversion of the relatively benign (or even neuroprotective) Aβ to the AD inducing form. Various factors can contribute to the aggregation propensity of the Aβ molecule, the best characterised of which is the additional two amino acids present at the C-terminal end of the Aβ42 molecule which bestow it with greatly enhanced aggregation propensity (Mucke and Selkoe 2012). However, other modifications including phosphorylation (Kumar et al. 2011), N-terminal truncation (Schilling et al. 2006) and mutations within the Aβ amino acid sequence (Di Fede et al. 2009) have been shown to influence its aggregation. The exact toxic species of aggregated Aβ responsible for neurodegeneration has been widely debated, with the finger of blame being pointed at various aggregated forms of Aβ including dimers (Jin et al. 2011), nanotubular protofibrils (Nicoll et al. 2013) and fibrils (Gotz et al. 2001), though perhaps most convincingly at a soluble oligomeric Aβ species which correlate most significantly with cognitive decline (Tomic et al. 2009). Various oligomeric forms of the peptide have been proposed in the heterogeneous mix found in the AD brain, with varying neurotoxic effects (Larson and Lesne 2012). Indeed, these oligomeric species, which can range from low molecular weight dimers and trimers to higher molecular weight assemblies such as Aβ*56, can show greater correlation with disease severity and progression (Larson and Lesne 2012). Much like in the human condition, mice with amyloid plaques but low levels of oligomeric Aβ show less cognitive deficit than those with high oligomer content within the brain (Lesne et al. 2008).

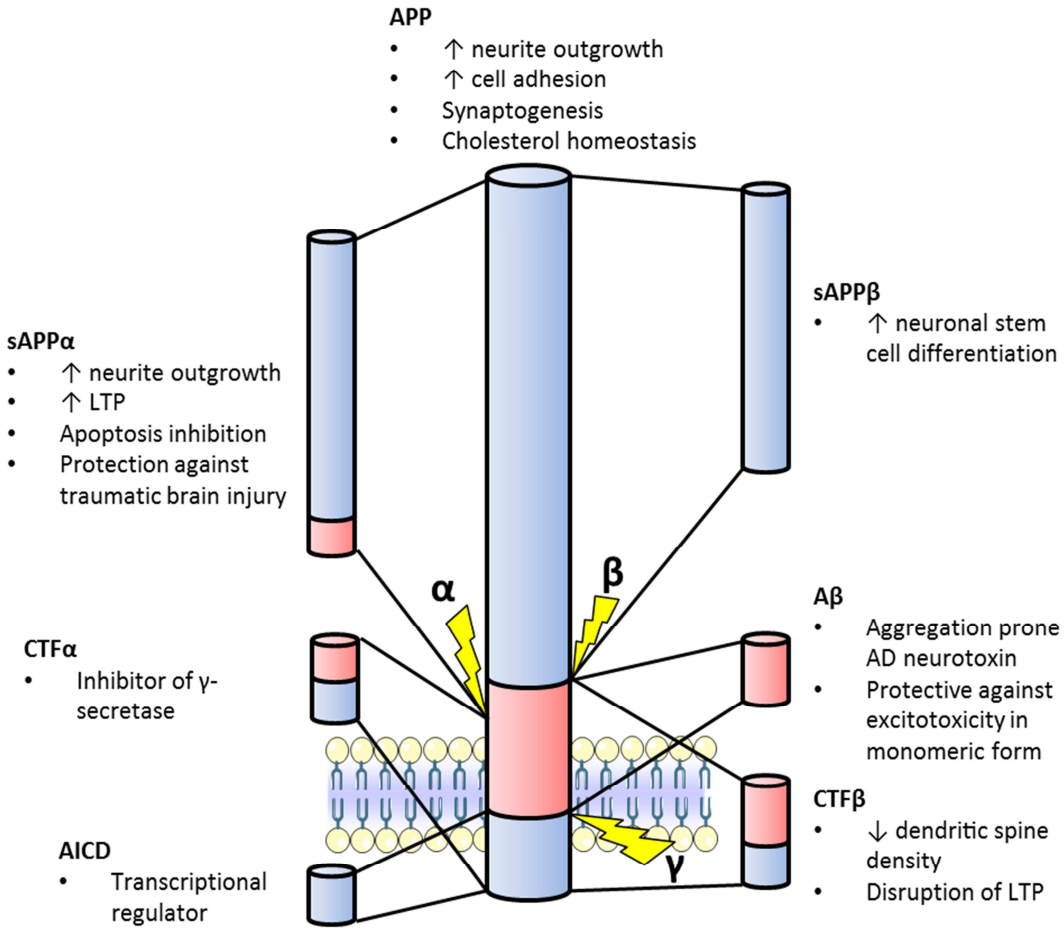

Figure 1.6 APP and fragments produced by its proteolysis have distinct and overlapping functions

Various functional properties have been attributed to APP and fragments produced by its proteolysis by α-secretase (α), β-secretase (β) and γ-secretase (γ). Aβ is perhaps the most studied due to its role in the amyloid cascade hypothesis of AD. However, other fragments have been implicated in a range of neurodegenerative and neuroprotective processes.

Mechanisms of toxicity

The role of Aβ in the 'amyloid cascade hypothesis' has been extensively studied and reviewed, and though an exact mechanism of toxicity is yet to be agreed upon, the increased presence of Aβ has been proposed to result in inflammatory responses, tau hyperphosphorylation, neuronal injury and other downstream effects leading to the massive neuronal death often seen in AD post-mortem brains (Haass and Selkoe 2007). Though different forms of Aβ have been shown to induce cell death in neurons (Deshpande et al. 2006), the period of time over which they accumulate in humans to cause disease means subtler phenotypes are perhaps of more interest. The presence of soluble forms of Aβ has been shown to reduce LTP in brain slices, induce the loss of spines in neurons and in mouse models and associate with synapses in the AD brain (Spires-Jones and Hyman 2014). The mechanism through which Aβ toxicity is transduced is still largely open to debate, and though AD is defined by the deposition of Aβ into extracellular plaques within the brain, extracellular oligomeric forms of Aβ has been shown to interact with various receptor proteins including the low-density lipoprotein receptor related protein 1 (LRP1), NMDA receptors and α-amino-3-hydroxy-5-methyl-4-isoxazolepropionic acid (AMPA) receptors facilitating its uptake (Chasseigneaux and Allinquant 2012). An array of data has implicated the cellular prion protein as a receptor for Aβ oligomers providing evidence of a link from Aβ to tau through activation the src family kinase Fyn which phosphorylates tau (Lauren et al. 2009;Rushworth et al. 2013;Um et al. 2013;Um et al. 2012). Further research into the tau-Aβ interaction has also suggested that Aβ on its own may not induce the deficits in LTP seen in AD, instead suggesting tau hyperphosphorylation is increased by excess Aβ and in turn causes the cognitive deficits (Shipton et al. 2011). Indeed, recent evidence suggests that tau hyperphosphorylation is dependent upon Aβ production, with inhibition of amyloidogenic APP proteolysis attenuating tau pathology in 3D models of human neural cell culture (Choi et al. 2014).

Aβ spreading and seeding

An interesting element of Aβ physiology recently coming to light is its capacity to spread from cell to cell through the brain and potentially act as a seed for further Aβ aggregation (Benilova et al. 2012). The exact mechanisms of Aβ transfer remain enigmatic, though it has been shown to be released in association with exosomes, possibly identifying a route through which cell to cell transfer could occur (Rajendran et al. 2006). Whether exosomal release of Aβ represents a clearance mechanism within the cell, or is an aberrant effect of increased cellular Aβ production remains unclear, but reduced clearance of Aβ may also contribute to its transfer (Domert et al. 2014). The hypothesis for a prion-like seeding property of Aβ comes from experiments showing

that intra-cerebral injection of human or mouse derived Aβ could increase amyloidosis in APP transgenic mice (Jucker and Walker 2013). The suggestion is that, similar to the Creuzfeldt-Jakob disease (CJD) causing prion protein, abnormal conformations of Aβ may act as seed, resulting in the templating and mis-folding of further Aβ molecules, contributing to their accumulation (Jucker and Walker 2015). Recent research has also provided some evidence for this process in humans who died of CJD as a result of receiving prion-contaminated, cadaver-derived human growth hormone (Jaunmuktane et al. 2015). Aβ deposition within the brain parenchyma and vasculature was observed in post-mortem examination of several patients who had died of CJD between 36-51 years of age, before Aβ plaques are usually observed (Jaunmuktane et al. 2015). This led the authors to hypothesize that plaque pathology was due to Aβ seed contamination within the human growth hormone preparations (Jaunmuktane et al. 2015). A previous study had however suggested no link between human growth hormone treatment and the development of AD or Parkinson's disease (Irwin et al. 2013), implying the Aβ deposition observed by Jaunmuktane et al. (2015) would not necessarily have caused AD in these patients.

A neuroprotective role?

Interestingly, monomeric Aβ has been suggested to have some neuroprotective roles, protecting neurons against excitotoxicity (Giuffrida et al. 2009) and oxidative stress (Lee et al. 2005). A role for Aβ in the modulation of vesicle release at presynaptic sites has been identified (Abramov et al. 2009) and is interesting in the context of Aβ release appearing to be activity dependent (Cirrito et al. 2008). However, Aβ has also been shown to reduce synaptic transmission in APP over-expressing neurons (Kamenetz et al. 2003) suggesting the role of Aβ in the synapse may be concentration dependent, and require tight control. Interestingly, carriers of the previously described A673T mutation in APP which reduces Aβ generation show reduced age related cognitive decline suggesting reduced (though perhaps not abolished) Aβ production is not detrimental (Jonsson et al. 2012).

1.4.2 sAPPα

In contrast to Aβ, sAPPα has been proposed to have an array of functions including roles in neuroprotection and neurogenesis (Chasseigneaux and Allinquant 2012). It has been suggested on the basis of this that sAPPα production may therefore represent an essential physiological role for APP (Nhan et al. 2015). In the cellular context, binding of sAPPα to integrins has been shown to indirectly increase neurite outgrowth by acting as a competitive inhibitor, binding to, and preventing integrins interacting with APP which reduces the ability of full length APP to

promote outgrowth (Young-Pearse et al. 2008). Roles in synaptic transmission (Gustafsen et al. 2013), cellular calcium homeostasis and protection against excitotoxic damage (Mattson et al. 1993) and inhibition of pro-apoptotic pathways in response to various stresses (Copanaki et al. 2010) have also been demonstrated for sAPPα. Recent evidence has also implicated the Akt survival pathway in the transduction of the protective effects of sAPPα following trophic factor deprivation (Milosch et al. 2014). *In vivo* sAPPα has been shown to protect against neuronal damage caused by traumatic brain injuries (Corrigan et al. 2012a;Corrigan et al. 2012b), while knock-in of DNA encoding sAPPα into the APP locus in a mouse model rescues the deficits previously observed in APP knockout mice (Ring et al. 2007). Blocking sAPPα with specific antibodies injected into the hippocampus of rats has been shown to block LTP, while direct infusion of exogenous sAPPα into the hippocampus showed the opposite affect (Taylor et al. 2008). The infusion of sAPPα into wild-type mice has also been shown to increase presynaptic boutons, suggesting a mechanism through which LTP could be enhanced (Bell et al. 2008). Importantly, sAPPα levels have been shown to be reduced in the CSF of AD patients (Nhan et al. 2015), perhaps as a result of the loss of ADAM10 activity previously described (see **Section 1.3.3**). Identifying a receptor(s) for sAPPα remains a main missing link between the extracellular secretion and reported activity of the fragment, though its downstream effects have been shown separately to be reliant on APP and SORLA expression (Hartl et al. 2013;Milosch et al. 2014).

1.4.3 sAPPβ

Relatively few functional roles have been ascribed to sAPPβ despite being only 16 amino acids shorter than sAPPα. Indeed, sAPPβ was shown to be 100 fold less effective at protecting mouse hippocampal neurons from excitotoxic stress than sAPPα (Furukawa et al. 1996). However, It was recently shown to increase neural differentiation in human embryonic stem cells to a greater extent than sAPPα (Freude et al. 2011). In a separate knock in study to that described for sAPPα, Li et al. (2010) demonstrated sAPPβ knock-in at the mouse APP locus allowed morphologically normal brain development, but the knock-in was unable to rescue lethality seen in $APP^{-/-}APLP2^{-/-}$ double knockout mice. The authors also suggested that sAPPβ may have a role in the regulation of the anti-ageing protein Klotho and transthyretin, though observations were based on liver expression in day 0 post-natal $APP^{-/-}/APLP2^{-/-}$ knockouts compared to $sAPP\beta^{+/-}/APLP2^{-/-}$ mice (Li et al. 2010) and further corroboration of this result has not been published.

1.4.4 AICD

AICD has been shown to act as a transcriptional regulator of various genes (Beckett et al. 2012), showing similarity to the proteolytic fragment produced by γ-secretase cleavage of the Notch protein (Edbauer et al. 2002). AICD in the cytoplasm is thought to be rapidly degraded by IDE, while translocation of AICD to the nucleus requires stabilisation through the binding of Fe65, a nuclear adapter protein, and binding of the histone acetyltransferase Tip60 within the nucleus to induce gene expression (Cao and Sudhof 2001;Goodger et al. 2009;Edbauer et al. 2002). More recently an interaction between AICD and MED12, an important component of the eukaryotic transcriptional mediator complex, was reported (Nalivaeva and Turner 2013). AICD has been implicated in the transcription regulation of various genes encoding proteins with implications in AD including NEP, LRP1, BACE1, glycogen synthase kinase 3 β (GSK3β) and APP itself (Beckett et al. 2012). AICD has been shown to occupy the promoter region of the *NEP* (*MME*) gene, leading to 6-fold increase in NEP mRNA levels (Belyaev et al. 2010). Not only was this effect APP isoform specific as previously described, but appeared to be dependent on amyloidogenic APP proteolysis (Belyaev et al. 2010). The mechanism through which AICD produced from APP695 is protected from degradation remains unknown, though stabilisation through Fe65 binding, and sequestration into cytoplasmic vesicles have both been hypothesised (Edbauer et al. 2002;Belyaev et al. 2010). The relatively distal nature of the production of AICD from α- and γ-secretase proteolysis may increase the likelihood of degradation before reaching the nucleus, when compared to AICD produced by β- and γ-secretase in the endocytic pathways (Rajendran and Annaert 2012). It has also been suggested that the phosphorylation state of two residues, T743 and Y756, within AICD could abolish interactions with certain proteins such as Fe65 or encourage the interaction of others (Aydin et al. 2012). Links between AICD and Alzheimer's like pathology in mice have also been made though, much like the role of AICD in transcriptional activation, these have courted controversy and it remains unclear as to whether this proteolytic fragment is pathological or not (Ghosal et al. 2009;Giliberto et al. 2010).

1.4.5 p3

Probably the least studied of all APP fragments, p3 is produced following sequential α-secretase and γ-secretase cleavage, and is essentially an N-terminally truncated Aβ peptide. In vitro oligomerisation protocols often applied to recombinant Aβ42 peptide were unable to induce p3 oligomerisation, leading to the suggestion that the N-terminal residues may play an important role in shielding the hydrophobic core of the Aβ molecule from water, and their removal results in destabilisation of the molecule (Dulin et al. 2008). On the other hand, p3 was identified in diffuse amyloid deposits within the brains of AD patients (Gowing et al. 1994), and given that it

should be abundantly produced in the brain following APP and CTFα proteolysis, its relevance to disease is perhaps under-explored.

1.4.6 CTFs

The CTFs of APP left following the primary α- or β-cleavage event have both been suggested to have negative effects on dendritic spine density as well as potential roles in synaptotoxicity (Bittner et al. 2009). CTFβ has also been shown be the earliest accumulating APP metabolite in the hippocampus in the brains of the triple transgenic AD mouse and the primary contributor to early lesions seen in the brain (Lauritzen et al. 2012). Concurrent with this, β-secretase inhibition, but not γ-secretase inhibition was able to rescue LTP deficits in a mouse model with enhanced β-secretase APP proteolysis due to *BRI2* knockdown, suggesting CTFβ may also disrupt LTP (Tamayev et al. 2012). Dosing Tg2576 mice with γ-secretase inhibitors (GSI) was shown to increase CTFβ accumulation in the hippocampus, and despite reducing Aβ and not appearing to alter processing of other γ-secretase substrates, did not improve memory and learning in the mice (Mitani et al. 2012). In fact, doses of one GSI were actually shown to significantly reduce cognitive function in wild-type mice over just 8 days of dosing (Mitani et al. 2012). CTFα has been shown to act as an inhibitor of γ-secretase through the action of an inhibitory domain in residues 17-21 of the Aβ region (Tian et al. 2010) though other roles for this fragment have not been explored.

1.5 Targeting Aβ therapeutically

1.5.1 BACE1 inhibitors

Since its discovery as the rate limiting protease in the generation of Aβ, BACE1 has remained a major target for pharmacological intervention in AD (Cole and Vassar 2007). Following the discovery of BACE1, first generation peptidic BACE1 inhibitors showed potent *in vitro* efficacy which often failed to translate into the *in vivo* scenario, where poor blood brain barrier penetrance and bioavailability were among the issues identified (Rajendran and Annaert 2012;Vassar 2014). The large active site of BACE1 has made the design of small molecule inhibitors difficult, while the endosomal site of BACE1 activity requires relatively specific delivery and lipophilicity of inhibitors (De Strooper et al. 2010;Vassar 2014). Innovative strategies for BACE1 inhibition including attachment of a cholesterol moiety to a transition state BACE1 inhibitor to improve its membrane targeting (Rajendran et al. 2008), use of inhibitory antibodies targeting the BACE1 cleavage site in APP (Boddapati et al. 2011) or BACE1 itself (Atwal et al. 2011), coupling a BACE1 inhibitory antibody to a transferrin receptor antibody to enhance

cellular uptake (Yu et al. 2011) and use of peptide inhibitors containing the APP_{SWE} sequence (Li et al. 2015) have all been proposed as mechanisms for inhibiting BACE1. The design of potent BACE1 inhibitors was aided by the resolution of the crystal structure of BACE1 bound to a peptidic inhibitor and a range of BACE1 inhibitors are currently in clinical trials (Vassar 2014). Though Elli Lilly recently withdrew a Phase II clinical trial of their BACE1 inhibitor due to liver toxicities, Merck have shown their BACE1 inhibitor, MK-8931, to be safe, tolerable and to significantly reduced CSF levels of Aβ, resulting in a current combined Phase II and III trial of the drug (Vassar 2014). Eisai have also shown good safety and tolerability of their BACE1 inhibitor coupled with Aβ reductions in the CSF and have recently entered a Phase II trial for mild AD patients (Vassar 2014). BACE1 inhibitors currently in clinical trials should therefore provide a definitive answer on whether BACE1 is a viable target for AD therapy. However, targeting BACE1 has two major problems. Specifically targeting APP proteolysis without affecting BACE1 proteolysis of other substrates may prove difficult and confound the potential success of these molecules and, furthermore, it is likely that BACE1 inhibition will only be effective in the early stages of AD, before significant cell death and related downstream toxicities have occurred (Vassar 2014).

1.5.2 γ-secretase inhibitors and modulators

Unlike BACE1, targeting γ-secretase with inhibitors which show high bioavailability and blood brain barrier penetrance has not been a significant issue (Golde et al. 2013). However, the same issues that undermine the targeting of BACE1, namely the stage at which it would be effective and specific substrate targeting also apply to GSIs. As discussed previously, the γ-secretase complex provides an extremely challenging target for therapeutic intervention due to wide-ranging biological roles, numerous substrates and inherent complexity (De Strooper 2014). Indeed, recent clinical trial data from the GSI Semagacestat showed cognitive worsening in the drug treated cohort compared to the placebo treated group, alongside an array of undesirable side effects including increased incidence of skin cancer (Doody et al. 2013). Rather than total inhibition, modulation of the activity of γ-secretase has been proposed as a potential mechanism through which Aβ42 generation could specifically be reduced (Crump et al. 2013). Various non-steroidal anti-inflammatory drugs have been identified as γ-secretase modulators (GSMs) and are proposed to enhance continued Aβ proteolysis following ε-cleavage to produce Aβ species with shorter C-termini (Golde et al. 2013). Only one GSM has made it through the clinic to publication but failed to slow cognitive decline in a cohort of patients with mild AD (Green et al. 2009), while Eisai Inc. also entered a clinical trial with a proposed GSM, but are yet

to publish results (Crump et al. 2013). Though GSM development may have continued, novel compounds have been slow to make it to the clinic.

1.5.3 α-secretase enhancers

Due to the postulated neuroprotective roles of sAPPα, and the fact that its production precludes the formation of Aβ, enhancing α-secretase activity has been proposed as a therapeutic target in AD (De Strooper et al. 2010). Indeed, AD mouse models that over-express ADAM10 show reduced Aβ deposition suggesting a reciprocal relationship between α- and β-secretase activity *in vivo* (Lichtenthaler 2011). Furthermore, sAPPα has been shown to act as an inhibitor of BACE1 (Obregon et al. 2012), and cleavage of the cellular prion protein (a proposed Aβ oligomer receptor) by ADAM10 results in reduced Aβ binding to neuroblastoma cells (Griffiths and Hooper, unpublished). While specific activators of α-secretase may be difficult to produce, α-nicotinic acetylcholine receptor agonists have been shown to indirectly activate α-secretase, and have been taken as far as phase II clinical trials for AD (De Strooper et al. 2010). Recently, upregulation of ADAM10 transcription has been targeted using acitretin which increases ADAM10 expression by increasing the availability of retinoic acid receptors, which in turn bind regulatory elements on the ADAM10 gene (Endres and Fahrenholz 2010). A recent clinical trial of acitretin showed good safety and tolerability, coupled with increased sAPPα in the CSF of patients with AD (Endres et al. 2014). However, like γ- and β-secretase, α-secretase has a large number of cellular substrates and it has been reported that increases in its activity can induce metastasis in tumours, complicating its potential application (Rajendran and Annaert 2012).

1.5.4 Promoting Aβ clearance

The proposal that AD stems from the accumulation and reduced clearance of Aβ within the brain has led to therapies targeting Aβ clearance as a potential therapeutic avenue for AD. Many of these Aβ clearing therapeutics had strong pre-clinical support suggesting the capacity to remove Aβ from the brain, and cause associated improvements in cognitive deficits (Wisniewski and Goni 2015). Despite this, definitive improvements in cognition in patients treated with these drugs have not been observed. One caveat for these forms of treatment is that, given that Aβ accumulation may occur long before symptomatic presentation with AD, patients may need treatment in very early stages of disease to observe any benefit.

Active immunotherapy

In active immunotherapy, patients were immunised with Aβ peptide in the hope that the immune system would naturally produce Aβ antibodies, resulting in clearance of Aβ from the

brain. In mouse models, Aβ active immunisation appeared successful, ameliorating plaque deposition and preventing astrocytosis (Schenk et al. 1999). However, in the case of the clinical trial of Elan's AN1792 vaccine, the trial was abandoned due to incidence of meningoencephalitis and amyloid related imaging abnormalities (ARIA) (Wisniewski and Goni 2015). Follow up analysis showed that, despite evidence of plaque clearance in patients, there was no slowing of cognitive decline, nor increases in longevity (Holmes et al. 2008). Several active immunisation clinical trials are still ongoing, with the new generation of vaccines designed to more specifically target the supposed toxic forms of Aβ, though none have yet reported results (for a summary see (Wisniewski and Goni 2015)).

Passive immunotherapy

Passive immune therapy seeks to remove Aβ from the brain through dosing patients with antibodies raised against Aβ to improve their removal by microglia, or prevent further aggregation into toxic species (Wisniewski and Goni 2015). Similar to active immunotherapy trials, passive immunotherapy has been shown to induce ARIA in some cases, particularly in patients who are carriers of the APOE4 allele (Salloway et al. 2009). Results from anti-amyloid passive immunotherapy trials have been mixed, in some cases showing negative outcomes and in others, some mild benefits have been observed. Janssen and Pfizer's joint venture anti-Aβ antibody Bapineuzumab, was unable to improve cognition in AD patients, despite significant amyloid clearance as determined by PiB PET (Liu et al. 2015b). Though this led to abandonment of Bapineuzumab, a second generation humanised version of the antibody has entered phase I clinical trials for safety and tolerability (Wisniewski and Goni 2015), though the results have not yet been reported. Elli Lilly's humanised anti-Aβ antibody Solanezumab, which is proposed to target soluble rather than plaque Aβ (Karran and Hardy 2014a), significantly raised Aβ40 and Aβ42 in plasma and CSF samples but failed to improve cognition across the cohort of AD patients in clinical trials (Doody et al. 2014). However, a recent re-analysis of the data suggested some benefit to cognition in the mildest AD patients leading to an initiation of a new clinical trial assessing the drug's efficacy in mild AD patients (Siemers et al. 2015). Due to the seemingly positive data in the mild AD cohort in the Solanezumab trial, it is now entering clinical trials aiming to prevent AD in those with inherited forms alongside Gantenerumab, an Aβ antibody which recognises fibrillar forms of Aβ (Wisniewski and Goni 2015). Results have also been mixed for Biogen's human antibody Aducanumab which, despite initial promising results, could not significantly slow cognitive decline despite amyloid clearance and caused ARIA and microhaemorrhaging in some cases (Underwood 2015). However, the full details of this trial remain to be published.

Aβ degrading enzymes

Enhancing the activity of Aβ degrading enzymes such as NEP or IDE have also been suggested as mechanisms through which AD could be treated without secretase inhibition (Nalivaeva et al. 2014). Indeed, the aggregation of Aβ is thought to be concentration dependent (De Strooper et al. 2010), suggesting that the removal of Aβ may aid in preventing further aggregation. However, the Aβ degrading enzymes which have been identified are not specific to Aβ, and thus their regulation brings with it many of the difficulties also associated with secretase inhibition (Nalivaeva et al. 2015). Over-expression of IDE or NEP in APP transgenic mice reduced monomeric Aβ levels and plaque pathology (Leissring et al. 2003) while increased NEP activity associated with expression or treatment with the neuropeptide somatostatin has been shown to increase Aβ clearance *in vivo* (Saito et al. 2005). Although IDE activators have been identified *in vitro* (Cabrol et al. 2009), activators of Aβ degrading enzymes have not as yet made it to the clinic, and their relatively slow development and non-specific modes of action may make Aβ removal through passive immunotherapy more attractive.

1.5.5 Preventing Aβ aggregation

Aβ aggregation is a key process in its capacity to induce the cascade of events that lead to AD. However, confusion surrounds the exact molecular identity of the 'toxic' Aβ species, stemming from inconsistencies in the source, preparation and characterisation of Aβ for experimental procedures (Benilova et al. 2012;Masters and Selkoe 2012) and potentially makes targeting the prevention of Aβ aggregation difficult. Rather than preventing the initial aggregation of Aβ monomer, anti-aggregation drugs may accelerate the transition of the proposed toxic oligomeric formations of Aβ to the less soluble conformations (Doig and Derreumaux 2015), which may have reduced cellular toxicity. The polyphenolic compound epigallocatechin-3-gallate (EGCG) is perhaps the best studied anti-aggregation molecule, and is proposed as a potential therapy for various diseases which are thought to be caused by amyloids (Eisele et al. 2015). EGCG has been shown to remodel synthetic Aβ oligomer conformation, altering its toxicity (Rushworth et al. 2013;Bieschke et al. 2010) and has been shown to ameliorate memory deficits in APP transgenic mice (Rezai-Zadeh et al. 2008). On this basis EGCG has entered clinical trials for AD (Doig and Derreumaux 2015).

1.6 The APP interactome

1.6.1 Studies of the APP interactome

Protein-protein interactions represent a mechanism through which APP processing and trafficking may be regulated and can provide insight into the molecular functions of a protein by

association. The APP interactome has been of interest both in terms of trying to ascertain its cellular function (Perreau et al. 2010), but also for the purpose of identifying proteins which may modulate its proteolysis (Rice et al. 2013). Given the previously discussed difficulties encountered for BACE1 and γ-secretase inhibitors with the large number of substrates in addition to APP for these proteases, the capacity of the APP interactome to modulate Aβ generation provides a novel avenue through which the production of Aβ could be targeted. Perreau et al. (2010) recently compiled a comprehensive list of APP interactors, where possible showing the exact domain and isoform of APP involved in the interaction. Through this work they identified interaction networks implicating APP in neuronal outgrowth and migration through interactions with extracellular and membrane bound proteins, and interaction with a large number of proteins known to be involved in protein trafficking (Perreau et al. 2010). A wide range of approaches have been taken to identify APP interacting proteins *in vitro*, *ex vivo* and *in vivo*.

In vitro, yeast two-hybrid studies of the APP interactome have been used to identify several proteins which interact with the intracellular domain of APP, including perhaps the best established APP interactor Fe65 (McLoughlin and Miller 1996). The yeast two-hybrid technique was also employed by Matsuda et al. (2005) to determine interactors of the holo-APP protein. The study, using a split-ubiquitin version of the yeast two-hybrid approach, identified several proteins which were later shown to influence the proteolysis of APP (Matsuda et al. 2005) (see **Section 1.5.2**). One *ex vivo* AICD interactome study used a system where AICD was recruited to proteo-liposomes and used as a bait to identify AICD interactors from mouse brain cytosol (Balklava et al. 2015). Through this study, the authors identified an interaction between AICD and components of the PIKfyve complex leading to its activation (Balklava et al. 2015). The activated PIKfyve complex can subsequently phosphorylate phospholipid phosphatidylinositol-3-phosphate (PI(3)P) which, in its phosphorylated form, can control TGN-endosome recycling and endosome morphology, leading the authors to suggest an essential role for AICD in endosomal trafficking (Balklava et al. 2015). In another *ex vivo* interactome study Gautam et al. (2015) used various glutathione-S-transferase-tagged APP ectodomain constructs to isolate interacting proteins from the soluble fraction of mouse brains. They identified novel interactions between the APP ectodomain and three members of the synaptotagmin (Syt) family of proteins, two of which were subsequently shown to influence APP proteolysis (see **Section 1.5.2**) (Gautam et al. 2015). Recently, the first study of the APP interactome in a cell culture context was reported using the commonly used, non-neuronal human embryonic kidney (HEK) cell line, where tagged-APP was immunoprecipitated from stable isotope labelled amino acids in cell culture (SILAC) labelled cells and interactors were identified by liquid chromatography-tandem mass

spectrometry (LC-MS/MS) (Hosp et al. 2015). This study identified interactions for wild-type and Swedish mutant APP (and other neurodegeneration linked proteins), focusing on the interaction between APP and the mitochondrial Leucine-rich PPR motif-containing protein (LRPPRC) (Hosp et al. 2015). The authors suggested this interaction (which was higher for the Swedish mutant APP) could lead to mitochondrial dysfunction as LRPPRC has a key role in mitochondrial gene regulation (Hosp et al. 2015). An interactome study for APP in a neuronal cell line has yet to be reported, and on the basis of previous *in vitro* data could provide valuable insight into APP function and the regulation of its proteolysis in this cell type.

Various studies have investigated the *in vivo* interactome of APP. One such study investigated the *in vivo* APP interactome in wild-type mice, comparing the interactome with that of APLP1 and APLP2 (Bai et al. 2008). This study identified 34 APP interactors, of which one, leucine-rich repeat and immunoglobulin-like domain-containing protein 1 (LINGO-1), was subsequently shown to influence Aβ generation in a HEK cell model (Bai et al. 2008). However, the reported effect of LINGO-1 on APP proteolysis was later contested by Rice et al. (2013) (see **Table 1.2**). In a similar *in vivo* mouse study, Kohli et al. (2012) generated a human APP mouse model with a tandem affinity purification tag inserted into the gene in the AICD region. This study identified various proteins involved in synaptic vesicle trafficking and members of the 14-3-3 family enriched in the APP interactome, leading the authors to propose an important role in synaptic signalling for APP (Kohli et al. 2012). A human *in vivo* APP interactome study was performed by Cottrell et al. (2005) and identified 21 proteins which interacted with human APP in AD and control brains. Though this study compared AD and control brains, no specific interactions were identified for APP in either group (Cottrell et al. 2005).

Individual studies have further identified interactions between APP and NMDA receptors via the NR1/GluN1 subunit (Cousins et al. 2009) and Nav1.6, a protein with important roles in sodium channel formation (Liu et al. 2015a), with both studies indicating APP increased cell surface expression of the proposed interactor suggesting an important role for APP in regulation of the transit of proteins to the cell surface. Many proteins which interact with the cytoplasmic tail of APP have been shown to alter its trafficking, including Mint3 which has a role in APP export for the Golgi (Caster and Kahn 2013).

1.6.2 APP interactors can alter its proteolysis

Many proteins have been shown to alter APP proteolysis through direct interaction with APP. The mechanism by which they modulate APP proteolysis may be through acting as a physical blockade (e.g. BRI2), preventing the access of the proteases to APP (Matsuda et al. 2008), or by

altering APP trafficking (e.g. sortilin related receptor (SORLA) and thus either enhancing or reducing the likelihood of APP encountering the secretases (Andersen et al. 2005). Perhaps the best studied APP interacting protein is Fe65 which is known to interact with the cytoplasmic tail of APP (via the YENPTY motif) and influence APP internalisation. Despite its intensive study, the effect of Fe65 on APP proteolysis has remained controversial (see (McLoughlin and Miller 2008)). In a similar manner, proteins from the mint family have been shown to interact with the APP YENTPY motif, with conflicting results reported on the effect on APP proteolysis (Ho et al. 2008). A list of other proteins previously identified to alter cellular APP proteolysis by direct binding to the protein can be found in **Table 1.2**. The capacity of the APP interactome to modulate APP proteolysis is of particular interest given that the proteins could offer a mechanism through which Aβ accumulation could be reduced. The specific interactomes of the APP isoforms are also of particular interest given the previously reported difference in their proteolysis (Belyaev et al. 2010). Perreau et al. (2010) highlighted several interactions which appeared to be specific to the KPI domain-containing APP isoforms, including the proposed interactions with LRP1, spondin-1, and two proteins from the kallikrein family. Interestingly LRP1, LRP1B and spondin-1 have previously been linked to alterations in APP proteolysis (see **Table 1.2**). Kallikrein-related peptidase 6, has been linked to AD in a GWAS study, where the gene was duplicated in an early onset case (Rovelet-Lecrux et al. 2012) and it has been suggested the protease can actually cleave APP to produce Aβ-like fragments (Little et al. 1997). These observations make the study of the interactomes of the APP isoforms interesting to determine the cause of differences in their proteolysis.

1.7 Aims

In this introduction, the importance of trafficking, interactions and mutations have been discussed in terms of their influence on APP proteolysis. These influences have been of particular interest to our lab due to our identification of differences in the proteolysis of APP isoforms when expressed in the same cellular system (Belyaev et al. 2010). While much higher levels of Aβ and sAPPβ, indicative of increased amyloidogenic proteolysis, were observed in the APP695 isoform compared to the KPI domain-containing APP isoforms (Belyaev et al. 2010), the cause of this difference has remained enigmatic. As reducing Aβ levels in the brain remains a major target for AD therapy, understanding the cause of this large difference in Aβ generation from the APP isoforms could highlight novel pathways for intervention in AD. In light of this the main aims of this thesis were to:

Protein	Interaction details	Effect on proteolysis	Reference
AP-4 complex	• Identified by yeast 2-hybrid • μ4 subunit Interacts with the YKFFE motif in APP cytoplasmic tail • Induces export of APP from the TGN	siRNA knockdown of AP-4 caused ↑Aβ, ↓CTFs	(Burgos et al. 2010)
BRI2	• Identified on the basis a yeast 2-hybrid screen • Masks the recognition site for α-secretase and BACE1	siRNA knockdown of BRI2 caused ↑sAPPβ, ↑Aβ40/↑Aβ42	(Matsuda et al. 2008)
BRI3	• Identified on the basis a yeast 2-hybrid screen • Specifically interacts with full length APP but not CTFs	siRNA knockdown of BRI3 caused ↑sAPPβ, ↑Aβ40/↑Aβ42 Overexpression of BRI3 caused ↓sAPPα/β, ↓Aβ40 /Aβ42	(Matsuda et al. 2009a)
CD74	• Identified on the basis a yeast 2-hybrid screen • Binds APP ectodomain	Over-expression of CD74 ↓Aβ40/Aβ42	(Matsuda et al. 2009b)
Dab2	• Binds the NPxY motif in the cytoplasmic tail of APP • Identified due to ability to bind a similar motif in LDLR • Mediates endocytosis of APP to endosomes	Dominant negative mutant ↓Aβ40/Aβ42 Over-expression caused ↑Aβ40/Aβ42	(Lee et al. 2008)
GRP78	• GRP78 binds APP and slows its maturation	Over-expression of GRP78 caused ↓Aβ40/↓Aβ42	(Yang et al. 1998)
LRP-1	• Identified due to similar ability to bind KPI domain containing tissue factor pathway inhibitor • Induces endocytosis of APP	LRP1 expression ↑Aβ, ↓sAPPα LRP1 antagonist RAP ↓Aβ	(Kounnas et al. 1995;Ulery et al. 2000)
LRP1B	• Investigated due to similarities to LRP1 • Binds full length APP • Increases cell surface levels of APP	Over-expression caused ↑sAPPα, ↓Aβ40/↓Aβ42, ↓CTFβ	(Cam et al. 2004)

Table 1.2 APP interactors which affect proteolysis

Table continued overleaf.

Protein	Interaction details	Effect on proteolysis	Reference
LRP10	• Investigated due to homology to LDLR family members • Interacts with the ectodomain of APP causing retention within the Golgi	Overexpression of LRP10 caused ↓Aβ40, ↓sAPPα/β	(Brodeur et al. 2012)
Lingo-1	• Extracellular ligand for APP identified through a brain interactome study	Bai et al. showed siRNA knockdown caused ↑ CTFα and ↓CTFβ Rice et al. showed over-expression caused ↓ sAPPα and ↓ sAPPβ	(Bai et al. 2008;Rice et al. 2013)
Nogo receptors (NgR)	• Investigated due to localisation to amyloid plaques in AD brains • Interacts with APP ectodomain in human brain and cells	Park et al. showed over-expression of NgR1 ↓Aβ Zhou et al. showed NgR2 and NgR3 ↑Aβ40/Aβ42	(Park et al. 2006;Zhou et al. 2011)
Pin1	• Identified due to capacity of Pin1 to bind pThr-Pro motifs • Binds APP and alters the cis/trans isomerisation of the P743/T744 bond	Akiyami et al. showed Pin1 overexpression ↑Aβ Pasterino et al. showed siRNA knockdown of Pin1 ↓sAPPα, ↑sAPPβ	(Akiyama et al. 2005;Pastorino et al. 2006)
Reelin	• Extracellular ligands for APP identified by brain interactome study	Rice et al. showed over-expression caused ↓sAPPα , ↓ sAPPβ, ↓CTFs and ↓Aβ40/Aβ42	(Rice et al. 2013)
SNX17	• Binds the NPxY motif in the cytoplasmic tail of APP • Identified due to ability to bind a similar motif in LRP1 • Proposed to increase APP recycling to cell surface	Dominant negative mutant and siRNA knockdown ↑Aβ40/Aβ42	(Lee et al. 2008)
SORCS1	• Investigated due to homology to SORLA • Binds full length APP • Genetic link to AD	Over-expression caused ↓Aβ40/Aβ42 siRNA knockdown caused ↑Aβ40	(Reitz et al. 2011)

Table 1.2 cont. APP interactors which affect proteolysis

Table continued overleaf.

Protein	Interaction details	Effect on proteolysis	Reference
SORLA	• Investigated due to reduced expression in AD brain • Binds to the GFLD and carbohydrate domains of APP • Causes retrograde transport of APP to the TGN	Over-expression of SORLA caused ↓Aβ and ↓sAPPβ	(Andersen et al. 2005;Andersen et al. 2006)
Spondin-1	• Identified through a brain interactome study • Binds extracellular domain of APP	Ho et al. showed over-expression caused ↓CTFs Rice et al. showed over-expression had no effect	(Ho and Sudhof 2004;Rice et al. 2013)
Syt-1 and Syt-9	• Identified in an *ex vivo* APP ectodomain interactome study. • Interacts with the APP ectodomain between the E1 and KPI domains	Syt-1 and Syt-9 over-expression caused ↑ sAPPβ and ↑Aβ40/Aβ42 Syt-1 knockdown caused ↓ sAPPβ and ↓Aβ40/Aβ42	(Gautam et al. 2015)

Table 1.2 cont. APP interactors which affect proteolysis

1. Identify differences in the subcellular location and trafficking of the APP isoforms which could contribute to the differences in proteolysis that have been reported previously.
2. Identify the interactomes of the APP isoforms in a cellular context and determine whether preferential interaction of particular proteins with the different APP isoforms can influence their proteolysis.
3. Determine the effect of recently discovered APP mutations at the A673 residue on the proteolysis of the APP isoforms, and their influence on the proteolysis of APP by different candidate β-secretases.

In **Chapter 3** FLAG-tagged forms of the APP isoforms APP695 and APP751 have been used to investigate their subcellular distribution by immunofluorescence microscopy. Several trafficking pathways which are reportedly involved in Aβ generation have also been investigated to determine their effect on the proteolysis of the APP isoforms. These include endocytosis, distribution to lipid rafts and the recycling endosome system. The effect of differences in the proteolysis of the APP isoforms on protein degradation, and the production of alternative proteolytic APP fragments have also been investigated.

In **Chapter 4** FLAG-tag labelled APP isoforms have been used to perform an interactomic study using stable isotope labelling of amino acids in cell culture, coupled to liquid chromatography-tandem mass spectrometry, to identify differences in the interactomes of the APP isoforms. The implication of these interactions for differences in APP isoform function has been investigated as well as the effect of several of the interactors on proteolysis of the different isoforms.

In **Chapter 5** the recently reported APP mutations at the residue A673 within the Aβ sequence have been investigated to determine their effect on APP proteolysis of the two APP study isoforms. Subsequently, the effect of these mutations on proteolysis by two postulated APP β-secretases, BACE1 and cathepsin B have been determined.

Chapter 2. Materials and methods

2.1 Materials

2.1.1 Molecular biology reagents

Human APP695, APP751 and APP770 cDNA in the pIREShyg vector and empty pIREShyg vector (Clontech; Mountain View, CA, USA) were provided by the Hooper Laboratory (University of Manchester, UK). The empty enhanced green fluorescent protein (EGFP) vector pEGFP-N1 (Clontech) and pCI-neo vector (Promega, Madison, WI, USA) were a kind gift from Professor Chris Miller (King's College London, UK). Human APP695 cDNA in the vector pEGFP-N1, human APP695 cDNA with a C-terminal mCherry tag in the vector pCI-neo were also a kind gift from Professor Chris Miller. All mutagenic and PCR primers were obtained from Sigma-Aldrich (St. Louis, MO, USA). Sequencing primers were obtained from Integrated DNA technologies (Coralville, IA, USA). Quikchange II Site-Direct Mutagenesis Kit and XL-1 blue competent *Escherichia coli* cells were purchased from Stratagene (Cambridge, UK). The HiSpeed Plasmid Maxi Kit, QIAprep Spin Miniprep Kit and QIAquick Gel Extraction Kit were purchased from Qiagen (Venlo, Netherlands). All restriction enzymes, the DNA ladder and the Quick Ligation Kit were purchased from New England Biolabs (Hitchin, UK). The KOD XL DNA Polymerase Kit was purchased from Merck Millipore (Darmstadt, Germany) and the Pfx DNA Polymerase Kit was from Life Technologies (Paisley, UK).

2.1.2 Cell culture reagents

The human SH-SY5Y neuroblastoma cell line was provided by the Hooper laboratory (University of Manchester, UK). Dulbecco's modified Eagle's medium (DMEM), Opti-MEM, phosphate buffered saline containing Ca^{2+} and Mg^{2+} ions ($PBSM^{+}$) and phosphate buffered saline with no metals ($PBSM^{-}$) were purchased from Lonza (Basel, Switzerland). Hygromycin B and foetal bovine serum (FBS) were purchased from Thermo Fisher Scientific (Paisley, UK). Isotope labelled DMEM and dialysed FBS (10 kDa molecular weight cut-off) were purchased from Dundee Cell Products (Dundee, UK). All on-target and non-targeting siRNAs and the DharmaFECT 1 transfection reagent were purchased from Dharmacon, Inc. (Lafayette, CO, USA). The TransIT-LT1 transfection reagent was purchased from Mirus Bio (Madison, WI, USA). The β-secretase inhibitor (βIV) and the cathepsin B inhibitor (Ca074Me) were purchased from Merck Millipore. Cycloheximide, Dynasore and dimethyl sulfoxide (DMSO) were purchased from Sigma-Aldrich.

2.1.3 Antibodies, ELISAs and Meso Scale Discovery assays

A list of the sources of all primary antibodies and horseradish peroxidase (HRP) and fluorescent conjugated secondary antibodies used in immunoblot, immunoprecipitation and immunofluorescence microscopy experiments can be found in **Table 2.1**. The dilutions at which they were used for each experimental technique can be found within their respective methods section. The pyroglutamate Aβ(N3pE40) assay was purchased from Cambridge Bioscience (Cambridge, UK). Meso Scale Discovery (MSD) sAPP and Aβ multiplexing assays were purchased from MSD (Rockville, MD, USA).

2.1.4 General laboratory reagents

Protein A Dynabeads, Protein G Dynabeads and sulfo-NHS-SS-Biotin EZ-Link were purchased from Thermo Fisher Scientific. Protein A sepharose and Protein G sepharose and anti-FLAG affinity gel were purchased from Sigma-Aldrich. EDTA-free protease inhibitor cocktail was purchased from Roche Diagnostics (Burgess Hill, UK). All general laboratory reagents and chemicals were purchase from standard scientific suppliers including Sigma-Aldrich and Thermo Fisher Scientific among others. In the case of chemicals, all purchases were of analytical grade and high purity.

2.2 Methods

2.2.1 Cloning of APP695-FLAG

APP695 cDNA in the vector pIREShyg was subjected to polymerase chain reaction (PCR) using the forward primer 5' – CATCGCATGCATATGCTGCCCGGTTTGGCACTG – 3' and reverse primer 5' – CATGCGGCGGCCGCCTACTTATCGTCGTCATCCTTGTAATCGTTCTGCATCTGCTCAAAGAACTTGTAGG – 3' (red – spacer, blue - NsiI restriction site, green - NotI restriction site, purple – stop, orange – FLAG sequence, black – APP specific). A standard PCR master mix for 4 reactions using the Pfx DNA Polymerase kit was prepared according to the manufacturer's instructions and aliquoted into 4 separate thin walled PCR tubes. The reactions were then subjected to two-step PCR thermal cycling according to the manufacturer's instructions. Following thermal cycling, the reactions were electrophoresed on a 1% agarose gel (TAE buffer (40 mM Tris, 20 mM acetic acid, 1 mM EDTA), 1% (w/v) agarose, 0.01% (v/v) ethidium bromide, pH 8.0) in TAE buffer for 70 min at 100 V with a 1 kB DNA ladder. Bands of the length corresponding to the desired APP695 cDNA PCR product (~2.1 kB) were excised from the gel under ultra violet light and purified from the gel slice using QIAquick Gel Extraction Kit according to the manufacturer's instructions.

Target	Antibody (code)	Source
GAP43 FE65 Rab7	EP809Y (Ab75810) EPR3538 (Ab91650) EPR7589 (Ab137029)	Abcam (Cambridge, UK)
Flotillin 1	(610820)	BD Transduction Laboratories (Oxford, UK)
ABCA1 Flotillin 2 p-APP(T668) PRDX1 Rab11a	D3HQ1 (12683S) C43A3 (3436) (3823) D5G12 (8499) (2431)	Cell Signalling Technologies (Danvers, MA, USA)
EGFP	(632569)	Clontech (Mountain View, CA, USA)
sAPPβ $sAPP\beta_{SWE}$	1A9 129	Dr Ishrut Hussain (Formerly GlaxoSmithKline; Harlow, UK)
TGN-46	TGN-46	Dr Sreenivasan Ponambalam (University of Leeds; Leeds, UK)
Anti-rabbit HRP Anti-mouse Alexa Fluor 488 Anti-rabbit Alexa Fluor 594 Transferrin receptor	(A16096) (A11059) (A21207) H68.4 (13-6800)	Invitrogen (Paisley, UK)
APP (full length) sAPPα	22C11 (MAB348) 6E10 (NE1003)	Merck Millipore (Darmstadt, Germany)
Ataxin-10 GRP78 HSPA8	(15693) (11587) (10654)	Proteintech (Manchester, UK)
DPP7 Rab5a	H8 (SC-390008) S-19 (SC-309)	Santa Cruz Biotechnology, Inc
β-Actin FLAG-tag monoclonal FLAG-tag polyclonal Anti-mouse HRP	AC-15 (A5441) (F3165) (F7425) (A9044)	Sigma-Aldrich (St. Louis, MO, USA)

Table 2.1 Primary and secondary antibody sources

Following purification of the PCR product, APP695-FLAG and empty pIREShyg vector were digested with NsiI and NotI restriction enzymes at 37°C for 2 h to produce compatible sticky ends for ligation. The digest products were electrophoresed on an agarose gel, excised from the gel and purified as previously described. Ligation of the insert and vector digest products was then carried out using a Quick Ligation Kit using a 3:1 molar ratio of insert to vector according to the manufacturer's instructions. After a 5 min incubation period, 2 µl of the reaction was used to transform XL-1 blue competent *E. coli* cells according to the manufacturer's instructions and the transformed bacteria were used to inoculate Luria-Bertani (LB) agar plates containing 0.1 mg/ml ampicillin and incubated at 35°C overnight. Colonies were selected and used to inoculate 5 ml of sterile LB Broth which were incubated overnight at 37°C with shaking at 220 RPM. DNA was then extracted from the bacteria using QIAprep Spin Miniprep Kit according to the manufacturer's instructions.

2.2.2 Cloning of APP751-GFP

APP751 cDNA in the vector pIREShyg was subjected to PCR using the forward primer 5' – CTCAGAAGCTTATGCTGCCCGGTTTGGCACTGC – 3' and reverse primer 5' – GAGTTCGTCGACTGGTTCTGCATCTGC – 3' (red – spacer, blue - HindIII restriction site, green - SalI restriction site, black – APP specific). A standard PCR master mix for 4 reactions was prepared using the Pfx DNA Polymerase kit according to the manufacturer's instructions and aliquoted into 4 separate thin walled PCR tubes. The reactions were then subjected to two-step PCR thermal cycling according to the manufacturer's instructions. Following thermal cycling, the reactions were electrophoresed on a 1% agarose gel for 70 min at 100 V with a 1 kB DNA ladder. Bands of the length corresponding to the desired APP751 cDNA PCR product (~2.3 kB) were excised from the gel and purified as previously described.

The APP751 PCR product and empty pEGFP-N1 vector were digested with HindIII and SalI restriction enzymes at 37°C for 2 h. The digest products were electrophoresed on an agarose gel, excised from the gel and purified as previously described. Ligations, transformations and cDNA preparations were then performed as previously described.

2.2.3 Site directed mutagenesis

A site-directed mutagenesis approach was used to produce APP751-FLAG using the forward primer 5' – GATTACAAGGATGACGACGATAAGTAGGCGGCCGATCCACTAGTAACGGCCG – 3' and the reverse primer 5' – CTTATCGTCGTCATCCTTGTAATCGTTCTGCATCTGCTCAAAGAACTTGTAGG – 3' (orange – FLAG tag sequence, purple – stop, blue – vector specific sequence, Black – APP

specific sequence) with the KOD Polymerase PCR Kit according to the manufacturer's instructions.

To create single amino acid mutations, APP695 and APP751 in the vector pIREShyg were subjected to site-directed mutagenesis using the Quikchange II Site-Directed Mutagenesis Kit according to the manufacturer's instructions. To create the Icelandic mutation (A673T) a single nucleotide G1960A mutation was introduced into the APP cDNA. The mutagenic primers were: forward primer, 5' – CTCTGAAGTGAAGATGGATACAGAATTCCGACATGACTC -3' and reverse primer, 5' – GAGTCATGTCGGAATTCTGTATCCATCCATCTTCACTTCAGAG -3'. The mutation is highlighted in green. To create the Italian mutation (A673V) a single nucleotide C1961T mutation was introduced into the APP cDNA. The mutagenic primers were: forward primer, 5' – CTCTGAAGTGAAGATGGATGTAGAATTCCGACATGACTC -3' and reverse primer, 5'-GAGTCATGTCGGAATTCTACATCCATCCATCTTCACTTCAGAG -3'.

The maternal DNA was then digested through addition of 1 µl of DpnI restriction enzyme and incubation at 37°C for 2 h. Transformations and DNA preparations were then performed as previously described. The prepared DNA was then screened for incorporation of the desired mutation by sequencing (See **Section 2.2.4**).

2.2.4 DNA sequencing

APP cDNA was sent for full forward and reverse sequencing by Beckman-Coulter Genomics using the forward primers: 5'- TGGTGAGTTTGTAAGTGATGCC -3', 5'-GGTAGAGGAAGAGGCTGAGGA-3', 5', 5'-GAGTGGAAGCCATGCTCAAT-3' and 5'-ATGCCATCTTTGACCGAAAC-3', and the reverse primers: 5'-TGAGTTTCGCAAACATCCAT-3', 5'-CAGACTCTGTGGTGGTGGTG-3', 5'-TTGAACACGTGACGAGGC-3', 5'-AAAAGAATGCCACGGCTG-3' and 5'-GTTCTGCTGCATCTTGGACA-3' which were designed to be spaced evenly through the APP cDNA sequence. In the cases of FLAG-tagged and GFP-tagged constructs, forward primer four (5'-ATGCCATCTTTGACCGAAAC-3') resulted in sequencing beyond the normal 3' end of the APP cDNA, meaning the removal of the normal stop codon and the incorporation of the FLAG-tag or GFP-tag could be confirmed.

2.2.5 Ethanol precipitation of DNA for stable transfection

DNA was quantified using an Implen NanoPhotometer (Implen; Munich, Germany) and 30 µg was added to a sterile eppendorf. A 1/10 volume of filter sterilised 3 M sodium acetate (pH 5.2) was then added to the DNA followed by two volumes of cold 100% ethanol. The eppendorfs were then incubated at -20°C for 1 h followed by 20 min centrifugation at 4°C at 12,460 x g. The supernatant was then discarded and 300 µl of cold 80% ethanol was added to the DNA pellet.

The eppendorf was then centrifuged for a further 5 min at 12,460 x g. The supernatant was discarded and DNA was dried at room temperature in a sterile environment for 30 min then re-suspended in 30 µl of sterile deionised water.

2.2.6 Cell culture

SH-SY5Y cells were cultured in DMEM supplemented with 10% FBS at 37°C, 5% CO_2. Cells were passaged as required by removing the culture medium and replacing it with $PBSM^-$. Cells were incubated at 37°C for ~5 min to remove them from the bottom of the flask, pelleted by centrifugation at 500 x g for 5 min and split into fresh flasks. In experiments requiring the analysis of metabolites within the conditioned medium, the DMEM was removed at the appropriate point and cells were washed with pre-warmed $PBSM^+$. The cells were subsequently incubated in an appropriate volume of Opti-MEM and cultured for a further 6 h or 24 h depending on the experiment.

2.2.7 Stable transfection of SH-SY5Y cells

Flasks of SH-SY5Y cells were grown to 70-80% confluence. The cell medium was removed and the cells were removed from the bottom of the flask by bathing in 5 ml $PBSM^-$. Once re-suspended, the cells were transferred to a 15 ml tube and centrifuged for 5 min at 500 x g to pellet the cells. The supernatant was removed and the cells were re-suspended in 700 µl of serum free DMEM and transferred to a 4 mm electroporation cuvette. The appropriate DNA (30 µg), or 30 µl of sterile deionised water for control flasks, was added to the cell suspension and mixed. Cuvettes were then pulsed with electricity at 250 V, 1650 µF for 20 ms. The cells were then transferred to a 25 cm^2 flask containing 5 ml of DMEM (with 10% FBS). The following day the cell medium was replaced to remove floating cell debris. Cells were then allowed to reach 70-80% confluence, changing the medium when appropriate. At 70-80% confluent cells were treated with 75 µg/ml hygromycin B to kill cells not expressing the desired construct. The cell medium was changed every 2 days and supplemented with hygromycin B for 10 days, or until all cells in the control transfected flask had died. Cells were then grown to ~90% confluence before being stored in liquid nitrogen until required.

2.2.8 Transient transfection of SH-SY5Y cells

SH-SY5Y cells were seeded in 6-well plates and grown to 80% confluence. Opti-MEM (250 µl), 7.5 µl of Trans-LT1 transfection reagent and 2.5 µg of the desired DNA were added to a sterile eppendorf and incubated at room temperature for 20 min. The cell medium was removed, cells were washed once with $PBSM^+$ and 2.5 ml of fresh cell culture medium was added to each well.

The transfection mix was then added to the cells in a dropwise manner and gently mixed. Cells were then cultured for 24 h. The cell medium was then removed and the cells were washed with $PBSM^+$. The cells were then cultured in 700 µl of Opti-MEM for 6 h.

2.2.9 Stable isotope labelling of amino acids in cell culture

To carry out SILAC, mock transfected cells, or cells expressing APP695-FLAG or APP751-FLAG were cultured in DMEM containing heavy (R10, K8), medium (R6, K4) or light (R0, K0) isotope labelled versions of the amino acids arginine (R) and lysine (K). The light isotope labelled medium contained unlabelled arginine and lysine, the medium isotope labelled medium contained ^{13}C labelled arginine and ^{2}D labelled lysine and the heavy isotope labelled medium contained ^{13}C and ^{15}N labelled arginine and ^{13}C and ^{15}N labelled lysine. The isotope labelled DMEM was supplemented with 10% dialysed FBS. The cells were cultured for at least 3 weeks, or until at least 6 doublings of the cell population had occurred.

2.2.10 Pharmacological cell treatments

Cells were cultured at described previously until confluent. Inhibitors were solubilised in an appropriate volume of sterile DMSO. The cell culture medium was removed and cells were washed once with $PBSM^+$ and replaced with Opti-MEM containing the inhibitor or DMSO only as a control. Cells were then cultured for a further 6 h or 24 h.

2.2.11 siRNA mediated protein knockdown

Cells were seeded in 6 well plates (10 cm^2) at 500,000 cells per dish and cultured overnight. Cells were then transfected with 50 nM siRNA for 48 h using 10 µl of DharmaFECT 1 transection reagent according to the manufacturer's instructions (in experiments where this protocol was adapted it is described in the results section). The cell medium was removed and replaced with Opti-MEM and the cells were cultured for a further 6 h.

2.2.12 Protein degradation assay

Cells were seeded into 6 well plates at 750,000 cells per well and cultured until reaching confluence. The cell culture medium was removed and replaced with serum-free DMEM containing 50 µg/ml cycloheximide and cultured for the time periods indicated.

2.2.13 Cell lysate and media preparation

The conditioned cell medium was removed from the cells and centrifuged at 500 x g for 5 min at 4°C to pellet floating cells and cell debris. For MSD analysis the conditioned cell medium was stored at -20°C if not being used immediately. For immunoblot analysis the conditioned cell medium was transferred to a 10 kDa molecular weight cut-off Vivaspin column (Generon Ltd; Maidenhead, UK) and centrifuged at 1400 x g at 4°C until the conditioned medium was concentrated to approximately 250 µl and stored at -20°C if not being used immediately. The cells were washed once in ice cold $PBSM^+$, then harvested and lysed in ice cold cell lysis buffer (50 mM Tris, 150 mM NaCl, 0.5% (w/v) Sodium deoxycholate, 1% (v/v) NP-40, EDTA-free protease inhibitor cocktail, pH 8.0) for 30 min on ice before being clarified by centrifugation at 12,460 x g for 10 min at 4°C. The supernatant was removed and stored at -20°C if not being used immediately.

2.2.14 Bicinchoninic acid (BCA) assay

Clarified cell lysates and conditioned cell medium samples were loaded in duplicate into the wells of a 96-well plate in volumes between 1-10 µl depending on the experiment and made up to 10 µl using sterile deionised water. Bovine serum albumin (BSA) standards ranging from 2-10 µg/µl and a sterile deionised water control were loaded in duplicate. BCA assay solution and 4% (w/v) $CuSO_4$ solution were then mixed at a ratio of 50:1 and 200 µl added to each assay well. Plates were incubated at 37°C for 30 min and the absorbance was measured at 562 nm.

2.2.15 Lipid raft preparations

Cells were grown to confluence and harvested in ice cold $PBSM^-$. Cells were pelleted by centrifugation at 500 x g for 5 min at 4°C. Cells were subsequently lysed in 750 µl of ice cold 2-(*N*-Morpholino)-ethanesulfonic acid (MES) buffered saline (MBS) (25 mM MES, 150 mM NaCl, pH 6.5) containing 1% (v/v) Triton X-100 by passing through a 21 gauge needle (0.5 mm thickness) five times. An equal volume (750µl) of ice cold 80% (w/v) sucrose in MBS was added to the cell lysate. A discontinuous sucrose gradient was formed by loading 1 ml of ice cold 5% (w/v) sucrose solution to the bottom of a 5 ml soft walled Beckmann centrifugation tube. Following this 3 ml of ice cold 35% (w/v) sucrose solution was loaded beneath the 5% solution using a syringe and needle, ensuring the 5% solution remained floating above the 35% solution. The cell lysate (1 ml) was then carefully loaded in the bottom of the tube ensuring the maintenance of all three layers of the gradient. Sample gradients were then centrifuged at 100,000 x g in a Beckmann L-90K centrifuge using a SW55 swing bucket rotor for 18 h at 4°C.

Following centrifugation, gradient samples were checked for the formation of an insoluble raft fraction, clearly visible within the gradient as a milky aggregate at the 5%-35% sucrose interface. Nine 0.5 ml fractions were collected at 4°C from the bottom of the tube using a 1ml syringe and transferred to sterile eppendorfs. Samples (100 µl) were mixed with 25 µl of 5 x dissociation buffer (0.5 mM Tris-Hydrochloride, 10% (w/v) sodium dodecyl sulphate (SDS), 50% (v/v) glycerol, 0.5 mM dithiothreitol, 0.1% (w/v) bromophenol blue, pH 6.8) and stored at 20°C.

2.2.16 Cell surface biotinylation

Cells were seeded in 25cm^2 flasks and grown to ~100% confluence. The cell medium was removed and cells were washed twice in ice cold PBSM$^+$. Cells were then incubated with ice cold PBSM$^+$ containing 0.5 mg/ml of Sulfo-NHS-Biotin EZ-link for 20 min at 4°C. Cells were washed a further three times with ice cold PBSM$^+$ before being lysed as previously described and were subjected to BCA assay to determine the protein concentration of the samples. Streptavadin agarose was equilibrated in cell lysis buffer for 20 min. Cell lysate samples were diluted to 0.5µg/µl and 250 µg was added to the equilibrated streptavidin agarose. Samples were incubated on a rotating wheel for 3 h at 4°C to precipitate biotin linked proteins. Samples were subjected to centrifugation at 500 x g for 45 s and the unbound fraction removed. The streptavidin pellet was then washed with 500 µl cell lysis buffer, centrifuged for 45 s at 500 x g, and the supernatant was removed. This process was repeated four times. The bound sample was dissociated from the agarose by adding 120 µl 2 x dissociation buffer (0.2 mM Tris-Hydrochloride, 4% (w/v) sodium dodecyl sulphate (SDS), 20% (v/v) glycerol, 0.2 mM dithiothreitol, 0.04% (w/v) bromophenol blue, pH 6.8) and boiling of the samples for 5 min at 95°C. Samples were subjected to centrifugation for 45 s at 500 x g and the bound fraction was removed and frozen at -20°C.

2.2.17 Protein co-immunoprecipitations

Cells were harvested and lysed in 800 µl of ice cold CHAPSO buffer (50mM Tris, 150mM NaCl, 1% (w/v) CHAPSO, 2mM EDTA, EDTA-free protease inhibitor cocktail, pH 7.5) or IP buffer (10mM Tris-Hydrochloride, 150mM NaCl, 0.5% NP-40 and 1x EDTA-free protease inhibitor cocktail, pH 7.5) for 30 min on ice. Lysates were then clarified by centrifugation and the protein concentration was determined by BCA assay as described previously.

Anti-FLAG affinity gel (30 µl), protein A sepharose (30 µl), protein G sepharose (30 µl), protein G Dynabeads (1.5 µg) or protein A Dynabeads (1.5 µg) were washed in PBSM$^-$. Anti-FLAG affinity gel was equilibrated in the appropriate lysis buffer for 30 min. Primary antibody (2.5 µg) was

diluted in 1 ml PBSM$^-$ and added to the Dynabeads or sepharose and incubated for 2 h at room temperature on a rotary mixer. The sepharose was pelleted by centrifugation at 500 x g for 1 min and Dynabeads were pelleted using a DynaMag magnetic rack and the supernatant was removed. Protein concentrations were diluted to 1mg/ml in the appropriate buffer and 1 mg of total protein was added to the anti-FLAG affinity gel, sepharose or Dynabeads and incubated for 2 h at 4°C on a rotary mixer. The sepharose and anti-FLAG affinity gel were pelleted by centrifugation at 500 x g for 1 min at 4°C. The Dynabeads were pelleted using a DynaMag magnetic rack. The supernatant was removed and saved as the unbound fraction. The anti-FLAG affinity gel, sepharose and Dynabeads were washed three times in PBSM$^-$ and the supernatant was removed each time as previously described. After washing, the pellet was re-suspended in 20-50 µl of 2 x dissociation buffer and boiled for 3 min to elute the bound proteins. The anti-FLAG affinity gel, sepharose and Dynabeads were pelleted as previously described and the supernatants were removed and saved as the bound fraction.

2.2.18 Human brain samples

Human brain tissue from the temporal cortex of AD and control patients was obtained from the South West Dementia Brain Bank (University of Bristol, UK). The study had ethical approval from the North Somerset and South Bristol Research Ethics Committee. Clinical diagnosis of AD was made on the according to the assessment criteria outlined by the Consortium to Establish a Registry for Alzheimer's disease (CERAD) (Morris et al. 1989). Homogenisation of the brain tissue samples has been previously described (Whitehouse et al. 2010). The protein concentrations were determined by BCA assay.

2.2.19 Sodium dodecyl sulphate polyacrylamide gel electrophoresis (SDS-PAGE)

Following the determination of protein concentration by BCA assay, samples were diluted to 1mg/ml by the addition of an appropriate volume of 5 x dissociation buffer and cell lysis buffer. The samples were boiled for 5 min at 95°C and briefly centrifuged before 30-50 µl of the sample was loaded on to the polyacrylamide gel. Proteins were separated on 7-17% acrylamide gradient gels in Tris-Glycine-SDS buffer (Biorad; Hemel Hempstead, UK) for ~1 h at 45 mA per gel.

2.2.20 Immunoblotting

Proteins were transferred to polyvinylidene difluoride membranes (GE Healthcare; Little Chalfont, UK) at 120 V for 75 min in transfer buffer (150 mM glycine, 20mM Tris, 20% (v/v) methanol, pH 8.4). Membranes were blocked for 1 h at room temperature in phosphate

buffered saline (PBS) (20 mM Na_2HPO_4, 2 mM NaH_2PO_4, 150 mM NaCl, pH 7.4) containing 0.01% Tween-20 (PBS-T) and either 5% (w/v) skimmed milk powder or 3% (w/v) BSA when using antibodies to phosphorylated epitopes. Membranes were washed briefly in PBS-T before being incubated with primary antibody diluted as described (**Table 2.2**) overnight at 4°C. Membranes were washed three times for 10 min in PBS-T followed by incubation with the appropriate HRP-conjugated secondary antibody (**Table 2.2**) for 1 h at room temperature. All secondary antibodies were diluted at 1:4000 in the same buffer as their respective primary antibody. Membranes were washed two times for 10 min in PBS-T followed by a final 10 min wash in PBS. Equal volumes of Pierce electrochemiluminescence western blotting substrate (Thermo Fisher Scientific) were combined and washed over the membrane for 1 min before the membrane was imaged using a Syngene Gbox X4 (Syngene; Cambridge, UK). Semi-quantitative densitometry was then carried out on blots using Syngene Genetools software (Syngene).

2.2.21 sAPP and Aβ quantification

Levels of sAPPα and sAPPβ or Aβ38, Aβ40 and Aβ42 in the conditioned cell medium were determined using the sAPP or Aβ multiplex assay plates from Meso Scale Discovery according to the manufacturer's instructions. Briefly, standards were diluted in Opti-MEM and standards and experimental samples were buffered with 50mM HEPES (pH 7.5). All incubations were carried out at room temperature with the plates on a plate shaker. Plates were blocked for 1 h, washed in their plate specific wash buffers, then incubated with 25 µl of conditioned cell medium for 1 h (sAPP plates) or with 25 µl of conditioned cell medium and 25µl of detection antibody solution (Aβ plates). Following the 1 h incubation with samples, the conditioned cell medium on sAPP plates was removed, plates were washed with the appropriate wash buffer and 25 µl of detection antibody was added to the plates which were incubated for a further 1 h. Plates were washed in the appropriate buffer and analyte levels were determined using the MESO QUICKPLEX SQ 120 and analysed using MSD Workbench 4.0 software (MSD; Rockville, MD, USA). The concentration of each measured analyte was corrected to the total protein concentration within the conditioned medium as determined by BCA assay. Due to variation in the absolute amount of Aβ and sAPP detected between experimental repeat, data for these analyses are always presented as a percentage of the control (e.g non-targeting siRNA or DMSO controls.

2.2.22 pGlu-Aβ3-40 ELISA

Conditioned cell medium was removed from the cells and centrifuged at 500 x g for 5 min at 4°C to pellet any floating cell debris. The conditioned cell medium was transferred to a 2 kDa molecular weight cut-off Vivaspin column (Hydrosart; Goettingen, Germany) and centrifuged at

Target	1° antibody dilution	2° antibody
ABCB1	1:1000, PBS-T, 2% (w/v) BSA	Goat anti rabbit
Actin	1:10000, PBS-T, 2% (w/v) BSA	Rabbit anti-mouse
APP	1:4000, PBS-T, 2% (w/v) BSA	Rabbit anti-mouse
Ataxin 10	1:1000, PBS-T, 2% (w/v) BSA	Goat anti-rabbit
DPP7	1:500, PBS-T, 2% (w/v) BSA	Rabbit anti mouse
Fe65	1:1000, PBS-T, 2% (w/v) BSA	Goat anti-rabbit
FLAG-tag monoclonal	1:1000, PBS-T, 5% (w/v) milk	Rabbit anti-mouse
FLAG-tag polyclonal	1:1000, PBS-T, 5% (w/v) milk	Goat anti-rabbit
Flotillin-1	1:1000, PBS-T, 5% (w/v) milk	Rabbit anti-mouse
Flotillin-2	1:1000, PBS-T, 2% (w/v) BSA	Goat anti-rabbit
GAP43	1:10000, PBS-T, 2% (w/v) BSA	Goat anti-rabbit
GFP	1:1000, PBS-T, 5% (w/v) milk	Rabbit anti-mouse
GRP78	1:1000, PBS-T, 2% (w/v) BSA	Goat anti-rabbit
HSPA8	1:1000, PBS-T, 2% (w/v) BSA	Goat anti-rabbit
p-APP	1:1000, PBS-T, 3% (w/v) BSA	Goat anti-rabbit
PRDX1	1:1000, PBS-T, 2% (w/v) BSA	Goat anti rabbit
Rab11a	1:1000, PBS-T, 2% (w/v) BSA	Goat anti-rabbit
sAPPα	1:4000, PBS-T, 2% (w/v) BSA	Rabbit anti-mouse
sAPPβ	1:4000, PBS-T, 2% (w/v) BSA	Rabbit anti-mouse
$sAPP\beta_{SWE}$	1:4000, PBS-T, 2% (w/v) BSA	Rabbit anti-mouse
Transferrin receptor	1:1000, PBS-T, 2% (w/v) BSA	Rabbit anti-mouse

Table 2.2 Primary antibody dilutions and secondary antibodies for immunoblot analysis

1400 x g at 4°C until the conditioned cell medium was concentrated to ~500 µl. The concentrated conditioned medium was then subjected to analysis for pGlu-Aβ3-40 using the Aβ N3pE-40 ELISA (IBL international; Hamburg, Germany) according to the manufacturer's instructions.

2.2.23 Immunofluorescence microscopy

Cells were seeded into 24 well plates containing cover slips at 30,000 cells per well and cultured overnight. Cells were briefly washed in $PBSM^+$ then fixed and permeablised with a 1:1 ratio of ice cold methanol and acetone for 10 min at room temperature. The cells were then washed with $PBSM^+$ and blocked in $PBSM^+$ containing 5% (v/v) fish skin gelatin (FSG) (Sigma-Aldrich) for 1 h at room temperature. Cover slips were incubated with primary antibody overnight at 4°C diluted as described (**Table 2.3**). Cover slips were washed three times for 10 min with $PBSM^+$ containing 0.2% (v/v) Tween-20 ($PBSM^+$-T) and incubated with donkey anti-mouse Alexa Fluor 488 and donkey anti-rabbit Alexa Fluor 594 antibodies diluted at 1:500 in $PBSM^+$ containing 5% (v/v) FSG for 1 h at room temperature. Coverslips were washed once for 10 min in $PBSM^+$ and then incubated with DAPI diluted at 1:1000 in $PBSM^+$ for 2 min at room temperature. The coverslips were then washed twice for 10 min with $PBSM^+$-T and once with $PBSM^+$ and mounted on slides using Fluoromount G (Southern Biotech; Birmingham, AL, USA). Images were taken using a DeltaVision Optical Restoration Microscopy System (GE Healthcare) and analysed using Image J software (National Institutes of Health; Bethesda, MD, USA).

2.2.24 Liquid chromatography – tandem mass spectrometry (LC MS/MS)

FLAG-tagged proteins were immunoprecipitated from mock transfected cells or those expressing APP695-FLAG or APP751-FLAG using the anti-FLAG affinity gel (see **2.2.16**). SDS-PAGE (see **2.2.17**) and immunoblot analysis (see **2.2.18**) were used to confirm APP immunoprecipitation and co-immunoprecipitation of Fe65. Bound fractions from the mock and APP695-FLAG and APP751-FLAG immunoprecipitation were then combined at a 1:1:1 ratio in preparation for LC MS/MS analysis.

LC MS/MS was carried out at the Proteomics Facility at the University of Bristol by Dr K. Heesom using the following methodology. Protein samples were separated by SDS-PAGE. The gel lane was cut into 3 slices and each slice subjected to in-gel tryptic digestion using a DigestPro automated digestion unit (Intavis Ltd.). The resulting peptides were fractionated using an Ultimate 3000 nanoHPLC system in line with an LTQ-Orbitrap Velos mass spectrometer (Thermo Scientific). In brief, peptides in 1% (v/v) formic acid were injected onto an Acclaim PepMap C18

Target	1° antibody dilution	2° antibody
FLAG	1:500, $PBSM^+$, 5% (v/v) FSG	Donkey anti-mouse Alexa Fluor 488
Rab5a	1:200, $PBSM^+$, 5% (v/v) FSG	Donkey anti-Rabbit Alexa Fluor 594
Rab7	1:250, $PBSM^+$, 5% (v/v) FSG	Donkey anti-Rabbit Alexa Fluor 594
Rab11a	1:200, $PBSM^+$, 5% (v/v) FSG	Donkey anti-Rabbit Alexa Fluor 594
TGN-46	1:750, $PBSM^+$, 5% (v/v) FSG	Donkey anti-Rabbit Alexa Fluor 594

Table 2.3 Primary antibody dilutions and secondary antibodies for immunofluorescence microscopy

nano-trap column (Thermo Scientific). After washing with 0.5% (v/v) acetonitrile, 0.1% (v/v) formic acid, peptides were resolved on a 250 mm × 75 µm Acclaim PepMap C18 reverse phase analytical column (Thermo Scientific) over a 150 min organic gradient, using 7 gradient segments (1-6% solvent B over 1 min, 6-15% solvent B over 58 min, 15-32% solvent B over 58 min, 32-40% solvent B over 3 min, 40-90% solvent B over 1 min, held at 90% solvent B for 6 min and then reduced to 1% solvent B over 1 min) with a flow rate of 300 nl min^{-1}. Solvent A was 0.1% formic acid and solvent B was aqueous 80% acetonitrile in 0.1% formic acid. Peptides were ionized by nano-electrospray ionization at 2.1 kV using a stainless steel emitter with an internal diameter of 30 µm (Thermo Scientific) and a capillary temperature of 250°C. Tandem mass spectra were acquired using an LTQ-Orbitrap Velos mass spectrometer controlled by Xcalibur 2.1 software (Thermo Scientific) and operated in data-dependent acquisition mode. The Orbitrap was set to analyse the survey scans at 60,000 resolution (at m/z 400) in the mass range m/z 300 to 2000 and the top ten multiply charged ions in each duty cycle selected for MS/MS in the LTQ linear ion trap. Charge state filtering, where unassigned precursor ions were not selected for fragmentation, and dynamic exclusion (repeat count, 1; repeat duration, 30 s; exclusion list size, 500) were used. Fragmentation conditions in the LTQ were as follows: normalized collision energy, 40%; activation q, 0.25; activation time 10 ms; and minimum ion selection intensity, 500 counts.

The raw data files were processed and quantified using Proteome Discoverer software v1.2 (Thermo Scientific) and searched against the UniProt Human database plus appropriate APP sequences using the SEQUEST algorithm. Peptide precursor mass tolerance was set at 10 ppm, and MS/MS tolerance was set at 0.8 Da. Search criteria included carbamidomethylation of cysteine (+57.0214) as a fixed modification and oxidation of methionine (+15.9949) and appropriate SILAC labels ($^{2}H_4$-Lys, $^{13}C_6$-Arg for Medium and $^{13}C_6{}^{15}N_2$-Lys and $^{13}C_6{}^{15}N_4$-Arg for Heavy) as variable modifications. Searches were performed with full tryptic digestion and a maximum of 1 missed cleavage was allowed. The reverse database search option was enabled and all peptide data was filtered to satisfy false discovery rate of 5%. The protein ratios presented in **Table 4.1** represent the average of the raw measured peptide ratios for each protein from two independent labelling, immunoprecipitation and LC-MS/MS experiments.

2.2.25 Bioinformatic analysis

Gene ontology analysis was performed with DAVID Bioinformatics Resources version 6.7 (available at http://david.abcc.ncifcrf.gov/) **(Huang et al. 2008;Huang et al. 2009)** using Uniprot accession numbers as identifiers. Manual curation was performed on the entire dataset to ensure recognition of UniProt identifiers by DAVID software.

2.2.26 Statistical analysis

Data were analysed using IBM SPSS Statistics 20 software. For analysis of data from experiments using large cell populations a normal distribution was assumed and parametric tests were used for analysis. Levene's test was first applied to all data to determine equality of variance between groups for comparison. For comparison between two data sets, an independent t-test was applied and the appropriate statistic determined depending on the equality of variance. For experiments using single cell analysis or human brain samples, normal distribution of the data was determined using a Kolmogorov-Smirnov test. If the data were normally distributed a t-test was used to determine significance. If the data were not normally distributed, statistical significance was determined by Mann-Whitney U test. For all analyses, statistical significance was taken at $p<0.05$.

Chapter 3. APP isoforms show differential subcellular localisation contributing to differential proteolysis

3.1 Introduction

3.1.1 The APP isoforms show differential proteolysis

As discussed in **Chapter 1,** various lines of evidence indicate a change in the expression profile of the APP isoforms in the brain in AD, with an increase in the expression of the longer APP isoforms observed in the disease state (see **Table 1.1**). This has led some in the field to suggest that the longer APP isoforms are more amyloidogenic and causative of the increased amyloid burden in the brains of AD patients (Barrachina et al. 2005;Moir et al. 1998). However, in an extensive study on various brain regions comparing AD and control tissue, a decrease in KPI domain-containing APP isoforms was observed in areas with high amyloid deposition, alongside an increase in KPI domain-containing isoforms in regions with low amyloid deposition in the AD brains, leading the authors to suggest that APP695 was the more amyloidogenic isoform (Golde et al. 1990). Very few of these studies have directly investigated APP isoform proteolysis in the cellular context. One study directly comparing the proteolysis of APP isoforms in murine and HEK cell models identified an increased ratio of amyloidogenic to non-amyloidogenic proteolysis in APP751 expressing cells compared to APP695 expressing cells (Ho et al. 1996). However, they did observe less sAPPα and importantly, less sAPPβ in the conditioned cell medium from APP751 expressing P19 cells compared to those expressing APP695 (Ho et al. 1996). When our lab studied APP isoform proteolysis in human SH-SY5Y cells we also observed significantly less sAPPβ (~3.5-fold) and Aβ (~2.5-fold) as well as a 10% reduction in sAPPα, in the conditioned medium from cells expressing the KPI domain-containing APP isoforms (APP751 and APP770), compared to those expressing APP695 (Belyaev et al. 2010). These data indicated a higher propensity for APP695 to undergo amyloidogenic proteolysis than APP containing the KPI domain and raise the interesting question of how APP containing the KPI domain is protected from amyloidogenic proteolysis, or indeed, how APP695 is predisposed to undergo more amyloidogenic proteolysis.

3.1.2 Does subcellular location contribute to the differential proteolysis of APP isoforms?

As eluded to in **Chapter 1**, the trafficking of APP is complex, and the exact subcellular location(s) for APP proteolysis, and importantly, Aβ generation are still not fully understood. Difficulties arise in the analysis of proposed subcellular locations for BACE1 cleavage of APP as rarely do the

cell systems within which APP proteolysis is analysed in different studies align. Variations in the choice of cell line and APP isoform, the incorporation of familial AD-linked mutations and addition of large fluorescent tags and different methods for analysis may all confound the potential for consensus.

Strong evidence implicates early endosomes as the primary site for amyloidogenic proteolysis of APP (Koo and Squazzo 1994), while further studies have also identified recycling endosomes (Das et al. 2013), the TGN (Choy et al. 2012), mitochondria (Pavlov et al. 2011), lysosomes (Tam et al. 2014) and lipid rafts (Bhattacharyya et al. 2013) as sites of amyloidogenic APP proteolysis. Plasma membrane insertion and subsequent endocytosis have been identified as key processes leading to the amyloidogenic proteolysis of APP (Schneider et al. 2008) and GWAS has implicated several proteins involved in endocytosis as risk loci for late onset AD (Guerreiro et al. 2013). Given the large differences in proteolysis we have previously identified in APP isoforms (Belyaev et al. 2010), it seems pertinent to investigate the subcellular location of these isoforms in order to determine differences which may contribute to either enhanced, or reduced, amyloidogenic proteolysis. Importantly, direct comparison of the subcellular distribution of these isoforms in the same model system should allow the identification of subcellular environments in which APP is subject to greater amyloidogenic proteolysis. Drugs targeting Aβ production at specific subcellular locations have had some recent success in cell models, suggesting comprehensive understanding of APP trafficking and subcellular sites of proteolysis could contribute to drug development (Mecozzi et al. 2014;Rajendran et al. 2008).

3.1.3 Aims

The main aim of this chapter was initially to identify differences in subcellular location of two APP isoforms (APP695 and APP751) which could cause the differential proteolysis we have previously observed in these isoforms in SH-SY5Y cells (Belyaev et al. 2010). To achieve this, we used FLAG-tagged versions of the APP isoforms to specifically study their subcellular distribution by IFM, cell surface biotinylation and subcellular fractionation. To determine the effect of the disruption of particular trafficking pathways, siRNA mediated protein knockdown of lipid raft proteins and proteins implicated in APP recycling as well as pharmacological inhibition of endocytosis were employed, followed by subsequent analysis of APP soluble fragments. We sought to determine whether the rates of APP degradation differed significantly between APP isoforms and whether alternative pathways of APP proteolysis could cause differences in the proteolysis of the APP isoforms by studying proteolytic fragments of APP in the conditioned cell medium from cells expressing the APP isoforms.

3.2 Results

3.2.1 FLAG-tagged APP isoforms, but not GFP-tagged APP isoforms show the expected differences in proteolysis

The subcellular location of APP has been highlighted within the literature as an important factor in the proteolysis of APP (for review see (Thinakaran and Koo 2008)). Thus, to allow differentiation between exogenously expressed APP and endogenous APP, a FLAG-tag and a GFP-tag were selected as an appropriate means of tagging two APP isoforms, APP695 and APP751. APP695 and APP751 in the pIREShyg vector (**Figure 3.1A**) at the Bst-X1 and Bam-H1 site, respectively, were FLAG-tagged by two different methods. APP695 was FLAG-tagged by a conventional PCR and cloning technique. APP695 cDNA was amplified from the pIREShyg vector containing APP695 using a PCR primer containing the sequence for the FLAG-tag. The amplified PCR product was subsequently ligated into empty pIREShyg vector and the resulting DNA was used to transform competent bacteria. During cloning, the bacterial colonies were screened to find colonies expressing DNA which cut with restriction enzymes according to i) expectations from the vector/insert map, and ii) compared to normal APP695 DNA. DNA from the colonies that showed the correct sized DNA fragments when cut with specific restriction enzymes, as seen in lane 1 (**Figure 3.1B**), were subsequently sequenced to confirm the addition of the FLAG tag (**Figure 3.1C**). Due to difficulties in ligating the APP751-FLAG PCR product into the pIREShyg vector, the FLAG-tag was added to the APP751 cDNA by site-directed mutagenesis, using primers containing the FLAG-tag sequence. Following the site-directed mutagenesis, the resulting DNA was used to transform competent bacteria and the colonies produced were then screened by sequencing to confirm the addition of the FLAG-tag. Full APP forward and reverse sequencing was used to confirm the correct cDNA sequence had been maintained, and the successful addition of the FLAG-tag (**Figure 3.1C**). Finally, two digests were carried out to confirm the correct amplification of the rest of the vector. DNA fragments corresponding to predicted sizes in both Bam-H1 (APP695 – 1665bp and 6000bp, APP751 – 1500bp and 6500bp) and AdhI (APP695 – 7800bp, APP751 – 8000bp (**Figure 3.1D**) restriction digests were observed confirming the constructs had been amplified correctly.

Following successful cloning of the FLAG-tag coding sequence to the C-terminus of the APP695 and APP751 cDNA, SH-SY5Y cells were stably transfected with the vector encoding APP695-FLAG, APP751-FLAG or with the vector only as a control (mock transfected) by electroporation. Cell lysates and the conditioned cell medium from APP-FLAG expressing and mock transfected SH-SY5Y cells were subjected to immunoblot analysis to determine the APP protein expression

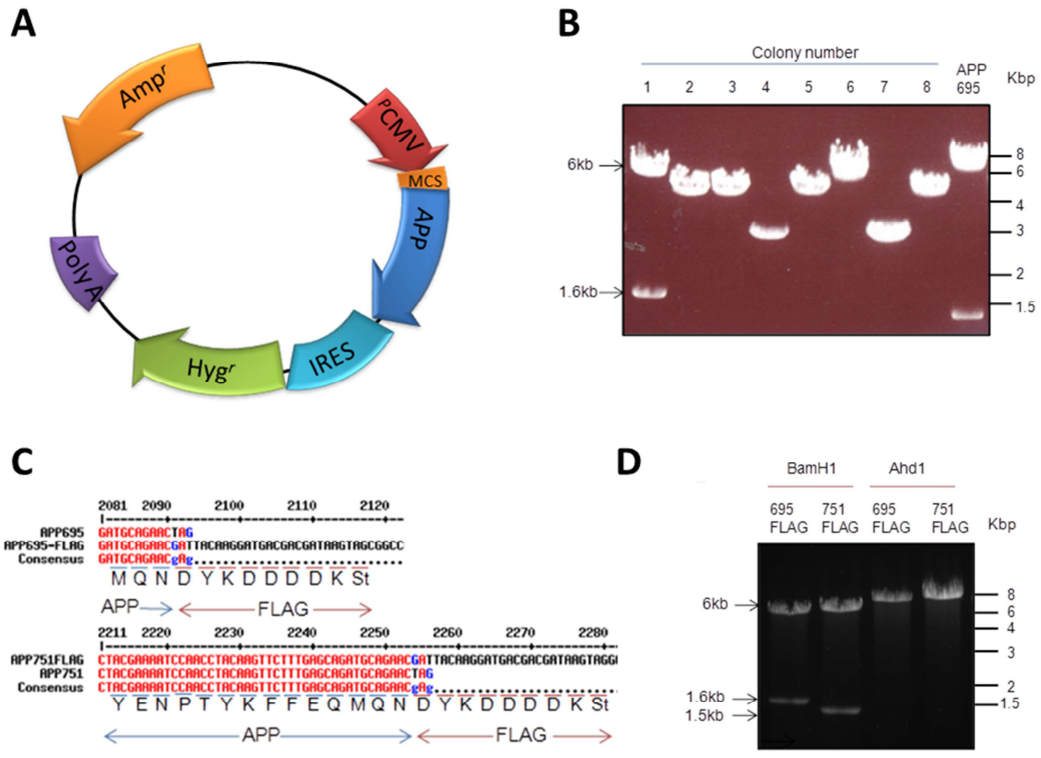

Figure 3.1 Production of APP-FLAG constructs

A) APP695 and APP751 were both in the vector pIREShyg (Clontech) (Amp^r - ampicillin resistance gene, ^{P}CMV – human cyclomegalovirus promoter, MCS – multiple cloning site, IRES – internal ribosome entry site, Hyg^r – hygromycin phosphotransferase gene). **B)** Following PCR to amplify the APP695 cDNA, subsequent ligation of the PCR product back into the pIREShyg vector and bacterial transformation, colonies were screened using the BamHI restriction enzyme to identify any DNA products which cut according to expectations as seen in lane 1 (APP695-FLAG – 6000bp and 1665bp). **C)** Following identification of DNA indicative of having incorporated the FLAG-tag from both APP695 PCR technique and APP751 site-directed mutagenesis, the DNA was sent for sequencing and sequences were aligned with the original APP sequences to identify those with the FLAG-tag. **D)** Following amplification of the DNA, FLAG-tagged constructs were screened a final time with restriction enzymes to ensure appropriate fragmentation predicted from the DNA sequence (APP695-FLAG; BamHI – 1665bp and 6000bp and AdhI – 7800bp, APP751-FLAG; BamHI – 1500bp and 6500bp and AhdI – 8000bp).

and ensure that the addition of the FLAG-tag to the C-terminus of APP did not alter its proteolysis (**Figure 3.2A**). The molecular weight marker (kDa) is indicated on the left of the blot panels in this, and all subsequent blots. Quantification showed comparable expression of the APP isoforms, when corrected for the level of APP in the mock transfected cells (**Figure 3.2B)**. Similar to the results presented by Belyaev et al. (2010) densitometric analysis showed 48% less sAPPα (**Figure 3.2C**) and 80% less sAPPβ (**Figure 3.2D**) in the conditioned cell medium from the APP751-FLAG expressing cells compared to the APP695-FLAG expressing cells. To confirm the results observed from immunoblotting, which is considered a semi-quantitative method, sAPPα, sAPPβ and Aβ in conditioned cell medium were all quantified using an ELISA based system developed by MSD. These multiplexing assays allow for the simultaneous quantification of sAPPα and sAPPβ (F**igure 3.3A**) or Aβ38, Aβ40 and Aβ42 (**Figure 3.3B**) in a single well of a 96-well ELISA plate, requiring greatly reduced volumes of conditioned cell medium, shorter incubation times and circumventing the need for the conditioned cell medium to be concentrated. MSD analysis showed 75% less sAPPα and 85% less sAPPβ in the conditioned cell medium from the APP751-FLAG expressing cells compared to the APP695-FLAG expressing cells when corrected to account for soluble fragments from endogenous APP (**Figure 3.3C**). Concomitantly, 85% less Aβ was observed for all three measured Aβ species, in the conditioned cell medium from the APP751-FLAG expressing cells compared to the APP695-FLAG expressing cells (**Figure 3.3D**). As the ε-cleavage by the γ-secretase influences the species of Aβ eventually liberated (see **Figure 1.2B**) and thus the amyloidogenic potential of the molecule, the ratio of the Aβ species were compared between the two cell lines. No significant differences were observed in the ratio of Aβ40:Aβ42 (**Figure 3.3E)**, Aβ38:Aβ42 (**Figure 3.3F**) or Aβ40:Aβ38+Aβ42 (**Figure 3.3G**) in the conditioned cell medium from the two APP isoforms.

In order to determine any differences in the dynamics of APP isoform trafficking, we sought to study live trafficking of APP in SH-SY5Y cells, and proposed co-transfection of APP695-Cherry and APP751-EGFP as a mechanism for determining whether APP isoforms co-localised when co-expressed. APP695-EGFP and APP695-Cherry constructs were in the vectors EGFP and pCi-Neo, respectively. In order to allow comparative analysis of APP695 and APP751, cDNA encoding APP751 was amplified by PCR and cloned into the pEGFP-N1 vector between the HindIII and SalI restriction sites. Full DNA sequencing was used to confirm the insertion of the APP coding sequence, with correct in-frame insertion to ensure the C-terminal expression of the EGFP fusion protein. The constructs were subsequently transiently transfected into SH-SY5Y cells and the expression of EGFP, APP695-EGFP, APP751-EGFP and AP695-Cherry was initially confirmed by IFM (**Figure 3.4**). Imaging indicated successful transfection of the cells and the fluorescence

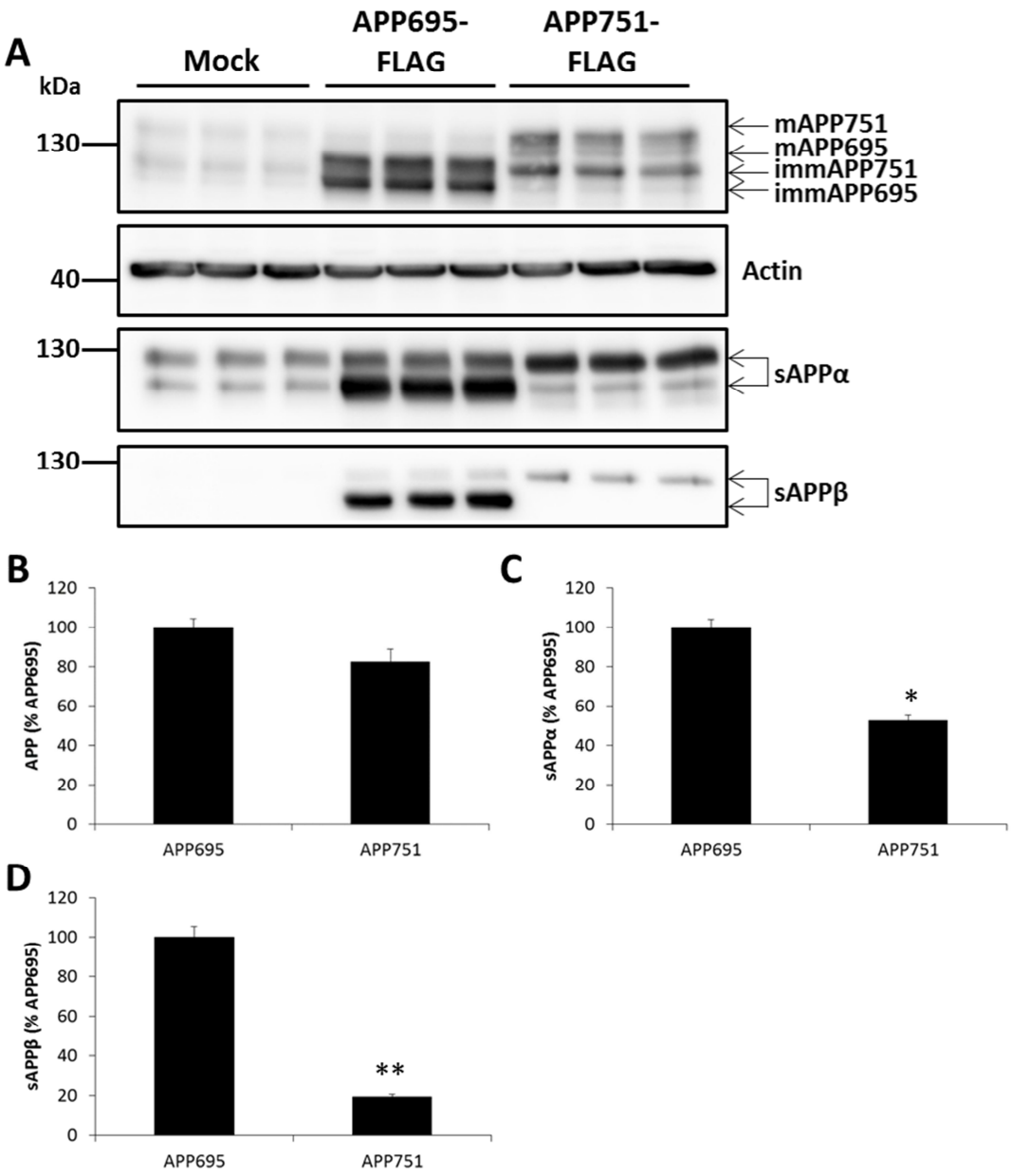

Figure 3.2 Expression and proteolysis of FLAG-tagged APP constructs

SH-SY5Y cells stably expressing APP695-FLAG or APP751-FLAG in the vector pIREShyg, or mock transfected cells expressing vector only were cultured for 24 h in Opti-MEM and the conditioned cell medium was collected and concentrated and cells were lysed in lysis buffer. **A)** The cell lysates were subjected to immunoblot analysis for APP, where four prominent bands were observed corresponding to immature (imm) and mature (m) forms of the two APP isoforms, and for actin. The concentrated conditioned cell medium was subjected to immunoblot analysis for sAPPα and sAPPβ. Densitometric analysis of **B)** APP **C)** sAPPα and **D)** sAPPβ corrected for the amount present in mock expressing cell lysates or conditioned cell medium. Bars represent the mean, error bars are ± S.E.M, *, $p<0.05$, **, $p<0.01$, n=3.

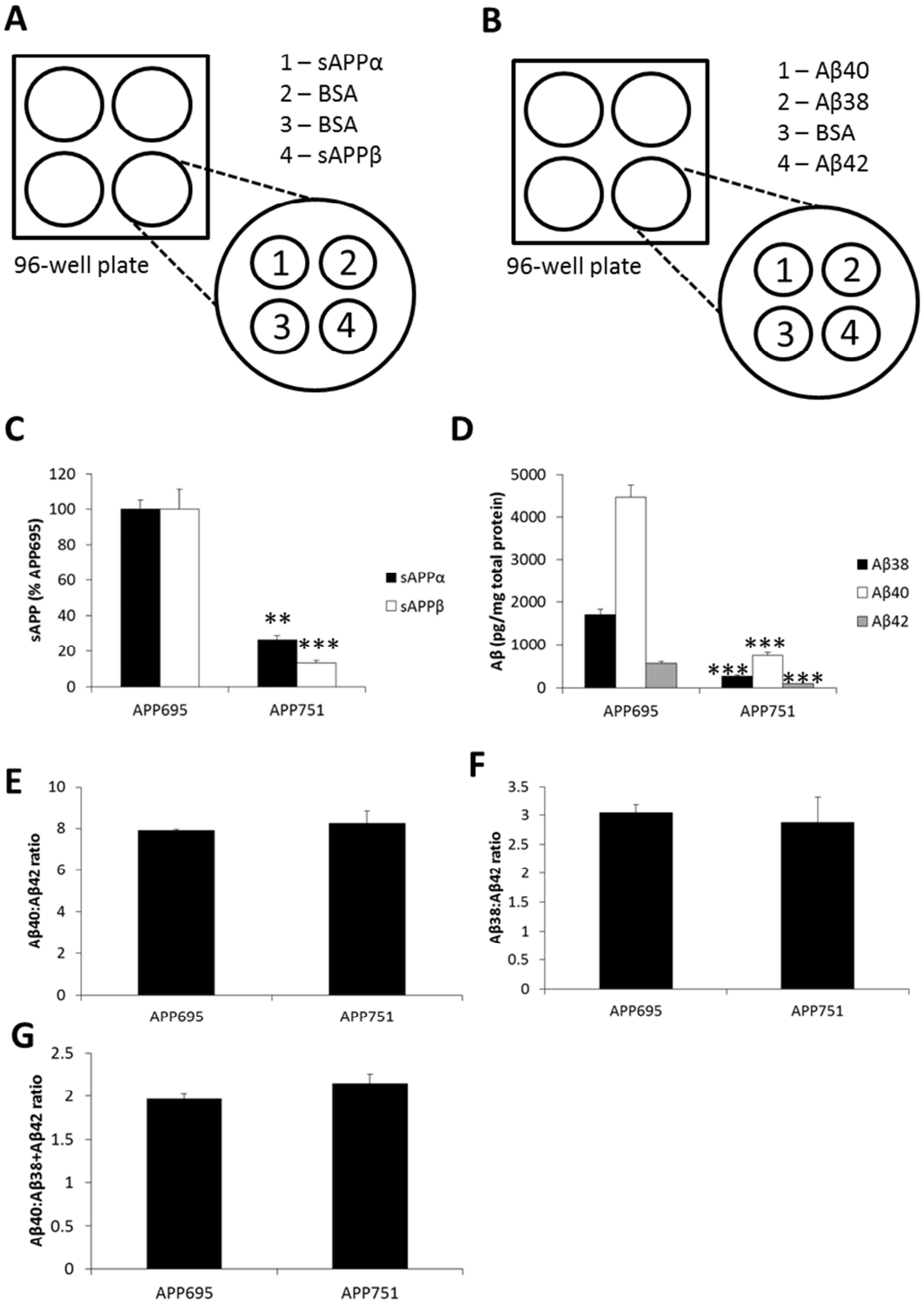

Figure 3.3 APP isoform proteolysis analysis by Meso Scale Discovery

Figure legend overleaf.

Figure 3.3 cont. APP isoform proteolysis analysis by Meso Scale Discovery

MSD assays provide a multiplexing platform allowing parallel measurement of **A)** sAPPα and sAPPβ or **B)** Aβ38, Aβ40 and Aβ42 in a single well of a 96 well plate on 25µl of conditioned cell medium with specific antibodies linked to four spots within each well. MSD analysis of **C)** sAPPα and sAPPβ and **D)** Aβ38, Aβ40 and Aβ42 in the conditioned cell medium from SH-SY5Y cells expressing APP695-FLAG or APP751-FLAG, corrected for the amount observed in mock transfected cell medium. The ratio of **E)** Aβ40:Aβ42, **F)** Aβ38:Aβ42, **G)** Aβ40:Aβ38+Aβ42. Bars represent the mean, error bars are ± S.E.M, **, $p<0.01$, ***, $p<0.001$, n=3.

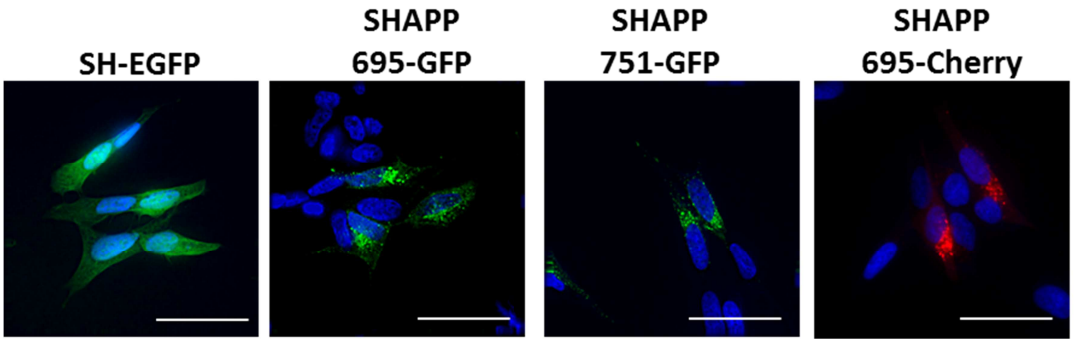

Figure 3.4 Expression of fluorescent APP constructs

SH-SY5Y cells were transiently transfected with 2.5µg of cDNA encoding GFP, APP695-GFP, APP751-GFP or APP695-Cherry using trans-LT1 transfection reagent for 24 h. Cells were subsequently fixed and mounted and the expression of exogenous protein was determined by IFM. Scale bar = 50 µm.

appeared largely perinuclear, with some punctate staining also observed, consistent with APP being present mainly in the TGN and endocytic vesicles (Thinakaran and Koo 2008).

Subsequently, SH-SY5Y cells were transiently transfected with the cDNA encoding APP695-GFP, APP751-GFP, APP695-Cherry or vector only controls (EGFP or pCI-Neo), and APP expression was confirmed by immunoblot analysis using anti-APP and anti-GFP antibodies (**Figure 3.5A**). Expression levels varied for all constructs between experiments. An average 2.9-fold, 3.1-fold, and 2.5-fold over-expression of APP was determined by densitometry for APP695-GFP, APP751-GFP and APP695-Cherry, respectively, compared to the amount of APP in their comparative mock transfected control cell line (determined from the APP blot with 22C11) (**Figure 3.5B**). No significant difference in sAPPα or sAPPβ was observed in the conditioned cell medium from cells expressing APP695-EGFP, APP751-EGFP or APP695-Cherry over their respective mock transfected controls (**Figure 3.5C**). No significant differences were observed for any Aβ species in the conditioned cell medium from cells expressing APP695-EGFP, APP751-EGFP or APP695-Cherry over their relative mock transfected control (**Figure 3.5D**) despite apparent over-expression determined by both IFM and immunoblot analyses. The lack of apparent proteolysis of these constructs also meant that no difference in isoform proteolysis could be observed. For this reason experiments were not continued with the APP-EGFP constructs.

3.2.2 The subcellular location of the APP isoforms varies and contributes to differential proteolysis

The subcellular location of APP has been widely reported to influence its proteolysis (for reviews see (Thinakaran and Koo 2008;Haass et al. 2012;Rajendran and Annaert 2012;Jiang et al. 2014)), and thus could be a contributing factor in the differential proteolysis of the APP isoforms. Following the addition of the FLAG-tag to our APP construct, we were able to compare the location of APP isoforms within SH-SY5Y cells by studying co-localisation with various subcellular markers. Cells expressing APP695-FLAG or APP751-FLAG were seeded onto glass coverslips and cultured overnight before being fixed and permeabilised. Anti-FLAG antibodies were then used to specifically identify the expressed APP isoform within the cell, alongside antibodies raised against TGN-46, a TGN marker (**Figure 3.6A**), Rab5a, an early endosome marker (**Figure 3.6B**), Rab11a, a recycling endosome marker (**Figure 3.6C**) and Rab7, a late endosome marker (**Figure 3.6D**). Mock transfected cells were also prepared to ensure specific labelling of APP-FLAG by the FLAG antibody (data not shown). Quantification of co-localisation between APP and the subcellular marker was performed using Image J and showed subtle differences in co-localisation of APP isoforms with specific subcellular markers. APP751 showed greater co-localisation with TGN-46 (**Figure 3.6E**) and Rab5a (**Figure 3.6F**), APP695

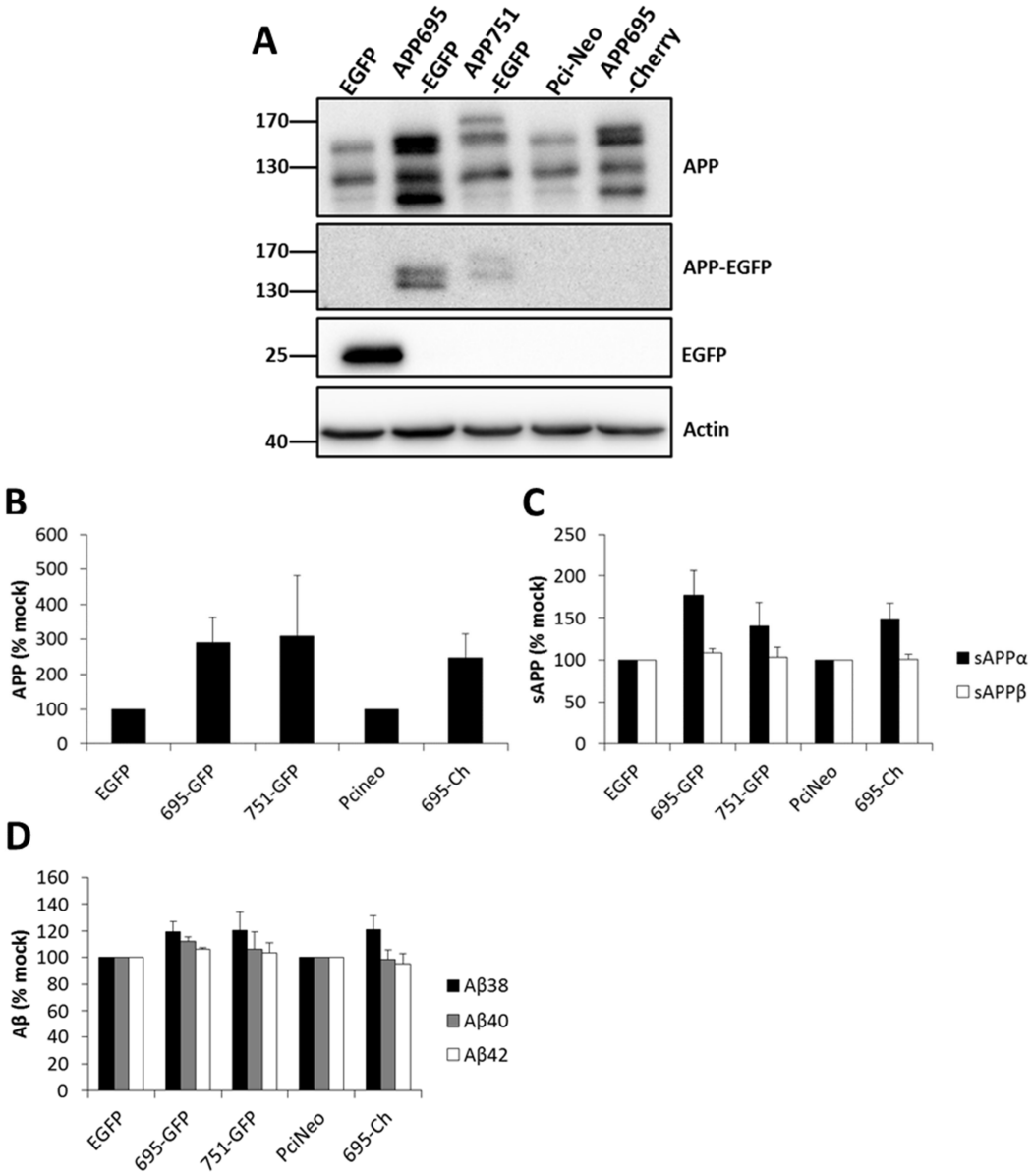

Figure 3.5 Expression and proteolysis of fluorescent APP

SH-SY5Y cells were transiently transfected with 2.5µg of cDNA encoding EGFP, APP695-GFP, APP751-GFP, APP695-Cherry or pCiNeo vector (as a vector only control for APP695-Cherry) using trans-LT1 transfection reagent and cultured for 24 h. The cell medium was subsequently replaced with Opti-MEM and cells were cultured for a further 6 h. **A)** Cells were lysed and subjected to immunoblot analysis for APP, GFP, and actin. **B)** Densitometric analysis of APP (from the APP blot, shown in the top panel) **C)** MSD analysis of sAPPα and sAPPβ in the conditioned cell medium from transiently transfected cells. D) MSD analysis of Aβ in conditioned medium from transiently transfected cells. Bars represent the mean, error bars are ± S.E.M, n=3.

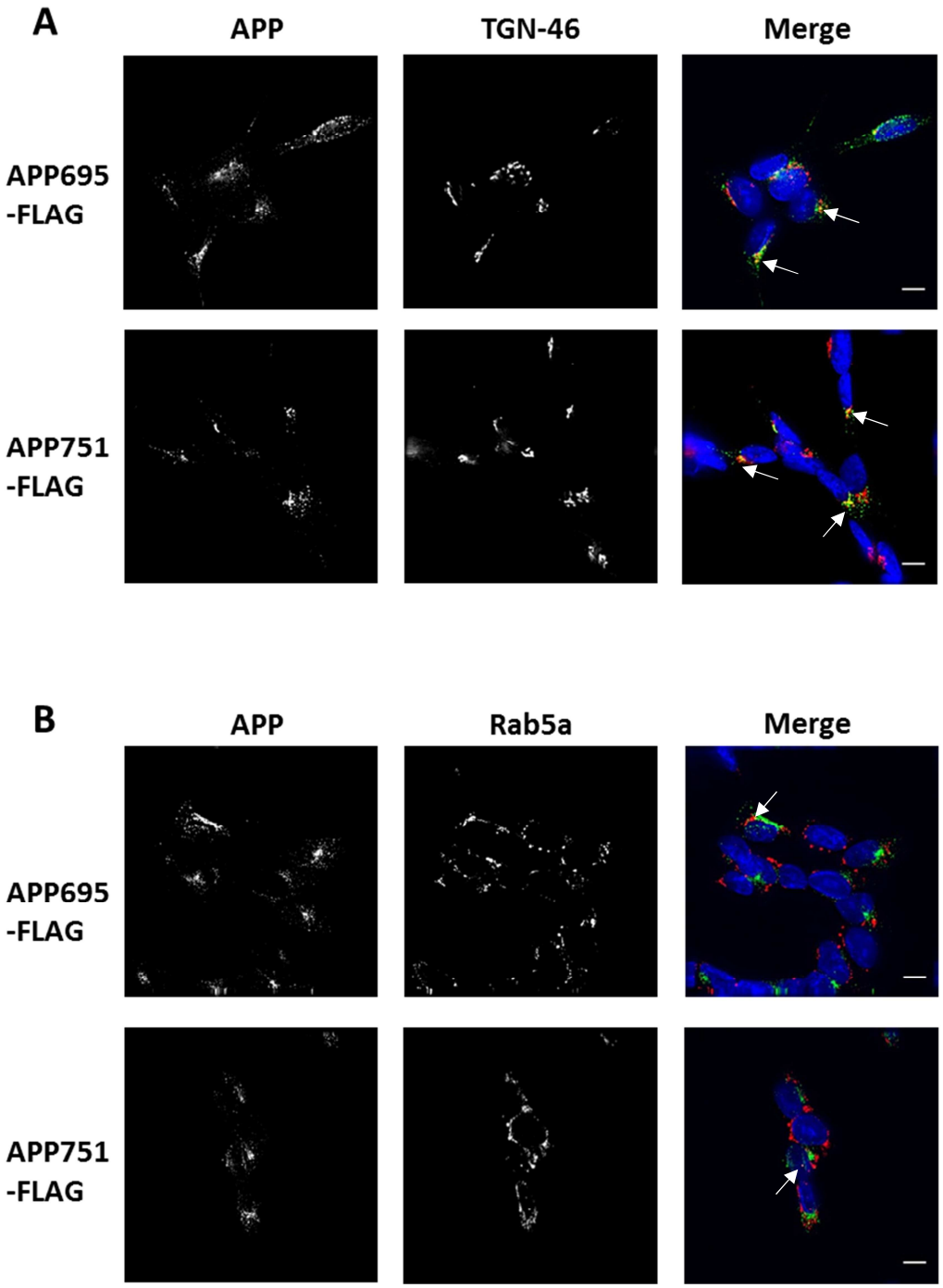

Figure 3.6 The APP isoforms show subtle variations in subcellular distribution

Figure continued overleaf.

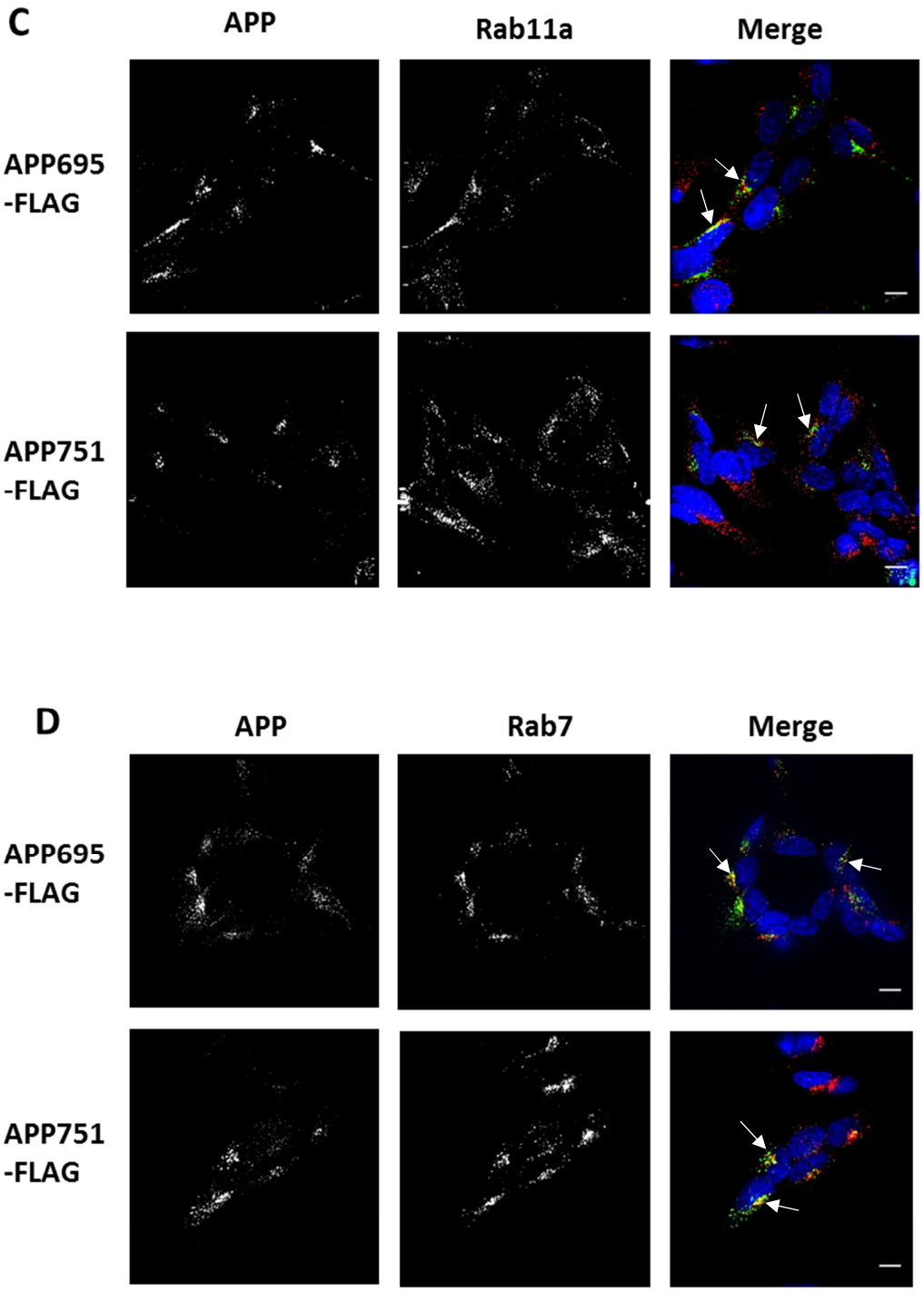

Figure 3.6 cont. The APP isoforms show subtle variations in subcellular distribution

Figure continued overleaf.

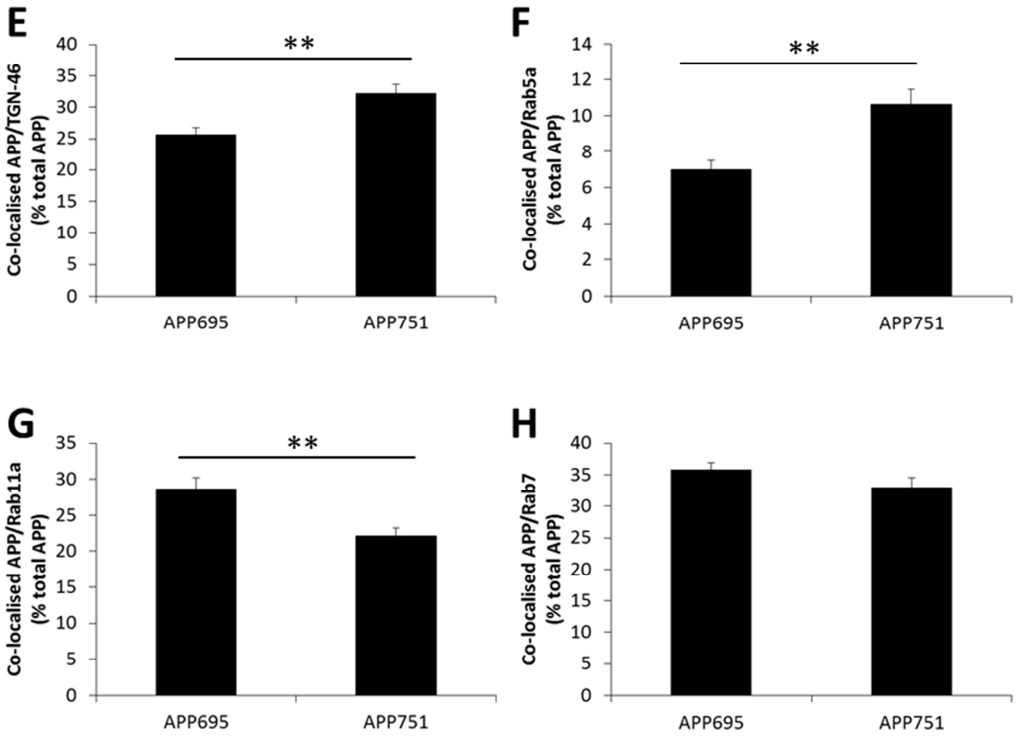

Figure 3.6 cont. The APP isoforms show subtle variations in subcellular distribution

SH-SY5Y cells expressing APP695-FLAG or APP751-FLAG cultured on glass cover slips were fixed and permeabilised. Coverslips were then incubated with anti-FLAG monoclonal antibody and an antibody raised against subcellular markers for **A)** the TGN (TGN-46), **B)** early endosomes (Rab5a), **C)** recycling endosomes (Rab11a) or **D)** late endosomes (Rab7). Mock transfected cells were also immunostained to ensure specific labelling of APP-FLAG (data not shown). Cover slips were subsequently incubated with anti-mouse Alexa fluor-488 fluorescent secondary antibody to detect APP-FLAG and anti-rabbit Alexa fluor-594 fluorescent secondary antibody to detect the subcellular marker. Cells were imaged and co-localisation between APP and the subcellular marker quantified for **E)** TGN-46, **F)** Rab5a, **G)** Rab11a and **H)** Rab7 using Image J. Scale bars = 10 µm. Bars represent the mean, error bars are ± S.E.M, **, $p < 0.01$, $n>75$ cells from 3 experimental replicates. In merge images, blue is nuclear (DAPI) staining, green is APP staining and red is subcellular marker staining. Regions of co-localisation are highlighted with white arrows.

showed greater co-localisation with Rab11a (**Figure 3.6G**) and no significant difference between the isoforms was observed in the co-localisation with Rab7 (**Figure 3.6H**).

Previous reports have indicated APP bearing the Swedish mutation is subjected to proteolysis in the secretory pathway (Haass et al. 1995) so we sought to determine whether the incorporation of this mutation into the APP isoforms reduced their differential proteolysis in our SH-SY5Y cells. Cell lysates and concentrated conditioned cell medium from SH-SY5Y cells expressing $APP695_{SWE}$ and $APP751_{SWE}$ were subjected to immunoblot analysis for APP and sAPPβ (**Figure 3.7A**). Due to mutation of the C-terminal residues of sAPPβ in the Swedish mutant, blots for $sAPP\beta_{SWE}$ had to be carried out separately meaning direct comparison of sAPPβ from APP_{WT} and APP_{SWE} is not possible by immunoblot analysis. Significantly less sAPPβ (reduced by 50%) was observed in conditioned cell medium from $APP751_{SWE}$ expressing cells compared to $APP695_{SWE}$ expressing cells (**Figure 3.7B**).

To determine whether the differences observed in subcellular location could influence APP proteolysis, we investigated the effect of Rab11a knockdown on APP proteolysis in APP695-FLAG and APP751-FLAG expressing cells. Rab11a has previously been identified as a modulator of BACE1 trafficking and was shown to influence APP proteolysis in a HeLa cell system (Udayar et al. 2013), while recycling endosomes have also been proposed as site of direct APP proteolysis (Das et al. 2013). IFM data had also indicated greater co-localisation between APP695 and Rab11a compared to APP751 (see **Figure 3.6**). APP695-FLAG and APP751-FLAG expressing SH-SY5Y cells were transfected with 50 nM siRNA against Rab11a for 48 h, and were subsequently cultured in Opti-MEM for 6 h. The conditioned cell medium was removed and the cells were lysed and the cell lysates were subjected to immunoblot analysis for APP, Rab11a and actin (**Figures 3.8A and 3.8B**). Rab11a was knocked down by 62% in the APP695-FLAG expressing cells (**Figure 3.8C**) and by 69% in the APP751-FLAG expressing cells (**Figure 3.8D**). APP was not significantly altered in either APP expressing cell line upon knockdown of Rab11a (**Figure 3.8E and 3.8F**). MSD analysis on the conditioned cell medium showed no significant difference in sAPPα or sAPPβ in either the APP695-FLAG expressing cells (**Figure 3.8G**) or the APP751-FLAG expressing cells (**Figure 3.8H**) upon Rab11a knockdown. MSD analysis for Aβ showed significantly less Aβ38 (reduced by 15%), Aβ40 (reduced by 17%) and Aβ42 (reduced by 18%) in the conditioned cell medium from the APP695-FLAG expressing cells upon Rab11a knockdown (**Figure 3.8I**). No significant difference was observed for any Aβ species in the conditioned cell medium from the APP751-FLAG expressing cells following Rab11a knockdown (**Figure 3.8J**).

The presence of APP at the cell surface and its subsequent endocytosis has been shown to be important in Aβ generation (Cirrito et al. 2008). Given that, in addition to the reduced sAPPβ

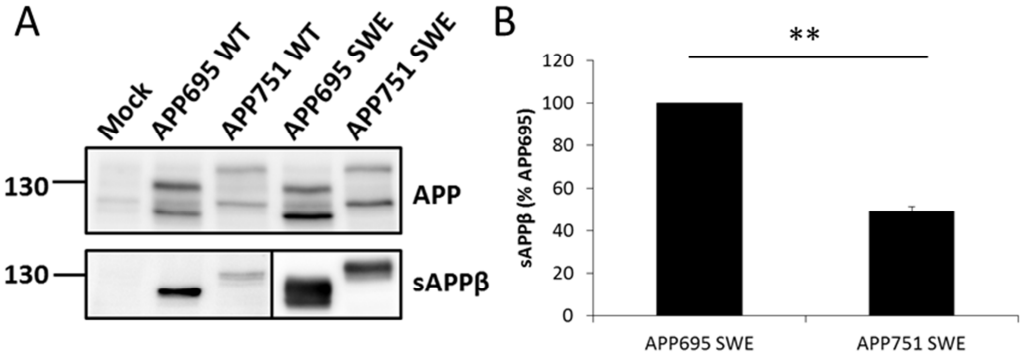

Figure 3.7 The APP isoforms bearing the Swedish mutation maintain their differential amyloidogenic proteolysis

SH-SY5Y cells expressing $APP695_{WT}$, $APP751_{WT}$, $APP695_{SWE}$ or $APP751_{SWE}$ were cultured in Opti-MEM for 24 h. The conditioned cell medium was concentrated and the cells were lysed. **A)** Cell lysates were subjected to immunoblot analysis for APP and the conditioned cell medium was subjected to immunoblot analysis for sAPPβ and $sAPP\beta_{SWE}$. **B)** Densitometric analysis of $sAPP\beta_{SWE}$. Bars represent the mean, error bars are ± S.E.M, **, $p < 0.01$, n=3.

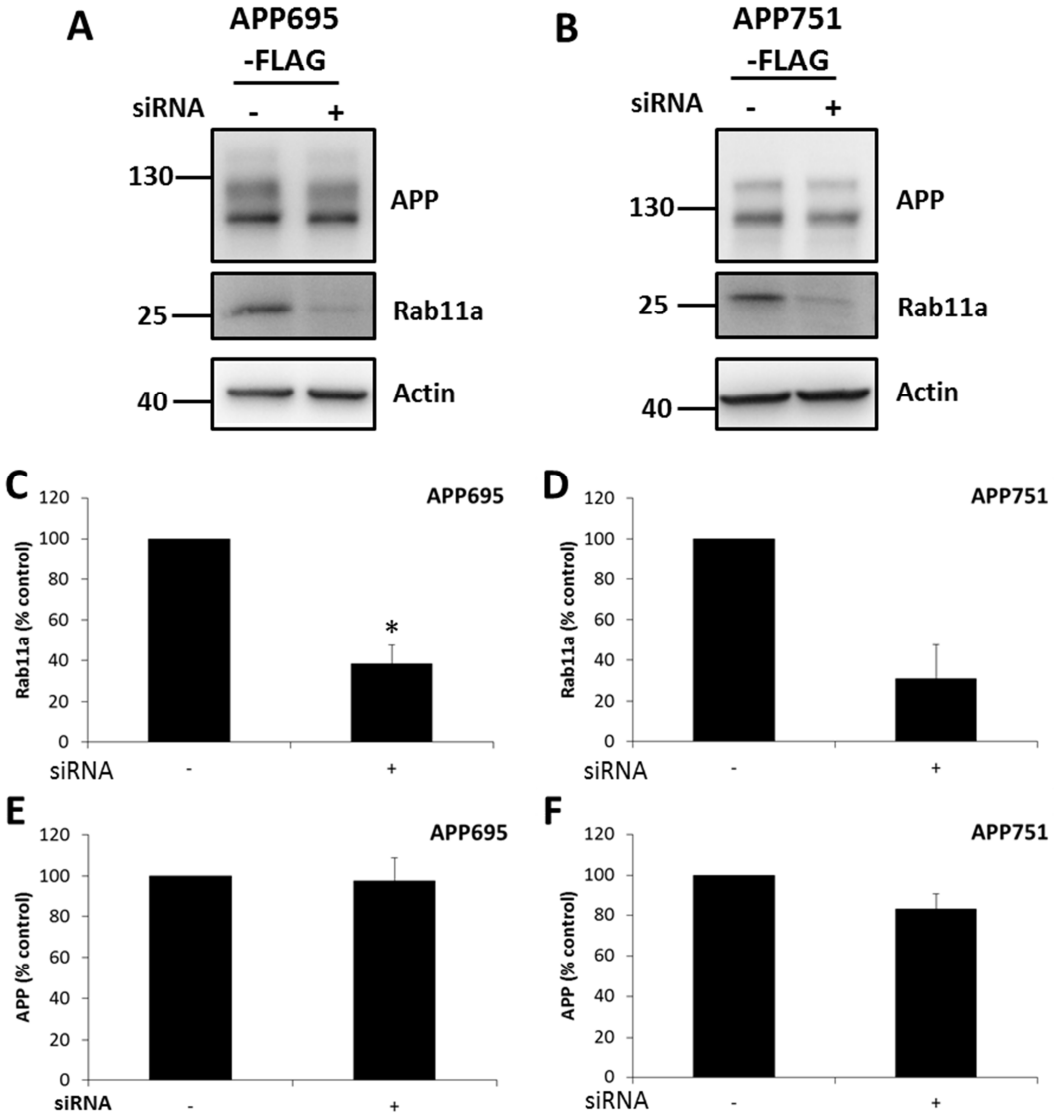

Figure 3.8 Rab11a knockdown decreases Aβ in APP695-FLAG, but not APP751-FLAG, expressing cells

Figure continued overleaf.

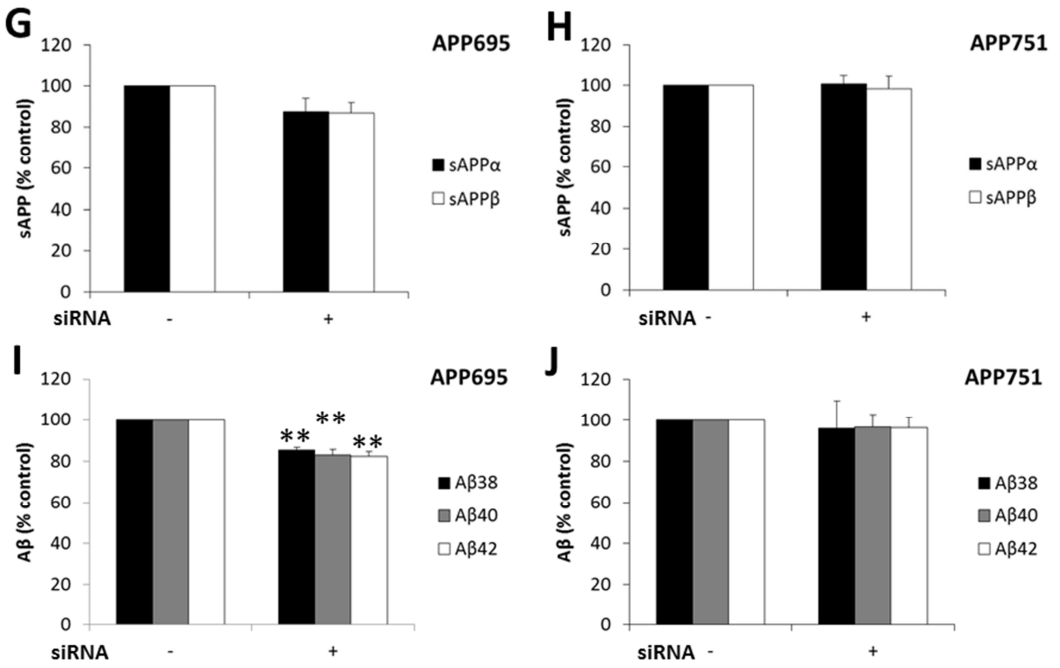

Figure 3.8 cont. Rab11a knockdown decreases Aβ in APP695-FLAG, but not APP751-FLAG, expressing cells

Rab11a was knocked down in **A)** APP695-FLAG expressing and **B)** APP751-FLAG expressing SH-SY5Y cells using 50 nM smartpool siRNA complexed with DharmaFECT 1 transfection reagent in DMEM for 48 h. The cell medium was replaced with Opti-MEM and cells were cultured for a further 6 h. Cells were lysed and subjected to immunoblot analysis for APP, Rab11a and actin. Densitometric analysis of Rab11a in **C)** APP695-FLAG expressing cells and **D)** APP751-FLAG expressing cells. Densitometric analysis of APP in **E)** APP695-FLAG expressing cells and **F)** APP751-FLAG expressing cells. MSD analysis for sAPPα and sAPPβ in the conditioned cell medium from **G)** APP695-FLAG expressing cells and **H)** APP751-FLAG expressing cells. MSD analysis for Aβ38, Aβ40, and Aβ42 in the conditioned cell medium from **I)** APP695-FLAG expressing cells and **J)** APP751-FLAG expressing cells. Bars represent the mean, errors bars are ± S.E.M., *, p-value<0.05, **, p-value <0.01, n=3.

and Aβ production, significantly less sAPPα was observed in the conditioned cell medium from APP751-FLAG expressing cells compared to APP695-FLAG expressing cells, we postulated that there may be increased APP695 localisation to the cell surface. SH-SY5Y cells expressing APP695-FLAG or APP751-FLAG were labelled with 0.5 mg/ml sulpho-NHS-SS-biotin or with DMSO as a control for 30 min at 4°C to label proteins at the cell surface, before being washed and lysed. Biotin labelled proteins were then immunoprecipitated from cell lysates using streptavidin agarose beads and the input and biotin labelled samples were subjected to immunoblot analysis for APP and actin. Control experiments (no biotin) showed no APP immunoprecipitated in the bound fractions. Biotin labelling resulted in the pulldown of APP from both the APP695-FLAG expressing cells and the APP751-FLAG expressing cells but no pulldown of actin which should not have been labelled due to its cytosolic nature (**Figure 3.9A**). Densitometric analysis showed 37% less APP751-FLAG was present at the cell surface compared to APP695-FLAG when corrected for the amount of APP in the input cell lysates (**Figure 3.9B**). Further attempts were made to confirm this result using flow cytometry. Unfortunately none of the antibodies employed for this technique showed consistently increased cell fluorescence compared to the mock transfected cells, suggesting they did not specifically bind APP on the cell surface in this live cell technique.

To determine whether subsequent endocytosis of APP from the cell surface differentially affects the proteolysis of the APP isoforms, SH-SY5Y cells expressing APP695-FLAG or APP751-FLAG were cultured in Opti-MEM containing the dynamin inhibitor Dynasore (100 μM) to inhibit endocytosis. This concentration was previously employed to determine the effect of APP endocytosis on Aβ production in a HeLa cell system (Chun et al. 2015). Cells were subsequently lysed and subjected to immunoblot analysis for APP and actin (**Figures 3.10A and 3.10B**). APP was significantly increased following treatment with Dynasore in APP695-FLAG expressing cells (2-fold increase) (**Figure 3.10C**) and in APP751-FLAG expressing cells (1.8-fold increase) (**Figure 3.10D**). The ratio of mature to immature APP in the cell lysates was significantly reduced by treatment with Dynasore in APP695-FLAG expressing cells (**Figure 3.10E**) and in APP751-FLAG expressing cells (**Figure 3.10F**). MSD analysis showed Dynasore treatment significantly reduced sAPPα and sAPPβ in the conditioned cell medium from the APP695-FLAG expressing cells (reduced by 71% and 70%, respectively) (**Figure 3.10G**) and the APP751-FLAG expressing cells (reduced by 70% and 63%, respectively) (**Figure 3.10H**). Dynasore treatment significantly reduced Aβ38, Aβ40 and Aβ42 in the conditioned cell medium from the APP695-FLAG expressing cells (reduced by 70%, 71% and 62%, respectively) (**Figure 3.10I**) and the APP751-FLAG expressing cells (reduced by 59%, 66% and 50%, respectively) (**Figure 3.10J**). No significant

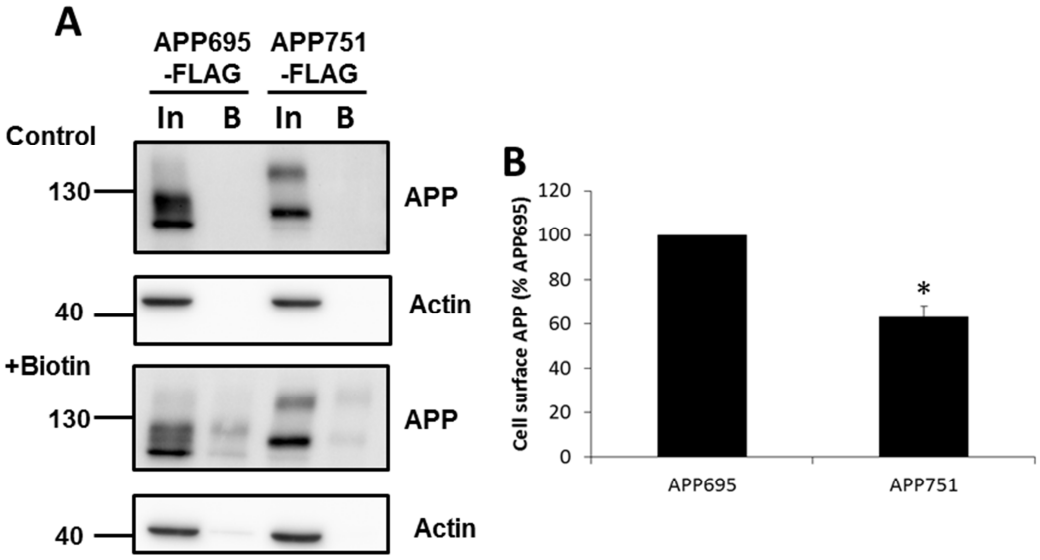

Figure 3.9 More APP695 is present at the cell surface than APP751

SH-SY5Y cells expressing APP695-FLAG or APP751-FLAG were incubated with 0.5 mg/ml sulpho-NHS-SS-Biotin or vehicle only control (DMSO) in $PBSM^{+}$ at 4°C to label cell surface proteins. Cells were washed to remove excess biotin then lysed and biotinylated proteins were pulled down using streptavidin agarose. **A)** Input (In) and bound (B) fractions were subjected to immunoblot analysis for APP and actin. **B)** Densitometric analysis of cell surface APP corrected for total APP in the cell lysates. Bars represent the mean, error bars are ± S.E.M, *, $p < 0.05$, n=3.

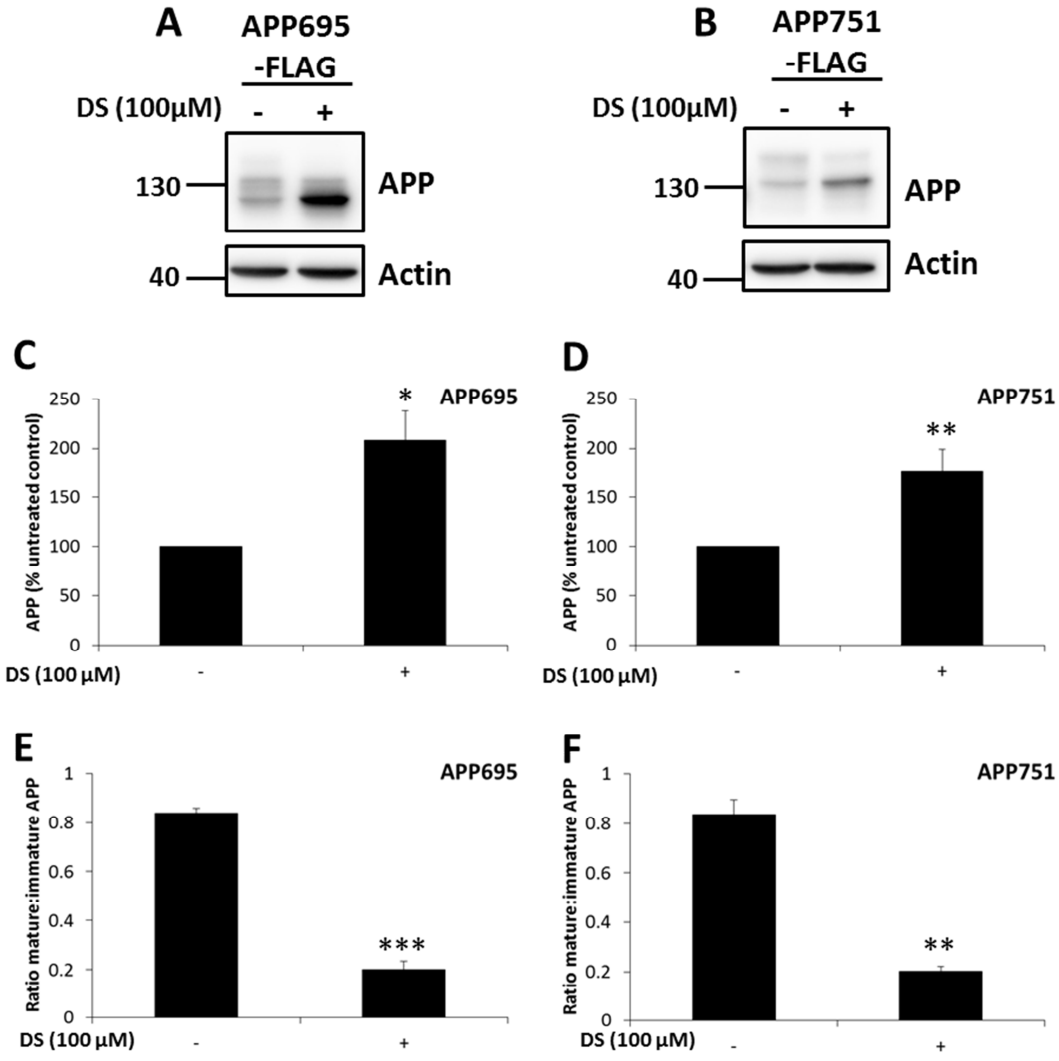

Figure 3.10 Inhibition of endocytosis decreases APP proteolysis but is not isoform specific

Figure continued overleaf.

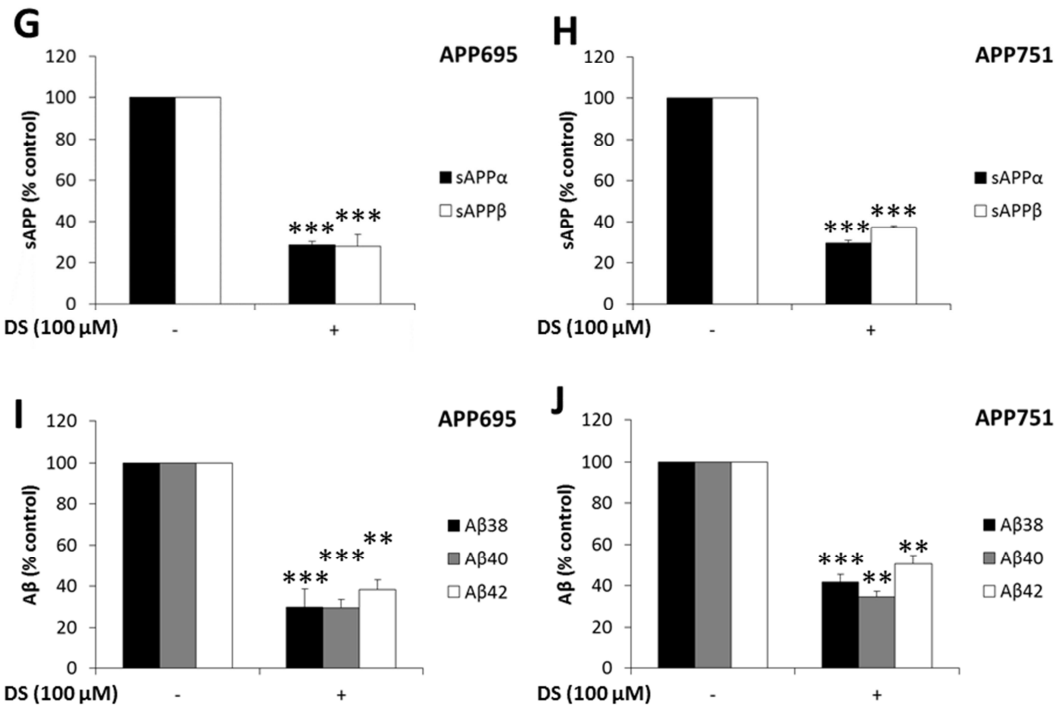

Figure 3.10 Inhibition of endocytosis decreases APP proteolysis but is not isoform specific

SH-SY5Y cell expressing **A)** APP695-FLAG or **B)** APP751-FLAG cultured for 6 h in Opti-MEM containing 100 µM Dynasore (DS) (**+**) or a DMSO only control (**-**). Cells were lysed and subjected to immunoblot analysis for APP and actin. Densitometric analysis of APP in **C)** APP695-FLAG and **D)** APP751-FLAG expressing cells. Densitometric analysis of the ratio of mature to immature APP in **E)** APP695-FLAG and **F)** APP751-FLAG expressing cells. MSD analysis for sAPPα and sAPPβ in the conditioned cell medium from **G)** APP695-FLAG and **H)** APP751-FLAG expressing cells. MSD analysis for Aβ38, Aβ40, and Aβ42 in the conditioned cell medium from **I)** APP695-FLAG and **J)** APP751-FLAG expressing cells. Bars represent the mean, errors bars are ± S.E.M., *, p-value<0.05, **, p-value <0.01, ***, p-value<0.001, n=3.

differences were observed between the two isoforms when statistical analysis was applied to the percentage reduction observed from each isoform for all measured soluble APP fragments.

Lipid rafts, cholesterol rich microdomains within the plasma membrane, have been widely implicated as sites of both APP proteolysis and toxic Aβ signalling (for a review see (Rushworth and Hooper 2010)). To investigate whether APP isoforms were specifically partitioned into these membrane microdomains, lipid raft domains were isolated using buoyant sucrose density gradient centrifugation in the presence of Triton X-100. Initial experiments showed the presence of APP in both the raft and the non-raft fractions of mock transfected SH-SY5Y cells (**Figure 3.11A**), APP695-FLAG expressing cells (**Figure 3.11B**) and APP751-FLAG expressing cells (**Figure 3.11C**). In all three cell lines, the lipid raft marker flotillin-1 was confined to fractions 6-9, with the majority present in fraction 7 in all cases. The non-raft marker, transferrin receptor, was primarily localised to fractions 1-4 in all cell lines. Despite the use of various concentrations of Triton X-100 in these experiments, all traces of transferrin receptor contamination could not be removed from the raft fractions. The raft fractions (fractions 6-8) and non-raft fractions (fractions 1-4) were subsequently pooled and subjected to immunoblot analysis for APP, flotillin-1 and transferrin receptor (**Figure 3.12A**). No significant difference was observed between raft localisation of the two APP isoforms (**Figure 3.12B**)**.** Higher transferrin receptor contamination was observed in raft fractions from APP695-FLAG expressing cells compared to APP751-FLAG expressing cells but was not statistically significant (**Figure 3.12C**).

To determine whether lipid raft disruption altered proteolysis in APP expressing SH-SY5Y cells, levels of flotillin-1 or flotillin-2 were knocked down in APP695-FLAG (**Figure 3.13A**) and APP751-FLAG expressing cells (**Figure 3.13B**) using 50 nM siRNA for 48 h. Knockdown of each flotillin was performed separately. In APP695-FLAG expressing cells 59% knockdown of flotillin-1 was observed, while a 43% knockdown was also observed for flotillin-2 (**Figure 3.13C**). In APP751-FLAG expressing cells, flotillin-1 was knocked down by 55% and flotillin-2 was knocked down by 39% (**Figure 3.13D**). No significant difference was observed on the amount of APP following knockdown of flotillin-1 or flotillin-2 in either the APP695-FLAG expressing cells (**Figure 3.13E**) or the APP751-FLAG expressing cells (**Figure 3.13F**). No significant difference was observed for sAPPα or sAPPβ in the conditioned cell medium from APP695-FLAG expressing cells following flotillin-1 or flotillin-2 knockdown (**Figure 3.13G**). No difference was observed for sAPPα in the conditioned cell medium from APP751-FLAG expressing cells following flotillin-1 or flotillin-2 knockdown (**Figure 3.13H**). A small but statistically significant reduction in sAPPβ (reduced by 5%), was observed following flotillin-1 knockdown, but no significant difference was observed following flotillin-2 knockdown in the conditioned cell medium from APP751-FLAG expressing cells (**Figure 3.13H**). No significant differences were observed in Aβ species following flotillin-1

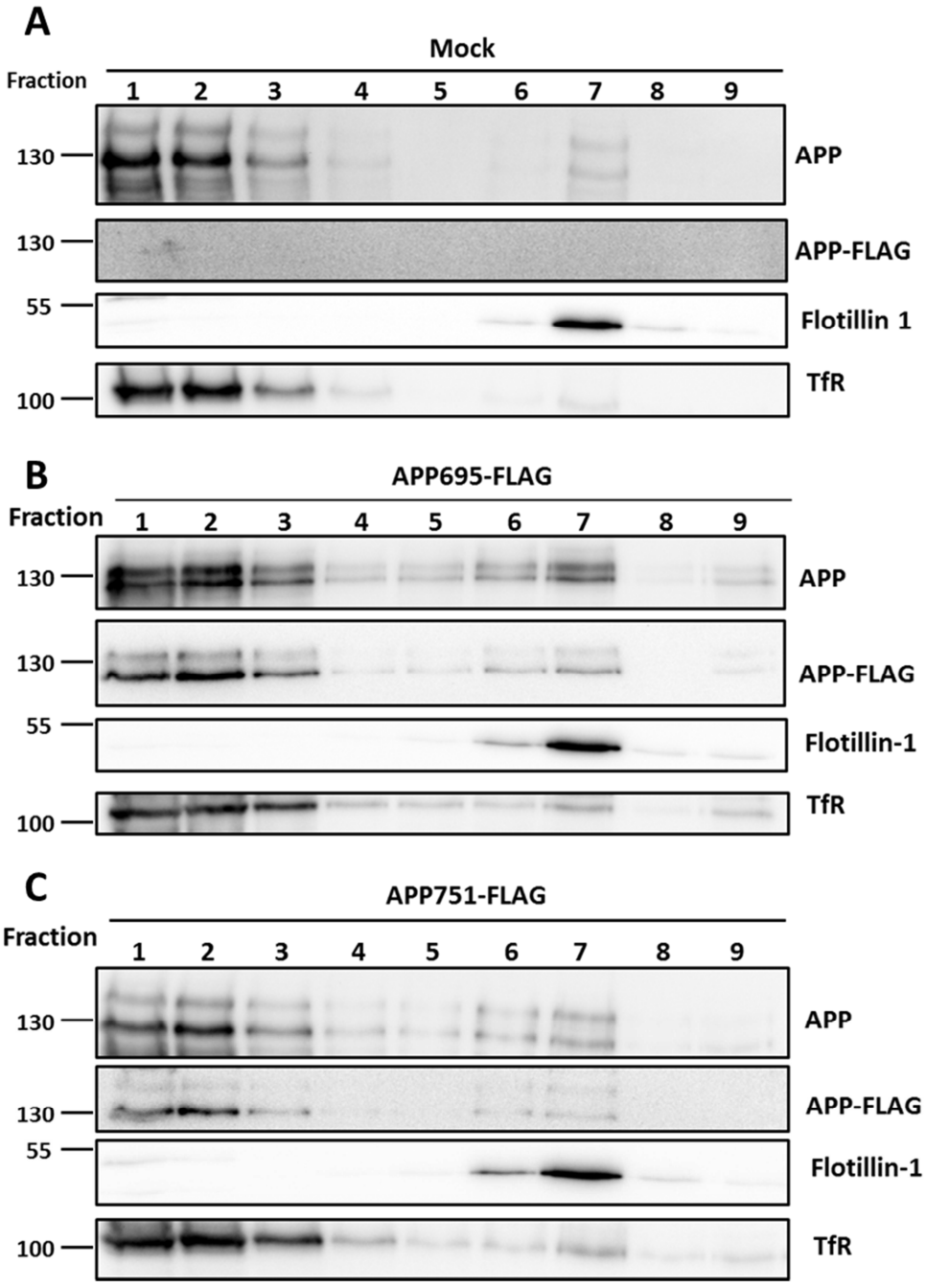

Figure 3.11 A pool of endogenous and over-expressed APP localises to lipid rafts

SH-SY5Y cells expressing A) vector only (Mock) B) APP695-FLAG or C) APP751-FLAG were subjected to lipid raft preparation. The collected fractions were subjected to immunoblot analysis for APP, APP-FLAG, Flotillin-1 and the transferrin receptor (Tfr).

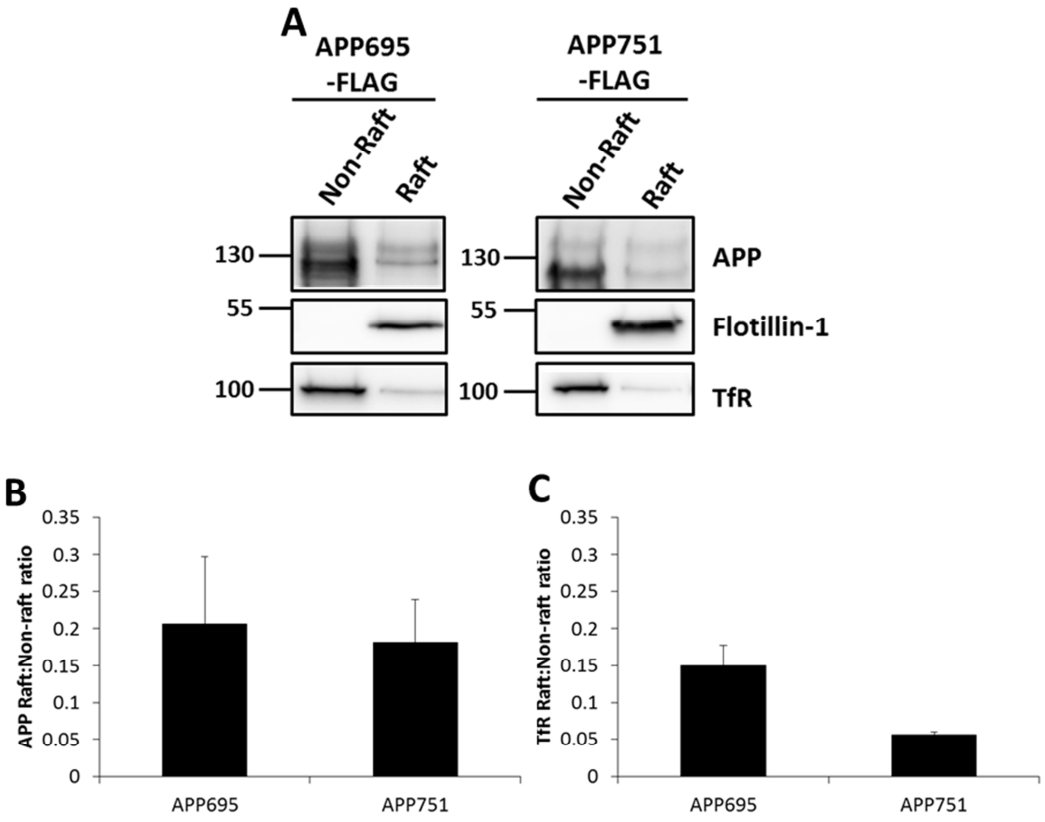

Figure 3.12 APP695-FLAG and APP751-FLAG show no difference in lipid raft distribution

Equal volumes of lipid raft preparation fractions 1-3 were combined as a total non-raft fraction and fractions 6-8 were combined as a total raft fraction. **A)** Raft and non-raft fractions from APP695-FLAG and APP751-FLAG subjected to immunoblot analysis for APP, flotillin-1 and the transferrin receptor (Tfr). **B)** The ratio of raft to non-raft APP and **C)** TfR was determined by densitometric analysis. Bars represent the mean, error bars are ± S.E.M, n=3.

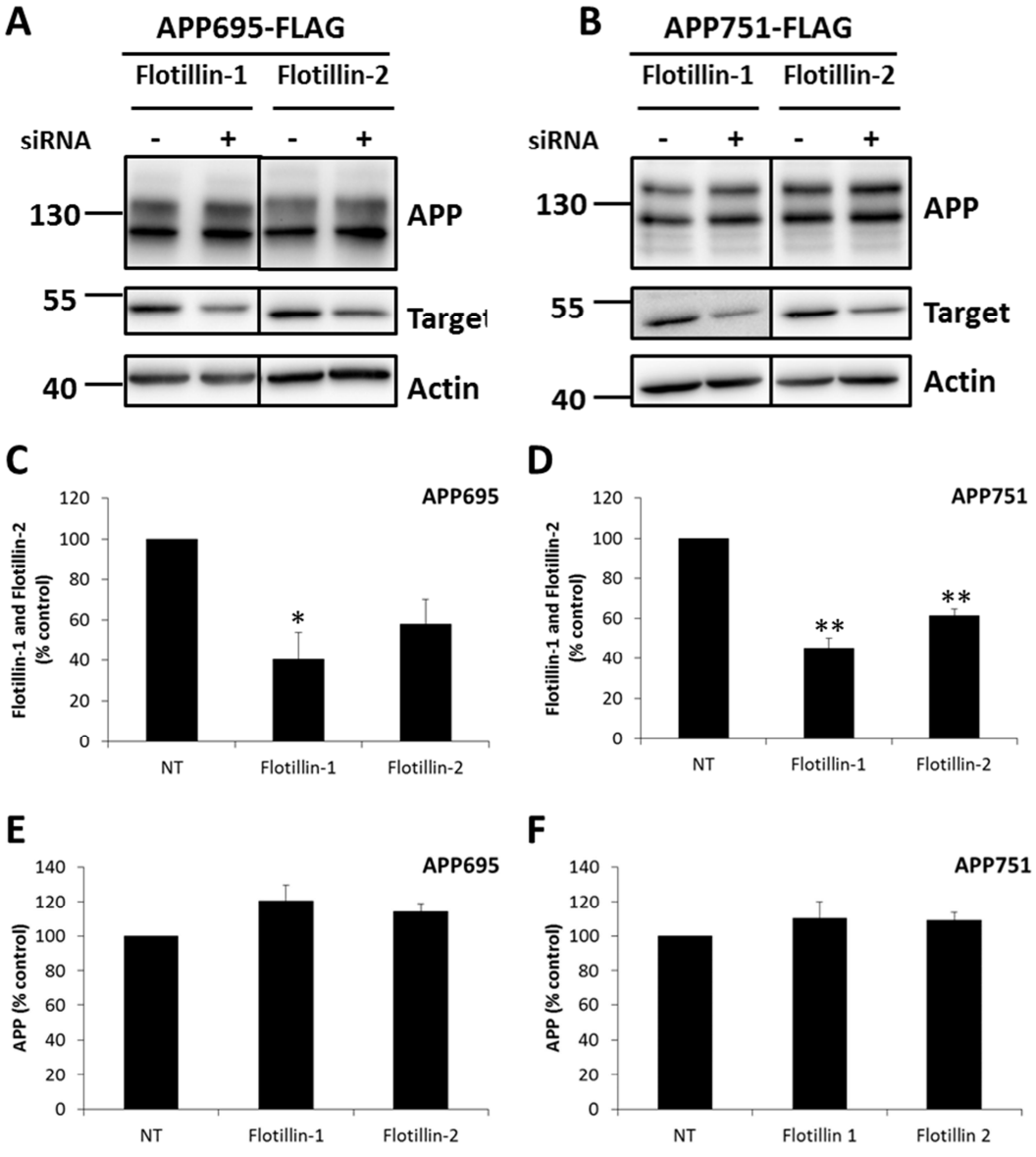

Figure 3.13 Flotillin-1 and flotillin-2 knockdown decreases Aβ in APP751-FLAG, but not APP695-FLAG, expressing cells

Figure continued overleaf.

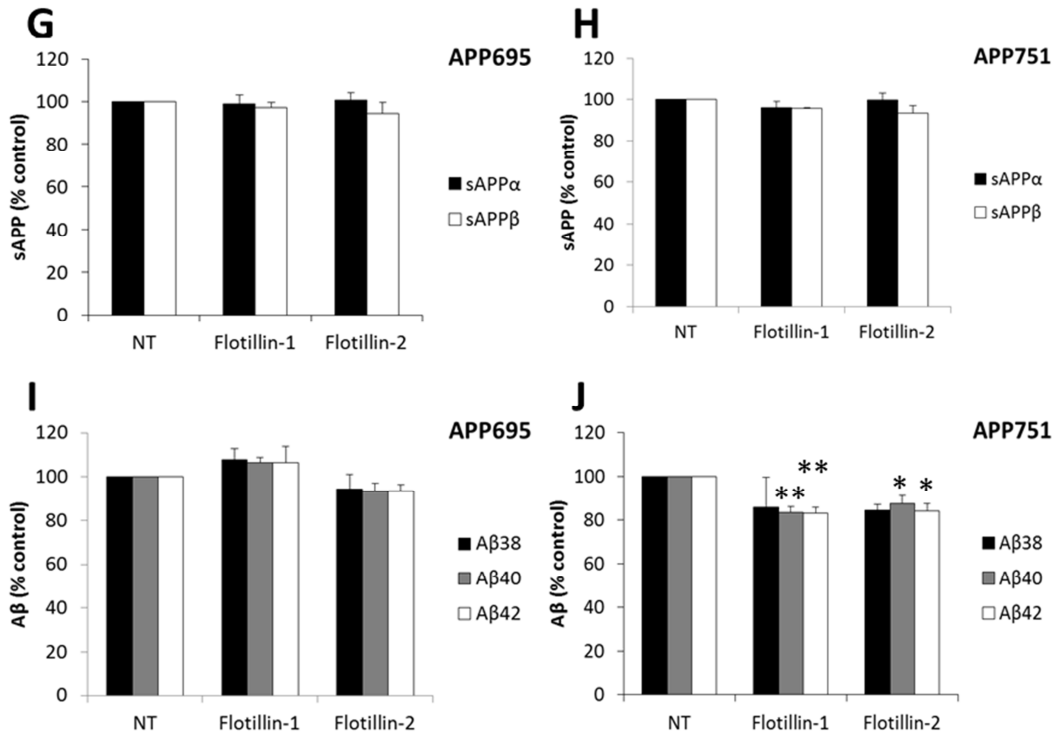

Figure 3.13 cont. Flotillin-1 and flotillin-2 knockdown decreases Aβ in APP751-FLAG, but not APP695-FLAG, expressing cells

Flotillin-1 or flotillin-2 were knocked down in **A)** APP695-FLAG expressing and **B)** APP751-FLAG expressing SH-SY5Y cells using 50nM smartpool siRNA complexed with DharmaFECT 1 transfection reagent in DMEM for 48 h. The cell medium was replaced with Opti-MEM and cells were cultured for a further 6 h. Cells were lysed and subjected to immunoblot analysis for APP, flotillin-1 or flotillin-2 and actin. Densitometric analysis of Flotillin-1 and flotillin-2 in **C)** APP695-FLAG expressing cells and **D)** APP751-FLAG expressing cells. Densitometric analysis of APP in **E)** APP695-FLAG expressing cells and **F)** APP751-FLAG expressing cells. MSD analysis for sAPPα and sAPPβ in the conditioned cell medium from **G)** APP695-FLAG expressing cells and **H)** APP751-FLAG expressing cells. MSD analysis for Aβ38, Aβ40, and Aβ42 in the conditioned cell medium from **I)** APP695-FLAG expressing cells and **J)** APP751-FLAG expressing cells. Bars represent the mean, errors bars are ± S.E.M., *, p-value <0.05, **, p-value <0.01, n=3, NT=non-targeting. In control experiments (NT) for APP695 average absolute Aβ38, Aβ40 and Aβ42 levels were 238 pg/mg, 695 pg/mg and 64 pg/mg, respectively. In control experiments (NT) for APP751 average absolute Aβ38, Aβ40 and Aβ42 levels were 92 pg/mg, 329 pg/mg and 39 pg/mg, respectively.

or flotillin-2 knockdown in the conditioned cell medium from APP695-FLAG expressing cells (**Figure 3.13I**). Aβ40 and Aβ42 were significantly reduced in the conditioned cell medium from APP751-FLAG expressing cells following both flotillin-1 knockdown (reduced by 17% for both knockdowns) and flotillin-2 knockdown (reduced by 13% and 16%, respectively) (**Figure 3.13J**). Aβ38 was only detectable in two experiments for both flotillin-1 and flotillin-2 knockdown in the APP751-FLAG expressing cells and therefore statistics were not applied to this result.

3.2.3 APP isoforms show no significant differences in protein degradation rate

The experiments described in this chapter demonstrated 4-fold higher sAPPα and 5-fold higher sAPPβ and Aβ in the conditioned cell medium from APP695-FLAG expressing cells compared to APP751-FLAG expressing cells. APP has been shown to have an extremely short half-life with nascent molecules rapidly transported and degraded within the cell (Gersbacher et al. 2013). We sought to determine whether the increased proteolytic cleavage of APP695 by α- and β-secretases was reflected in the overall protein degradation rate. Incubation of cells with cycloheximide prevents *de novo* protein synthesis by prevention of translational elongation of nascent peptides by the ribosome (Schneider-Poetsch et al. 2010). SH-SY5Y cells expressing APP695-FLAG or APP751-FLAG were incubated in serum-free DMEM containing 50 μg/ml cycloheximide, a method previously used for the determination of APP degradation rate (Lane et al. 2013). The effect on APP was determined by immunoblot analysis at 30 min intervals over 150 min (**Figure 3.14A**). Densitometric analysis indicated that approximately 75% of APP was degraded over the 150 min incubation and there was no significant variation in the degradation rate between the two APP isoforms (**Figure 3.14B**).

3.2.4 Various proteolytic fragments of APP are present in the conditioned medium, and vary between the isoforms

Several recent reports have indicated APP can be cleaved at multiple sites by different proteases to produce soluble N-terminal fragments. Proteolysis by membrane type-5 matrix metalloproteinase (MT5-MMP)/η-secretase has been shown to produce a fragment referred to as sAPPη (Willem et al. 2015) and meprin β has been shown to liberate a short N-terminal fragment of APP named N-APP20 (Jefferson et al. 2011) (**Figure 3.15A**). To determine whether the APP isoforms are proteolytically cleaved to produce any other proteolytic fragments, concentrated conditioned cell medium from SH-SY5Y cells expressing APP695-FLAG or APP751-FLAG, or from mock transfected cells was subjected to immunoblot analysis using two different APP antibodies; 6E10, raised to the N-terminal residues of the Aβ region with APP (**Figure 3.15B**), and 22C11, raised against an epitope encompassing residues 66-81 of APP (**Figure**

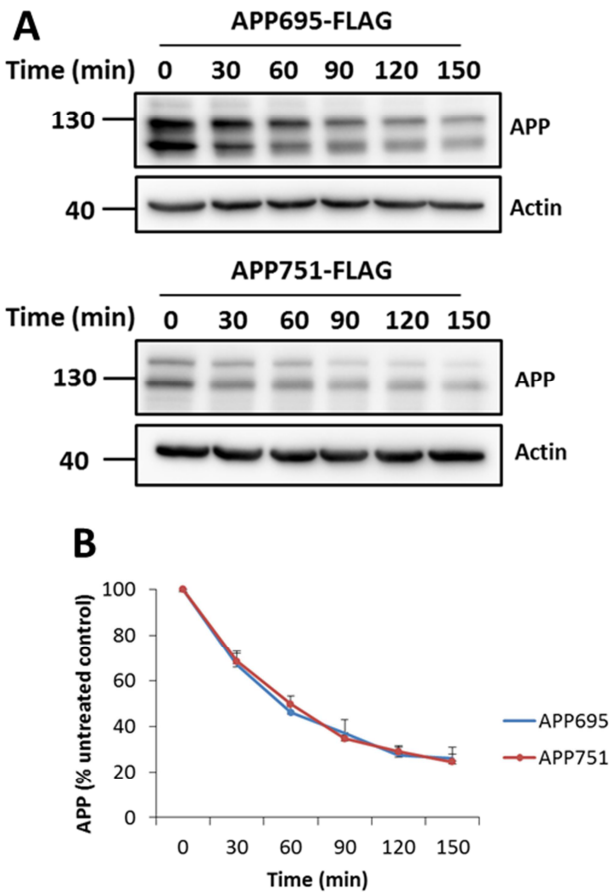

Figure 3.14 Degradation rates of the APP isoforms show no significant differences

SH-SY5Y cells expressing APP695-FLAG or APP751-FLAG were cultured in serum free DMEM containing 50 µg/ml cycloheximide for time periods ranging from 30 min to 150 min. **A)** Cells were lysed and subjected to immunoblot analysis for APP and actin. **B)** Densitometric analysis of APP at the specified time points. Points represent the mean, error bars are ± S.E.M, n=4.

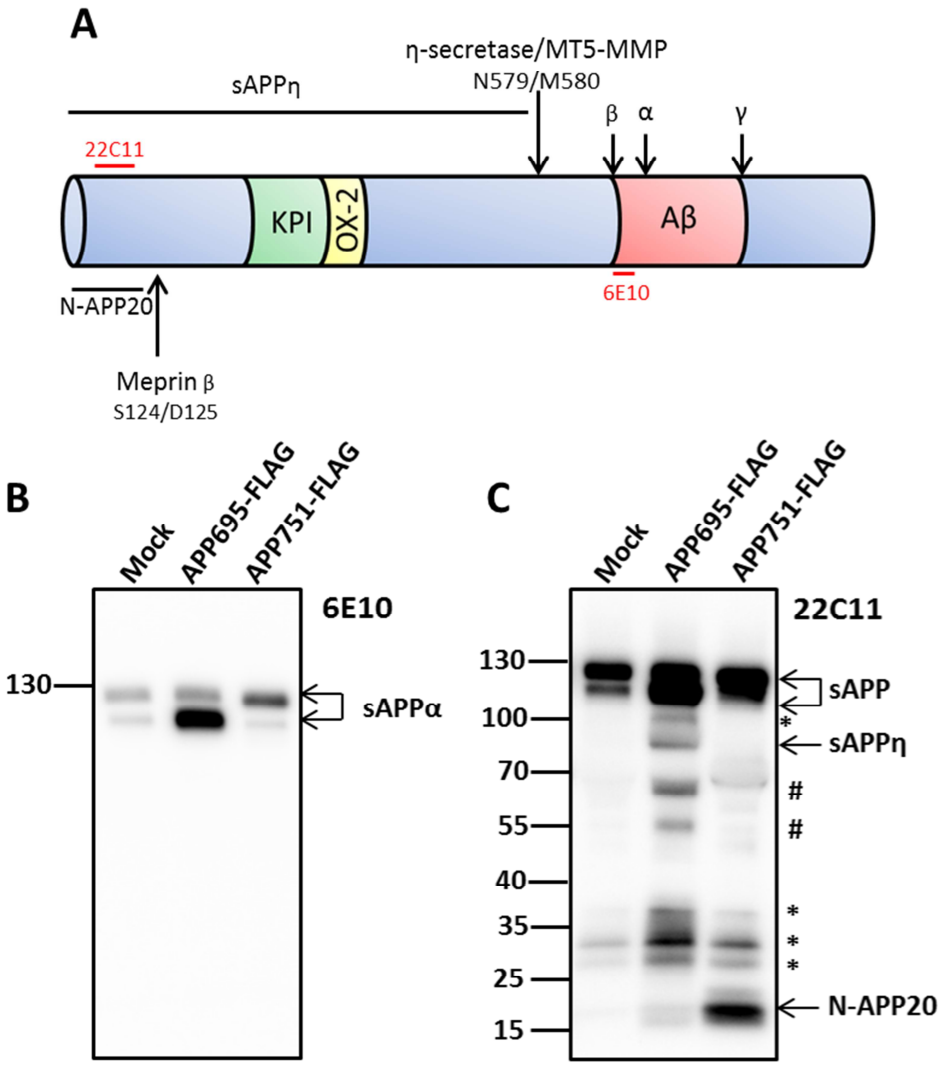

Figure 3.15 APP soluble fragments of various lengths are present in conditioned media from APP expressing cell lines

A) APP can be cleaved at sites other than the α-, β- and γ-secretase sites. Cleavage of APP in the ectodomain by meprin β and MT5-MMP produce soluble APP fragments meprin β and sAPPη, respectively. Due to their different epitopes, 22C11 and 6E10 (red) can be used to identify soluble APP fragments in the conditioned cell medium. Immunoblot analysis of the concentrated conditioned medium from mock transfected, APP695-FLAG and APP751-FLAG expressing SH-SY5Y cells to detect soluble APP fragments using **B)** 6E10 antibody raised against an epitope at the N-terminus of the Aβ region (amino acids 3-8) and **C)** 22C11 antibody raised against the N-terminus of APP (amino acids 66-81). Bands marked * denote cleavage products which follow APP expression but show no molecular weight difference. Bands marked # denote cleavage products which follow the APP expression and show a molecular weight difference.

3.15C). Comparative blots showed that the 6E10 antibody picked up only the doublet banding pattern which represents sAPPα produced from the APP695 and APP751 isoforms, while blotting with 22C11 showed a range of protein fragments within the conditioned cell medium from all the cell lines. Most of these additional fragments varied in chemiluminescent intensity in a similar pattern to that seen in the two sAPPα bands observed in the 6E10 immunoblot (marked with *). Some appeared to show molecular weight differences in the conditioned cell medium from APP695-FLAG and APP751-FLAG, suggesting production from both isoforms (marked with #). Some bands were observed in only the conditioned cell medium from APP695-FLAG expressing cells including a band of ~80 kDa assumed to be sAPPη (Willem et al. 2015). A prominent band of ~20 kDa was observed in the conditioned cell medium from APP751-FLAG expressing cells which was almost absent from the conditioned cell medium from APP695-FLAG expressing cells and mock transfected cells and was assumed to be the previously described N-APP20 (Jefferson et al. 2011).

3.3 Discussion

We have shown that proteolysis of two APP isoforms in our SH-SY5Y cellular system is markedly different, and believe understanding the cause of that difference could lead to the identification of novel pathways to modulate Aβ generation. As discussed in **Chapter 1,** the amyloidogenic potential of each APP isoform has been contested, and data presented in this chapter supports the original work by Belyaev et al. (2010) which implicated APP695 as the major amyloidogenic APP isoform. As differences are observed in both sAPPβ and Aβ when comparing isoform proteolysis, it is likely that the cause of the differential proteolysis we observe acts at the level of BACE1 cleavage, and we were therefore interested in pursuing cellular location and trafficking differences we believed may contribute to differential proteolysis.

3.3.1 Does differential subcellular localisation contribute to differential proteolysis of the APP isoforms?

The exact mechanisms of APP trafficking and subcellular distribution have been the subject of a wide range of analyses, in many cell lines, often with conflicting results (for reviews see (Jiang et al. 2014;Rajendran and Annaert 2012;Haass et al. 2012;Thinakaran and Koo 2008;Musardo et al. 2013). What is clear is that trafficking and subcellular distribution of APP and the proteases responsible for its cleavage is a dynamic process, with a wide range of potential modulating factors and influences. The production of Aβ appears to be intrinsically linked to the subcellular domains that APP and the secretases are trafficked through and/or retained within, and alterations in these could potentially contribute to AD.

In order to specifically study the subcellular location of the APP isoforms, tagged versions of the two APP isoforms were generated as described. A FLAG-tag was initially selected due to its small size in comparison to larger tags such as EGFP, which we postulated would reduce the possibility of trafficking perturbations caused by the presence of the tag. Indeed, data presented herein suggests that APP proteolysis was unaffected by the addition of a FLAG-tag as the generation of proteolytic APP fragments was increased on their expression within our SH-SY5Y cell system and proteolytic differences in the APP isoforms were still observed (See **Figures 3.2 and 3.3)**. Despite heavy reliance within the field on GFP-tagged proteins, we found that addition of EGFP to the C-terminus of APP altered proteolysis of over-expressed APP. We observed little increase in sAPP or Aβ production over endogenous levels in our system, despite confirmation of APP over-expression (See **Figure 3.5**). In addition, no differences in APP isoform expression could be observed and therefore use of APP-EGFP expressing cells was deemed not suitable for this project.

The secretory pathway

As described in **Chapter 1**, APP is synthesised in the ER and trafficked to the Golgi apparatus where various PTMs occur. According to some studies, APP is already subject to amyloidogenic proteolysis within these two subcellular organelles, resulting in Aβ generation. Within the ER, it has been suggested that this is due to presence of APP and the secretases in a specific sub-compartment of the ER known as mitochondrial-associated ER membranes (MAMs) within which APP proteolysis and Aβ generation has been shown to occur (Schreiner et al. 2015). The consequence of APP presence in the Golgi, particularly the TGN, remains a contentious issue within the field. While some studies have shown that retention within (Schmidt et al. 2007), or recycling to (Andersen et al. 2005) the TGN results in reduced amyloidogenic proteolysis of APP, others argued that increased Aβ generation follows retrieval of APP to the TGN (Choy et al. 2012). Mecozzi et al. (2014), recently showed retromer stabilisation caused a reduction in proteolysis at the rate-limiting, β-secretase step, though it is unclear whether this is due to the capacity of retromer to recycle APP back to the cell surface or to the TGN. We show here that APP751 shows higher localisation to TGN-46 labelled subcellular compartments than APP695 (See **Figure 3.6**). Though the mechanism by which APP751 is retained within, or trafficked back to the TGN has not been investigated here, it suggests presence within this subcellular site may contribute to the reduced APP751 proteolysis we observe. Further support for the notion that recycling of APP to the TGN can prevent Aβ generation comes from the identification of several proteins involved in protein recycling in GWAS and genetic expression profiling. These proteins are involved in retrieval of APP from the cell surface or early endosomes and recycling to the TGN, and include the sortilin-related VPS-10 domain containing receptor 1 (SorCS1) (Reitz et al. 2011) and the major retromer components SORL1 (SORLA) (Rogaeva et al. 2007) and vacuolar protein sorting (VPS)-35 (Small et al. 2005). Retromer comprises a constitutive trimer of VPS proteins; VPS-35, VPS-29 and VPS-26 along with varying combinations of proteins belonging to the sorting nexin family and other protein complexes related to its function in trafficking (Burd and Cullen 2014). Pharmacological chaperones which stabilise the retromer complex have been shown to reduce Aβ production in neurons and have therefore been suggested as potential therapeutics for AD (Mecozzi et al. 2014). A more in depth understanding of exactly how these drugs alter APP trafficking would provide much needed insight into the potential contribution of BACE1 proteolysis in the TGN to Aβ production.

We were interested to observe whether familial AD linked mutations within APP could affect the differential proteolysis we observed in the APP_{WT} isoforms. APP_{SWE} has been widely reported to undergo amyloidogenic proteolysis in the secretory pathway (Haass et al. 1995;Thinakaran et al.

1996b). We observed by immunoblot that 80% less sAPPβ was present in the conditioned cell medium from APP751-FLAG expressing cells compared to APP695-FLAG expressing cells (**Figure 3.2**). With APP_{SWE} immunoblot data indicated that, though the difference between the two isoforms is still statistically significant, $APP751_{SWE}$ only produces 50% less sAPPβ than $APP695_{SWE}$ (**Figure 3.7**). Though not completely over-riding the protective effect of the KPI domain, it appears that enhancing APP proteolysis in the TGN through the addition of the Swedish mutation reduces the differential proteolysis of these two isoforms. This adds weight to the hypothesis that retention within the early secretory pathway could indeed protect APP751 from proteolysis by BACE1.

Plasma membrane and endocytosis

Following trafficking through the secretory pathway, APP can be inserted in the plasma membrane, with approximately 10% of APP thought to be present at the cell surface (Thinakaran and Koo 2008). Data presented here suggests that less APP751 is constitutively present at the cell surface (see **Figure 3.9**). This may explain why we observe less sAPPα in the conditioned cell medium from APP751 expressing cells, as α-secretase cleavage is thought to occur predominantly at the cell surface (Parvathy et al. 1999). We observed both immature and mature APP present at the cell surface, which is perhaps surprising given that APP maturation is thought to occur in the Golgi (Haass et al. 2012). However, the presence of both bands at the cell surface has previously been observed (Jager et al. 2009) and raises questions about the control of cell surface APP and the mechanisms contributing to the presence of PTMs. When dynamin mediated endocytosis was pharmacologically inhibited by Dynasore, sAPPβ and Aβ in the conditioned cell medium were reduced to a similar extent in both the APP expressing cell lines (**Figure 3.10**). This would suggest that, despite less APP751 being present at the cell surface in the first place, once at the cell surface, the APP isoforms are subject to similar levels of amyloidogenic proteolysis. Again, this suggests that the cause of the proteolytic difference in APP isoforms occurs prior to its trafficking to the cell surface. Surprisingly, sAPPα was also significantly reduced in the conditioned cell medium when cells were treated with Dynasore, despite the fact that α-secretase cleavage occurs at the cell surface. Of course, it is possible, given that Dynasore does not specifically modulate APP endocytosis, that the increased presence of other α-secretase substrates at the cell surface out-competes APP for proteolytic cleavage. Indeed, the conditioned cell medium from Dynasore treated cells had a much higher total protein concentrations compared to control treated cells as determined by BCA assay, suggesting that shedding of other proteins into the medium was significantly increased. Interestingly, neither of the two papers identified within the literature which had previously

used Dynasore to inhibit endocytosis, determined the effect on sAPPα, or at least did not present those data (Chun et al. 2015;Zhu et al. 2012). Dynasore treatment also had a significant effect on total APP suggesting inhibition of proteolysis can increase APP within the cell. Interestingly, this increase was largely down to an increase in the immature APP. It is unclear exactly which form of APP is more readily cleaved down either proteolytic pathway, though some work has suggested that PTMs can alter APP proteolysis (Chun et al. 2015). Given that we observed two distinct bands when immunoblot analysis was performed on APP in the cell lysates, it is perhaps surprising that we generally only observed two bands (presumed to be from each isoform) when the conditioned cell medium is subjected to immunoblotting for sAPPα, and only a single band for sAPPβ. Whether this indicates that PTMs may drastically influence proteolysis in our system would require further experimentation, but poses further interesting questions on the factors affecting proteolysis.

GWAS have identified *PICALM/CALM*, *CD2AP*, *BIN1* and *GAB2* as AD risk alleles, all of which have roles in endocytic sorting (Rajendran and Annaert 2012), highlighting the importance of endocytosis in AD. Though GWAS does not assess the functional implications of the risk alleles identified, and single nucleotide polymorphisms are often in non-coding regions of genes, recent work showed loss of CALM selectively decreased Aβ42 levels through altering γ-secretase endocytosis (Kanatsu et al. 2014). Endocytosis of APP and BACE1 may occur through distinct pathways, with APP endocytosis being clathrin-dependent (Schneider et al. 2008;Cossec et al. 2010), and BACE1 endocytosis controlled by the GTPase, ADP ribosylation factor 6 (ARF6) (Sannerud et al. 2011) and it has been suggested that endocytosis is a key process in the generation of Aβ in neurons (Cirrito et al. 2008). APP and BACE1 may converge later in the endocytic pathway allowing proteolytic cleavage (Rajendran and Annaert 2012). These data suggest that the difference in APP proteolysis is independent on endocytosis, and could potentially be caused by reduced exocytosis of APP751, or by differential intracellular trafficking. Trafficking of APP and BACE1 to the cell surface was also recently shown to occur in separate vesicles (Bauereiss et al. 2015), suggesting mechanisms exist which tightly regulate the convergence of these two proteins during transit through the secretory pathway.

Lipid rafts are membrane microdomains enriched in cholesterol, sphingolipids and a subset of membrane proteins which have been proposed as important sites in both production of Aβ, and in mediating its toxicity (Rushworth and Hooper 2010). Indeed, APP (Bhattacharyya et al. 2013), BACE1 (Vetrivel et al. 2009) and the γ-secretase complex components NCT and APH-1 (Cheng et al. 2009) have all been shown to undergo palmitoylation, a PTM which can predispose the proteins to become enriched in lipid rafts (Blaskovic et al. 2013). It has been previously suggested that APP segregated into lipid raft domains undergoes proteolysis by BACE1, while

remaining cell surface APP undergoes α-secretase cleavage (Ehehalt et al. 2003). Therefore, we hypothesised that APP695 may be preferentially sorted to lipid rafts, resulting in increased amyloidogenic proteolysis. Our data shows that endogenous APP localises to lipid rafts, and that a similar distribution of APP between raft and non-raft fractions can be observed with APP which is over-expressed and endogenous APP in mock transfected cells (See **Figure 3.11**). However, we were unable to identify significant differences between the isoforms in their raft distribution (See **Figure 3.12**). This is despite the fact that addition of a GPI-anchor to BACE1, which results in increased raft distribution of BACE1, has previously been shown to enhance APP695 proteolysis to a much greater extent than APP751 (Cordy et al. 2003). Given that the fractionation protocol is relatively crude, and difficulties arose in completely removing transferrin receptor contamination from the raft fractions, more quantitative methods were devised to determine the importance of lipid raft localisation in APP isoform proteolysis. To more quantitatively assess the effect of raft localisation of APP isoforms, we used flotillin-1 and flotillin-2 knockdown to disrupt raft integrity and observed the effect on APP proteolysis (See **Figure 3.13**). Flotillins are palmitoylated and myristoylated (Neumann-Giesen et al. 2004) and are thus targeted to lipid rafts domains where they act as structural components in the clathrin-independent endocytosis pathway (Frick et al. 2007). They have previously been implicated in the generation of Aβ through direct interactions with the C-terminus of APP (Chen et al. 2006), causing accumulation of APP in lipid rafts. Flotillin-2 knockdown has previously been shown to significantly reduce the production of sAPPβ and Aβ from Swedish mutant APP695 in mouse neuron-like cells (Schneider et al. 2008), while flotillin-1 knock out in the APPPS1 mouse (APP751 with Swedish mutation and PSEN L166P mutation (Radde et al. 2006)), also reduced soluble and plaque Aβ (Bitsikas et al. 2014). The data presented here suggested, contrary to our original hypothesis, that flotillin-1 and flotillin-2 knockdown only significantly altered APP751 proteolysis, with a more significant effect observed at the level of γ-secretase proteolysis. This would suggest distribution to lipid rafts does not cause the consistent difference in isoform proteolysis at the β-secretase step we observe. Interestingly, while investigating the effect of APP palmitoylation on APP proteolysis, Bhattacharyya et al. (2013) identified a small but significant difference in APP isoform palmitoylation. Despite indicating that N-terminal Cysteine residues, C186 and C187, are sites for APP palmitoylation, more palmitoylated APP was observed for the APP751 isoform than the APP695 isoform, possibly increasing APP751 localisation to lipid rafts (Bhattacharyya et al. 2013). However, given that BACE1 proteolysis was only significantly reduced in the APP751-FLAG cell line following flotillin-1 knockdown, it would appear that localisation to lipid rafts does not contribute to the difference in isoform proteolysis we observe. While knockdown of flotillin-1 or flotillin-2 may disrupt raft organisation or

stability, it may not affect membrane cholesterol levels, which have previously been identified as an important factor in amyloidogenic APP proteolysis (Ehehalt et al. 2003;Marquer et al. 2014). Understanding the effect of cholesterol depletion may therefore be of further interest to determine the effect of lipids and lipid rafts on the differential proteolysis we observe for the APP isoforms.

Endosomal sorting and APP recycling

The overriding consensus in the field is that proteolysis of APP by BACE1 occurs predominantly in early endosomes, where the acidic luminal pH optimises its proteolytic capability (Vassar et al. 2009). Endosomal enlargement and acidification may be an important factor in the development of AD (Cataldo et al. 1997). Indeed, early endosomes have been shown to be enlarged in AD patient neurons, a phenomenon that has been shown to correlate with increased endosomal activity, suggesting increased rate of internalisation into the endocytic pathway (Cataldo et al. 1997). The application of Förster resonance energy transfer has shown distinct co-localisation of BACE1 and APP specifically at the cell surface and in early endosomes following endocytosis, again highlighting an important role for endocytosis in BACE1 cleavage of APP (Kinoshita et al. 2003). Given this consensus, it is counterintuitive that we observed APP751 co-localising to a greater extent with Rab5a, an early endosome marker, than APP695 (See **Figure 3.6**). However, it should be noted that in our analysis, only a small amount (10% or less) of APP co-localised with Rab5a. It is possible, though the hypothesis would need testing experimentally, that the routes by which the APP isoforms reach the endosomal system vary, and potentially affects localisation with BACE1. As discussed previously, it has been suggested that several concurrent mechanisms for the endocytosis of APP exist, which could result in endosomal vesicles containing different protein subsets (Rajendran and Annaert 2012). Manipulation of endosomal maturation through the use of GTP-locked mutant Rab5-Q79L could prove useful in further dissecting if APP751 trafficking to the endosome differs from APP695 and how this contributes to differential proteolysis (Sannerud et al. 2011).

Following its internalisation APP can be recycled to the plasma membrane in recycling endosomes which have also been postulated as a site of BACE1 proteolysis of APP (Das et al. 2013). APP and BACE1 have been shown to converge in recycling endosomes in response to glycine-mediated stimulation of NMDA receptors in neurons, leading to increased CTFβ production (Das et al. 2013). Recycling endosomes have also been shown to have a role in Aβ production through their role in recycling BACE1 to the cell surface following endocytosis (Udayar et al. 2013). Our data show APP695 co-localises with Rab11a to a greater extent than APP751 (See **Figure 3.6**) and, concurrent with this, Aβ was significantly reduced following

Rab11a knockdown only in APP695-FLAG expressing cells (See **Figure 3.8**) indicating localisation to recycling endosomes contributes to amyloidogenic proteolysis of APP695. Whether this is due to proteolysis within recycling endosomes, or due to its recycling back to the cell surface where it can be reinternalized with BACE1 is not clear. Though not reaching statistical significance in either case, sAPPα and sAPPβ were both reduced by Rab11a knockdown only in APP695 expressing cells suggesting a role for Rab11a in the initial APP cleavage event in our cell model as well. While Udayar et al. (2013) previously showed 50-70% decrease in sAPPβ and Aβ following Rab11a knockdown, we observed only 15% reduction in Aβ in our SH-SY5Y cell line, albeit at a lower knockdown level. The use of a non-neuronal cell system and APP bearing the Swedish mutation by Udayar et al. (2013) may account for some these differences. Interestingly, when investigating the effect of Rab11a knockdown in primary neurons from wild-type mice and HEK cells expressing wild-type APP, the effect of Rab11a knock down on sAPPβ and Aβ production was less pronounced (Udayar et al. 2013).

Lysosomal sorting and degradation

APP can be trafficked from early endosomes to the lysosomal system via late endosomes, where proteolytic degradation of APP can occur (Haass et al. 2012). APP can also be trafficked directly to the lysosomes either from the cell surface through the process of micropinocytosis involving Arf6 (Tang et al. 2015;Lorenzen et al. 2010), or directly from the Golgi apparatus (Tam et al. 2014). Notably, all three of these reports used APP751 expression, begging the question as to whether these could be isoform specific trafficking pathways. It has been reported that γ-secretase cleavage of APP can occur in the lysosome (Tam et al. 2014), and that APP CTFs can accumulate in the lysosomes when PS function is lost or reduced (Chen et al. 2000). Whether this requires prior cleavage by BACE1 in an alternative subcellular compartment remains unclear. In co-localisation studies, we observed no significant differences between the APP isoforms in their co-localisation with Rab7 (see **Figure 3.6**), a key regulator of late endosome fusion with the lysosome (Bucci et al. 2000). We did however, see much higher co-localisation for both APP isoforms with Rab7 than with Rab5a, supporting the hypothesis that lysosomes may be an important subcellular location in the proteolysis and/or degradation of APP. Similar to previous reports (Gersbacher et al. 2013;Lane et al. 2013), we have observed rapid degradation of APP following the inhibition of protein biosynthesis using cycloheximide, though again observed no significant differences between the degradation rates of the APP isoforms (See **Figure 3.14**). It would be interesting to investigate the role of proteosomal degradation of APP further, particularly given that we see no differences in APP degradation rate following the inhibition of protein biogenesis using cycloheximide. APP has been shown previously to

undergo proteosomal degradation, particularly in response to ER stress, suggesting the proteasome plays an important part in the degradation of APP (Jung et al. 2015). The key question here would be whether APP751 is more readily or rapidly degraded by the proteasome than APP695, thus reducing its proteolysis by α- and β-secretase.

3.3.2 Does retention within the early secretory pathway attenuate amyloidogenic APP proteolysis?

Evidence presented in this study implies that retention within the early secretory pathway may contribute to the differences we observe in the proteolysis of the APP751 as compared to the APP695 isoform. In support of this we observed greater co-localisation between the TGN marker TGN-46 and APP751 than APP695, and that comparatively less APP751 was present at the cell surface compared to APP695. Inhibition of endocytosis reduced amyloidogenic proteolysis of APP to a similar extent for both isoforms, suggesting that the cause of the difference in proteolysis occurs prior to APP endocytosis. It is possible therefore that APP751 is retained within the TGN to a greater extent than APP695, though the cause of this would need further investigation. To add weight to this hypothesis, disruption of the exocytosis effector Rab3 (Stenmark 2009), would aid in the identification in differences in exocytosis of the APP isoforms and its influence on Aβ generation. Knockdown of Rab3a in a recent high-throughput screen of Rab GTPases to determine effects on APP proteolysis resulted in decreased sAPPβ and Aβ generation (Udayar et al. 2013), again implying retention of APP within the TGN can protect it from amyloidogenic proteolysis. Alternatively the use of tetanus toxin, which inhibits the exocytosis of secretory vehicles (Zheng et al. 2012), could be employed to test the same hypothesis. While disruption of APP recycling and lipid rafts have been shown in this chapter to influence Aβ production from the APP695 and APP751 isoforms, respectively, neither is causative of the 80% difference we observe in sAPPβ and Aβ production when comparing APP695 and APP751.

While APP751 appeared to show greater co-localisation with an endosomal marker (Rab5a), only low levels of either APP isoform were localised to the early endosomes. To follow up on this, it would be interesting to disrupt early endosome trafficking to observe the effect of this on the proteolysis of the APP isoforms. Two mechanisms of APP endocytosis have been described, but it remains unclear whether these mechanisms give rise to different subpopulations of endosomes with different subsets of proteins (Rajendran and Annaert 2012). While it has been shown that APP can be directly trafficked to the lysosomal compartment from the TGN (Tam et al. 2014), there is no specific evidence for direct transport of APP from the TGN to early endosomes. However, there is evidence that this trafficking pathway exists and involves the Rab

GTPase Rab22, which aids in bi-directional transport between the TGN and endosomes (Stenmark 2009). Interestingly, in their Rab GTPase screen, Udayar et al. (2013) showed Rab22 knockdown increased sAPPβ and Aβ, while expression of its activating RabGAP reduced them. The bi-directional action of Rab22 makes interpreting these data difficult, but may indicate Rab22 is required for the export of BACE1 from the TGN, or that APP can be transported via this mechanism to endosomes which do not contain BACE1, or alternatively, that similar to retromer, Rab22 can induce APP trafficking back to the TGN. Given that we observed less APP751 at the cell surface, but observed higher co-localisation with Rab5a, it would be interesting to test whether direct trafficking to endosomes occurs and whether this influences proteolysis. A summary of the trafficking pathways we have investigated in this study are highlighted in green in **Figure 3.16**, while those we suggest are of potential interest to further dissect the influence of trafficking on APP isoform proteolysis are highlighted in red.

3.3.3 Do the APP isoforms undergo differential proteolysis at other sites?

Recent data has suggested that APP can undergo proteolytic cleavage at an alternative site, resulting in the shedding of a distinct sAPP species termed sAPPη (Willem et al. 2015). This proteolytic cleavage was shown to liberate the 80 kDa soluble N-terminal sAPPη fragment through cleavage between amino acids N588 and M589 by the matrix metalloproteinase MT5-MMP (Willem et al. 2015). We therefore thought it pertinent to determine whether the APP isoforms undergo differential proteolysis at sites other than the β-secretase site, including the newly discovered η-secretase site. Though the 22C11 antibody is not sAPPη specific, when the conditioned cell medium from SH-SY5Y cells was subjected to immunoblot analysis with this antibody, a band of the correct molecular weight for the proposed sAPPη fragment (80 kDa) was observed (see **Figure 3.15**). Interestingly, the production of sAPPη appears to be solely from the APP695 isoform, as no corresponding band appeared in the conditioned cell medium from the APP751 expressing cell line. This is despite Willem et al. (2015) showing evidence that reduced β-secretase activity led to higher production of the sAPPη fragment in mouse hippocampal neurons and human induced pluripotent stem cell (iPSC) derived neurons. Only a single band at ~20 kDa is more prominent in the conditioned cell medium from the APP751-FLAG expressing cells than in the conditioned cell medium from the APP695-FLAG expressing cells. A proteolytic APP fragment of this size has previously been reported in the conditioned cell medium from SH-SY5Y cells (Vella and Cappai 2012) and HEK cells (Jefferson et al. 2011) and it has been proposed that this is an N-terminal cleavage product produced by proteolytic cleavage of APP by meprin β (Jefferson et al. 2011). Meprin β has also been shown to cleave APP in a manner resembling a β-secretase, and can be responsible for the liberation of Aβ (Bien et al. 2012). It is

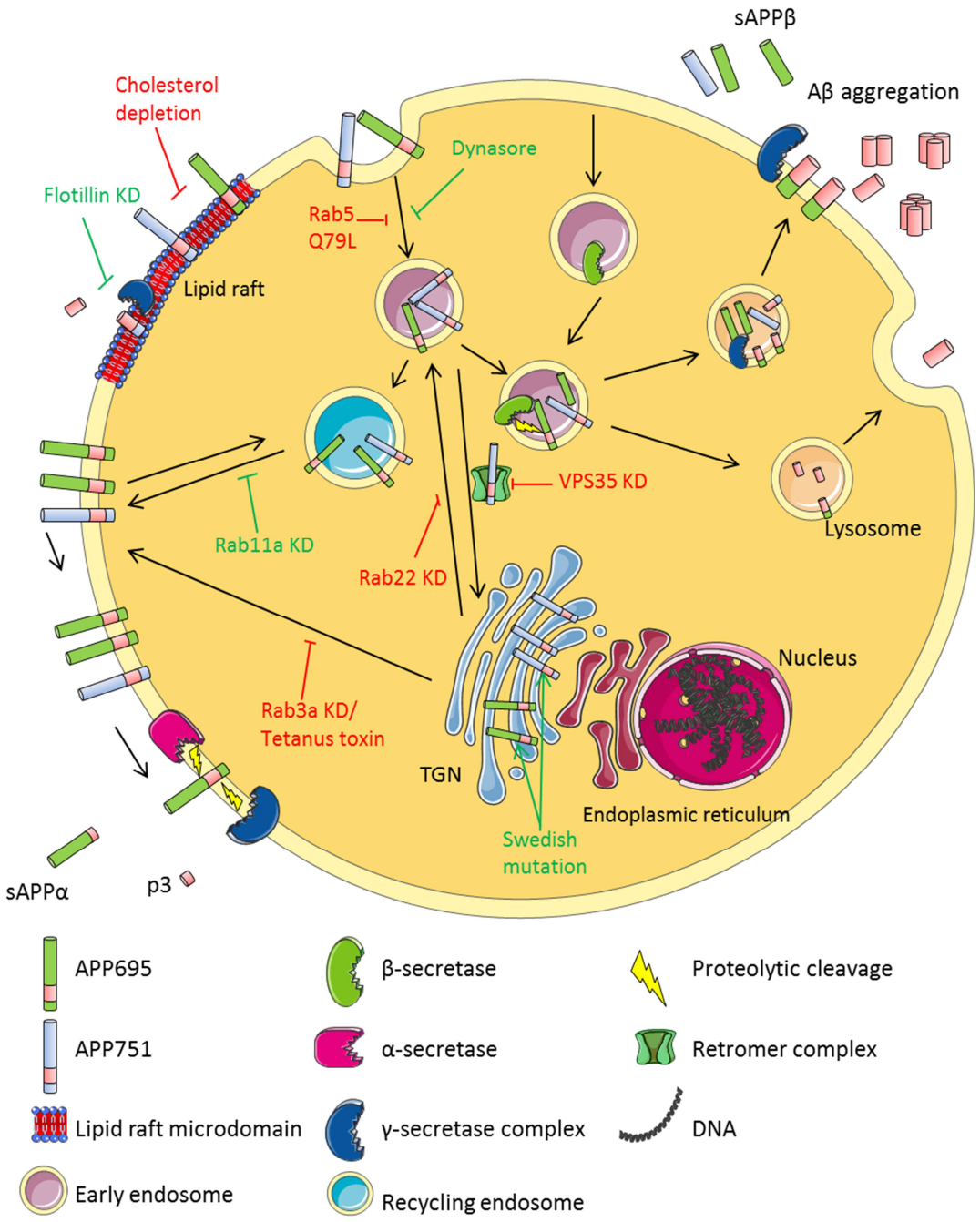

Figure 3.16 APP trafficking complexities and proposed targets

A schematic representation of the mechanisms used to inhibit or disrupt the various trafficking pathways in this study are highlighted in green. Those we propose as further targets to elucidate other trafficking pathways involved in differential isoform proteolysis are highlighted in red. KD = knockdown.

interesting that in APP751-FLAG expressing cells we see much more of the ~20kDa fragment and less sAPPα, sAPPβ and Aβ, even though a reciprocal relationship has not been described for BACE1 and meprin β mediated cleavage before. Following the meprin β cleavage, which releases the 20 kDa, the BACE1 and α-secretase sites would still be intact, so APP could still theoretically be cleaved by BACE1 and α-secretase. Therefore it would need further investigation to determine whether this difference in proteolysis is causative of the differences in isoform proteolysis by BACE1 or α-secretase, and what the fate of APP with the N-terminal removed is. Interestingly, membrane bound meprin β, which is responsible for the β-secretase cleavage of APP requires activation by the serine protease matriptase-2 which could potentially be inhibited by APP751 due to the presence of the KPI domain (Jackle et al. 2015). The interplay between these proteolytic pathways would certainly be of interest given the results we observe here and could go some way to explaining the differences in APP isoform proteolysis.

In summary we have shown that, once reaching the cell surface, both the APP isoforms we have studied here undergo similar levels of proteolysis. However, less APP751 appears to be constitutively present at the cell surface indicating differences in exocytosis. Supporting this, co-localisation experiments indicate that the APP751 isoform localises to the TGN to a greater extent than APP695 and incorporation of the Swedish mutation reduces the difference in proteolysis observed for the APP695 and APP751 isoforms. Proteolysis of the APP isoforms may occur in different subcellular locations, as shown by differences in the effects observed when disrupting recycling endosomes or lipid raft domains. However, these differences are subtle and do not appear to be solely responsible for the large difference in proteolysis we see between the isoforms. Further work investigating the importance of exocytosis and endosomal trafficking is also suggested in **Figure 3.16** and may aid in further identification of the pathways involved in differential proteolysis of APP isoforms. Further investigation of other proteolytic pathways may also be of interest given that there appear to be differences in APP isoform proteolysis by the relatively novel APP cleaving enzymes, η-secretase and meprin β.

Chapter 4. Investigating the APP isoform interactomes and their implications for APP proteolysis

4.1 Introduction

4.1.1 Proteomic analysis and its application to neurodegenerative diseases

Proteomic analyses are now being used widely in the AD field for a range of applications including identification of biomarkers from cerebrospinal fluid (Wildsmith et al. 2014), identification of insoluble aggregates within degenerated brains (Bai et al. 2013), to elucidate changes in protein expression profiles in different cell or tissue states (Chaput et al. 2012) and to interrogate the interactome of various disease-linked proteins (Hosp et al. 2015). While traditional mass spectrometry is not inherently quantitative, linking its use to prior sample labelling through the use of methods such as isobaric tags for absolute and relative quantitation (iTRAQ) and SILAC can extend its use into quantitative proteomics, allowing comparative analysis of large datasets (Mann 2006). Developments in the application of SILAC now means comparative analyses of up to 5 different conditions can be carried out simultaneously, giving huge scope for analysis of various experimental conditions in comparison to a control condition.

4.1.2 Can interactome studies imply novel molecular functions for APP?

A definitive role for APP remains enigmatic, though it is becoming apparent that it may be involved in several processes as discussed in **Chapter 1,** rather than having a single function. Through various experimental analyses, the data presented in **Chapter 3** highlights that the APP isoforms may be differentially trafficked in the same cell system, and therefore may be exposed to different protein-protein interactions within these subcellular compartments. In turn these protein-protein interactions may influence APP proteolysis, or allow inference of functions specific to the APP isoforms. Perreau et al. (2010) attempted to curate all reported APP interactors within the literature giving details of the domain involved in the interaction, as well as carrying out in depth ontology analysis to decipher functions enriched within the APP interactome. These included enrichment of proteins localised to synapses, growth cones, cytoplasmic membrane bound vesicles and the plasma membrane and those involved in extracellular matrix formation among others (Perreau et al. 2010). Despite this, at the point at which this project was initiated, no interactomic analysis of the APP in a cellular context had been carried out despite huge reliance within the field on cellular analysis of APP metabolism and function.

4.1.3 Can interactomic studies identify novel modulators of APP proteolysis?

Direct inhibition of the secretases responsible for APP proteolysis is fraught with difficulties given the large number of additional substrates which have been identified for both BACE1 and γ-secretase. In light of this, it seems pertinent to investigate other potential mechanisms through which the accumulation of Aβ could be attenuated. Protein-protein interactions specific to BACE1, γ-secretase and APP have all previously been shown to influence Aβ generation (Wakabayashi et al. 2009;He et al. 2004;Park et al. 2006). This led us to postulate that a cellular interaction specific to either APP695 or APP751 could either enhance, or prevent, their proteolysis leading to the differences in isoform proteolysis we observed in cells expressing these two isoforms. As discussed in **Chapter 1** various APP interactors have been shown to influence proteolysis, and several of these, including members of the LRP family have been shown to exert their effect in an isoform specific manner (Cam et al. 2004;Kounnas et al. 1995).

4.1.4 Aims

The main aim of this chapter was initially to identify any protein-protein interactions which could be responsible for the difference in proteolysis observed in APP isoforms. In addition, we aimed to determine whether the interactome networks of APP isoforms could identify differences in protein function and/or protein subcellular distribution. To achieve this, a quantitative interactomic study of different APP isoforms was performed using SILAC coupled to LC-MS/MS. Proteins within the interactome were investigated to determine whether they influenced APP proteolysis through siRNA knockdown and subsequent determination of the production of APP soluble fragments. Finally, we sought to determine whether any proteins that appeared to influence APP proteolysis showed altered expression profiles in post mortem brain tissue from AD patients compared to that from non-cognitively impaired subjects.

4.2 Results

4.2.1 APP-FLAG immunoprecipitation optimisation and SILAC

As described in **Chapter** 2, APP695 and APP751 were C-terminally FLAG tagged to allow their specific immunoprecipitation from cell lysates. In order to achieve the best possible APP isolation from cell lysates, several methods of APP-FLAG immunoprecipitation were trialled. Following cell lysis in IP buffer and clarification, cell lysates from APP695-FLAG or APP751-FLAG expressing SH-SY5Y cells were incubated with either FLAG monoclonal antibody bound to protein G sepharose beads, FLAG polyclonal antibody bound to protein A sepharose beads or with anti-FLAG affinity gel to immunoprecipitate APP. Proteins were then eluted from the sepharose or anti-FLAG affinity gel by the addition of 2x dissociation buffer and boiling for 5 min. Input, unbound and bound fractions from each cell line and each immunoprecipitation condition were analysed by immunoblot analysis with anti-APP antibody (**Figure 4.1**). Results showed much greater immunoprecipitation of APP from cells lysates using the anti-FLAG affinity gel than with either the FLAG monoclonal, or the FLAG polyclonal antibody linked to sepharose beads.

In order to successfully determine proteins specifically interacting with APP by mass spectrometry, cell lysis conditions were optimised to ensure protein-protein interactions were not disrupted during cell lysis. To determine optimal co-immunoprecipitation conditions two buffers were trialled, one containing the detergent CHAPSO (CHAPSO buffer), and the other containing the detergent NP-40 (IP buffer) which was adapted from a previous SILAC LC-MS/MS study (Wu et al. 2012). Interactions between APP and Fe65 are probably the most extensively studied direct interaction for the APP protein and was therefore used as a determinant of successful co-immunoprecipitation conditions. Cells expressing APP695-FLAG, APP751-FLAG or mock transfected cells were lysed in either CHAPSO buffer or IP buffer. APP-FLAG immunoprecipitation was then performed using the anti-FLAG affinity gel and input, unbound and bound fractions were then subjected to immunoblot analysis for APP-FLAG, APP and Fe65.

The results showed that in both CHAPSO buffer (**Figure 4.2A**) and IP buffer (**Figure 4.2B**) APP was successfully immunoprecipitated from cell lysates as determined using both monoclonal FLAG antibody and anti-APP antibody (top panels). Successful co-immunoprecipitation of Fe65 was observed in both buffers (bottom panel), though a stronger signal was seen following lysis in IP buffer. Following this result, and given that the IP buffer had previously been used in similar SILAC based interactomic studies (Wu et al. 2012), we carried out all subsequent immunoprecipitation experiments following cell lysis in this buffer.

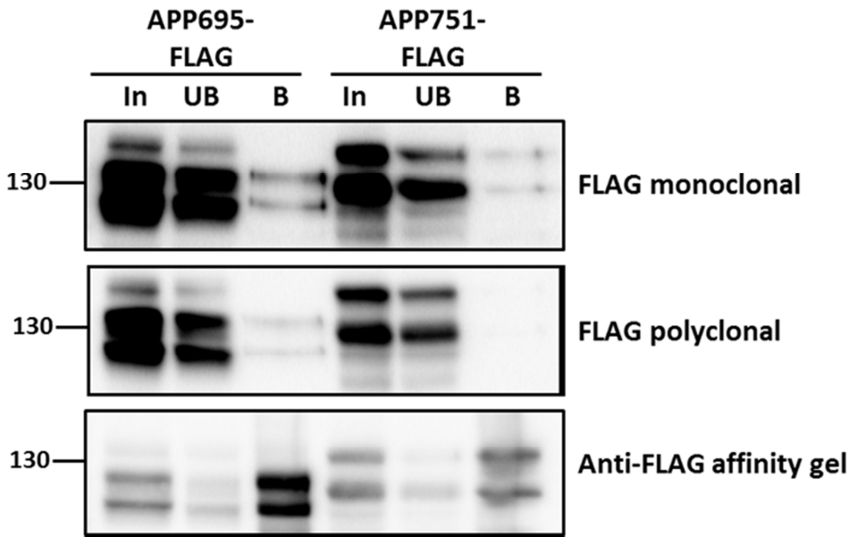

Figure 4.1 FLAG-tag affinity gel efficiently immunoprecipitates FLAG tagged APP

Immunoprecipitation of FLAG-tagged APP the from lysates of SH-SY5Y cells expressing APP695-FLAG or APP751-FLAG was carried using 3 different immunoprecipitation techniques; streptavidin beads linked to FLAG monoclonal (top panel) or polyclonal (middle panel) antibodies and FLAG-tag affinity gel (bottom panel). Following immunoprecipitation input (In), unbound (UB) and bound (B) fractions from immunoprecipitations were separated by SDS-PAGE and immunoblotted for APP using 22C11.

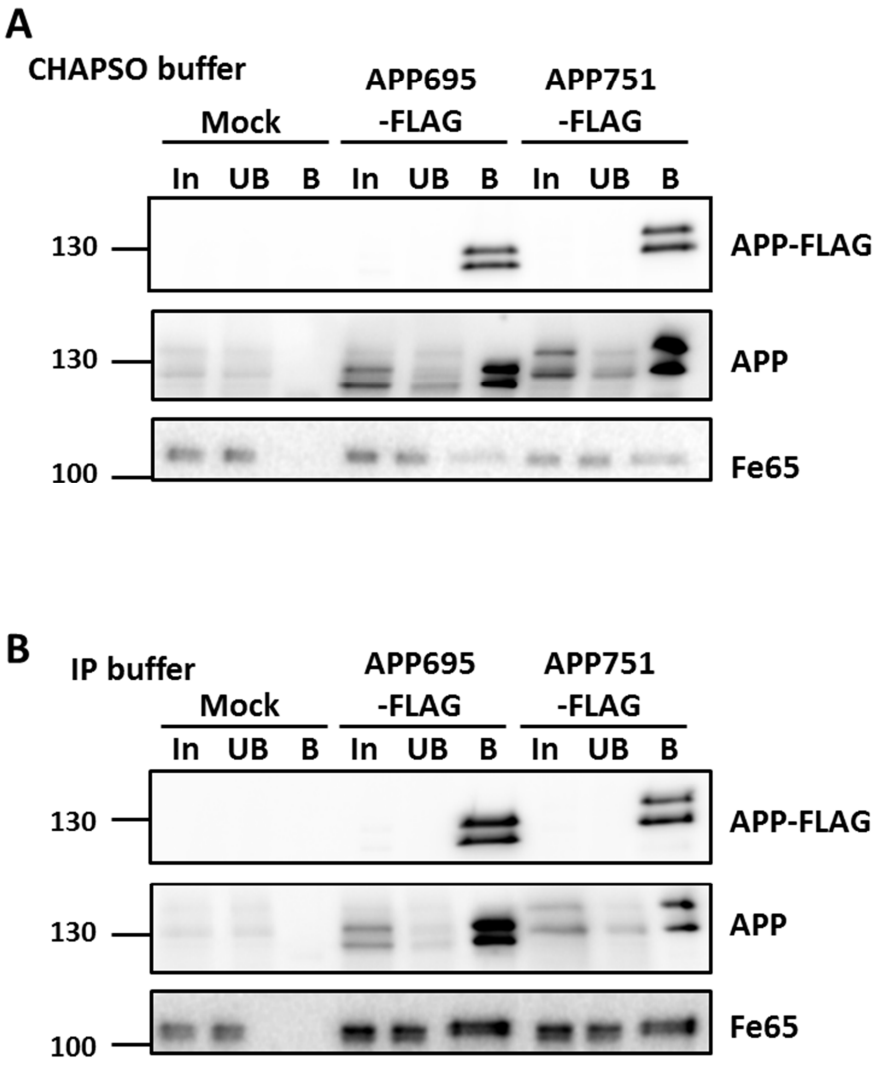

Figure 4.2 Cell lysis in IP buffer results in higher co-immunoprecipitation of Fe65 with APP than lysis with CHAPSO buffer

Mock transfected SH-SY5Y cells and SH-SY5Y cells expressing APP695-FLAG or APP751-FLAG were lysed in either **A)** CHAPSO buffer or **B)** IP buffer, and APP-FLAG was immunoprecipitated using FLAG-tag affinity gel. Input (In), unbound (UB) and bound (B) fractions from the immunoprecipitations were subjected to immunoblot analysis with anti-FLAG (top panel), 22C11 (middle panel) and Fe65 (bottom panel) and co-immunoprecipitated Fe65.

4.2.2 APP isoforms show differences in interactomes which indicate differential functions

Following the optimisation of co-immunoprecipitation conditions, an experimental strategy was defined to allow analysis of the interactomes of the two APP isoforms (**Figure 4.3A**). Briefly, mock transfected, APP695-FLAG and APP751-FLAG expressing SH-SY5Y cells were cultured over a 3 week period in heavy, medium and light isotope labelled medium, respectively. Over the 3 week period cells were passaged over 6 times suggesting at least 6 doublings, which has previously been identified as ensuring over 95% labelling of proteins within the cells (Emmott et al. 2013). APP was subsequently immunoprecipitated using the conditions previously optimised and confirmation of immunoprecipitation of both APP and co-immunoprecipitation of Fe65 was carried out by immunoblot analysis using a small aliquot of the bound fraction (**Figure 4.3B**). The three bound fractions were then combined in a 1:1:1 ratio and subjected to mass spectrometry analysis which was carried out by Dr Kate Heesom at the University of Bristol Proteomics Facility.

Application of this technique not only allows the identification of proteins present from each co-immunoprecipitation on the basis of isotope labelling, but also allows their quantification. Comparing protein abundance from each bound fraction (from mock, APP695-FLAG and APP751-FLAG expressing cells) allows the generation of a ratio of interaction comparing each experimental immunoprecipitation. By setting a ratio cut-off value, proteins identified in the mass spectrometry analysis that were not deemed to be enriched above the level seen in the control immunoprecipitation can be excluded, meaning remaining proteins identified should be true interactors. Several parameters were set for the inclusion of an interactor in the final data set. i) The LC-MS/MS identification was carried out on two separate SILAC labelled immunoprecipitations and only proteins with peptide ratios calculated on the basis of at least 4 peptides over the two experiments were included in the analysis. ii) Interaction ratios for each APP cell line compared to mock for the remaining 297 proteins were Log2 converted and plotted as a scatter graph (**Figure 4.4A**). iii) To determine whether a protein was specifically enriched in the immunoprecipitated samples from each APP-expressing cell line, all proteins whose interaction ratio did not exceed the average interaction ratio of its own data set were removed, a method previously employed to determine the *in vivo* mouse interactome of APP (Kohli et al. 2012). This cut off value was 5.0 for the APP695 interactome and 2.6 for the APP751 interactome, and represents a more conservative cut off than the arbitrary 2-fold one used in similar SILAC based interactome studies (Wu et al. 2012;Hosp et al. 2015). Enriched proteins were re-plotted in (**Figure 4.4B**), revealing 35 proteins enriched in both datasets. In addition 11 proteins were specifically enriched in the APP695 dataset and 23 were specifically enriched in the APP751 dataset. A comprehensive list of Uniprot protein accession numbers and gene

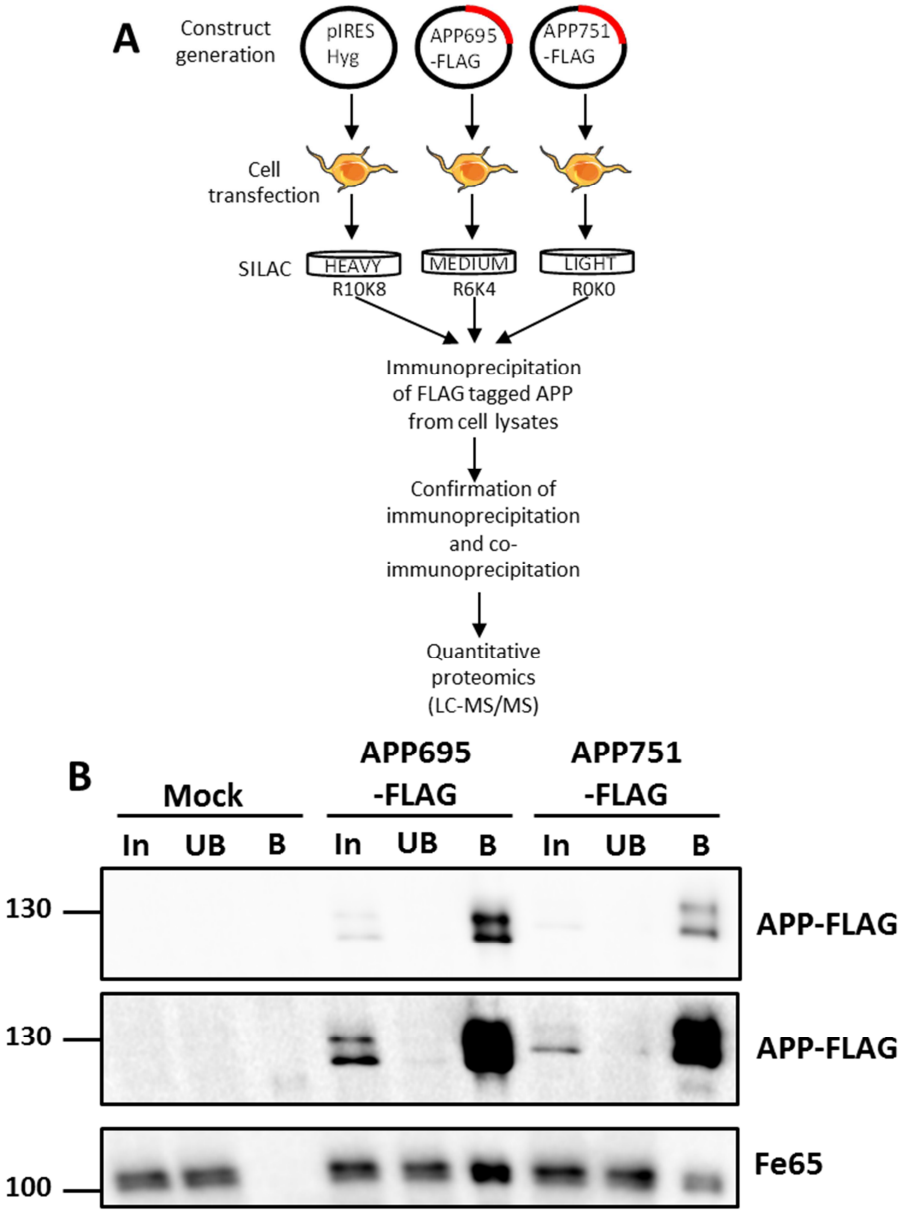

Figure 4.3 SILAC and LC-MS/MS used to identify proteins differentially interacting with FLAG-tagged APP695 and APP751 isoforms

A) Schematic representation of the SILAC LC-MS/MS strategy. SH-SY5Y cells expressing APP695-FLAG, APP751-FLAG or mock transfected cells were labelled by SILAC. FLAG-tagged APP was immunoprecipitated from cell lysates and analysis of the bound immunoprecipitation fractions was carried out by LC-MS/MS. **B)** Following SILAC, immunoprecipitation of FLAG-tagged proteins was performed using anti-FLAG affinity gel. Input (In), unbound (UB) and bound (B) fractions from the three immunoprecipitations were subjected to immunoblot analysis using anti-FLAG antibody (shown at normal (top) and higher (middle panel) exposure) to confirm APP immunoprecipitation and co-immunoprecipitation Fe65, before the mass spectrometry analysis.

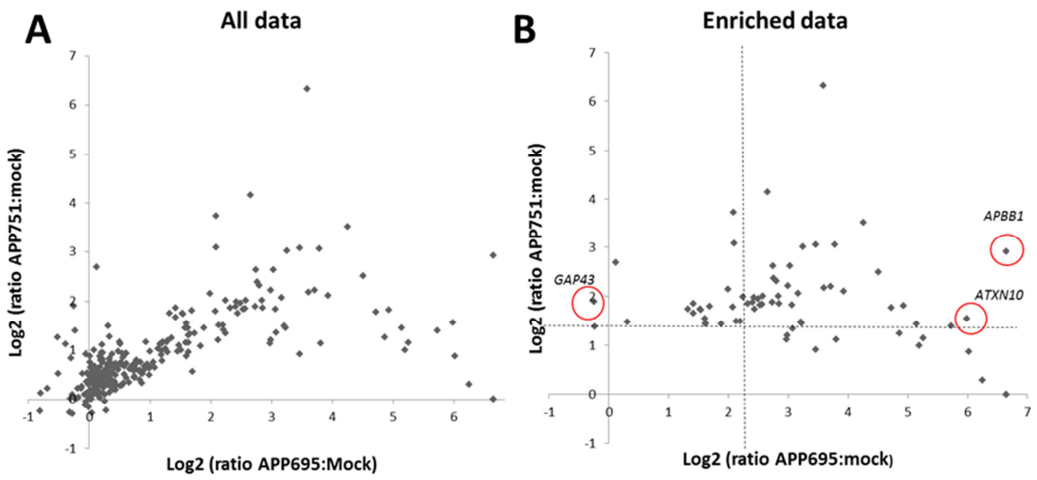

Figure 4.4 Identification of enriched data from mass spectrometry analysis

Of the 410 proteins which were identified within both of the two mass spectrometry analyses performed, 297 were identified on the basis of at least 4 peptides over the two experiments. **A)** Protein interaction ratios were Log2 converted and plotted as the ratio of APP695:mock against the ratio of APP751:mock. **B)** Cut offs of 5.1-fold and 2.6-fold enrichment over the mock transfected cell line (dotted lines) were used to identify proteins which were enriched in the interactome of APP695 and APP751 respectively. Cut off values were Log2 converted giving cut off values of 2.325 and 1.379 for APP695 and APP751, respectively, and were applied to the data set to provide an enriched data set indicating specific interactors for each isoform. Circled are *GAP43*, *APBB1* and *ATXN10.*

names is displayed in **Table 4.1** along with scores (an indicator of the certainty of protein identification), peptide numbers (number of peptides used to calculate the interaction ratio) and protein sequence coverage (% of the whole protein amino acid sequence covered by all peptides) for the two separate experiments, and binding ratios (comparison of the abundance of each protein in co-immunoprecipitations from each experimental cell line) averaged from the two experiments.

Gene ontology analysis on proteins in each interactome was then performed using DAVID software (Huang et al. 2008;Huang et al. 2009). Several ontology groupings were significantly enriched in the APP interactomes (**Table 4.2**). For APP695, ontology groupings showed interaction with various mitochondrial proteins involved in the biosynthesis of ATP, as well as interaction with various nuclear pore proteins and transporters. APP751 on the other hand showed enrichment for proteins enriched in cytoplasmic vesicles. When analysis was performed on proteins showing >2-fold interaction with APP695 compared to APP751, nuclear pore proteins became even more significantly enriched, while mitochondrial proteins also remained enriched (**Table 4.3**).

4.2.3 Validation of the APP interactome data

It has been suggested that high throughput analyses, such as the one employed in this study, often generate false positive results, making the data less reliable than low throughput analyses (Perreau et al. 2010). For this reason, we sought to confirm some of the interactions using FLAG monoclonal antibody for APP immunoprecipitation or, where available, an antibody against the reported interactor. Cell lysates from mock, APP695-FLAG and APP751-FLAG expressing SH-SY5Y cells were subjected to immunoprecipitation with FLAG monoclonal antibody linked to protein G Dynabeads and immunoblot analysis was used to confirm the interaction between APP and ataxin-10, Fe65, growth associated protein 43 (GAP43), 78 kDa glucose regulated protein (GRP78) and heat shock cognate 71 kDa protein 8 (HSPA8) using this low throughput technique (**Figure 4.5**). The majority of antibodies which worked for immunoblot were not suitable for immunoprecipitation. Successful co-immunoprecipitation of APP695 was shown following immunoprecipitation of ataxin-10 and GAP43 (**Figure 4.6A**) while successful co-immunoprecipitation of APP751 only occurred in the GAP43 immunoprecipitation (**Figure 4.6B**).

Uniprot Accession	Gene name	Score Expt 1 /Expt 2	Peptide Expt 1 /Expt 2	Coverage Expt 1/ Expt 2 (%)	APP695:Control ratio		APP751:Control ratio		APP695:APP751 ratio	
					Binding ratio	Peptide	Binding ratio	Peptide	Binding ratio	Peptide
Q5JTZ9	AARS2	7.2/24.1	2/4	2.4/5.6	100.00	4	1.00	4	71.41	6
O00213	APBB1	19.0/42.8	4/6	10.4/12.7	100.00	10	7.55	11	61.67	10
Q9UBX3	SLC25A10	9.4/24.5	1/2	3.5/8.7	75.71	4	1.22	4	60.55	5
Q9UBB4	ATXN10	11.7/14.9	3/2	8.2/6.1	63.03	5	2.94	5	60.52	5
O43592	XPOT	15.3/20.0	3/3	4.0/4.o	35.21	3	2.72	3	19.99	5
P55060	CSE1L	32.4/35.3	6/5	7.6/11.8	64.53	8	1.82	8	8.27	11
O95373	IPO7	13.4/44.5	4/6	5.1/8.3	13.95	8	2.19	8	6.92	10
Q9H9B4	SFXN1	11.2/32.5	2/7	7.1/21.4	7.88	4	3.45	5	4.74	8
P53985	SLC16A1	11.1/22	2/3	6.7/7.3	15.16	4	4.33	4	4.67	5
O00483	NDUFA4	5.1/19.0	2/3	27.1/37.0	9.33	5	2.74	5	4.60	5
Q92973	TNPO1	16.5/15.9	3/2	3.9/2.8	9.21	5	2.80	5	4.17	5
P55084	HADHB	38.2/15.1	6/3	13.7/7.8	7.84	6	2.19	5	3.98	7
O75473	LGR5	37.6/8.4	5/1	7.0/1.4	36.49	5	2.00	5	2.47	8
E1NZA1	PRIC295	33.8/93.5	7/18	2.8/9.3	30.41	14	3.54	14	2.33	22
P08183	ABCB1	27.8/7.8	4/1	4.0/1.2	7.05	2	2.22	3	2.23	4
O14980	XPO1	9.8/54.6	2/7	3.3/8.7	13.06	8	4.65	8	1.99	9
P12236	P12236	78.8/135.7	7/9	24.5/27.2	9.77	6	5.68	7	1.98	10
P36542	P36542	15.0/16.6	1/4	13.6/31.5	11.00	8	1.88	8	1.96	8
P78527	PRKDC	142.7/309.7	23/48	6.8/13.7	12.11	50	4.54	50	1.92	66
Q9ULH0	KIDINS220	32.6/8.8	5/1	3.3/1.0	8.92	7	4.18	7	1.89	7
P16615	ATP2A2	28.2/87.0	4/11	4.8/13.0	28.95	14	2.38	14	1.88	17
P05141	SLC25A5	94.9/131.2	8/9	27.9/25.5	6.64	10	3.71	10	1.79	12
O43175	PHGDH	26.4/23.2	6/5	13.4/11.8	7.89	6	2.30	6	1.70	10
P31689	DNAJA1	32.6/71.7	8/7	20.9/22.7	8.34	13	3.56	12	1.64	15
Q9UJS0	SLC25A13	76.8/142.0	9/14	18.5/27.6	7.92	19	4.67	20	1.63	28
Q53H12	AGK	13.3/3.4	3/1	8.6/5.3	4.57	4	2.83	4	1.59	4
Q9NQX7	ITM2C	59.9/13.1	7/2	31.8/18.3	52.68	11	2.64	11	1.59	15
P53007	SLC25A1	6.4/28.1	1/3	5.8/11.3	100.00	1	1.00	1	1.56	5
P25705	ATP5A1	69.5/106.49	8/12	18.8/26.8	4.35	25	2.83	25	1.53	27
P57088	TMEM33	5.8/40.2	2/5	9.9/18.2	6.29	6	4.07	6	1.52	7
Q15758	SLC1A5	15.1/28.4	2/4	3.9/10.9	8.37	7	2.55	7	1.50	8
O60762	DPM1	13.9/29.5	2/5	10.6/31.8	6.93	6	4.98	6	1.48	9
P02786	TFRC	52.5/19.8	8/3	12.2/5.7	4.97	10	3.65	10	1.48	11
Q96HS1	PGAM5	104.3/152.4	4/8	12.5/31.5	19.01	26	11.42	26	1.46	30
P04843	RPN1	71.3/92.3	6/11	13.6/26.8	5.74	19	3.57	19	1.46	23
Q96AY4	TTC28	12.5/18.6	1/3	0.5/1.4	6.75	2	5.20	2	1.46	4
O14828	SCAMP3	17.5/42.7	2/3	8.4/14.1	5.92	6	4.05	6	1.46	7
P68363	TUB1A	171.0/477.9	12/17	38.9/56.5	5.61	5	3.87	5	1.45	5
Q71U36	TUBA1A	177.6/479.0	12/17	38.9/56.5	7.19	5	3.63	5	1.45	5
P43307	SSR1	6.7/11.3	2/2	7.2/9.8	5.40	2	3.37	2	1.40	4
Q9Y277	VDAC3	10.7/10.3	3/2	14.5/7.4	3.68	4	2.73	4	1.38	4
P56134	ATP5J2	9.8/26.4	2/2	49.0/49.0	5.35	6	3.97	6	1.37	6

Table 4.1 The APP695 and APP751 interactome

Table continued overleaf.

Uniprot Accession	Gene name	Score Expt 1 /Expt 2	Peptide Expt 1 /Expt 2	Coverage Expt 1/ Expt 2 (%)	APP695:Control ratio		APP751:Control ratio		APP695:APP751 ratio	
					Binding ratio	Peptide	Binding ratio	Peptide	Binding ratio	Peptide
A6NKG5	RTL1	29.2/140.5	5/16	4.0/16	5.28	18	3.70	18	1.35	23
Q16891	IMMT	65.0/86.2	6/9	15.3/17.0	4.23	10	3.60	9	1.34	10
P27708	CAD	16.8/32.3	2/3	1.2/1.9	5.89	4	3.59	4	1.33	5
P62491	RAB11A	19.2/15.9	3/2	22.6/15.5	3.07	5	2.72	5	1.31	6
P50416	CPT1A	14.5/31.0	2/3	3.4/5.2	11.02	3	8.37	3	1.30	5
P05023	ATP1A1	75.8/67.5	10/8	13.6/11.1	8.12	6	6.20	6	1.29	10
P04792	HSPB1	30.5/53.2	4/4	23.4/25.9	4.72	9	4.02	9	1.27	11
Q00325	SLC25A3	46.8/67.6	2/4	8.6/21.3	7.14	11	4.04	12	1.22	12
Q13409	DYNC1I2	24.2/11.8	3/1	16.1/19.1	6.66	4	6.18	4	1.19	5
P39656	DDOST	18.6/25.6	3/3	7.5/10.5	4.25	6	8.47	6	1.15	7
P40939	HADHA	35.6/48.4	6/7	9.5/13.5	4.21	12	3.46	12	1.14	13
P08195	SLC3A2	15.8/30.01	2/2	5.3/5.1	3.05	4	2.74	4	1.13	4
P53618	COPB1	14.2/28.1	3/3	8.4/5.4	2.88	4	3.37	4	1.08	5
Q96N67	DOCK7	20.7/23.1	4/3	2.3/2.0	2.49	6	3.37	6	1.07	7
P53621	COPA	40.8/21.1	7/3	7.3/3.4	3.02	8	2.93	9	1.04	10
P27824	CANX	35.3/35.1	3/5	9.1/10.0	3.21	8	3.49	8	1.04	9
Q92504	SLC39A7	15.0/26.0	1/1	3.7/3.7	9.47	6	8.09	6	1.03	7
P11021	HSPA5	310.3/272.1	23/25	40.2/41.1	3.96	55	4.45	55	0.87	62
P61026	RAB10	24.2/54.0	3/4	17.0/22.5	2.91	5	3.34	5	0.83	6
P09172	DBH	5.4/92.8	1/13	1.6/24.3	2.66	11	3.63	11	0.82	15
Q09028	RBBP4	25.9/6.89	5/1	18.1/3.8	1.23	5	2.80	4	0.81	4
P49411	TUFM	40.1/71.9	3/9	9.3/27.2	2.66	14	3.18	13	0.77	14
O95831	AIFM1	5.8/11.6	2/3	11.5/6.4	13.71	3	8.33	4	0.71	4
Q9UHL4	DPP7	9.9/26.6	2/3	6.7/8.5	1.08	4	6.46	4	0.39	4
Q06830	PDRX1	20.3/75.2	3/7	21.6/51.3	0.85	13	2.63	13	0.35	13
P17677	GAP43	9.1/34.7	1/2	9.7/16.4	0.84	4	3.74	4	0.23	4
Q92870	APBB2	32.6/49.8	3/3	4.4/10.7	1.00	8	79.59	10	0.01	8

Table 4.1 cont. The APP695 and APP751 interactome

A comprehensive list of all proteins identified as enriched across the two experiments including details of the Uniprot identifier used for subsequent ontology analyses, gene name, score, peptide count and sequence coverage, as well as interaction ratios comparing all three experimental cell lines. Proteins are ordered in the table on the basis of the ratio of interaction between the two APP study isoforms, with those showing higher interaction with APP695 at the top of the table, while those showing higher interaction with APP751 are found at the bottom of the table.

Interactome	Category	Function term	Fold enrichment	P-value (Benjamini)
APP695	Biological process	ATP biosynthetic pathway	18.1	$1.6x10^{-2}$
APP695	Biological process	Nuclear transport	18.4	$1.9x10^{-3}$
APP695	Cellular component	Nuclear pore	18.4	$1.9x10^{-3}$
APP751	Cellular component	Cytoplasmic membrane-bounded vesicle	5.8	$7.91x10^{-6}$

Table 4.2 Gene ontology analysis of APP interacting proteins

The interactomes of the APP isoforms were subjected to gene ontology analysis to identify functions enriched in their interactomes. Gene ontology analysis was performed on proteins that were considered to be enriched in each APP isoform interactome. Uniprot accession numbers were used as gene identifiers and ontology analysis carried out using DAVID software (http://david.abcc.ncifcrf.gov/).

Category	Function term	Fold enrichment	P-value (Benjamini)
Biological process	Protein import into nucleus, docking	159.2	$3.9x10^{-2}$
Cellular component	Mitochondrial part	7.1	$4.4x10^{-2}$

Table 4.3 Mitochondrial and nuclear proteins are enriched in the APP695 interactome

Further gene ontology analysis was performed on proteins which showed large differences in interaction ratios between the two APP isoforms. Proteins which showed at least 2 fold higher interaction with either isoform were analysed using DAVID software. Functions displayed in the table were only enriched in the APP695 interactome.

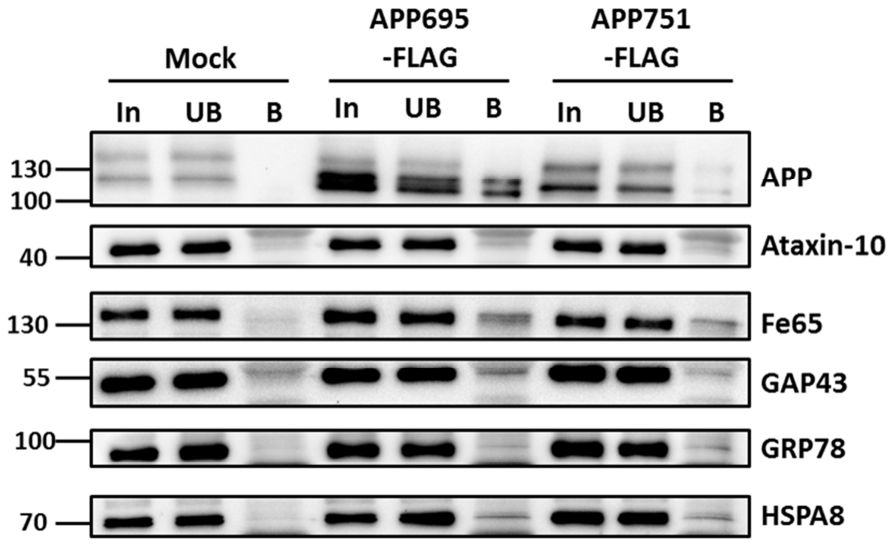

Figure 4.5 Co-immunoprecipitation for the confirmation of APP interactors

Immunoprecipitations were performed on cell lysates from mock, APP695-FLAG and APP751-FLAG expressing SH-SY5Y cells using FLAG monoclonal antibody linked to protein A Dynabeads. Input (In), unbound (UB) and bound (B) fractions were immunoblotted for APP alongside Ataxin-10, Fe65, GAP43, GRP78 and HSPA8, all of which were identified as enriched in the interactome for at least one APP isoform (see Table 4.1).

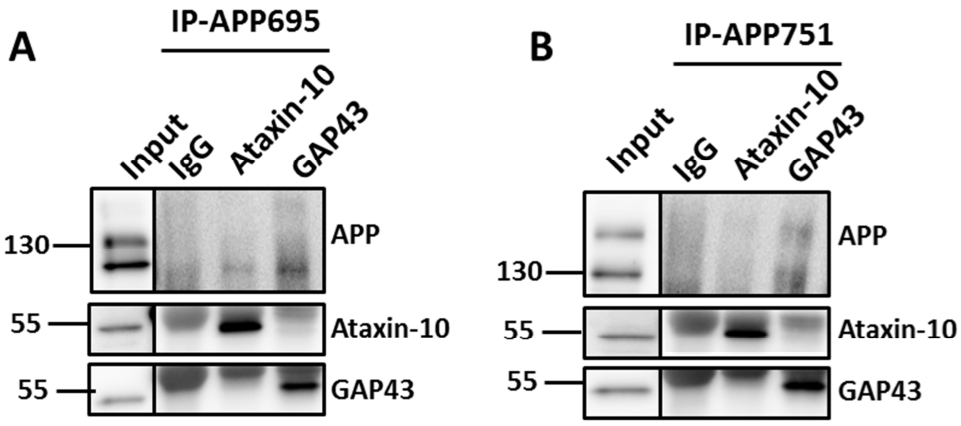

Figure 4.6 Immunoprecipitation of Ataxin-10 or GAP43 results in co-immunoprecipitation of APP

Ataxin-10 and GAP43 were immunoprecipitated from cell lysates from A) APP695-FLAG expressing or B) APP751-FLAG expressing SH-SY5Y cells with an IgG control immunoprecipitation. Input and bound fractions from each IP were then subjected to immunoblot analysis for APP, Ataxi-n10 and GAP43 to confirm immunoprecipitation of the target protein and co-immunoprecipitation of APP.

4.2.4 The APP interactome yields modulators of APP proteolysis

Several interactors were screened for their effect on APP proteolysis. As data presented in **Chapter** 3 recapitulated the increased propensity for the APP695 isoform to follow amyloidogenic proteolysis observed by Belyaev et al. (2010), we focused on proteins which showed differences in their interaction with the two APP isoforms. Proteins were selected on the basis of previous studies within the literature suggesting interaction or co-localisation either with full length APP, or APP fragments or on the basis of their function potentially leading to reduced APP proteolysis by β- or α-secretase.

We initially focused on seven proteins; four showing higher interaction with APP695 (Fe65, ATP-binding cassette sub-family B member 1 (ABCB1), integral membrane protein 2C (ITM2C) and ataxin-10), and three showing higher interaction with APP751 GAP43, peroxiredoxin-1, and dipeptidyl peptidase 2 (DPP7)). Fe65 has previously been shown to influence APP proteolysis (Ando et al. 2001;Suh et al. 2011), though the effect of this interaction on Aβ generation has remained controversial (Pastorino et al. 2013). It has previously been shown that ABCB1 can bind extracellular Aβ and influence its transport across the cell membrane (Kuhnke et al. 2007), while ABCB1 knockout mice show enhanced Aβ accumulation (Cirrito et al. 2005) and a polymorphism in the ABCB1 gene has recently been linked to AD (Feher et al. 2014). Ataxin-1, a member of the same protein family as ataxin-10, has previously been shown to alter proteolysis of APP (Zhang et al. 2010). ITM2C or BRI3 has also been suggested to influence APP proteolysis (Matsuda et al. 2009a), while a related family member, BRI2, has been shown to inhibit Aβ generation through direct interaction with APP (Matsuda et al. 2008). GAP43 has previously been shown to co-localise in various experimental models with APP (Masliah et al. 1992a;Masliah et al. 1992b;Zhan et al. 1995), while peroxiredoxin-1 is involved in the cellular response to oxidative stress which has been reported to be a contributing factor in AD pathogenesis (reviewed in (Zhao and Zhao 2013)). As APP751 appears to undergo significantly less BACE1 proteolysis, we hypothesised an alternative protease may be responsible for APP751 proteolysis. As the protease DPP7 showed higher interaction with APP751 in the mass spectrometry data we also sought to determine whether it could be responsible for the differences observed in proteolysis of the APP isoforms. Experiments on APP695-FLAG and APP751-FLAG expressing cells were carried out in parallel to determine any isoform dependent effects of protein interactions.

Fe65

The effect of the APP-Fe65 interaction on APP proteolysis remains unclear, with several experimental models giving conflicting results (reviewed in (McLoughlin and Miller 2008)). Mass

spectrometry data indicated a 60-fold higher interaction between APP695-FLAG and Fe65 compared to APP751-FLAG, and we therefore investigated the effect of Fe65 knockdown on APP isoform proteolysis. APP695-FLAG and APP751-FLAG expressing SH-SY5Y cells were transfected with 50 nM siRNA against Fe65 for 48 h, and were subsequently incubated with serum free Opti-MEM for 6 h. The conditioned cell medium was removed and the cells were lysed and the cell lysates were subjected to immunoblot analysis for APP, Fe65 and actin (**Figures 4.7A and 4.7B**). Quantification showed 65% knockdown of Fe65 in both the APP695-FLAG and the APP751-FLAG expressing cells (**Figures 4.7C and 4.7D**). The amount of APP was not significantly altered following Fe65 knockdown in either the APP695-FLAG or the APP751-FLAG expressing cells (**Figures 4.7E and 4.7F**). A significant increase in sAPPβ (increased by 17%), but no significant difference in sAPPα, was observed in the conditioned cell medium from the APP695-FLAG expressing cells following Fe65 knockdown (**Figure 4.7G**). No significant difference was observed in the amount sAPPα or sAPPβ in the conditioned cell medium from the APP751-FLAG expressing cells following Fe65 knockdown (**Figure 4.7H**). A significant increase in Aβ38 (increased by 26%) and Aβ40 (increased by 15%) was observed in the conditioned cell medium from the APP695-FLAG expressing cells following Fe65 knockdown (**Figure 4.7I**). No significant differences were observed for any Aβ species in the conditioned cell medium from the APP751-FLAG expressing cells following Fe65 knockdown (F**igure 4.7J**). These data suggest that the APP-Fe65 interaction protects APP from BACE1 proteolysis and subsequent γ-secretase proteolysis, but is specific to the APP695 isoform. Though the knockdown of Fe65 appeared to alter the generation of Aβ38, Aβ40 and Aβ42 to differing extents from the APP695 isoform, no significant differences were observed in the Aβ40:Aβ42, Aβ38:Aβ42 or Aβ40:Aβ38+Aβ42 ratio (data not shown).

The phosphorylation status of APP at residue T743 has been shown to influence the extent to which APP interacts with Fe65, and also influence the rate at which APP undergoes amyloidogenic proteolysis (Ando et al. 2001). Given Fe65 was shown by mass spectrometry to interact to a greater extent with APP695, but APP695 also undergoes more amyloidogenic proteolysis, we sought to determine whether the two APP isoforms are differentially phosphorylated at the amino acid residue T743 (p-APP). Attempts were made to perform immunoblot analysis on phosphorylation of T743 directly in cell lysates, but the selected antibody was not sensitive enough to detect p-APP. Instead, APP695-FLAG and APP751-FLAG were immunoprecipitated from SH-SY5Y cell lysates using anti-FLAG affinity gel and probed for total APP and p-APP with a phosphorylation specific antibody (**Figure 4.8A**). Levels of p-APP were corrected for total APP pull-down and showed a no significant difference in APP at T743 (**Figure 4.8B**).

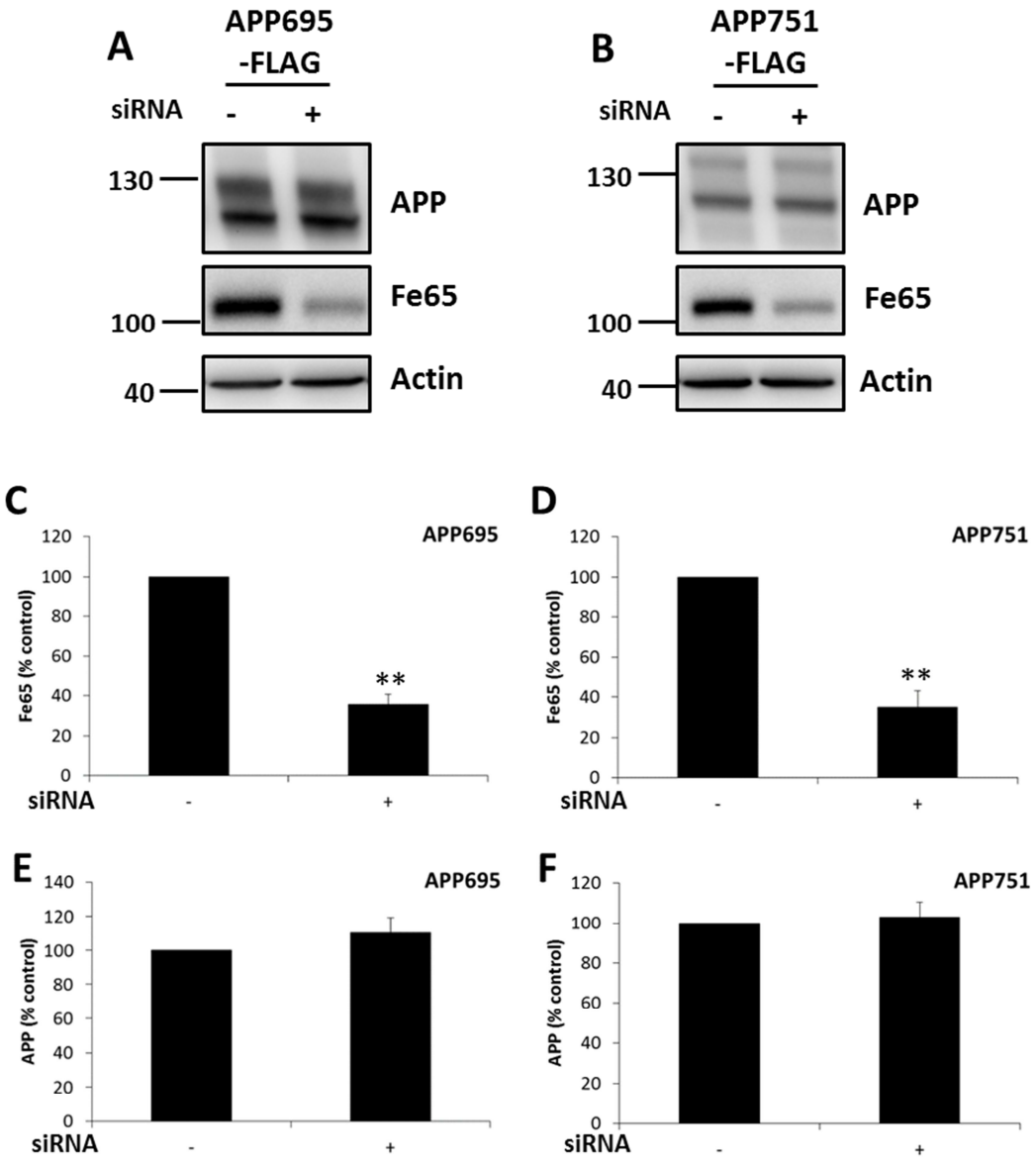

Figure 4.7 Fe65 knockdown increases amyloidogenic proteolysis in APP695-FLAG, but not APP751-FLAG, expressing cells

Figure continued overleaf.

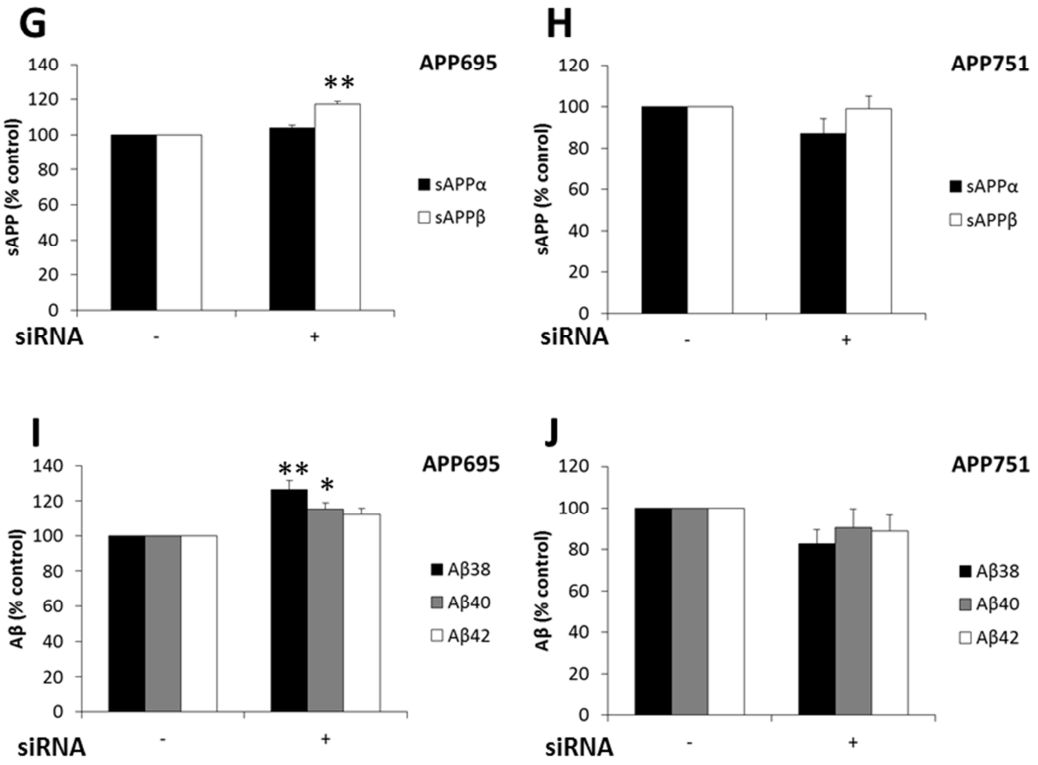

Figure 4.7 cont. Fe65 knockdown increases amyloidogenic proteolysis in APP695-FLAG, but not APP751-FLAG, expressing cells

Fe65 was knocked down in **A)** APP695-FLAG expressing and **B)** APP751-FLAG expressing SH-SY5Y cells using 50nM smartpool siRNA complexed with Dharmafect 1 transfection reagent in DMEM for 48 h. The cell medium was replaced with Opti-MEM and cells were cultured for a further 6 h. Cells were lysed and subjected to immunoblot analysis for APP, Fe65 and actin. Densitometric analysis of Fe65 in **C)** APP695-FLAG expressing cells and **D)** APP751-FLAG expressing cells. Densitometric analysis of APP in **E)** APP695-FLAG expressing cells and **F)** APP751-FLAG expressing cells. MSD analysis for sAPPα and sAPPβ in the conditioned cell medium from **G)** APP695-FLAG expressing cells and **H)** APP751-FLAG expressing cells. MSD analysis for Aβ38, Aβ40, and Aβ42 in the conditioned cell medium from **I)** APP695-FLAG expressing cells and **J)** APP751-FLAG expressing cells. Bars represent the mean, errors bars are ± S.E.M., *, p-value<0.05, **, p-value <0.01, n=3. In control experiments (-) for APP695 average absolute Aβ38, Aβ40 and Aβ42 levels were 211 pg/mg, 779 pg/mg and 83 pg/mg, respectively. In control experiments (-) for APP751 average absolute Aβ38, Aβ40 and Aβ42 levels were 223 pg/mg, 616 pg/mg and 64 pg/mg, respectively.

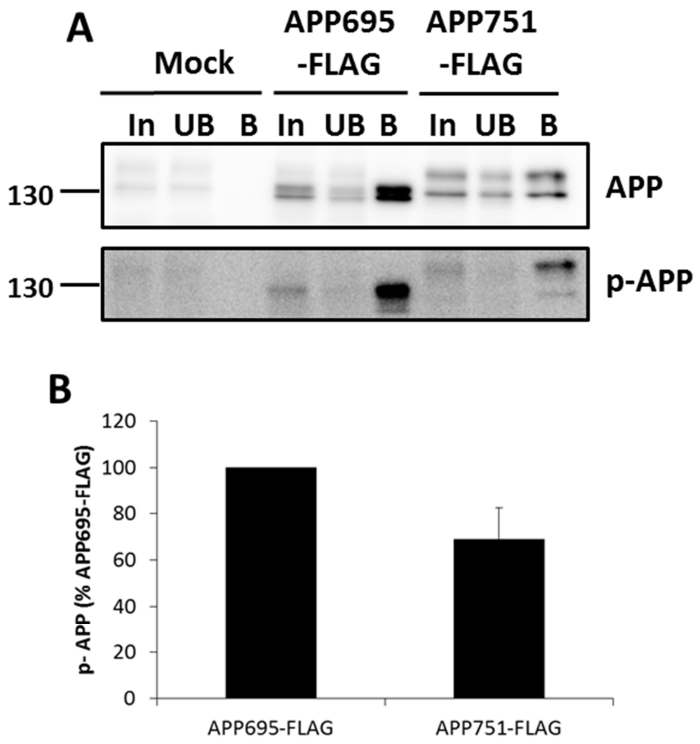

Figure 4.8 The amount of phosphorylated APP does not differ significantly between the APP isoforms

Immunoprecipitations were carried out on cell lysates from mock transfected, APP695-FLAG and APP751-FLAG expressing SH-SY5Y cells using FLAG-tag affinity gel. **A)** Input (In), unbound (UB) and bound (B) fractions were subjected to immunoblot analysis for APP and APP phosphorylated at T743 using a phosphor-epitope specific antibody (p-APP). **B)** Densitometric analysis was performed on APP and p-APP and the level of p-APP corrected for total APP. Bars represent the mean, error bars are S.E.M., n=3.

Ataxin-10

We next investigated the effect of ataxin-10 knockdown on APP proteolysis. As with Fe65, ataxin-10 showed 60-fold higher interaction with APP695 in the mass spectrometry analysis. APP695-FLAG and APP751-FLAG expressing SH-SY5Y cells were transfected with 50 nM siRNA against ataxin-10 for 48 h, and were subsequently cultured in Opti-MEM for 6 h. The conditioned cell medium was removed and the cells were lysed and the cell lysates were subjected to immunoblot analysis for APP, ataxin-10 and actin (**Figures 4.9A and 4.9B**). Quantification showed 45% and 38% knockdown of ataxin-10 in APP695-FLAG and APP751-FLAG expressing cells, respectively (**Figures 4.9C and 4.9D**). No significant differences were observed in the amount of APP in either the APP695-FLAG or the APP751-FLAG expressing cells (**Figures 4.9E and 4.9F**). No significant differences in sAPPα or sAPPβ were observed in the conditioned cell medium from APP695-FLAG expressing cells upon knockdown of ataxin-10 (**Figure 4.9G**). No significant difference was observed in sAPPα in the conditioned cell medium from APP751-FLAG expressing cells, while a statistically significant 5% increase in sAPPβ was observed following ataxin-10 knockdown (**Figure 4.9H**). Aβ38, Aβ40 and Aβ42 were all significantly reduced by 15% in the conditioned cell medium from the APP695-FLAG expressing cells upon ataxin-10 knockdown (**Figure 4.9I**). No significant difference was observed in any Aβ species in the conditioned cell medium from the APP751-FLAG expressing cells following ataxin-10 knockdown (**Figure 4.9J**).

GAP43

The effect of GAP43 knockdown on APP proteolysis was investigated in APP expressing SH-SY5Y cells. Mass spectrometry data indicated 4-fold greater interaction between GAP43 and APP751-FLAG than APP695-FLAG. APP695-FLAG and APP751-FLAG expressing SH-SY5Y cells were transfected with 50 nM siRNA against GAP43 for 48 h, and were subsequently cultured in Opti-MEM for 6 h. The conditioned cell medium was removed and the cells were lysed and the cell lysates were subjected to immunoblot analysis for APP, GAP43 and actin (**Figures 4.10A and 4.10B**). Quantification showed GAP43 knockdown of 37% and 35% in the APP695-FLAG and APP751-FLAG expressing cells, respectively (**Figures 4.10C and 4.10D**). No significant difference was observed in the amount of APP in APP695-FLAG expressing cells (**Figure 4.10E**) or APP751-FLAG expressing cells (**Figure 4.10F**) following GAP43 knockdown. No significant difference was observed in sAPPα or sAPPβ in the conditioned cell medium from the APP695-FLAG expressing cells (**Figure 4.10G**) or the APP751-FLAG expressing cells (**Figure 4.10H)** following GAP43 knockdown. No significant difference was observed in any Aβ species in the conditioned cell medium from the APP695-FLAG expressing cells following GAP43 knockdown (F**igure 4.10I**). No

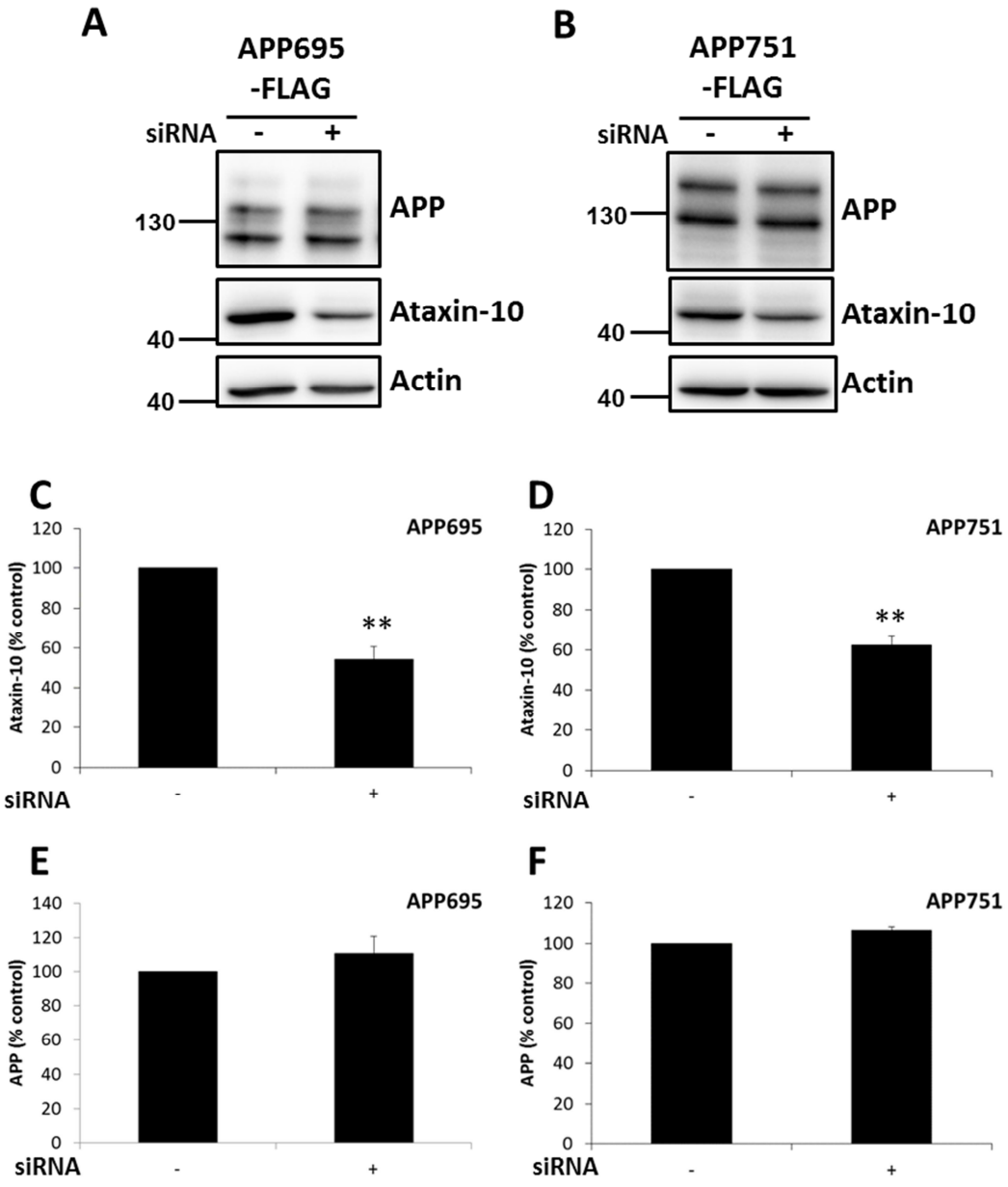

Figure 4.9 Ataxin-10 knockdown reduces Aβ in APP695-FLAG, but not APP751-FLAG expressing cells

Figure continued overleaf.

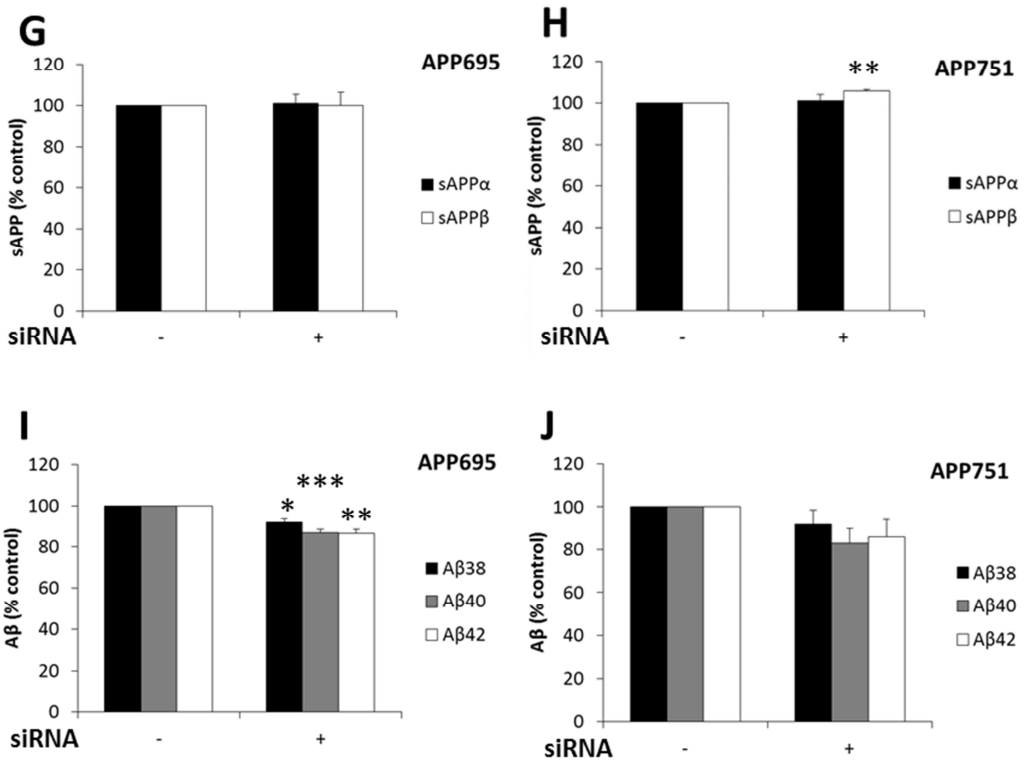

Figure 4.9 cont. Ataxin-10 knockdown reduces Aβ in APP695-FLAG, but not APP751-FLAG, expressing cells

Ataxin-10 was knocked down in **A)** APP695-FLAG expressing and **B)** APP751-FLAG expressing SH-SY5Y cells using 50nM smartpool siRNA complexed with Dharmafect 1 transfection reagent in DMEM for 48 h. The cell medium was replaced with Opti-MEM and cells were cultured for a further 6 h at 37°C, 5% CO_2. Cells were lysed and subjected to immunoblot analysis for APP, ataxin-10 and actin. Densitometric analysis of ataxin-10 in **C)** APP695-FLAG expressing cells and **D)** APP751-FLAG expressing cells. Densitometric analysis of APP in **E)** APP695-FLAG expressing cells and **F)** APP751-FLAG expressing cells. MSD analysis for sAPPα and sAPPβ in the conditioned cell medium from **G)** APP695-FLAG expressing cells and **H)** APP751-FLAG expressing cells. MSD analysis for Aβ38, Aβ40, and Aβ42 in the conditioned cell medium from **I)** APP695-FLAG expressing cells and **J)** APP751-FLAG expressing cells. Bars represent the mean, errors bars are ± S.E.M., *, p-value<0.05, **, p-value <0.01, ****, p-value <0.001, n=5 for APP695, n=3 for APP751.

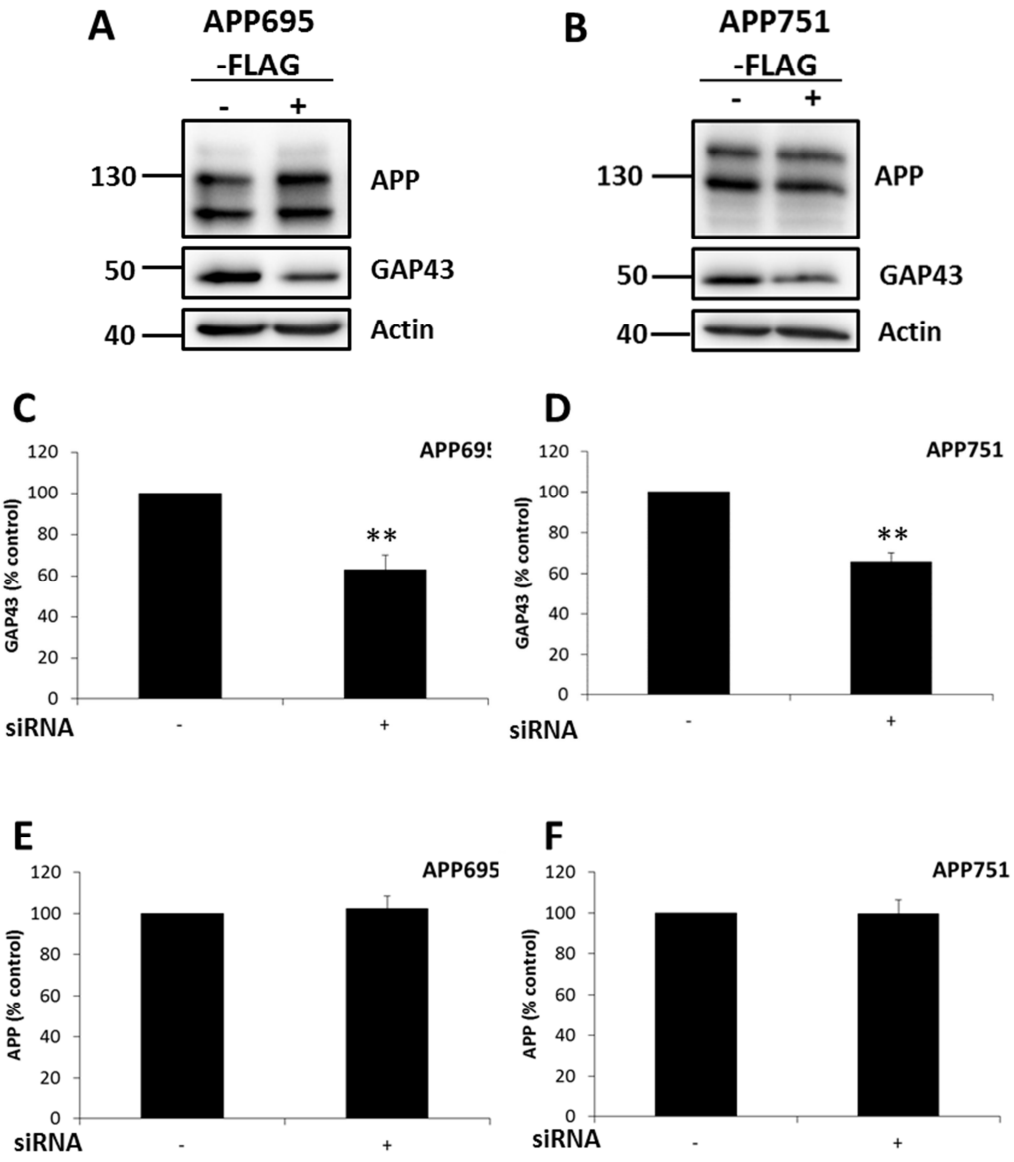

Figure 4.10 GAP43 knockdown reduces Aβ in APP751-FLAG, but not APP695-FLAG expressing cells

Figure continued overleaf.

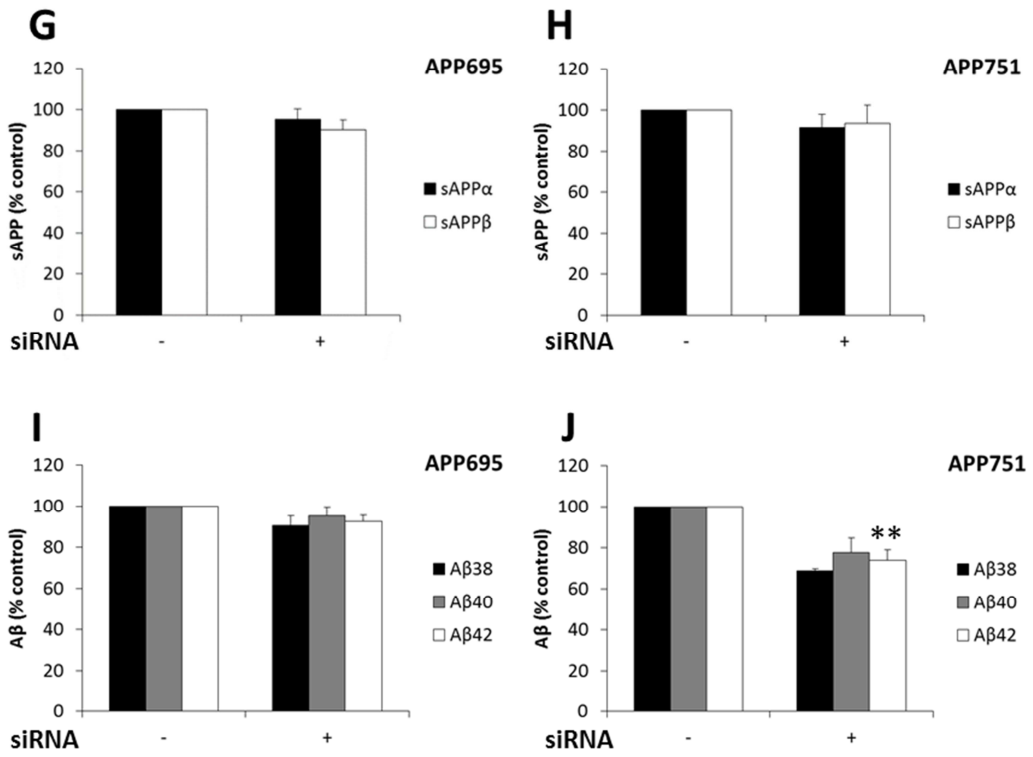

Figure 4.10 cont. GAP43 knockdown reduces Aβ in APP751-FLAG, but not APP695-FLAG expressing cells

GAP43 was knocked down in **A)** APP695-FLAG expressing and **B)** APP751-FLAG expressing SH-SY5Y cells using 50nM smartpool siRNA complexed with DharmaFECT 1 transfection reagent in DMEM for 48 h. The cell medium was replaced with Opti-MEM and cells were cultured for a further 6 h. Cells were lysed and subjected to immunoblot analysis for APP, GAP43 and actin. Densitometric analysis of GAP43 in **C)** APP695-FLAG expressing cells and **D)** APP751-FLAG expressing cells. Densitometric analysis of APP in **E)** APP695-FLAG expressing cells and **F)** APP751-FLAG expressing cells. MSD analysis for sAPPα and sAPPβ in the conditioned cell medium from **G)** APP695-FLAG expressing cells and **H)** APP751-FLAG expressing cells. MSD analysis for Aβ38, Aβ40, and Aβ42 in the conditioned cell medium from **I)** APP695-FLAG expressing cells and **J)** APP751-FLAG expressing cells. Bars represent the mean, errors bars are ± S.E.M., *, p-value<0.05, **, p-value <0.01, n=3. Aβ38 for APP751-FLAG, n=2).

significant difference was observed for Aβ40, but Aβ42 was significantly reduced by 27% in the conditioned medium from the APP751-FLAG expressing cells following GAP43 knockdown (**Figure 4.10J**). Due to the lower production of Aβ in the APP751-FLAG cell line Aβ38 could only be measured in the conditioned cell medium in two experiments and therefore statistics were not applied to this result.

ABCB1 and peroxiredoxin-1 do not consistently alter APP proteolysis

The mass spectrometry data indicated greater interaction between APP695 and ABCB1 compared to APP751, while peroxiredoxin-1 interacted to a greater extent with APP751. APP695-FLAG and APP751-FLAG expressing SH-SY5Y cells were transfected with 50 nM siRNA against ABCB1 or peroxiredoxin-1 for 48 h, and were subsequently cultured in Opti-MEM for 6 h. The conditioned cell medium was removed and the cells were lysed and the cell lysates were subjected to immunoblot analysis for APP, ABCB1 or peroxiredoxin-1 and actin (**Figures 4.11A and 4.11B**). APP was not significantly altered in either APP expressing cell line upon knockdown of ABCB1 or peroxiredoxin-1 (**Figure 4.11C and 4.11D**). No significant difference was observed in sAPPα or sAPPβ in the conditioned cell medium from either the APP695-FLAG expressing cells (**Figure 4.11E**) or the APP751-FLAG expressing cells (**Figure 4.11F**) upon ABCB1 or PRDX1 knockdown. No significant difference was observed for any Aβ species in the conditioned cell medium from the APP695-FLAG expressing cells following ABCB1 or PRDX1 knockdown (**Figure 4.11G**). No significant difference was observed for any Aβ species in the conditioned cell medium from the APP751-FLAG expressing cells following peroxiredoxin-1 knockdown or in Aβ42 following ABCB1 knockdown (**Figure 4.11H**). A significant 6% reduction was observed in Aβ40 following ABCB1 knockdown (**Figure 4.11H**). Due to the lower production of Aβ in the APP751-FLAG cell line Aβ38 could only be measured in the conditioned cell medium in two experiments following ABCB1 and peroxiredoxin-1 knockdown and therefore statistics were not applied to these results.

ITM2C and DPP7 could not be significantly knocked down in SH-SY5Y cells

ITM2C and DPP7 were also determined to be of interest in the proteolysis of the APP isoforms. APP695-FLAG and APP751-FLAG expressing SH-SY5Y cells were transfected with 25 or 50 nM siRNA against ITM2C (**Figure 4.12A**) or DPP7 (**Figure 4.12B**) for 24 or 48 h or with 50 nM siRNA for 72 h and were subsequently cultured in Opti-MEM for 6 h. The conditioned cell medium was removed and the cells were lysed and the cell lysates were subjected to immunoblot analysis for APP and ITM2C or DPP7. Immunoblot analysis showed variation in the siRNA concentration over the different time periods did not alter the knockdown of the target proteins. Similarly, variations in the amount of DharmaFECT 1 used for the siRNA transfection could not induce

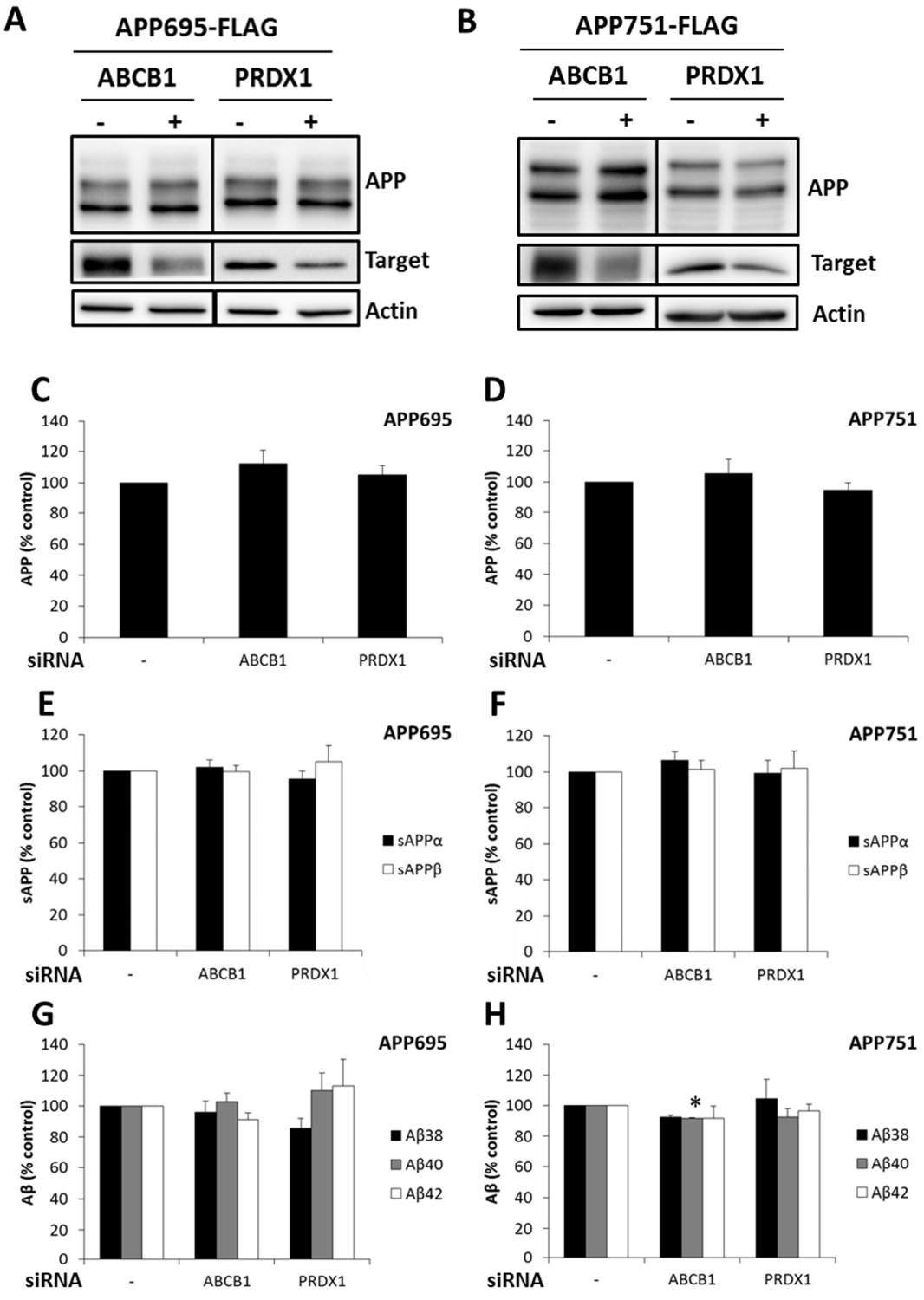

Figure 4.11 ABCB1 and peroxiredoxin-1 knockdown do not consistently alter APP proteolysis in APP695-FLAG or APP751-FLAG expressing cells

Figure legend overleaf.

Figure 4.11 cont. ABCB1 and peroxiredoxin-1 knockdown do not consistently alter APP proteolysis in APP695-FLAG or APP751-FLAG expressing cells

ABCB1 or peroxiredoxin 1 (PRDX1) were knocked down in **A)** APP695-FLAG expressing and **B)** APP751-FLAG expressing SH-SY5Y cells using 50nM smartpool siRNA complexed with Dharmafect 1 transfection reagent in DMEM for 48 h. The cell medium was replaced with Opti-MEM and cells were cultured for a further 6 h. Cells were lysed and subjected to immunoblot analysis for APP, ABCB1 or PRDX1 and actin. Densitometric analysis of APP in **C)** APP695-FLAG expressing cells and **D)** APP751-FLAG expressing cells. MSD analysis for sAPPα and sAPPβ in the conditioned cell medium from **E)** APP695-FLAG expressing cells and **F)** APP751-FLAG expressing cells. MSD analysis for Aβ38, Aβ40, and Aβ42 in the conditioned cell medium from **G)** APP695-FLAG expressing cells and **H)** APP751-FLAG expressing cells. Bars represent the mean, errors bars are ± S.E.M., *, p-value<0.05, n=3. APP751-FLAG (Aβ38 APP751-FLAG n=2).

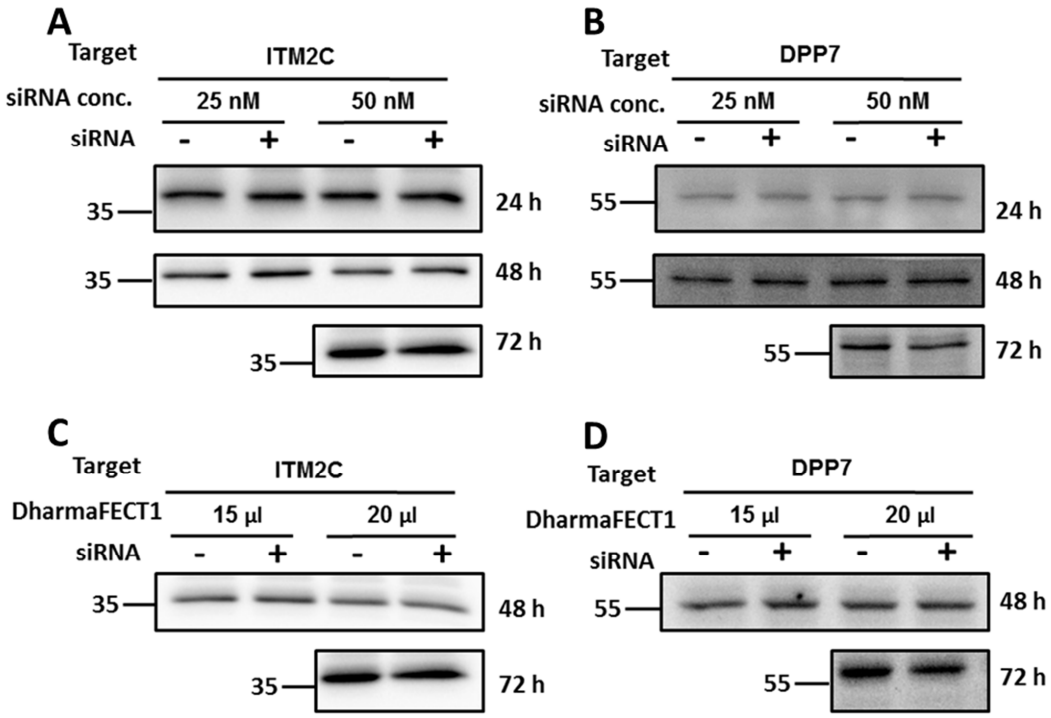

Figure 4.12 ITM2C and DPP7 could not be significantly knocked down in SH-SY5Y cells

SH-SY5Y cells were subjected to standard siRNA knockdown over a period of 24, 48 or 72 h with variations in the siRNA concentration for A) ITM2C or B) DPP7. The siRNA knockdown was also performed for C) ITM2C and D) DPP7 with increased amounts of DharmaFECT 1 transfection reagent. Cells were lysed and subjected to immunoblot analysis for ITM2C and DPP7.

significant knockdown of ITM2C (**Figure 4.12C**) or DPP7 (**Figure 4.12D**) over 48 or 72 h knockdown periods. The blots shown in **Figure 4.12** are representative blots from knockdowns in either the APP695-FLAG or the APP751-FLAG expressing cells. Significant knockdown could not be achieved in either cell line.

4.2.5 Ataxin-10, but not GAP43, is altered in the AD brain

To determine whether the interactions identified in our cell model could have relevance to AD progression or development, brain samples from the temporal cortex of AD and control donors were subjected to immunoblot analysis to determine the amount of ataxin-10 and GAP43 (**Figure 4.13A**). A cell lysate sample was loaded on each gel to ensure quantification of the correct band in the brain samples. Densitometric analysis showed significantly less ataxin-10 in the samples from the AD patients compared to the control samples (**Figure 4.13B**), while no differences were observed in the amount of GAP43 between the AD and control brains (**Figure 4.13C**). The blots shown are representative of the cohort.

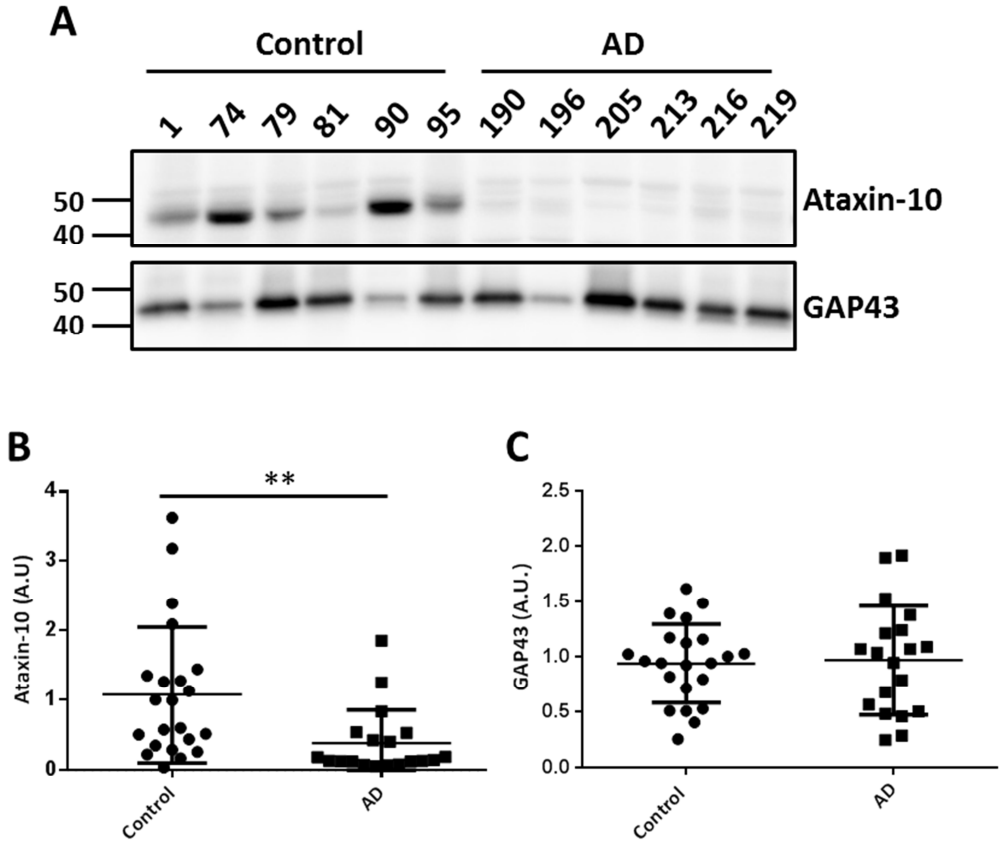

Figure 4.13 Ataxin-10 is significantly reduced, and GAP43 is unchanged, in the temporal cortex of AD patients

A) Human temporal cortex samples from control and AD patients were subjected to immunoblot analysis for ataxin-10 and GAP43. The blot shown is a representative blot for the cohort**.** Densitometric analysis of **B)** ataxin-10 and **C)** GAP43 is represented as a scatter plot of all samples. Lines represent the mean, error bars are ± standard deviation, **, p-value <0.01, n=22 control and 19 AD. A.U. = Arbitrary units. Numbers above the blots represent patient numbers.

4.3 Discussion

4.3.1 Application of SILAC to APP interactomic analysis

Interactomic analyses can give insight into protein function and subcellular location and reveal interactors important in the modulation of function. Despite the complexities surrounding APP function and metabolism, an unbiased study of the APP interactome in a neuronal cell line had not been performed until now. The methodology employed in our study, through the application of SILAC, overcomes the difficulties with the relatively non-quantitative nature of normal mass-spectrometry and gives high labelling efficiency, ensuring confidence in the data obtained (Munday et al. 2012). The isotopic labelling of arginine and lysine residues ensures the capacity for mass spectrometry to distinguish between peptides derived from specific cell conditions, or in our case cell lines, as trypsin digestion prior to mass spectrometry analysis ensures the presence of at least one labelled amino acid in each tryptic peptide, barring the final C-terminal peptide (Munday et al. 2012).

We have used an unbiased mass spectrometry screening approach to identify proteins that interact with two APP isoforms in a cell culture context. Through this screening method we have identified 69 proteins which meet the criteria we have used to determine whether proteins are true interactors or not. These parameters are of course arbitrary, but we believe represent a stringent enough cut off to identify only proteins which are direct interactors. Through the use of a C-terminally FLAG-tagged APP constructs we have avoided the use of any anti-APP antibody for the immunoprecipitation, the immunoreactivity of which may be blocked by interacting partners. In addition, we have shown that the addition of this 8 amino acid tag sequence does not affect the proteolysis of APP in our model system in **Chapter 3**. Our experimental design, using C-terminally tagged APP constructs means that identified proteins may interact with full length APP, CTFs produced by α- or β-secretase proteolysis or AICD.

Given the sensitivity of mass spectrometry, it is almost impossible to completely control for false positives in the dataset, as any immunoprecipitation based experiment will result in the presence of proteins within a sample which are not necessarily directly interacting with the bait protein (Mann 2006). In order to reduce the presence of proteins which were not interacting directly with APP we used fairly stringent criteria for the inclusion of a protein in the final dataset. LC-MS/MS analysis was performed on SILAC labelled cell lysate samples from two individual experiments and only those proteins identified in both experiments were taken forward into the final analysis. In an attempt to remove the presence of false positives from the dataset we set a cut-off for each APP isoform based on the average protein ratio of the APP to

mock transfected cell lines of the whole data set. The use of this average as the threshold for considering a protein a true interactor has previously been applied in a similar study of the APP interactome in the mouse brain (Kohli et al. 2012) and may represent a more stringent method for the removal of false positive interactors than the standard 2-fold cut off used in several other SILAC based interactome studies (Hosp et al. 2015;Emmott et al. 2013).

One major limitation of large scale proteomic studies is the apparent lack of consistency in the analysis of data produced with high-throughput data often not replicable in low-throughput analyses (Perreau et al. 2010). Indeed, despite wide reports of strong interaction between APP and Fe65, several studies have failed to identify this interaction in mass spectrometry based experiments (Bai et al. 2008;Hosp et al. 2015;Kohli et al. 2012). Due to its widely reported interaction with APP, we used Fe65 to confirm successful co-immunoprecipitation conditions prior to the LC-MS/MS analyses and were able to show interaction with both APP isoforms, a result confirmed in the LC-MS/MS analysis. Difficulty often arises in comparing across proteomic analyses due to differences in experimental approaches or lack of access to full proteomic datasets. Our dataset identified several proteins previously identified as APP interactors in mass spectrometry based studies including calnexin (CALX) and GRP78 (or HSPA5) (Bai et al. 2008), HSPA8 (Hosp et al.;Cottrell et al. 2005) and voltage-dependent anion selective channel protein (VDAC)3, Sodium/potassium-transporting ATPase subunit alpha-1 (ATP1A1) and Solute carrier family 25 member 3 (SLC25A3) (Kohli et al. 2012). Despite their well-studied roles in the proteolytic cleavage of APP, neither β- nor α-secretase were identified in the dataset, nor were any of the components of the γ-secretase complex. In a recent paper published during the preparation of this thesis, another SILAC LC-MS/MS based analysis of APP interactors failed to show co-immunoprecipitation of the secretases, suggesting that the transient nature of their interaction may prevent their co-immunoprecipitation (Hosp et al. 2015).

4.3.2 Functional clues from the APP interactome

As discussed in **Chapter 1** of this thesis, the exact molecular function of APP remains enigmatic despite its highly characterised structure and a wide range of postulated roles. Difficulties in deciphering a single role for APP may be down to the presence in the brain of several APP isoforms, and proteolytic fragments as well as the presence of the closely related homologs APLP1 and APLP2 (Kohli et al. 2012).

The study we have performed here does not provide definitive proof of a single function for APP, but provides support for several functions identified in the literature. The ontology analyses presented in this thesis, using our stringent cut off values for true interaction have

highlighted association between APP and various mitochondrial proteins. Intriguingly this association appears to be stronger for the APP695 isoform. APP has previously be implicated in altered mitochondrial function (Chua et al. 2013) and has been shown to accumulate in mitochondrial import channels in AD (Devi et al. 2006), while disruption of mitochondrial function has been widely reported in Alzheimer's disease (for review see (Ankarcrona et al. 2010)). Chua et al., (2013) observed a greater increase in mitochondrial activity and gene expression upon expression of APP695 than APP751 in an APP null cell line, data which appears to corroborate the isoform difference we have observed here. However, these data are not necessarily in agreement with that suggesting APP within the mitochondria can lead to mitochondrial dysfunction. It is plausible that accumulation in the mitochondrial import channels is indeed an aberrant process and AD related, while steady state APP presence in the mitochondrial membrane could have functional implications. The APP amino acid sequence contains a cryptic mitochondrial signal sequence suggesting that its presence in mitochondria is not solely due to aberrant localisation induced by over-expression (Anandatheerthavarada et al. 2003). Aβ and AICD have both been shown to be produced in the mitochondrial membrane, particularly in MAMs (Schreiner et al. 2015). These domains have been shown to resemble the lipid raft domains found within the plasma membrane, and are enriched in cholesterol, in which palmitoylated proteins including APP (Bhattacharyya et al. 2013), BACE1 (Vetrivel et al. 2009) and the nicastrin and APH-1 subunits of the γ-secretase complex (Cheng et al. 2009) are likely to accumulate. Lipid rafts have been postulated as important signalling platforms for intercellular signalling (Rushworth and Hooper 2010), and disruption in MAMs has been implicated in AD pathogenesis (Hedskog et al. 2013). Like plasma membrane lipid rafts, MAMs form important signalling domains for mitochondrial function (Schon and Area-Gomez 2013), but it has not been determined whether APP, or indeed the secretases have a specific role in this process. Despite the fact that APP is orientated within the mitochondrial membrane with its N-terminus in the mitochondrial matrix and C-terminal in the cytosol, AICD has been shown to be present within the mitochondrial matrix (Pavlov et al. 2011). Given the postulated roles for AICD as a transcriptional regulator, it would be interesting to investigate whether this proteolytic APP fragment has a role in the regulation mitochondrial genes. Indeed, this may explain the increased presence of mitochondrial proteins in this, and other interactomic analyses of APP. Whether their presence is due to direct interaction, or is a result of their increase expression may therefore be of interest to pursue further. Hosp et al. (2015) reported that APP bound the protein LRPPRC in the mitochondrial lumen, and thus affected the regulation of mitochondrial gene expression as LRPPRC has been shown to have an important role in post-transcriptional regulation on mitochondrial genes. LRPPRC itself was identified in our interactomic study but

only when a 2-fold cut off was employed, as was used by Hosp et al. (2015) and actually interacted to a greater extent with APP751. Again this may explain why Chua et al. (2013) identified differences in the regulation of mitochondrial genes and activity with APP751 and APP695, as the interaction with APP751 may inhibit the ability of LRPPRC to regulate transcription.

Gene ontology analysis also revealed enrichment of proteins involved in the formation of the nuclear pore specifically in the APP695 interactome, while these proteins were not enriched in the APP751 interactome. We would postulate that this interaction is with AICD which will retain the C-terminal FLAG-tag following proteolysis, rather than full length APP. These data support previous data from our lab which suggested transcriptionally active AICD was produced preferentially from the APP695 isoform (Belyaev et al. 2010). The exact mechanism by which this preferential production of transcriptionally active AICD occurs remains enigmatic, though it may be due to reduced APP751 proteolysis by BACE1, as transcriptionally active AICD has been suggested to be dependent on amyloidogenic proteolysis (Belyaev et al. 2010;Grimm et al. 2015;Goodger et al. 2009). Interestingly, differences in the production of nuclear signalling complexes have also been reported for APLP1 and APLP2. Gersbacher et al. (2013) recently showed that ICD from APLP2 was able to form transcriptionally active complexes with Tip60 and Fe65 and regulate gene expression, while ICD from APLP1 was not. This may go some way to explain why knockout of APP is not embryonically lethal unless combined with APLP2 knockout (Heber et al. 2000). As we have shown in **Chapter 3** of this thesis, APP isoforms do show distinct subcellular distribution, and given APP751 appears to be trafficked to the cell surface to a lesser extent than APP695, it may be that APP751 encounters less Fe65. These data appear to be supported by that in our interactomic analyses, which showed much greater interaction of APP695 with Fe65. In the interactome dataset produced by Hosp et al. (2015), no significant enrichment of nuclear proteins was observed, nor did they observe an interaction between APP and Fe65. In fact, only one protein (VDAC3) in the interactome data set produced by Hosp et al. (2015) met the cut-off criteria we set here (though a further 16 were identified but did not make our final data set due to the stringent cut off criteria we employed). The interactions which were identified may vary significantly between cell lines and it has been shown previously that the nuclear signalling capabilities of AICD appear to be specific to neuronal cells lines (Belyaev et al. 2010), suggesting specific interactions and trafficking pathways in these neuronal cells. It is also worth noting that the strategy adopted by Hosp et al. (2015) used N-terminally tagged APP meaning that CTFs and AICD would be excluded from their immunoprecipitations.

The bioinformatics analyses performed here add weight to the argument that APP, or fragments produced by its proteolysis, can be localised to the mitochondria and are involved in nuclear

signalling. Though the analysis does not highlight any particularly novel functional clues as to the role of APP, it does highlight that the functions of APP in the regulation of protein function need further understanding. Evidence is now mounting for APP and secretase localisation to the mitochondria (Anandatheerthavarada et al. 2003;Devi et al. 2006;Pavlov et al. 2011), yet their role in this organelle has not been extensively studied. Given the reported mitochondrial dysfunction in AD, the exact role and consequences of APP in the mitochondria could be of great interest.

4.3.3 The APP interactome identifies isoform specific modulators of Aβ production

Fe65

The effect of Fe65 on APP proteolysis has been disputed, with some publications suggesting it enhances amyloidogenic proteolysis of APP (Xie et al. 2007;Sabo et al. 1999), while others have suggested the opposite effect (Ando et al. 2001;Wiley et al. 2007). The apparent lack of consistency in results has previously been put down to differences in experimental cell line and methodology (McLoughlin and Miller 2008). Here we show that, concurrent with the increased interaction ratio observed for APP695, Fe65 knockdown appears to specifically increase the amyloidogenic proteolysis of APP695 but not of APP751. Fe65 has been reported to function in aiding nuclear transport of AICD following β-secretase proteolysis, stabilising the labile nature of this fragment and aiding its transport to the nucleus (Goodger et al. 2009;Belyaev et al. 2010). In light of evidence suggesting transcriptionally active AICD is produced predominantly from the APP695 isoform (Belyaev et al. 2010), it is not surprising that Fe65 appears to interact more with this APP isoform and affects the proteolysis of the APP695 isoform to a greater extent than the APP751 isoform. However, it has also been suggested that transcriptionally active AICD is produced preferentially from the amyloidogenic processing pathway (Belyaev et al. 2010;Goodger et al. 2009;Grimm et al. 2015). This makes the result slightly counterintuitive as it would appear Fe65 is blocking BACE1 proteolysis in our cell system. One possibility is that Fe65 binding represents a mechanism through which regulated amyloidogenic proteolysis occurs, allowing for the production of functional AICD. It has been suggested that phosphorylation of T743 may modulate Aβ generation through induction of specific conformational changes in the APP cytosolic domain (Haass et al. 2012). This phosphorylation event however has been suggested to reduce interaction with Fe65 and promote amyloidogenic proteolysis (Lee et al. 2003;Ando et al. 2001), though a threonine to alanine mutation introduced to APP in a transgenic mouse model at this site did not appear to alter APP proteolysis *in vivo* (Sano et al. 2006). Again, these data do not all support the same hypothesis given that we have observed more amyloidogenic proteolysis of APP695 observed a higher degree of interaction of this APP

isoform with Fe65, but did not observe a significant difference in the phosphorylation of the APP isoforms at T743 (though perhaps a trend towards increased phosphorylation in the APP695 isoform is evident). It has been suggested that APP can be phosphorylated by various kinases including cdc2, CDK5 and GSK3β (Pastorino et al. 2013), though the exact kinase responsible for phosphorylating APP at residue T743 remains unresolved. Of course, the difference we see here in the APP isoforms interaction with Fe65 also begs the question as to how the additional extracellular domain influences cytosolic interactions. Again, this could be down to the subcellular environment in which the APP isoforms predominantly localise or due to differences in phosphorylation at the various other phosphorylatable amino acids in the APP cytosolic domain. The T743 residue is not the only residue within the APP cytosolic tail which is phosphorylated and other work has also linked phosphorylation at Tyr682 to increased amyloidogenic proteolysis (Barbagallo et al. 2010), suggesting that these phosphorylated amino acids could have an important role in determining the proteolytic fate of APP. Current data on the mechanisms of APP phosphorylation, and their roles in various protein-protein interactions and Aβ generation paint a confusing picture, and require further study to definitively answer their roles in the development of AD.

Ataxin-10

The ataxin family of proteins are well recognised due to their causative roles in the ataxias. A pentanucleotide repeat in the ataxin-10 gene has been identified as the cause of Spinocerebellar ataxia type 10 but the normal protein function remains largely unknown (Tian et al. 2015). Study of protein knockdown in cerebellar neurons results in increased apoptosis, leading to the suggestion that the disease causing mutation may cause loss of function of ataxin-10 and cell death (Marz et al. 2004). Ataxin-10 has also been linked to the induction of neurite extension and neuronal differentiation , roles not dissimilar to those described for APP in **Chapter 1** of this thesis, indicating possible functional similarities between the two proteins. A stark reduction in ataxin-10 protein in the temporal lobe samples was observed in AD cases compared to control cases. Though this may suggest that ataxin-10 may not contribute significantly to amyloid burden late in the disease process, it is well known that Aβ may begin to accumulate long before the onset of AD. Combined with the similarities in proposed function between APP and ataxin-10, the relationship between these two proteins poses interesting questions. Indeed, the difference in levels of Ataxin-10 between control and AD cases could suggest loss of this protein may contribute significantly to AD pathology through other mechanisms in addition to influencing APP proteolysis. Though we did not screen cells targeted with siRNA with a cell death assay, no observable increases in cell death were noted by microscopy prior to cell lysis, and secretion of the soluble fragments sAPPα and sAPPβ were unaffected in our experiments,

suggesting decreases in Aβ were not as a result of cell death. Ataxin-10 contains an armadillo repeat domain which, in many proteins, enhances their capacity to form protein-protein interactions, potentially identifying a domain for interaction between APP and ataxin-10 (Marz et al. 2004). Despite a lack of knowledge as to the function of ataxin-10, the related protein ataxin-1 has previously been identified as a modulator of APP proteolysis, with its down-regulation causing an increase in the production of Aβ in APP751 expressing H4 cells (Zhang et al. 2010), and was identified as a possible AD risk gene in genome wide association studies (Bertram et al. 2008). It is interesting that these two related proteins have apparently opposite effects on APP proteolysis. The exact mechanism through which ataxin-10 exerts its effect on γ-secretase proteolysis is beyond the scope of the current study but would certainly be of interest given that disruption of the interaction between APP and ataxin-10 could serve as a method for disrupting Aβ production without the requirement for γ-secretase inhibition. Given the proposed neurotoxicity of CTFβ, it would be advisable in further study of this interaction to monitor the effect of knockdown on CTF accumulation.

GAP43

GAP43 has previously been shown to localise with APP in presynaptic boutons in the frontal cortex of AD brains (Masliah et al. 1992b), in outgrowing neurites of the neonatal rat brain (Masliah et al. 1992a) and in neurites surrounding amyloid plaque cores (Zhan et al. 1995). However, this is the first time a direct interaction between the two proteins has been reported. GAP43 is known to be a presynaptic protein (Wang et al. 2014), and the presynaptic membrane has previously been implicated as a site of BACE1 accumulation and amyloidogenic proteolysis of APP (DeBoer et al. 2014;Buggia-Prevot et al. 2014), while Aβ generation has also been shown to be activity dependent in neurons (Kamenetz et al. 2003). It is possible that interaction with GAP43 may contribute to retention of APP within presynaptic regions, resulting in increased proteolysis. Palmitoylation of GAP43 has been shown to increase its sorting to the cell surface (Gauthier-Kemper et al. 2014), presumably into lipid rafts where both APP and γ-secretase are present. A very recent publication identified GAP43 as an interactor of the γ-secretase complex in the mouse brain and, similar to the results shown herein, showed that GAP43 knockdown reduced Aβ in the conditioned cell medium of HEK cells expressing APP (Inoue et al. 2015). On the basis of this, it is tempting to speculate that GAP43 may play a role as a linker between γ-secretase and its APP CTF substrate, perhaps in lipid raft microdomains. Despite being a synaptic protein, no significant difference was observed in the expression of GAP43 in AD compared to control brains suggesting that GAP43 could continue to contribute to Aβ generation late in AD progression. As the samples probed in this study were from the temporal

cortex of human brains it may be of interest to determine levels of these proteins in regions of the brain affected by severe pathology such as the hippocampus.

It appears from the data presented within this chapter that the proteins identified within the APP interactome can significantly alter the production of Aβ. Therefore targeting these interactions may be a viable alternative to secretase inhibition to reduce Aβ production. Though targeting protein-protein interactions may not reduce proteolysis to the same extent as direct BACE1 or γ-secretase inhibition, it may avoid off-target effects of their inhibition on other substrates. Of course, for any interaction to be targeted directly, much greater understanding of the domains of each protein involved would be required. Recently, computational analysis was used to identify drugs which were able to stabilise the retromer complex and reduce Aβ production suggesting, this method of drug targeting could prove fruitful (Mecozzi et al. 2014). One would also have to bear in mind that any protein–protein interaction may be indicative of a functional relationship, so complete understanding of any functional consequences of disrupting such an interaction would be required. This would be particularly true for proteins with unresolved cellular functions such as ataxin-10. Although the data do not identify a single protein-protein interaction which is causative of the differential proteolysis we observe in the APP isoforms, evidence presented in this chapter does suggest differences in isoform function and interacting partners, all of which may contribute to the differential proteolysis and Aβ generation we observe in the isoforms.

Chapter 5. Investigating the effect of a familial and a protective APP mutation on APP proteolysis

5.1 Introduction

As discussed in **Chapter 1,** the amyloid cascade hypothesis posits that the amyloidogenic proteolysis of APP, and the resultant generation and accumulation of oligomeric Aβ species and deposition of Aβ in plaques, drives the initial cell aberrations and toxicity that lead to AD. Key support for the amyloid cascade hypothesis of AD has come from the study of familial forms of the disease, which can be caused specifically by mutations in either APP or in the protease subunits of the γ-secretase complex, PS1 and PS2. Many of these mutations have been shown to alter the proteolysis of APP. A comprehensive list of all known APP, PS1 or PS2 mutations is available at: www.alzforum.org/mutations. However, some in the field have criticised the amyloid cascade hypothesis due to its failure to yield disease modifying therapeutics and have postulated that other dysfunctions within the brains of AD patients may be to blame for neurodegeneration (See (Herrup 2015)).

5.1.1 The Icelandic mutation protects carriers from AD and age related cognitive decline and reduces Aβ production in a non-neuronal cell model

In 2012, a large genetic study of 1,795 Icelandic participants discovered a mutation within the *APP* gene which appeared to protect carriers from developing AD and age-related cognitive decline (Jonsson et al. 2012). This single nucleotide mutation within the *APP* gene causes an alanine to threonine substitution at the amino acid position 673 (A673T) of the APP sequence. This places the mutation at the second residue of the Aβ sequence of APP. This mutated form of APP was shown to produce 50% less sAPPβ and 40% less Aβ compared to APP_{WT} when expressed in HEK cells (Jonsson et al. 2012). Interestingly, this amino acid substitution is at the same site as an alanine to valine substitution (A673V) identified in an Italian pedigree with familial AD (Di Fede et al. 2009). The A673V mutation was shown to increase sAPPβ and Aβ production 3-fold, suggesting the amino acid at position 2 of the Aβ sequence can influence BACE1 proteolysis (Jonsson et al. 2012). While showing convincing evidence for reduced amyloidogenic proteolysis of APP containing the A673T mutation in HEK cells (Jonsson et al. 2012), the authors did not analyse the proteolysis of either mutated form of APP in a neuronal cell line. Nor did they investigate whether the amino acid substitution could alter proteolysis by other proposed β-secretases.

5.1.2 N-terminally truncated Aβ displays enhanced toxicity and aggregation

APP proteolysis can result in the generation of Aβ with C-terminal heterogeneity due to the 'nibbling' action of γ-secretase (Takami and Funamoto 2012). However, numerous lines of evidence now point to the production of N-terminally truncated Aβ species (Saido et al. 1995;Masters et al. 1985;Bien et al. 2012;Portelius et al. 2014;Deng et al. 2013) with varying toxicity and aggregation properties (Schilling et al. 2006;Schlenzig et al. 2012). Pyroglutamate Aβ (pGlu-Aβ) is an N-terminally truncated form of Aβ in which the first two, or first 10 amino acids of the Aβ 1-X sequence are absent and the glutamic acid residue normally at position 3 or 11 of the Aβ sequence becomes cyclised by the enzyme glutaminyl cyclase (QC) (Schilling et al. 2006). Of these two Aβ species, pGlu-Aβ3-X is probably the most studied and is referred to from here on as pGlu-Aβ. This N-terminal truncation and cyclisation has been shown to enhance aggregation propensity and stability and evidence exists proposing pGlu-Aβ as the predominant Aβ species in the brains of AD patients (Portelius et al. 2015). Indeed, this has led to pilot studies using specific antibody mediated clearance of pGlu-Aβ in AD transgenic mice to determine the potential of targeting this form of Aβ as a therapeutic target in AD (Frost et al. 2012). While BACE1 has been postulated as the major β-secretase responsible for the production of Aβ1-X, recent evidence has suggested the protease cathepsin B may be responsible for cleavage of APP to generate Aβ1-X (Hook et al. 2008) and may result in the production of more pGlu-Aβ (Hook et al. 2014).

5.1.3 Aims

The aim of this chapter was initially to determine whether the newly discovered Icelandic mutation protected APP from proteolysis in a neuronal cell line in our two study APP isoforms. Site-directed mutagenesis was performed on APP cDNA to produce APP bearing the protective A673T mutation (APP_{ICE}) or the AD-linked A673V mutation (APP_{ITA}) and comparative analysis of APP proteolysis in SH-SY5Y cells expressing wild-type (APP_{WT}) and mutant APP was carried out by immunoblot analysis. We then sought to determine whether the addition of the Italian mutation over-rides the protective effect of the KPI domain by comparing sAPP and Aβ generation when these mutations were incorporated into the APP isoforms (APP695 and APP751). Finally, we investigated the effect of both BACE1 and cathepsin B inhibitors on proteolysis of $APP695_{WT}$, $APP695_{ICE}$ and $APP695_{ITA}$ and sought to determine whether the inhibition of either enzyme altered the production of pGlu-Aβ.

5.2 Results

5.2.1 APP_{ICE} undergoes less, and APP_{ITA} undergoes more, amyloidogenic proteolysis than APP_{WT}

In order to study the effect of the reported APP mutations at the A673 amino acid residue of APP in neuronal cells, $APP695_{WT}$ and $APP751_{WT}$ in the vector pIRESHyg were mutated using site-directed mutagenesis and stably transfected into SH-SY5Y cells by electroporation.

SH-SY5Y cells expressing $APP695_{WT}$, $APP695_{ICE}$ or $APP695_{ITA}$ were cultured for 24 h in Opti-MEM and the conditioned cell medium was collected and concentrated. Cells were lysed and the lysates were subjected to immunoblot analysis for APP and actin, and the concentrated conditioned cell medium was subjected to immunoblot analysis for sAPPα and sAPPβ (**Figure 5.1A**). All immunoblot results and MSD analysis results were corrected to account for the amount of endogenous APP in lysates from mock transfected cells and the amount of endogenous sAPP and Aβ in the conditioned cell medium from mock transfected cells. No significant differences were observed in the amount of APP in either $APP695_{ICE}$ or $APP695_{ITA}$ compared to $APP695_{WT}$ (**Figure 5.1B)**. Quantification indicated sAPPα was significantly increased (reduced by 13%) in the conditioned cell medium from $APP695_{ICE}$ expressing cells and significantly decreased (reduced by 28%) in the conditioned cell medium from $APP695_{ITA}$ expressing cells compared to those expressing $APP695_{WT}$ (**Figure 5.1C**). Significantly less sAPPβ (reduced by 45%) was observed in the conditioned cell medium from $APP695_{ICE}$ expressing cells compared to those expressing $APP695_{WT}$, while significantly more sAPPβ (2.3-fold increase) was observed in the conditioned cell medium from cells expressing $APP695_{ITA}$ compared to those expressing $APP695_{WT}$ (**Figure 5.1D**).

To confirm the results obtained from immunoblot analysis, the conditioned cell medium from SH-SY5Y cells stably expressing $APP695_{WT}$, $APP695_{ICE}$ or $APP695_{ITA}$ was subjected to MSD analysis for soluble APP fragments. Significantly less sAPPα (reduced by 36%) was observed in the conditioned cell medium from cells expressing $APP695_{ICE}$ compared to those expressing $APP695_{WT}$, while no significant differences were observed for sAPPα in the conditioned cell medium between cells expressing $APP695_{WT}$ or $APP695_{ITA}$ (**Figure 5.2A)**. Significantly less sAPPβ (reduced by 53%) was observed in the conditioned cell medium from cells expressing $APP695_{ICE}$, while significantly more was observed in the conditioned cell medium from cells expressing $APP695_{ITA}$ (3.75-fold increase) compared to $APP695_{WT}$ expressing cells (**Figure 5.2B**). Significantly less Aβ38 (reduced by 32%), Aβ40 (reduced by 46%) and Aβ42 (reduced by 55%) was observed in the conditioned cell medium from cells expressing $APP695_{ICE}$ compared to cells

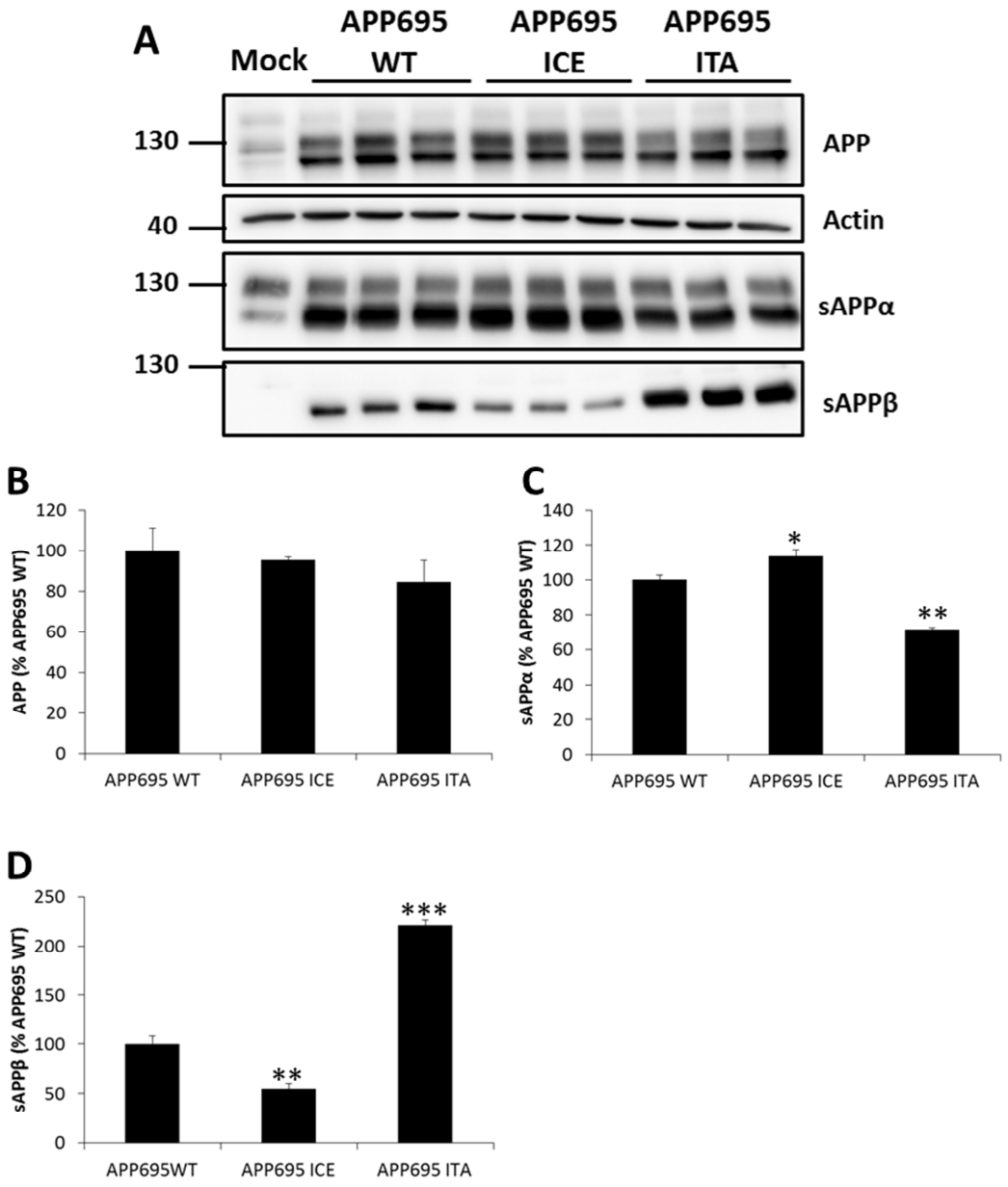

Figure 5.1 Immunoblot analysis shows APP695$_{ICE}$ undergoes less, and APP695$_{ITA}$ undergoes more, amyloidogenic proteolysis than APP695$_{WT}$

Mock transfected SH-SY5Y cells, or cells expressing APP695$_{WT,}$ APP695$_{ICE}$ or APP695$_{ITA}$ were cultured in Opti-MEM for 24 h. **A)** Cells were lysed and lysates were subjected to immunoblot analysis for APP and actin and the conditioned cell medium was collected and concentrated and subjected to immunoblot analysis for sAPPα and sAPPβ. Densitometric analysis of **B)** APP **C)** sAPPα **D)** sAPPβ. The amounts of APP and sAPP in APP expressing cells were corrected for the amount in mock transfected cells to account for endogenous APP and sAPP. Bars represent the mean, error bars are ± S.E.M. *, p-value<0.05, **, p-value<0.01, ***, p value<0.001 compared to APP695$_{WT}$, n=3.

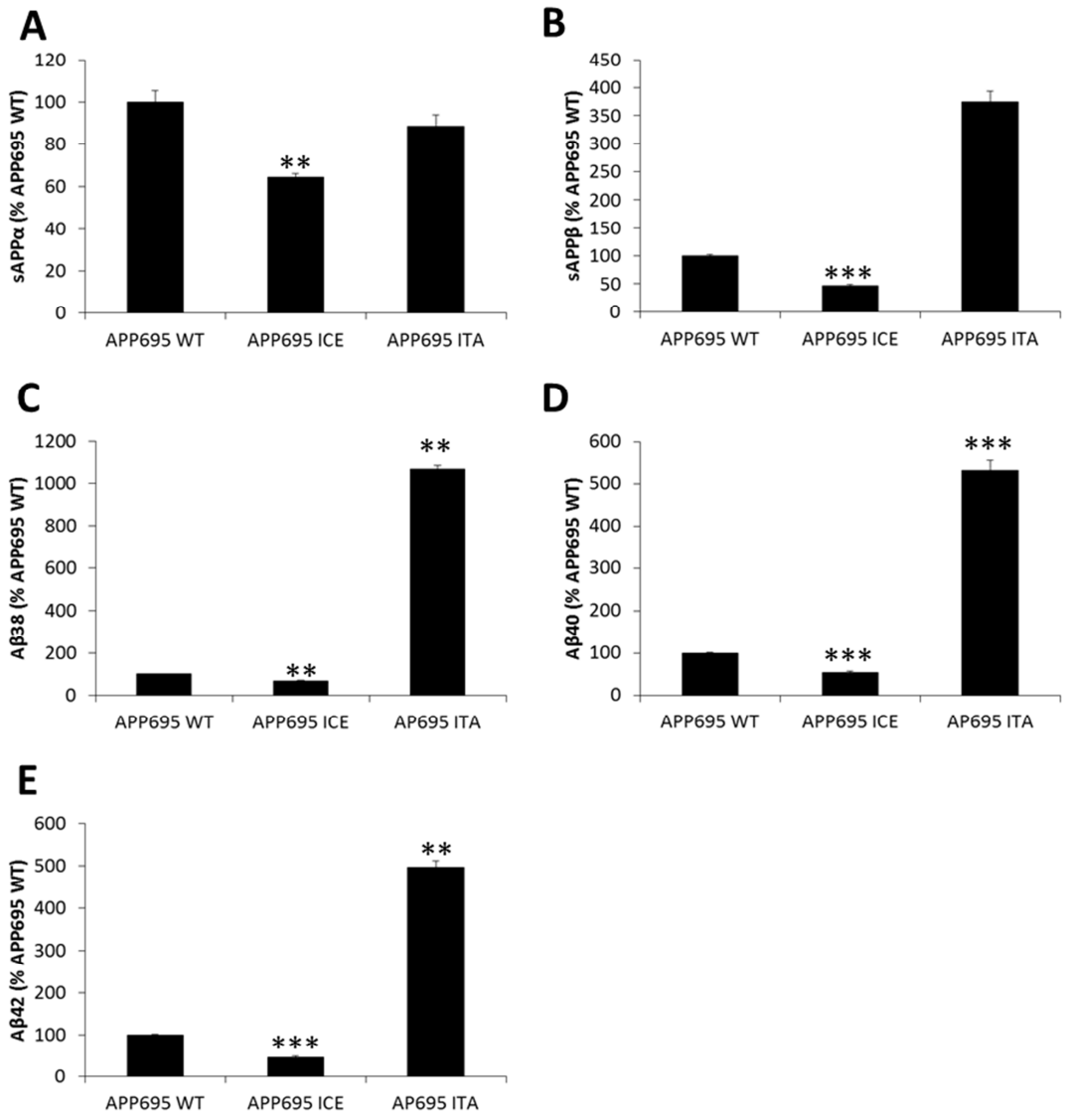

Figure 5.2 Meso Scale Discovery analysis confirms $APP695_{ICE}$ undergoes less, and $APP695_{ITA}$ undergoes more, amyloidogenic proteolysis than $APP695_{WT}$

Mock transfected SH-SY5Y cells, or cells expressing $APP695_{WT,}$ $APP695_{ICE}$ or $APP695_{ITA}$ were cultured in Opti-MEM for 24 h. The conditioned cell medium was subsequently collected and subjected to MSD analysis for **A)** sAPPα, **B)** sAPPβ, **C)** Aβ38, **D)** Aβ40 and **E)** Aβ42. The amounts of sAPPα, sAPPβ and Aβ in APP expressing cells were corrected for the amount in mock transfected cells to account for endogenous sAPP and Aβ. Bars represent the mean, error bars are ± S.E.M. **, p-value<0.01, ***, p-value<0.001, compared to $APP695_{WT}$, n=3. In $APP695_{WT}$ expressing cells the average absolute Aβ38, Aβ40 and Aβ42 levels were 219 pg/mg, 893 pg/mg and 77 pg/mg, respectively.

expressing $APP695_{WT}$ (**Figures 5.2C-E**). Significantly more Aβ38 (10-fold increase), Aβ40 (5.3-fold increase), and Aβ42 (5-fold increase) was observed in the conditioned cell medium from cells expressing $APP695_{ITA}$ compared to those expressing $APP695_{WT}$ (**Figures 5.2C-E**).

We then sought to determine whether the A673 mutations could alter the relative production of different species of Aβ by comparing the amount of each Aβ species in the conditioned medium cell from cells expressing $APP695_{WT}$, $APP695_{ICE}$ and $APP695_{ITA}$. The ratio of Aβ40:Aβ42 was significantly higher in the conditioned cell medium from cells expressing $APP695_{ICE}$ and cells expressing $APP695_{ITA}$, compared to cells expressing $APP695_{WT}$ (**Figure 5.3A**). The ratio of Aβ38:Aβ42 was significantly higher in the conditioned cell medium from cells expressing $APP695_{ICE}$ and cells expressing $APP695_{ITA}$ compared to those expressing $APP695_{WT}$ (**Figure 5.3B**). The ratio of Aβ40:Aβ38+Aβ42 was significantly lower in the conditioned cell medium from cells expressing $APP695_{ICE}$ and those expressing $APP695_{ITA}$ compared to those expressing $APP695_{WT}$ (**Figure 5.3C**).

We investigated whether the effect of the Icelandic or Italian mutations on amyloidogenic proteolysis was also observed in the APP751 isoform. As previously, mutants were generated by performing site-directed mutagenesis on APP751 cDNA and SH-SY5Y cells were stably transfected with the cDNA by electroporation. SH-SY5Y cells expressing $APP751_{WT}$, $APP751_{ICE}$ or $APP751_{ITA}$ or mock transfected cells were cultured for 24 h in Opti-MEM and the conditioned cell medium was collected and concentrated. All immunoblot results were corrected to account for the amount of endogenous APP in the cell lysates and the amount of endogenous sAPP and Aβ in the conditioned cell medium from mock transfected cells. Cells were lysed and subjected to immunoblot analysis for APP and actin and the concentrated conditioned cell medium was subjected to immunoblot analysis for sAPPα and sAPPβ (**Figure 5.4A**). No significant differences were observed in the amount of APP between cells expressing $APP751_{ICE}$ or $APP751_{ITA}$ compared to cells expressing $APP751_{WT}$ (**Figure 5.4B**). When compared to the conditioned cell medium from cells expressing $APP751_{WT}$, significantly less sAPPα was observed in the conditioned cell medium from cells expressing $APP751_{ICE}$ (reduced by 44%) and the conditioned cell medium from cells expressing $APP751_{ITA}$ (reduced by 83%) (**Figure 5.4C**). When compared to the conditioned cell medium from $APP751_{WT}$ expressing cells, significantly less sAPPβ was observed in the conditioned cell medium from $APP751_{ICE}$ expressing cells (reduced by 85%) and significantly more was observed in the conditioned cell medium from $APP751_{ITA}$ expressing cells (3.3-fold increase) (**Figure 5.4D**).

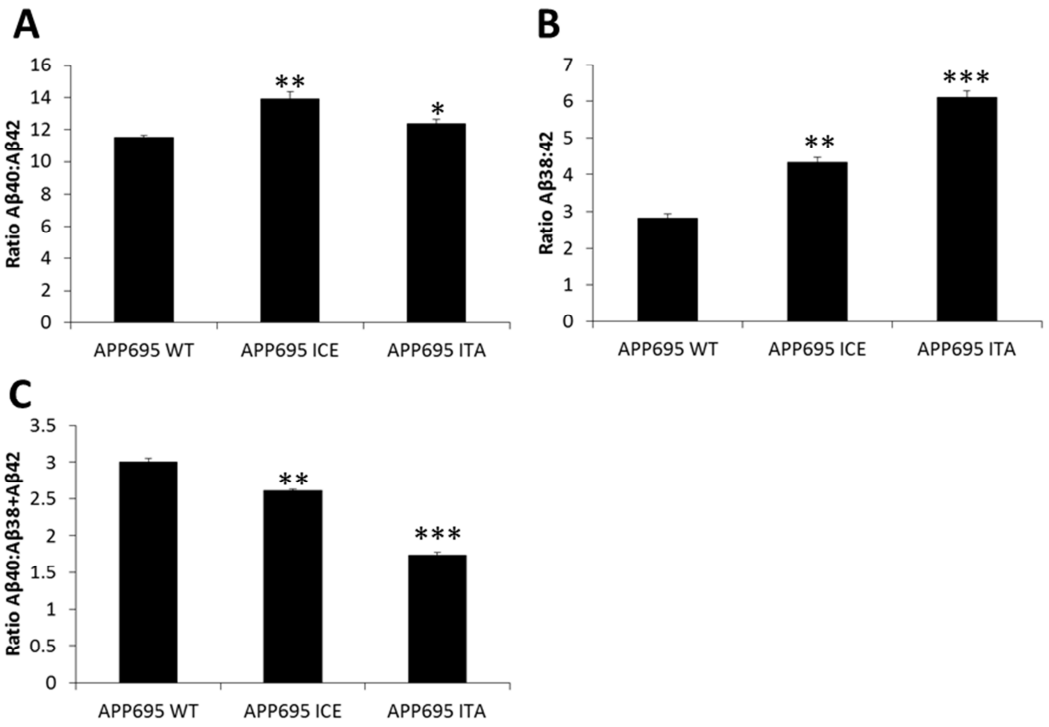

Figure 5.3 Mutations at the β-secretase site in APP can alter γ-secretase proteolysis

Mock transfected SH-SY5Y cells, or cells expressing $APP695_{WT,}$ $APP695_{ICE}$ or $APP695_{ITA}$ were cultured in Opti-MEM for 24 h. The conditioned cell medium was subsequently collected and subjected to MSD analysis for Aβ38, Aβ40 and Aβ42. Ratios of **A)** Aβ40:Aβ42, **B)** Aβ38:Aβ42 and **C)** Aβ40:Aβ38+Aβ42 were calculated. The amounts of Aβ in APP expressing cells were corrected for the amount in mock transfected cells to account for endogenous Aβ. Bars represent the mean, error bars are ± S.E.M. *, p-value<0.05, **, p-value<0.01, ***, p-value<0.001, compared to $APP695_{WT}$, n=3.

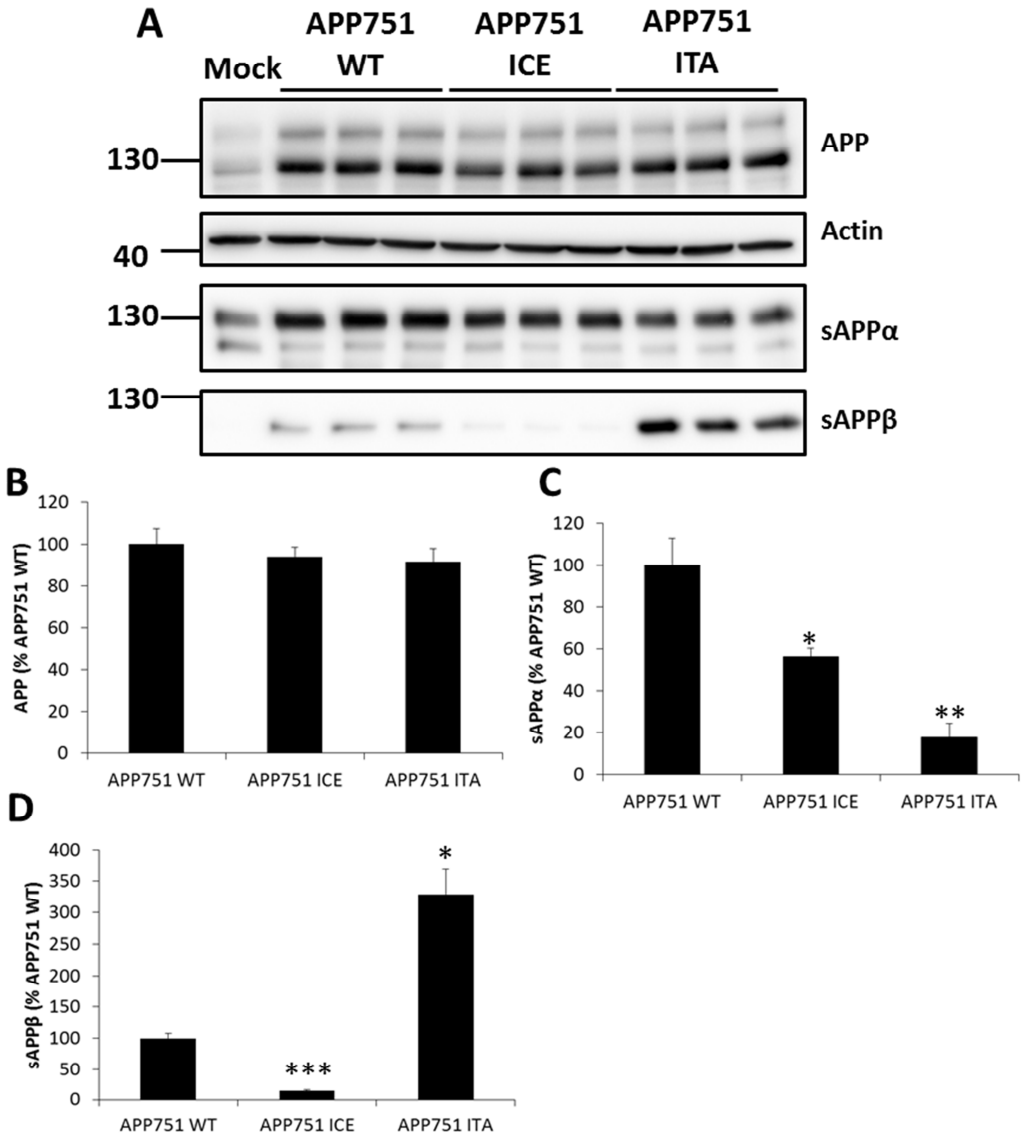

Figure 5.4 Immunoblot analysis shows $APP751_{ICE}$ undergoes less, and $APP751_{ITA}$ mutation undergoes more, amyloidogenic proteolysis than $APP751_{WT}$

Mock transfected SH-SY5Y cells, or cells expressing $APP751_{WT,}$ $APP751_{ICE}$ or $APP751_{ITA}$ were cultured in Opti-MEM for 24 h. **A)** Cells were lysed and lysates were subjected to immunoblot analysis for APP and actin and the conditioned cell medium was collected and concentrated and subjected to immunoblot analysis for sAPPα and sAPPβ. Densitometric analysis of **B)** APP. **C)** sAPPα and **D)** sAPPβ. The amounts of APP, sAPPα and sAPPβ in APP expressing cells were corrected for the amount in mock transfected cells to account for endogenous APP and sAPP. Bars represent the mean, error bars are ± S.E.M. **, p-value < 0.01 compared to $APP751_{WT}$, n=3.

5.2.2 APP isoforms with the Italian mutation undergo differential proteolysis

In **Chapter 3** we observed that the introduction of the Swedish mutation appeared to reduce the differential proteolysis we observed between the APP isoforms. We hypothesised that introduction of the Italian mutation into APP751 may overcome any protective effect of the additional KPI domain in APP751 in a similar manner to the Swedish mutation (see **Figure 3.7**).

Cell lysates and the concentrated conditioned cell medium from SH-SY5Y cells expressing $APP695_{ITA}$ and $APP751_{ITA}$ were subjected to immunoblot analysis for APP and sAPPβ (**Figure 5.5A**). Quantification of sAPPβ from $APP695_{ITA}$ and $APP751_{ITA}$ expressing cells showed significantly less sAPPβ (reduced by 68%) was present in the conditioned cell medium from cells expressing $APP751_{ITA}$ compared to those expressing $APP695_{ITA}$ (**Figure 5.5B**).

5.2.3 BACE1 and cathepsin B inhibitors both reduce amyloidogenic proteolysis of APP

Given recent reports of β-secretase activity of cathepsin B (Hook et al. 2014), we sought to determine the relative contribution of BACE1 and cathepsin B proteolysis to the amyloidogenic proteolysis of APP in our SH-SY5Y cell model.

SH-SY5Y cells expressing $APP695_{WT}$, $APP695_{ICE}$ or $APP695_{ITA}$, or mock transfected control cells were cultured in Opti-MEM supplemented with 1 μM of the BACE1 inhibitor βIV, or a vehicle only control (DMSO) for 24 h. Cells were lysed and subjected to immunoblot analysis for APP and actin (**Figure 5.6A**). Treatment with βIV caused a significant increase in APP in cells expressing $APP695_{WT}$ (43% increase) and $APP695_{ITA}$ (36% increase) but no significant change in APP in cells expressing $APP695_{ICE}$ compared to their respective DMSO control (**Figure 5.6B**). Separate quantification of mature and immature APP showed a significant increase in the ratio of mature to immature APP in cells expressing $APP695_{WT}$ but no significant change in the mature to immature ratio of APP in cells expressing $APP695_{ICE}$ or $APP695_{ITA}$ compared to their respective DMSO control (**Figure 5.6C**). The conditioned cell medium was subjected to MSD analysis for soluble APP fragments. A significant increase was observed in sAPPα (66% increase) following βIV treatment in the conditioned cell medium from $APP695_{ITA}$ expressing cells compared to the respective DMSO control (**Figure 5.7A**). No significant differences were observed for sAPPα in the conditioned cell medium from $APP695_{WT}$ or $APP695_{ICE}$ expressing cells following βIV treatment compared to their respective DMSO control (**Figure 5.7A**). Treatment with βIV significantly reduced sAPPβ in the conditioned cell medium from cells expressing $APP695_{WT}$

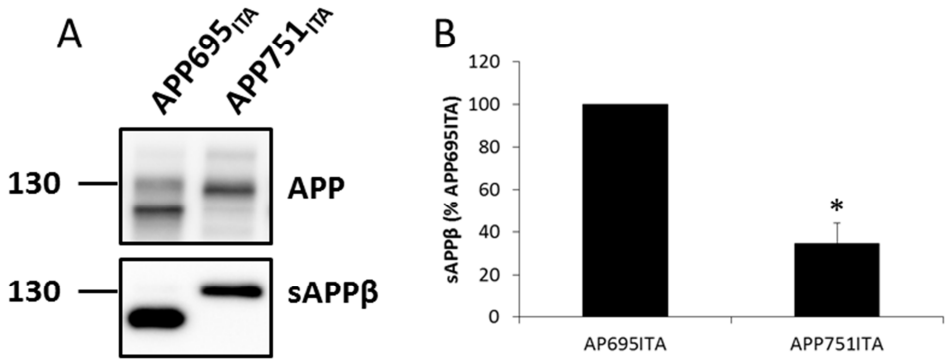

Figure 5.5 The Italian mutation does not over-ride the protective effect of the KPI-domain to the same extent as the Swedish mutation

Cells expressing $APP695_{ITA}$ or $APP751_{ITA}$ were cultured in Opti-MEM for 24 h. The conditioned cell medium was collected and concentrated and cells were lysed. **A)** Cell lysates were subjected to immunoblot analysis for APP and the conditioned cell medium was concentrated and subjected to immunoblot analysis for sAPPβ. **B)** Densitometric analysis of sAPPβ. Bars represent the mean, error bars are ± S.E.M., *, p-value<0.05, n=3.

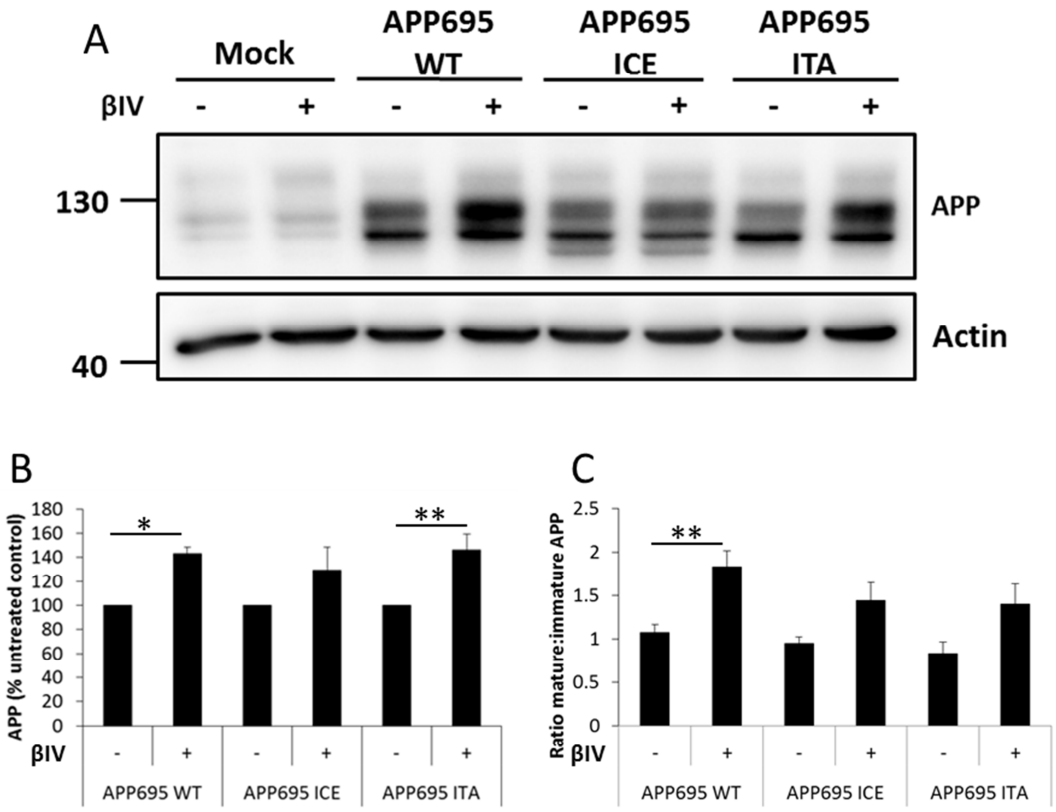

Figure 5.6 BACE1 inhibition alters APP profiles in cells expressing APP695$_{WT}$ and APP695$_{ITA}$ but not those expressing APP695$_{ICE}$

Mock transfected SH-SY5Y cells, or cells expressing APP695$_{WT,}$ APP695$_{ICE}$ or APP695$_{ITA}$ were cultured in Opti-MEM containing the BACE1 inhibitor βIV (1 μM) (+) or a DMSO only control (-) for 24 h. **A)** Cells were lysed and lysates were subjected to immunoblot analysis for APP and actin. Densitometric analysis of **B)** APP **C)** the ratio of mature to immature APP. The amounts of APP in APP expressing cells were corrected for the amount in mock transfected cells to account for endogenous APP . Bars represent the mean, error bars are ± S.E.M., *, p-value ,0.05, **, p-value < 0.01 compared to the DMSO controls, n=3.

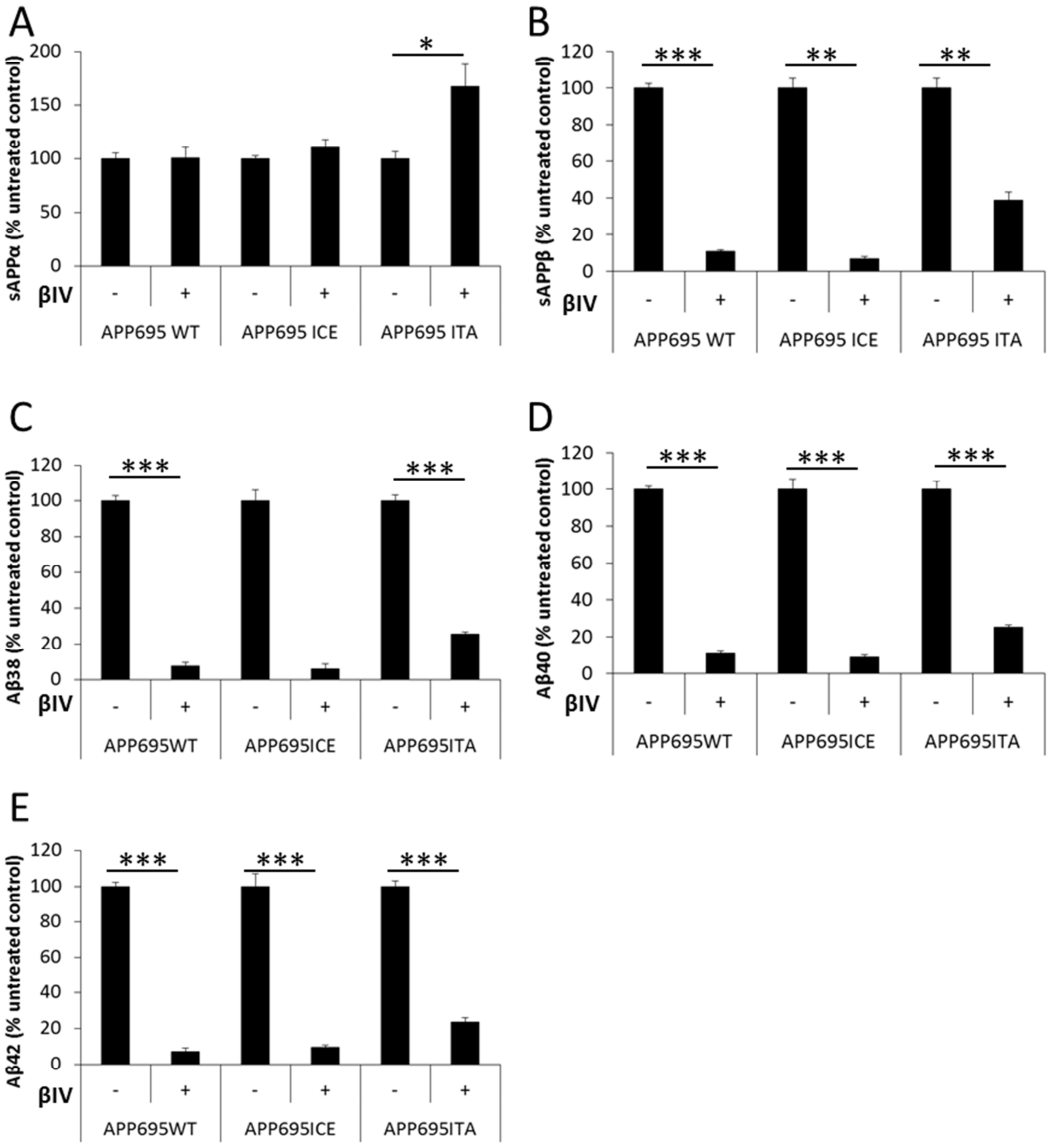

Figure 5.7 BACE1 inhibition reduces amyloidogenic APP proteolysis of APP695$_{WT}$, APP695$_{ICE}$ and APP695$_{ITA}$

Mock transfected SH-SY5Y cells, or cells expressing APP695$_{WT,}$ APP695$_{ICE}$ or APP695$_{ITA}$ were cultured in Opti-MEM containing the BACE1 inhibitor βIV (1 μM) (+) or a DMSO only control (-) for 24 h. The conditioned cell medium was subsequently collected and subjected to MSD analysis for **A)** sAPPα, **B)** sAPPβ, **C)** Aβ38, **D)** Aβ40 and **E)** Aβ42. The amounts of sAPP and Aβ in APP expressing cells were corrected for the amount in mock transfected cells to account for endogenous sAPP and Aβ. Bars represent the mean, error bars are ± S.E.M. *, p-value<0.05, **, p-value<0.01, ***, p-value<0.001 compared to the DMSO controls, n=3.

(reduced by 89%), $APP695_{ICE}$ (reduced by 97%) and $APP695_{ITA}$ (reduced by 61%) compared to their respective DMSO control (**Figure 5.7B**). Significant reductions in Aβ38 following βIV treatment were observed in the conditioned cell medium from cells expressing $APP695_{WT}$ (reduced by 93%) and $APP695_{ITA}$ (reduced by 74%) compared to their respective DMSO control (**Figure 5.7C**). The Aβ38 concentration was below the detection limit for the MSD assay in the conditioned cell medium from cells expressing $APP695_{ICE}$ following βIV treatment in two experiments and therefore statistics were not applied to this result. Aβ40 was significantly reduced in the conditioned cell medium from cells expressing $APP695_{WT}$ (reduced by 89%), $APP695_{ICE}$ (reduced by 96%) and $APP695_{ITA}$ (reduced by 76%) by βIV treatment compared to their respective DMSO control (**Figure 5.7D**). Aβ42 was also significantly reduced in the conditioned cell medium from cells expressing $APP695_{WT}$ (reduced by 83%), $APP695_{ICE}$ (reduced by 90%) and $APP695_{ITA}$ (reduced by 74%) by βIV treatment compared to their respective DMSO control (**Figure 5.7E**).

To determine whether cathepsin B acts as a β-secretase in our model system, SH-SY5Y cells expressing $APP695_{WT}$, $APP695_{ICE}$ or $APP695_{ITA}$, or a mock transfected control cells were cultured in Opti-MEM supplemented with 50 μM of the cathepsin B inhibitor Ca074Me or a vehicle only control (DMSO) for 24 h. Cells were lysed and subjected to immunoblot analysis for APP and actin (**Figure 5.8A**). Treatment with the cathepsin B inhibitor caused a significant increase in APP in cells expressing $APP695_{ICE}$ (47% increase) compared to untreated control cells but no significant differences were observed between Ca074Me treated and control treated cells for cells expressing $APP695_{WT}$ or $APP695_{ITA}$ (**Figure 5.8B**). Separate quantification of mature and immature APP showed no significant differences in the mature to immature APP ratio in any APP expressing cell line following Ca074Me treatment compared to their respective DMSO control (**Figure 5.8C**). The conditioned cell medium was subjected to MSD analysis for soluble APP fragments. Treatment with Ca074Me caused no significant differences in sAPPα in the conditioned cell medium in any of the APP expressing cell lines compared to their respective DMSO control (**Figure 5.9A**). Treatment with Ca074Me significantly reduced sAPPβ in the conditioned cell medium from cells expressing $APP695_{WT}$ (reduced by 54%) and $APP695_{ITA}$ (reduced by 45%) compared to their respective DMSO control but had no significant effect on $APP695_{ICE}$ expressing cells (**Figure 5.9B**). Significant reductions were also observed in Aβ38 in the conditioned cell medium from cells expressing $APP695_{WT}$ (reduced by 90%) and $APP695_{ITA}$ (reduced by 73%) following Ca074Me treatment compared to their respective DMSO control (**Figure 5.9C**). As with βIV treatment, treatment with Ca074Me resulted in Aβ38 levels in the conditioned cell medium from $APP695_{ICE}$ expressing cells which were below the detection limit of the MSD assay in two experiments and therefore statistical analysis was not applied to this

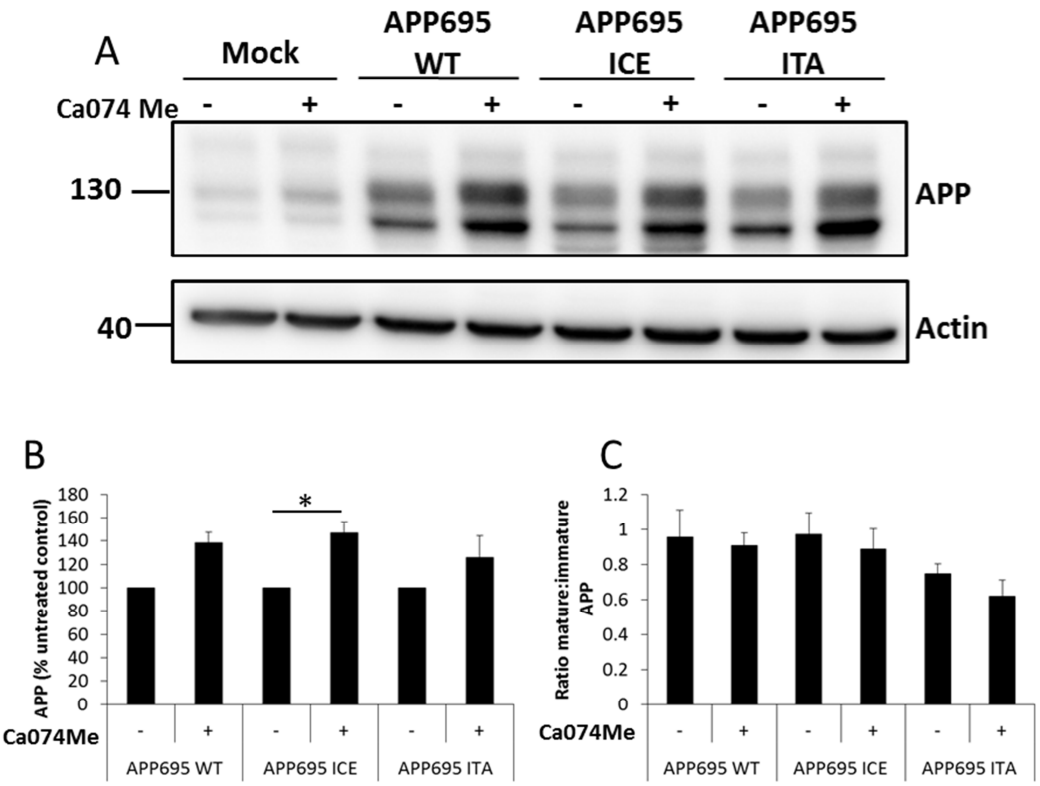

Figure 5.8 Cathepsin B inhibition does not alter mature to immature APP ratios but significantly increases APP695$_{ICE}$ levels

Mock transfected SH-SY5Y cells, or cells expressing APP695$_{WT,}$ APP695$_{ICE}$ or APP695$_{ITA}$ were cultured in Opti-MEM for containing the cathepsin B inhibitor Ca074Me (50 µM) (+) or a DMSO only control (-) for 24 h. **A)** Cells were lysed and lysates were subjected to immunoblot analysis for APP and actin. Densitometric analysis of **B)** APP **C)** the ratio of mature to immature APP. The amounts of APP in APP expressing cells were corrected for the amount in mock transfected cells to account for endogenous APP. Bars represent the mean, error bars are ± S.E.M., *, p-value<0.05, compared to the DMSO controls, n=3.

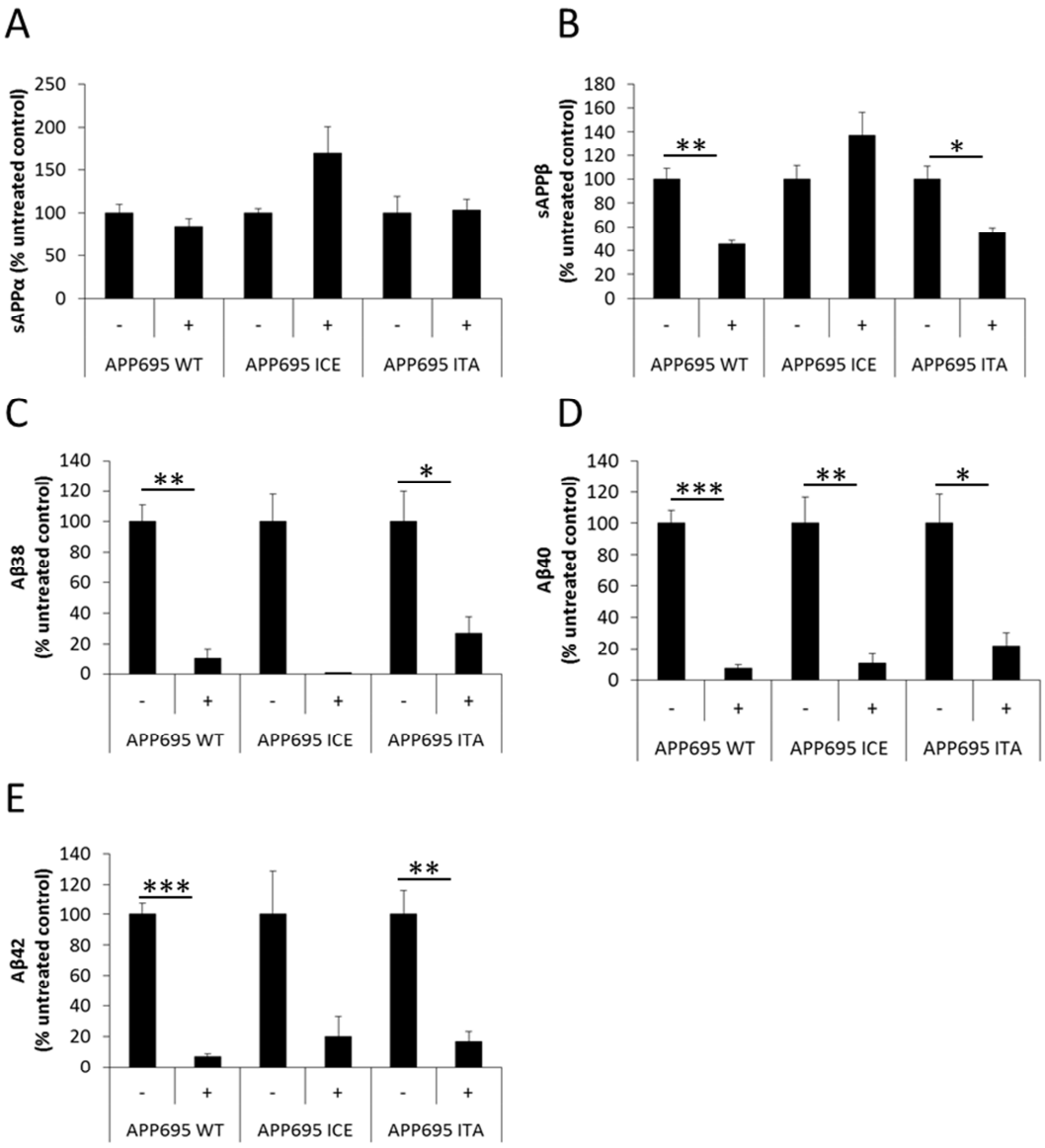

Figure 5.9 Cathepsin B inhibition reduces amyloidogenic APP proteolysis of APP695$_{WT}$ and APP695$_{ITA}$

Mock transfected SH-SY5Y cells, or cells expressing APP695$_{WT,}$ APP695$_{ICE}$ or APP695$_{ITA}$ were cultured in Opti-MEM for containing the cathepsin B inhibitor (50 µM) (+) or a DMSO only control (-) for 24 h. The conditioned cell medium was subsequently collected and subjected to MSD analysis for **A)** sAPPα, B) sAPPβ, **C)** Aβ38, **D)** Aβ40 and **E)** Aβ42. The amounts of sAPP and Aβ in APP expressing cells were corrected for the amount in mock transfected cells to account for endogenous sAPP and Aβ. Bars represent the mean, error bars are ± S.E.M., *, p-value<0.05, **, p-value<0.01, ***, p-value<0.001 compared to the DMSO controls, n=3.

group. Treatment with Ca074Me significantly reduced Aβ40 in the conditioned cell medium from cells expressing $APP695_{WT}$ (reduced by 93%), $APP695_{ICE}$ (reduced by 89%) and $APP695_{ITA}$ (reduced by 79%) compared to their respective DMSO controls (**Figure 5.9D**). Significantly reduced Aβ42 was also observed in the conditioned cell medium from cells expressing $APP695_{WT}$ (reduced by 94%) and $APP695_{ITA}$ (reduced by 83%), compared to their relative DMSO control while no significant difference was observed in Aβ42 in the conditioned cell medium from $APP695_{ICE}$ expressing cells following Ca074Me treatment (**Figure 5.9E**).

5.2.4 SH-SY5Y cells expressing WT and mutant APP do not produce detectable levels of pGlu-Aβ3-40

Mock transfected SH-SY5Y cells or SH-SY5Y cells expressing $APP695_{WT}$, $APP695_{ICE}$ and $APP695_{ITA}$ were cultured for 24 h in Opti-MEM containing either βIV (1 μM) or CA074Me (50 μM) or a DMSO only control. The conditioned cell medium was collected and concentrated in a 2 kDa molecular weight cut off spin column. The concentrated conditioned cell medium was then subjected to ELISA to detect pGlu-Aβ3-40. The results showed that in all cases, concentrations of pGlu-Aβ3-40 were below the detection limit of the assay employed.

5.3 Discussion

For many in the field, inhibiting the production of Aβ represents a feasible mechanism of preventing the onset of AD and there are still ongoing clinical trials of BACE1 inhibitors (Vassar 2014). Support for this therapeutic strategy has come mainly from the many studies of familial cases of AD. Various mutations within the APP gene, causing amino acid substitutions within, or adjacent to the β- or γ-secretase cleavage sites of the Aβ region have been identified. These mutations are proposed to cause AD in these familial cases by increasing the production of Aβ (e.g. APP_{SWE} – KM670/671NL), specifically increasing the production of the more amyloidogenic Aβ42 species (eg. APP_{LONDON} – V717I) or altering the aggregation propensity of the Aβ peptide (e.g. APP_{IOWA} – D694N) (http://www.alzforum.org/mutations). Until the identification of an apparent AD protective mutation within an Icelandic cohort (Jonsson et al. 2012), all the previously studied mutations in APP were identified on the basis of being causative of early onset, familial forms of AD. The fact that this protective mutation reduced the production of Aβ through reduced β-secretase cleavage of APP (Jonsson et al. 2012) adds weight to the theory that prevention of Aβ generation could protect against AD. Furthermore, those with the mutation appeared to have reduced age-related cognitive decline (Jonsson et al. 2012), suggesting specific long term inhibition of BACE1 proteolysis of APP does not have detrimental effects on cognition.

5.3.1 Familial mutations have the same effect on proteolysis in the APP isoforms

Few publications have emerged on the Icelandic APP mutation since the initial report of its neuroprotective capabilities. We initially sought to confirm the effects on β-secretase proteolysis reported by Jonsson et al. (2012) in a neuronal cell line in our two APP study isoforms. Following site-directed mutagenesis of the APP cDNA, and expression in our SH-SY5Y cell model we saw 44% less sAPPβ in the conditioned cell medium from the $APP695_{ICE}$ expressing cells by immunoblot and 53% by MSD analysis. We also observed 2.25-fold more sAPPβ in the conditioned cell medium from cells expressing $APP695_{ITA}$ compared to $APP695_{WT}$. These results were broadly similar to the results presented by Jonsson et al. (2012) who observed 55% less sAPPβ in $APP695_{ICE}$ expressing HEK cells and a 2.9-fold increase in sAPPβ from $APP695_{ITA}$ expressing cells compared to cells expressing $APP695_{WT}$. Results for sAPPα were also similar to those observed by Jonsson et al. (2012) for the APP695 isoform by immunoblot, though this result was not recapitulated by the MSD data. Explaining this discrepancy is difficult, though perhaps it exposes the semi-quantitative nature of immunoblot analysis in comparison to ELISA. Another possibility is that the mutation interferes with the capacity of the sAPPα antibody in the

MSD assay to immunoprecipitate sAPPα from the APP_{ICE} (and possibly the APP_{ITA}) is compromised by the amino acid substitution. A further repeat of this data would aid in confirming the result.

Amyloidogenic proteolysis of APP751 was also reduced by the addition of the Icelandic mutation and increased by the addition of the Italian mutation, perhaps to an even greater extent than with APP695. Immunoblot analysis showed sAPPβ was 3.25-fold higher in the conditioned cell medium from $APP751_{ITA}$ expressing cells and 75% lower in the conditioned cell medium from cells expressing $APP751_{ICE}$ compared to those expressing $APP751_{WT}$. Similar to the results from APP695 expressing cells, less sAPPα was observed by immunoblot analysis in the conditioned cell medium from cells expressing $APP751_{ITA}$ compared to $APP751_{WT}$, though less sAPPα was also observed in the conditioned cell medium from $APP751_{ICE}$ expressing cells. This indicates that the effect on β-secretase cleavage of the mutations at the residue A673 in APP is maintained in the APP751 isoform.

Since the original publication, further work has confirmed the findings of Jonsson et al. (2012) and those presented in this thesis, showing APP_{ICE} undergoes significantly less amyloidogenic proteolysis than APP_{WT} in primary mouse neurons transfected with the cDNA for wild-type or mutated APP (Benilova et al. 2014;Maloney et al. 2014), and in iPSC derived cortical neurons engineered to express APP bearing the Icelandic mutation (Maloney et al. 2014). Conflicting results have however been presented on whether the mutations at the A673 site alter the aggregation propensity of the Aβ molecule compared to the wild-type molecule. While Maloney et al. (2014) suggested the A673T mutation reduced Aβ42, but not Aβ40, aggregation compared to wild-type Aβ, Benilova et al. (2014) reported no differences in aggregation for Aβ42. However, they observed reduced aggregation of Aβ40 compared to wild-type Aβ. Similarly, the A673V mutation has been shown to increase only Aβ42 species aggregation in some cases (Messa et al. 2014;Maloney et al. 2014) and only the Aβ40 species in others (Benilova et al. 2014) compared to wild-type Aβ. Here we showed that the Aβ40:Aβ42 ratio for $APP695_{ICE}$ was significantly higher than that for $APP695_{WT}$, suggesting another mechanism through which APP_{ICE} could be neuroprotective. The ratio of Aβ38:Aβ42 was also significantly higher in APP_{ICE} and APP_{ITA} compared to APP_{WT}. Though probably not beneficial in APP_{ITA}, where Aβ42 is still produced at levels 3-fold higher than in APP_{WT}, the increased proteolytic processing of Aβ42 down to Aβ38 in APP_{ICE} could again act as another neuroprotective feature of this mutated form of APP. Though the mechanisms governing the production of specific Aβ species remain unclear, it has been suggested that it could be intrinsically linked to the composition of the γ-secretase complex, where alterations in the PS1 and PS2 subunits affect the initial endopeptidase cleavage and the APH1 subunit influences further carboxypeptidase activity (Acx

et al. 2014). As discussed previously, APP proteolysis appears to be intrinsically linked to its subcellular location, requiring the co-localisation of substrate and enzyme. However, mutations in APP have been shown to alter the subcellular location of APP proteolysis by BACE1. Could the same be true for γ-secretase proteolysis? Whether the differences in γ-secretase complex composition result in differential subcellular localisation of the complex has not been determined (Acx et al. 2014), but given another mutation at the N-terminus of Aβ cleavage has also been shown to influence Aβ at the C-terminus (Chen et al. 2012), this may aid in explaining the variations we have observed here. These data may therefore indicate that, in addition to the reduced production of Aβ in the Icelandic cohort (Jonsson et al. 2012), reduced aggregation propensity of the Aβ peptides produced (Benilova et al. 2014), along with increased Aβ40:Aβ42 ratio and increased Aβ38:Aβ42 ratio may also contribute to the protective effect. A summary of the data currently available for the A673 site mutants, alongside the data we have produced here can be found in **Table 5.1**.

Similar to APP_{SWE}, APP_{ITA} undergoes significantly more amyloidogenic proteolysis than APP_{WT}, though the subcellular site of APP_{ITA} proteolysis by BACE1 has not been identified. The APP_{SWE} mutation increases APP proteolysis in the secretory pathway (Haass et al. 1995), and its introduction into the APP751 isoform appears to overcome some of differential proteolysis we observe in APP isoform proteolysis (see **Figure 3.7**). As with APP_{SWE}, significant differences in the amount of sAPPβ in the conditioned cell medium were still observed between the two APP isoforms when the Italian mutation was introduced. In immunoblots, 70% less sAPPβ was observed in the conditioned cell medium from $APP751_{ITA}$ expressing cells than in $APP695_{ITA}$ expressing cells (**Figure 5.5**). This compares to 80% less sAPPβ observed in $APP751_{WT}$ in **Chapter 1** (**Figure 3.2**). Therefore differential isoform proteolysis appears to be reduced slightly by the addition of the Italian mutation, though not to the same extent as that seen in the APP_{SWE} isoforms. These differences may be of interest to follow up on, particularly given that the subcellular environment in which these APP A673 site mutants undergo proteolysis remains unknown.

5.3.2 BACE1 and cathepsin B inhibition both reduce APP proteolysis

BACE1 has been postulated as the major β-secretase responsible for the rate limiting step in Aβ production (Cole and Vassar 2007). However, recent evidence has suggested that cathepsin B may also be a constitutive β-secretase, and may significantly contribute to Aβ liberation both *in vitro* and *in vivo* (Hook et al. 2014). Herein we show that sAPPβ is significantly reduced by BACE1 inhibition in $APP695_{WT}$, $APP695_{ICE}$ and $APP695_{ITA}$ with a concomitant decrease in all three Aβ species (**Figure 5.5**). Significant increases in APP were also observed in APP_{WT} and APP_{ITA}

	Jonsson et al. 2012	Benilova et al., 2014	Maloney et al., 2014	Data presented here
Cell types	HEK293	Mouse primary neurons	HEK293 Human iPSC derived neurons	SH-SY5Y neuroblastoma
sAPPα	↓ APP_{ITA}	↓ APP_{ITA}	↓ sAPPβ:$sAPP\alpha_{ICE}$ ↑ sAPPβ:$sAPP\alpha_{ITA}$	Inconsistent between immunoblot and MSD
sAPPβ	↓ APP_{ICE} ↑ APP_{ITA}	↓ APP_{ICE} ↑ APP_{ITA}	See above	↓ APP_{ICE} ↑ APP_{ITA}
Aβ	↓ APP_{ICE} ↑ APP_{ITA}	↓ APP_{ICE} ↑ APP_{ITA}	↓ APP_{ICE} ↑ APP_{ITA}	↓ APP_{ICE} ↑ APP_{ITA}
Aggregation	-	↓ $A\beta40_{ICE}$ ↑ $A\beta40_{ITA}$	↑ $A\beta40_{ITA}$ ↓ $A\beta42_{ICE}$	-
Ratios	-	-	-	↑ $A\beta40{:}A\beta42_{ICE}$ ↑ $A\beta38{:}A\beta42_{ICE}$ ↓ $A\beta40{:}A\beta38{+}A\beta42_{ICE}$ ↑ $A\beta40{:}A\beta42_{ITA}$ ↑ $A\beta38{:}A\beta42_{ITA}$ ↓ $A\beta40{:}A\beta38{+}A\beta42_{ITA}$

Table 5.1 The effect of the APP A673T and A673V mutations on Aβ generation and properties

Several groups have studied the effect of the mutations in APP at the A673 site. Comparison shows consistency in the results for sAPPβ and Aβ production between groups. Some discrepancies exist in studies of the aggregation propensity of the Aβ molecule with these mutations. All the information in the table describes how the properties of the mutated APP/Aβ relates to the wild-type situation.

indicating that inhibition of BACE1 can also alter the amount of APP in cells. In APP_{ICE}, which we and others (Benilova et al. 2014;Jonsson et al. 2012;Maloney et al. 2014) have shown undergoes less BACE1 proteolysis, no significant difference in APP was observed following BACE1 inhibition. Interestingly, the ratio of mature to immature APP is also significantly increased in $APP695_{WT}$, again begging the question as to which form of APP is preferentially cleaved by BACE1. If APP O-GlcNacylation can protect APP from amyloidogenic proteolysis (Chun et al. 2015;Jacobsen and Iverfeldt 2011), it may be that inhibition of BACE1 results in more mature APP, resulting in the differences we observe by immunoblot analysis.

Inhibition of cathepsin B also significantly reduced sAPPβ in cells expressing $APP695_{WT}$ and $APP695_{ITA}$ but not those expressing $APP695_{ICE}$ (See **Figure 5.9)**. All three species of Aβ measured were shown to be significantly reduced in the conditioned cell medium from cells expressing $APP695_{ITA}$ and $APP695_{WT}$ that were treated with the cathepsin B inhibitor. However, the reductions observed in Aβ did not show a direct, concomitant relationship with the reduction in sAPPβ, as was seen following BACE1 inhibition with βIV. This was particularly true for $APP695_{ICE}$ where sAPPβ was not significantly altered by the cathepsin B inhibitor but Aβ40 was (and, though not reaching significance, other Aβ species also appeared to be reduced). Though Hook et al. (2014) postulated cathepsin B as a major β-secretase, no analysis was performed on sAPPβ, which may have been interesting given the results presented here. Indeed, other research had suggested that cathepsin B is capable of degrading APP CTFs, and inhibition of cathepsin B caused the accumulation of CTFs with no discernible effect on sAPPα or sAPPβ in human H4 neuroblastoma cells (Asai et al. 2011). However, this paper also indicated that Ca074Me inhibition had no effect on Aβ secretion, despite CTF accumulation (Asai et al. 2011), and contrary to what we observed in our SH-SY5Y model. It is surprising that in our cell system, treatment with the cathepsin B inhibitor significantly reduced Aβ to such an extent with little apparent continued BACE1 and γ-secretase proteolysis. Though Hook et al. (2014) provide compelling evidence for the production of Aβ in a cathepsin B dependent manner in their animal and cell models, further understanding of the processes involved is required. If cathepsin B is indeed acting as a β-secretase in our system, then it is interesting that its inhibition has no effect on APP_{ICE}. This would suggest cathepsin B does not cleave APP_{ICE}, and given Hook et al. (2014) linked cathepsin B cleavage to pGlu-Aβ generation, this may offer another mechanism by which the Icelandic mutation is protective. However, given that inhibition of BACE1 resulted in 90% reduction of sAPPβ and Aβ in APP_{WT} it is possible that there may be either some non-specific inhibitory effect or experimental artefact related to the high concentrations of inhibitor being used. Indeed, Asai et al. (2011) used 0.1 μM, 1 μM, and 10 μM concentrations of Ca074Me in their experiments (Asai et al. 2011), compared to the 50 μM used in the experiments presented

in this chapter and by Hook et al. (2014). Ideally, a concentration range should be employed to determine any interplay between these two proteolytic pathways in our system. It has been suggested that inhibition of lysosomal degradation through cathepsin inhibition can increase the retention of waste products including Aβ within neurons (Pimplikar et al. 2010). Whether this offers an alternative explanation for the reduced Aβ we have observed in the conditioned cell medium following cathepsin B inhibition in these experiments would need further investigation. APP has also been shown to be proteolytically cleaved by meprin β to produce Aβ1-X and Aβ2-X directly in cell models, and meprin β also cleaved synthetic peptides resembling the β-secretase cleavage site between positions two and three of the Aβ region (in theory creating Aβ3-X) (Bien et al. 2012). This is another event which may be influenced by the amino acid substitutions at A673 in APP, and could be of interest in the context of the amyloidogenic potential of these mutant forms of APP.

5.3.3 SH-SY5Y cells expressing APP695 do not produce detectable pGlu-Aβ3-40

Hook et al. (2014) showed that cathepsin B inhibition resulted in reduced pGlu-Aβ in their neuronal-like chromaffin cell model, a phenomenon not previously observed with other β-secretases. However, there is no evidence that cathepsin B cleaves APP between the alanine at position 2 and the glutamate at position 3 of the Aβ sequence to directly liberate Aβ3-X. The production of pGlu-Aβ must then require the activity of an exopeptidase to remove the aspartate and alanine residues and allow the nascent N-terminal glutamate residue to be cyclised by QC. As the Icelandic and Italian mutations are at the second amino acid in the Aβ sequence, we postulated they may affect the production of pGlu-Aβ species, potentially contributing to the neuroprotective or neurodegenerative phenotypes of these two APP mutants, respectively. Unfortunately, the levels detected were beneath, or at the very limit of the lowest detectable point of the standard curve of the pGlu-Aβ assay employed. Whether this is due to absence of the enzyme(s) responsible for producing N-terminally truncated Aβ or a lack of QC activity in our cell system is unclear and would require further investigation. In other experimental systems, co-expression of APP and QQ was required to produce detectable levels of pGlu-Aβ42, and these were still ~7-fold lower than that of normal Aβ (Schilling et al. 2008). However, there is emerging evidence that the presence of N-terminally truncated Aβ species may be extremely important to AD pathogenesis. A recent study showed that patients presenting with the pathological hallmarks of AD but without significant cognitive impairment had significantly less brain pGlu-Aβ than those with the same hallmarks and AD diagnosis (Portelius et al. 2015). Various lines of evidence have also suggested pGlu-Aβ is more toxic (which may be tau dependent) (Nussbaum et al. 2012), aggregation prone (Schilling et al. 2006)

and interferes to a greater extent with LTP than the Aβ1-X peptide (Deng et al. 2013) while QC is significantly upregulated in AD brains (Schilling et al. 2008). pGlu-Aβ has thus become a therapeutic target in AD, with QC inhibitors (Schilling et al. 2008) and specific pGlu-Aβ immunotherapy treatments both suggested to be potential specific modulators of pGlu-Aβ production and clearance, respectively (Frost et al. 2012). Understanding the process by which normal Aβ becomes N-terminally truncated through identification of proteases for its direct liberation, or exopeptidases which truncate the Aβ1-X form could provide further therapeutic targets for intervention, while understanding the contribution of amino acid substitutions at the N-terminus of the Aβ region alter pGlu-Aβ formation could further understanding of familial forms of the disease.

In summary, our results on amyloidogenic proteolysis of APP_{WT}, APP_{ICE} and APP_{ITA} in a neuronal model recapitulated the results first presented in the HEK cell line (Jonsson et al. 2012). They also support findings from other labs in primary mouse neurons and human neurons (Benilova et al. 2014;Maloney et al. 2014). In addition we show that the mutations may alter the ratio of Aβ species produced, potentially contributing to the phenotypes observed. While BACE1 and Cathepsin B were both shown to reduce Aβ production in the cell lines, further work using a wider range of drug concentrations and different cell lines, should be undertaken to fully understand the interplay between these proteolytic pathways. It would also be of interest to find a system in which pGlu-Aβ could be studied to determine the effects of these mutations on its formation, while the effect of meprin β would also be of interest to pursue further.

Chapter 6. Discussion

6.1 Introduction

Substantial and convincing evidence implicates APP and more importantly, its proteolytic cleavage product Aβ, as the main protagonist in AD. Despite this, the molecular function(s) of APP and the mechanisms which modulate its proteolysis remain poorly understood. Furthermore, confusion surrounds the relevance of the different isoforms of APP, the expression profiles and amyloidogenic potential of which have remained a contentious issue. While consensus within the literature points towards increased expression of longer APP isoforms in the brains of AD patients (**see table 1.1**), few comparative analyses of the differences in function and proteolysis of these isoforms have been performed. Work from our lab had previously shown that in a human neuroblastoma cell line, APP isoforms undergo differential proteolysis to Aβ, with the APP695 isoform undergoing more amyloidogenic proteolysis than the KPI domain-containing isoforms (Belyaev et al. 2010). Though the consequence of this difference in proteolysis for AICD transcriptional activity was examined by Belyaev et al. (2010), the causes of the difference in proteolysis have remained enigmatic. Therefore the main aim of the body of work presented in this thesis has been to determine the factor(s) influencing this stark difference in proteolysis. Here the potential implications of the research presented herein will be discussed with reference to the wider field of AD research. The remaining unanswered questions relating to the work and potential future directions of the research will also be discussed.

6.2 The APP isoforms undergo differential proteolysis and show differences in subcellular location and interactomes

Our lab has previously shown that, in our SH-SY5Y cell line, APP695 undergoes significantly more amyloidogenic proteolysis than the KPI domain-containing APP isoforms (Belyaev et al. 2010). This intriguing difference in the proteolysis of the APP isoforms raises several interesting questions: 1) how are different APP isoforms subject to differential amyloidogenic proteolysis, 2) can the cause of differences in proteolysis be targeted therapeutically, 3) what are the causes and consequences of a shift in the expression profile of APP isoforms? Though the work presented in this thesis has mainly focused on trying to answer the first of these questions, the other questions will also be discussed as part of this chapter.

Through studying the subcellular location and trafficking of the APP695 and APP751 isoforms we have shown that lipid raft disruption, and the action of recycling endosomes differentially affects APP proteolysis in these two isoforms, without being solely causative of the large difference in APP isoform proteolysis observed. We have provided evidence which suggests the cause of the differences in proteolysis may occur in the secretory pathway as more APP751 is present in the TGN and less APP751 reaches the cell surface, and yet amyloidogenic proteolysis of APP once reaching the cell surface appears to be the same for both isoforms. Though not yet a complete picture, this provides support for the notion that endocytosed APP contributes most significantly to Aβ generation regardless of the APP isoform. We have also shown some evidence that the APP isoforms may be processed differentially by other proteolytic pathways potentially involving meprin β and η-secretase/MT5-MMP, which may contribute to the differential proteolysis by α-secretase and β-secretase we observe in the APP isoforms. We have shown that the APP isoforms have over-lapping interactomes but the extent to which the APP isoforms interact with certain proteins can vary significantly. These differences may well have functional consequences and raise interesting questions regarding the nuclear signalling capabilities of APP isoforms and the role of APP in mitochondrial function or dysfunction. We have also shown that some of the protein-protein interactions identified can influence the amyloidogenic proteolysis of APP and again, this varies between the isoforms. As with the trafficking studies, no single interaction was identified that was solely responsible for the differences observed in isoform proteolysis. Finally, we have confirmed the effect of the recently discovered A673T mutation in APP (Jonsson et al. 2012) and attempted to answer questions regarding the influence of amino acid substitutions at the A673 site in APP on proteolysis by BACE1 and cathepsin B. The results presented raise further questions about the interplay between the various proposed β-secretases, their roles in different cell systems and the specificity and efficacy of their pharmacological targeting.

6.3 The case for targeting Aβ

The temporal sequence of events in the progression of AD has been controversial, though the overarching consensus remains that Aβ lies upstream of tau hyperphosphorylation (Hardy and Selkoe 2002;Frost et al. 2015). Yet the link between these two pathologies remains to be fully elucidated. While tau transgenic mice develop no overt amyloid pathology, studies have shown increases in Aβ in the brains of mice expressing a tau transgene can accelerate tau tangle formation (Gotz et al. 2001;Lewis et al. 2001) and that the toxic nature of Aβ may actually be mediated by tau (Roberson et al. 2007). Interactions between oligomeric forms of Aβ and the prion protein have been shown to result in fyn kinase phosphorylation (Rushworth et al. 2013)

and fyn kinase can directly interact with (Haass and Mandelkow 2010) and phosphorylate tau (Lee et al. 2004). Several lines of evidence interconnect Aβ and this trio of proteins as a major molecular mechanism resulting in the loss of synaptic proteins, neuronal network dysfunction, excitotoxicity and memory impairment in mice (Ittner et al. 2010;Chin et al. 2005;Roberson et al. 2011;Um et al. 2012). Recent evidence from 3D cell culture models using human neural cells with familial AD-linked APP or PS1 mutations has also supported the notion that Aβ lies upstream of tau, with Aβ accumulation shown to precede phosphorylated tau accumulation, and inhibition of Aβ generation was shown to prevent tau pathology (Choi et al. 2014). Therefore reducing Aβ (or more specifically Aβ42) which appears to be upstream of the various tau and fyn mediated toxicities should remain a major therapeutic strategy in the field.

6.4 Trafficking as a determinant of APP proteolysis and a potential therapeutic target

In order to explain APP trafficking, simplistic views of the production, maturation, proteolysis and degradation of APP are often presented (see **Figure 1.5**). However, the complexities of APP trafficking and its influence on APP proteolysis are probably still not fully understood and difficulties in comparing the proposed mechanisms involved in the trafficking of APP may stem from differences in the models used. By studying the trafficking of two APP isoforms which undergo differential proteolysis in our model system, we hoped to elucidate the trafficking pathway(s) involved in the differential proteolysis and indicate subcellular domains within which APP is protected from, or subjected to amyloidogenic proteolysis.

An array of evidence implicates endocytosis and the endosomal system in the generation of Aβ and endosomal dysfunction has been highlighted as a key driver of AD pathology, occurring early in disease pathogenesis (Rajendran and Annaert 2012). Data presented in this thesis suggests that upon reaching the cell surface, APP isoforms undergo similar amyloidogenic proteolysis, despite our observation of increased co-localisation of APP751 with an early endosome marker compared to APP695. This would suggest that the cause of the reduced amyloidogenic proteolysis of the APP751 isoform occurs before its insertion into the plasma membrane. Therefore regulating APP endocytosis offers a mechanism through which Aβ production could be attenuated without any isoform specific differences. However, the feasibility of specifically targeting APP endocytosis is questionable. Several proteins have been shown to influence APP endocytosis including sorting nexin 17 and Dab2 (Lee et al. 2008), LRP1B (Cam et al. 2004), Mint proteins (Sullivan et al. 2014) and LRP1 (Cam et al. 2005) which may provide more specific mechanisms through which APP internalisation could be modulated. Failure of our interactomic analyses to identify any of these previously proposed interactions

further highlights the requirement for in depth characterisation of interactors in disease relevant models.

We have also provided evidence here that less APP751 is present at the cell surface and more co-localises with a TGN marker when compared to APP695, suggesting I) limiting exocytosis or II) increasing trafficking of APP back to the TGN represents a means through which APP751 is spared from amyloidogenic proteolysis. The first concept is perhaps more likely given the results we have observed in the APP_{SWE} isoforms and as discussed previously, aligns with data showing retention of APP within the TGN may prevent its amyloidogenic proteolysis (Schmidt et al. 2007). In addition, evidence showing APP and BACE1 are trafficked to the cell surface in separate vesicles (Bauereiss et al. 2015) may indicate mechanisms exist which could keep these APP and BACE1 separate within the ER and Golgi apparatus prior to their exocytosis. Whether this difference in exocytosis exists in neurons, in which BACE1 and APP trafficking shows additional complexities (recently reviewed in: (Buggia-Prevot and Thinakaran 2015)) would need further investigation. The second of these concepts is perhaps more controversial. As discussed previously, drugs which enhance the retromer complex stability have been identified as Aβ reducing agents (Mecozzi et al. 2014), but it is unclear how these drugs alter APP trafficking (though the increase in sAPPα the authors observed may suggest it is through enhanced trafficking back to the cell surface). The effect of retromer stabilisation may be two fold in that, in addition to altering APP trafficking, the retromer component sorting nexin 6 binds BACE1 and regulates its trafficking, also reducing Aβ generation (Okada et al. 2010). Okada et al. (2010) did report however that sorting nexin 6 negatively regulated BACE1 retrograde transport, a counterintuitive result considering the proposed function of the retromer complex. Other reports have suggested the involvement of GGA proteins in the retrograde transport of BACE1 (Wahle et al. 2005). Rather than just increasing or decreasing APP proteolysis, GGA proteins appear to alter the secretion of sAPPβ and also cause the accumulation of CTFβ suggesting changes in the subcellular location of the secretases or APP can influence the fate of APP and its proteolytic fragments (von Einem et al. 2015). The effect of retrograde transport of APP and BACE1 is therefore complex and may involve several mechanisms. Despite these complexities, it has been proposed that retromer dysfunction is linked to other neurodegenerative diseases and therefore restoring retromer function has therapeutic potential which extends beyond AD (Small and Petsko 2015). However, the same issues which undermine the potential to target endocytosis would apply to therapeutics targeting the retromer complex, namely their capacity to specifically alter the trafficking of APP and/or BACE1 without perturbing other essential biological processes. In addition, perturbation of normal APP trafficking may have functional

consequences and could be particularly ill advised given a specific function of APP is yet to be defined.

6.5 APP interactions as an alternative target in Aβ generation

6.5.1 The caveats of BACE1 and γ-secretase as therapeutic targets

β-secretase cleavage of APP is the rate limiting step in the production of Aβ and thus BACE1, proposed to be the major β-secretase in the brain (Cole and Vassar 2007), has remained a major target for pharmacological intervention in AD. However, BACE1 substrate specificity is certainly not limited to APP and various other neuronal substrates have been identified (Kuhn et al. 2012;Dislich et al. 2015). Therefore a lack of understanding of the full repertoire of BACE1 substrates may confound the potential of this therapeutic strategy (Vassar et al. 2014). γ-secretase has remained an alternative therapeutic target to prevent the generation of Aβ, though perhaps presents an even more challenging proposition than BACE1. The inherent complexity of the γ-secretase complex makes its study difficult and only extremely recently has a detailed atomic structure of the γ-secretase complex as a whole been resolved (Bai et al. 2015). As with BACE1, the already large number of postulated substrates for γ-secretase is continually growing, making targeting only APP proteolysis essential for any therapeutic intervention. While studies often determine the off target effects of inhibition or modulation of γ-secretase activity on notch processing, there are no real high throughput methods of examining the effect on other γ-secretase targets (Golde et al. 2013). While GSIs have previously failed in clinical trials (Doody et al. 2013), undesirable side effects including inhibition of notch processing and the accumulation of APP CTFs may confound their capacity to either prove or disprove the amyloid cascade hypothesis (De Strooper 2014). However, GSMs which act to increase the carboxy-peptidase activity of γ-secretase to reduce Aβ42 specifically in favour of Aβ38 (and without causing CTF accumulation), have been shown to ameliorate memory deficits in AD mouse models without causing significant cognitive dysfunctions in wild-type mice (Mitani et al. 2012). GSMs were also recently shown to decrease neuronal tau levels in neurons derived from human iPSCs, suggesting a link between APP proteolysis and tau, and adding further weight to their potential as AD therapeutics (Moore et al. 2015). However, their effect on the proteolysis of any number of other γ-secretase substrates has not been determined and could again prove a confounding factor in the success of this type of drug.

6.5.2 Do modulators of APP proteolysis overcome the inherent difficulties of direct inhibition of the secretases?

Our results show that the RNAi induced knockdown of specific proteins in the interactomes of the APP isoforms we have studied can modify the production of Aβ. Fe65 was shown to affect APP proteolysis at the β-secretase step and both ataxin-10 and GAP43 were shown to affect the γ-secretase proteolysis step indicating that proteins within the interactome could be targeted to attenuate either cleavage event in the generation of Aβ. Knockdown of ataxin-10 and GAP43 both decreased Aβ generation, while Fe65 knockdown increased Aβ generation indicating that proteins within the interactome can either enhance or attenuate Aβ generation. While the application of RNAi removes the interactor rather than specifically disrupting the interaction, it appears that that the disruptions of these interactions could serve as alternative mechanisms through which to target Aβ generation without requiring direct inhibition of β- or γ-secretase. These data are of course preliminary and increased understanding of the mechanisms involved and the possible functional implications of these interactions may be required to determine whether they are suitable therapeutic targets. As we have shown that their affects appear to be isoform specific, further understanding of the expression of APP isoforms in the AD brain would prove useful in proposing any interactor as a valid target. Determining the domains involved in the protein-protein interactions we have shown modulate APP proteolysis may also be necessary to specifically disrupt these interactions. The capacity of drugs targeting protein-protein interactions to attenuate Aβ production has been shown with small molecule inhibitors of APP dimerization (So et al. 2012) and drugs which stabilise the retromer complex (Mecozzi et al. 2014) which have been both shown to inhibit Aβ production. Though the reductions in Aβ generation reported here are small in comparison to the efficacy of direct BACE1 inhibition in this cell model, more specific disruption of these APP interactions could produce more efficacious inhibition of Aβ production. In addition, a previous report suggested that a 30% reduction in soluble Aβ levels in the brains of transgenic mice (albeit through enhanced Aβ clearance rather than impaired Aβ generation) was enough to reduce memory deficits (Cramer et al. 2012). The modulators of APP proteolysis we have identified in this study would potentially have the same caveats of γ-secretase inhibition, namely accumulation of CTFs, and loss of potential nuclear signalling capabilities of AICD. However, the APP interactome could be further interrogated to identify modulators of BACE1 proteolysis which would prevent the accumulation of CTFs and Aβ.

Interruption of the interaction between APP and the proposed interactors overcomes the issue of substrate specific proteolysis inhibition for β- and γ-secretase inhibitors. However, as with

BACE1 and γ-secretase inhibitors or modulators, disruption of these interactions will only serve as a mechanism to reduce Aβ production. While potentially allowing the recovery of natural Aβ clearing mechanisms, these types of therapeutics are probably unlikely to improve or slow the progression of the disease in late stages (Golde et al. 2013). Indeed the ability to intervene early in the disease progression is likely paramount to the success of therapies targeting Aβ (Selkoe 2011). The discovery of the A673T protective mutation in APP acts as proof of principle for the amyloid cascade hypothesis and it indicates that inhibition of APP proteolysis by BACE1 and the resultant reduction in Aβ production has no deleterious effects and may in fact protect against AD (Jonsson et al. 2012). However, as carriers of this mutation would have reduced Aβ generation from birth, it may imply the need for BACE1 inhibition well before the decades of life in which AD is typically diagnosed. Drugs specifically targeting interactions which either enhance or attenuate Aβ production may therefore circumvent the difficulties encountered with BACE1 and γ-secretase inhibition in relation to their substrate specificity, but would still require early intervention. Though reducing the generation of Aβ in the brains of patients with significant prior Aβ accumulation may have some cognitive benefit (Karran and Hardy 2014b), it seems that drugs targeting Aβ production may be better thought of as preventative therapeutics, rather than 'cures' for those with later stage disease (Vassar 2014).

6.5.3 The effect of protein-protein interactions on Aβ production is not limited to the interactome of APP

When studying the interaction networks involved in AD progression and their influence on Aβ generation the interactomes of BACE1 and γ-secretase may also be of interest. Interaction between BACE1 and reticulon 3 has been shown to attenuate Aβ production by up to 60% through direct interaction in the ER, Golgi and TGN compartments (He et al. 2004), indicating that the BACE1 interactome also contains proteins capable of influencing Aβ generation and offering another mechanism by which BACE1 proteolysis may be decreased in the secretory pathway. Similarly, interaction between PS1 and phospholipase D1 has been shown to attenuate Aβ production through retention of PS1 within the Golgi, preventing the formation of the γ-secretase complex (Cai et al. 2006), while an interaction between PS1 and the protein Arc has been shown to increase Aβ production through promoting the intracellular trafficking of γ-secretase to endocytic vesicles without the requirement for endocytosis (Wu et al. 2011). Furthermore, interaction of β-arrestin 2 with the APH-1a subunit of the γ-secretase has also been shown to enhance Aβ production by 50% by increasing trafficking of the γ-secretase subunit to lipid raft domains (Thathiah et al. 2013) suggesting interactions of the various components of the γ-secretase complex could influence its proteolytic capabilities. The

identification of GAP43 as a modulator of Aβ generation in our own and another recent publication on γ-secretase interactions in the mouse brain (Inoue et al. 2015) adds weight to the argument for interrogating the interactomes of multiple AD linked proteins in order to elucidate further targets. Convergence on the same protein through different isolation techniques, along with data showing the same consequence of GAP43 knockdown gives increased confidence in the result. Similar to interactions we have observed for APP, the functional implications of the interactions observed in studies of the secretase interactomes would also require further understanding, but they may also offer potential avenues for therapeutic intervention in AD.

6.6 Alternative pathways of APP proteolysis

Perhaps BACE1 is the wrong target for therapeutic intervention in AD, not because the amyloid cascade hypothesis is wrong, but because there are other proteases with β-secretase activity or which cleave APP at alternative sites producing functional, benign or neurotoxic fragments. Inhibition of BACE1 proteolysis can dramatically reduce Aβ generation in our model system (see **Figure 5.5**) but there is emerging evidence that other proteases can initiate Aβ generation through β-secretase activity or cleave APP at alternative sites and further understanding of the processes involved in their action may be required (see **Figure 6.1**). One aspect of BACE1 proteolysis which is often overlooked (including in this thesis) is the fact that APP can be cleaved at two sites by BACE1. Though cleavage between M671 and D672 (the cleavage responsible for Aβ1-X production) is most often studied, BACE1 can also cleave between Y681 and E682 (resulting in Aβ11-X production) (Nhan et al. 2015). This may be important as the missing N-terminus of Aβ or C-terminus of sAPPβ may affect their detection by immunoblot analysis and ELISA (Vetrivel et al. 2011). Determination of cleavage of the APP isoforms at the Y681 by investigating APP CTF generation should be a priority in any further research on the proteolysis of the isoforms. In addition to the differences in Aβ production from the APP isoforms our lab has previously published (Belyaev et al. 2010), work presented in this thesis suggests that the APP isoforms may well undergo differential proteolysis by other proteases. While we cannot unequivocally confirm the identity of some of the proteolytic fragments we have observed, comparison to other observations within the literature suggest that APP695, in addition to increased β-secretase cleavage, may undergo more η-secretase/MT5-MMP cleavage, while APP751 appears to undergo preferential ectodomain shedding by meprin β to produce a small N-terminal APP fragment previously identified (Jefferson et al. 2011) (see **Figure 6.1**). Given these differences, and the fact that we see no differences in the degradation rates of the APP isoforms despite much higher β-secretase proteolysis of APP695, pursuing other proposed

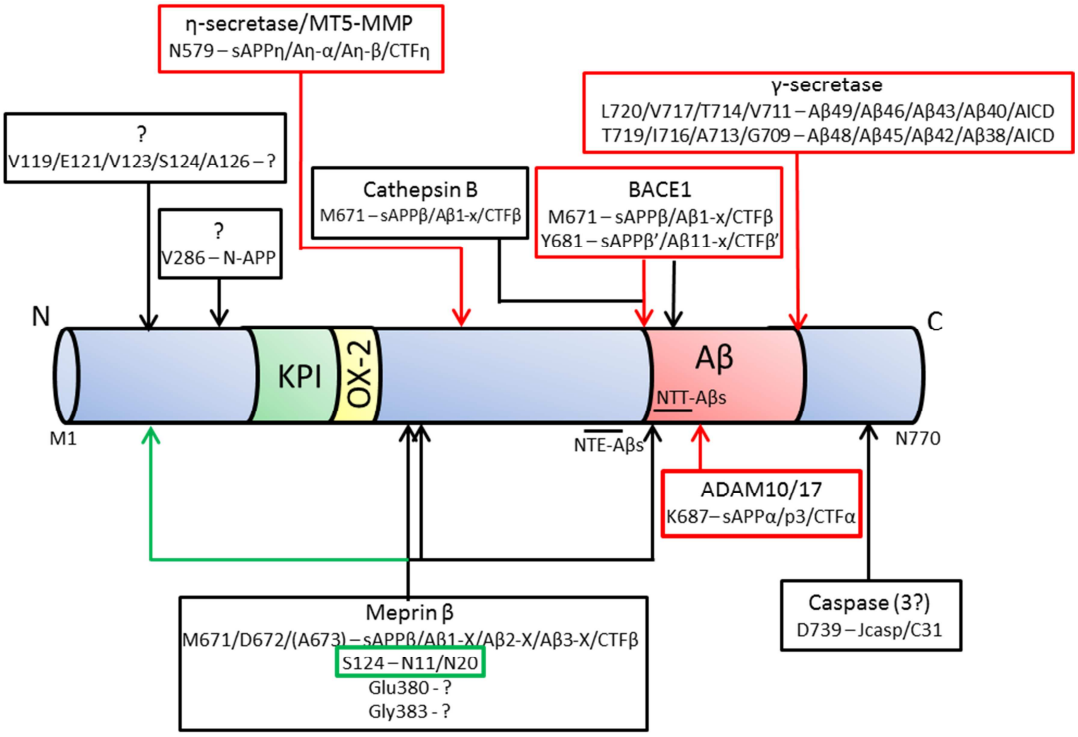

Table 6.1 The complexities of APP proteolysis

The typical view of APP proteolysis presented in Chapter 1 may be over simplified. Numerous other proteases have been identified as APP cleaving enzymes with a number of cleavage sites identified along the length of the APP molecule. The proteases responsible for the many proteolytic fragments identified within the literature have not been identified and some enzymes (including BACE1, γ-secretase and meprin β) cleave at more than one site. In all cases the proteolytic cleavage occurs on the carboxy-terminal side of the amino acid identified in the figure. Where fragments are named in the literature, their names are given or are alternatively marked '?'. Similarly, where proteases have not been identified, these are also designated '?'. Due to the huge number identified within the literature, N-terminally truncated Aβs (NTT-Aβs) and N-terminally extended Aβs (NTE-Aβs) are not specifically described. The proteases responsible for the production of NTE-Aβs and NTT-Aβ remain to be completely resolved. Red boxes represent proteolytic cleavage events we believe may be elevated in APP695 and green boxes represent cleavage events which may be elevated in APP751. N = n-terminus, C = C-terminus.

proteolytic pathways could provide alternative explanations for the differences we observe. This may also aid in clarifying the interplay between the different proteolytic pathways APP encounters. In addition to BACE1; cathepsin B (Hook et al. 2014) and meprin β (Bien et al. 2012) have both been proposed as putative β-secretases and meprin β (Jefferson et al. 2011) and MT5-MMP/η-secretase (Baranger et al. 2015;Willem et al. 2015) have both been shown to cleave APP at alternative sites in the APP ectodomain. Willem et al. (2015) also showed that the APP fragments produced by MT5-MMP/η-secretase proteolysis have functional relevance as the soluble fragment produced by sequential APP proteolysis by η-secretase and α-secretases was also shown to inhibit LTP in the hippocampal brain slices from mice. Furthermore, the production of soluble metabolites from the η-secretase pathway was shown to be >9-fold higher than the production of metabolites from the amyloidogenic pathway (Willem et al. 2015). Interestingly MT5-MMP knockout mice still produced considerable η-secretase fragments suggesting MT5-MMP may not be the sole protease responsible for η-secretase activity, at least in mice (Willem et al. 2015). Despite not possessing β-secretase like activity, MT5-MMP has been shown to influence Aβ generation and therefore has important implications in AD (Baranger et al. 2015). Small C-terminal APP fragments can be produced by caspase cleavage of AICD, CTFs or of the holo-APP molecule (Nhan et al. 2015). The proteolytic cleavage between D739 and A740 liberates the CTF C31 which can cause to cell apoptosis (Lu et al. 2000) and appears to contribute to behavioural deficits in APP transgenic mice independently of Aβ (Galvan et al. 2006). If produced from AICD, an N-terminal fragment identified as Jcasp is also produced, the function of which has remained controversial (Nhan et al. 2015). Several other APP fragments have also been identified in the literature without the specific protease or cleavage site being identified. One study identified N-terminally extended Aβ proposed to contain at least 34 amino acids N-terminal to the β-secretase site in the conditioned cell culture medium from 7PA2 cells which were shown to impair synaptic plasticity (Welzel et al. 2014). Initial reports that alternative N-terminal APP fragment (possibly containing amino acids 1-286 of the APP ectodomain) was responsible for the induction of axonal pruning (Nikolaev et al. 2009) were later disproved (Olsen et al. 2014), but alternative physiological functions for this fragment have not been determined nor has the protease responsible for its liberation been identified. A recent publication did show that a peptide containing the 286 N-terminal amino acids of APP could bind neurons, but the functional implications of this binding, and the receptor to which it bound were not identified (Dawkins et al. 2014). An array of N-terminal APP fragments have also been isolated from human CSF which were elevated in AD patients above the level seen in control patients (Portelius et al. 2010). Various N-terminally truncated Aβ peptides have been identified in the brain which may correlate better with AD diagnosis

(including the pGlu-Aβ already discussed) (Portelius et al. 2015). Others such as Aβ5-X increase in CSF from humans treated with a BACE inhibitor suggesting they are not direct products of BACE1 cleavage (Portelius et al. 2014).

In addition to the typically monitored fragments (sAPPα, sAPPβ, Aβ CTFs and AICD) a plethora of N-terminal and C-terminal APP fragments, may be present in the brain though it is unclear which of these are biologically relevant or functional, how they are regulated and how the proteolytic pathways interrelate. Until the interrelationship between these distinct pathways is reconciled, the failure of therapeutics targeting amyloid generation may not truly disprove the amyloid cascade hypothesis.

6.7 Outstanding questions on the causes and consequences of differences in the APP isoforms

6.7.1 The causes of changes in APP expression profile remain enigmatic

The lack of consensus on the expression profile of APP isoforms in ageing and AD is further confounded by a lack of understanding of the factors which cause changes in their expression profiles. Splicing factors involved in the regulation of APP splicing have been identified, which recognise specific sequences within the APP mRNA. The neuron specific splicing factor RBFox1 has been shown to increase exclusion of exon 7, encoding the KPI domain (Alam et al. 2014) and CUGBP2 has been shown to induce the exclusion of exon 8 encoding the OX-2 domain (Poleev et al. 2000). It would be interesting, on the basis of these data, to know the neuronal expression levels of these two splicing proteins and to determine whether the levels present in the ageing and AD brain decline in a concomitant manner with the reported increases in larger APP isoforms (see **Table 2.1**). An extensive study of the insoluble protein aggregates in AD brains also identified the accumulation of various components of the U1 small ribonucleoprotein (U1 snRNP) spliceosome complex in AD brains and global deficiencies in the splicing of various gene products (Bai et al. 2013). While the knockdown of the U1-70K subunit of the U1 snRNP complex appeared to increase, rather than decrease APP mRNA splicing, the authors observed no obvious change in isoform expression in their analysis, but did observe deficiencies in APP mRNA intron splicing (Bai et al. 2013). Alterations in the splicing of the APP transcript may also not be limited to AD, with one study finding significant increases in longer APP isoform mRNA in dementia with Lewy bodies and cerebral amyloid angiopathy, but not in Parkinson's Disease or PSP (Barrachina et al. 2005). Interestingly, this study observed changes in APP splicing only in late Braak stages of AD, and not in early stages (Barrachina et al. 2005).

It has been proposed that the increase in KPI domain-containing isoforms occurs due to excitotoxic stress or sustained synaptic NMDA receptor activation resulting in increased cellular Ca^{2+} levels with downstream effects on the mRNA splicing mechanism (Lesne et al. 2005). Evidence has also highlighted the importance of microRNAs (miRNAs) in APP alternative splicing with reduced miRNA levels, specifically miR-124, in AD brains being associated with increased inclusion of exons 7 and 8 in the APP transcript (Smith et al. 2011).

6.7.2 Specific functions for APP isoforms have not been determined

Despite the various differences in expression profile, proteolysis (Belyaev et al. 2010) and functional domains identified in the literature for the APP isoforms, specialised functional roles for each of the different isoforms are yet to be determined. Thus, the functional consequences of a switch in APP isoform expression also remain enigmatic.

A mitochondrial role for APP?

One study suggested that the expression of KPI-containing APP isoforms could contribute to mitochondrial dysfunction through reduction in the expression of several mitochondrial genes (Chua et al. 2013). Expression of APP695 in an APP null cell line increased mitochondrial metabolic enzyme levels to a greater extent than APP751 resulting in higher mitochondrial activity as measured by NAD+/NADH ratio, cytochrome c oxidase activity and mitochondrial membrane potential (Chua et al. 2013). In line with this, we have observed increased mitochondrial proteins in the APP695 interactome. However, APP has also been widely reported to disrupt mitochondrial function and significantly higher accumulation of APP in mitochondria isolated from AD patient brains compared to control brains has previously been observed (Pavlov et al. 2009). In contrast to the report from Chua et al. (2013), in a mouse model of AD, high expression of APP bearing the Swedish and London mutations was shown to induce various mitochondrial dysfunctions (Hauptmann et al. 2009). Given the reported mitochondrial dysfunction in AD this may be of interest to pursue further, particularly given that VDAC family members appear most consistently across the APP interactomic studies within the literature (Hosp et al. 2015;Kohli et al. 2012). Whether the association between APP and VDACs we and others have identified occurs in the mitochondrial membrane or in plasma membrane lipid rafts as has previously been identified (Fernandez-Echevarria et al. 2014), remains uncertain. However, VDAC1 in particular has been identified as a potential therapeutic target in AD due to its postulated role in mitochondrial dysfunction and interactions with APP and Aβ (Reddy 2013). Furthermore, it has been shown that VDAC1 interacts with the γ-secretase complex, and its knockdown reduced Aβ production (though its over-expression did not increase Aβ production) (Hur et al. 2012).

Nuclear signalling capacity of APP

Previous research from our lab suggested the nuclear signalling capabilities of APP are specific to AICD produced from the APP695 isoform (Belyaev et al. 2010). These data are supported by the data in this thesis indicating the APP695 isoform (or C-terminal fragments thereof) interacts to a greater extent with nuclear pore proteins than does the APP751 isoform. Further investigation of the C-terminus of the APP isoforms may aid in clarifying causes of the differences in transcriptional regulation observed by Belyaev et al. (2010) and the differences in Fe65 binding we observe here. In particular, analysis of the seven proposed phosphorylation sites in the APP cytosolic domain (van der Kant and Goldstein 2015) would be of interest. The capacity for AICD to regulate transcriptional activity remains controversial (Nalivaeva and Turner 2013). However, it may be an important consideration in the development of therapeutics targeting BACE1 given that transcriptionally active AICD is produced preferentially from the amyloidogenic proteolysis pathway and regulates the expression of the Aβ degrading enzyme NEP (Belyaev et al. 2010;Grimm et al. 2015) and transthyretin which has a role in Aβ clearance (Kerridge et al. 2014). This may be important as deficiencies in clearance of Aβ may contribute significantly to sporadic forms of AD (Octave et al. 2013). On the other hand, AICD over-expression in a mouse model was shown to replicate some of the pathological features of AD (Ghosal et al. 2009), though this finding has been contested (Giliberto et al. 2010). In addition, AICD has been reported to control the expression of various AD related genes including APP, BACE1 and GSK3β (Kim et al. 2003;von Rotz et al. 2004), the expression of which could all potentially contribute to the development of AD.

Other isoform specific roles

Very few specific roles for the different APP isoforms have been identified or studied in depth. The secreted form of KPI containing APP isoforms are analogous to protease nexin-2 (PN2), a secreted proteinase inhibitor capable of forming inhibitory complexes with epidermal growth factor binding proteins, nerve growth factors and trypsin (Nostrand et al. 1989). One distinct role of KPI domain-containing APP proteins in the clotting process has been described (Xu et al. 2005). Again, the implications of this function are uncertain. The KPI domain acts as an inhibitor of various prothrombotic enzymes and expression of KPI-containing APP in platelets reduces the risk of thrombosis in vascular injury in mice but increases haemorrhagic pathology following intracerebral haemorrhage (Xu et al. 2009;Xu et al. 2005). A recent report suggested the incidence of lobar microbleeds in AD patients are higher than in the cognitively normal, and are particularly associated with high amyloid burden (Yates et al. 2014). Microhaemorrhages have also been observed in participants in clinical trials for the amyloid clearing antibody

bapineuzumab, appearing to occur particularly in association with regions of high amyloid clearance (Sperling et al. 2012). Increased expression of KPI domain containing APP in these cases could therefore have detrimental effects and lead to increased damage of brain tissue. This suggests that, aside from their relative amyloidogenic potential, tight regulation of APP isoforms is essential in the brain.

6.7.3 The spatial and temporal expression of APP isoforms remains poorly understood

As highlighted in T**able 1.1,** a number of studies have investigated the expression profile of APP in the AD brain in comparison to control brains, often with contradictory results. Many of these studies relied upon quantification of APP mRNA in post-mortem tissue which is often subject to degradation and may not always reliably reflect protein expression (Rohan de Silva et al. 1997;Thathiah et al. 2013). A study of APP protein levels in AD brains in a large cohort of patients, in several brain regions of interest to AD pathogenesis could provide invaluable insight into the disease specific alteration in APP expression. Advances in quantitative proteomics may now allow this sort of study to be undertaken, though difficulties would still be faced in trying to decipher comparative APP isoform expression profiles due to the relatively small difference in amino acid sequence between the isoforms. However, the KPI domain of APP should produce five specific tryptic peptides potentially allowing this technique to be used to identify differences in the presence of this isoform (see **Figure 6.2**). One distinct tryptic peptide would also be produced for APP695 though this would contain only a single amino acid difference when compared to the APP751 amino acid sequence.

Though APP695 is often thought to be the main neuronally expressed APP isoform (Haass et al. 2012), appreciable levels of all three major APP isoforms have been shown to be present in a wide range of regional brain tissues, including the hippocampus (Golde et al. 1990;Johnson et al. 1990). While iPSC derived cortical neurons produced in our lab appear to express only the APP695 isoform (Edwards and Hooper, unpublished), the physiology of these cells is still being investigated, with data indicating that they show a foetal phenotype (Zameel Cader, keynote lecture, ARUK Manchester and Northwest Network meeting, 2015). This may be important given that expression profiles of APP may change in ageing and AD (see **Table 1.1**). Beyreuther et al. (1993) observed that, while making up 90% of APP transcripts in the foetal brain, APP695 mRNA accounts for only 50% or less of mRNA transcripts in the adult brain, while others have reported as much as 70% of APP mRNA in the brain contains the KPI domain coding region (Johnston et al. 1996). Therefore, finding methods to 'age' iPSC derived cortical neurons may be essential in their application to the study of AD. It would be interesting then to compare the expression profiles of APP isoforms in 'aged' and 'young' neurons. Astrocytes are proposed to

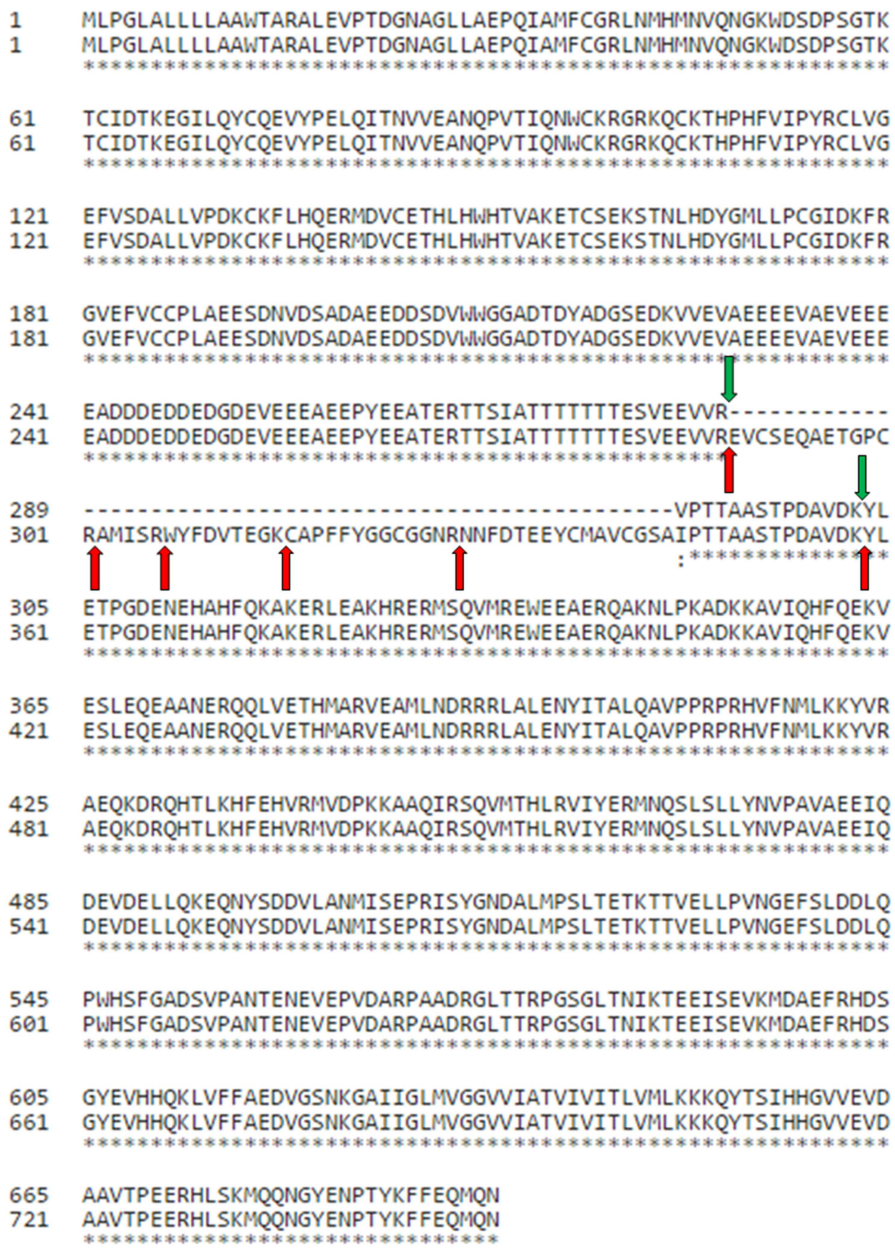

Table 6.2 The potential isoform specific APP fragments produced by tryptic digestion

Quantitative proteomics would allow the prevalence of the KPI domain containing APP isoforms within the brain to be quantified and compared due to potential trypsin cleavage sites within the KPI domain. These tryptic sites would produce 5 peptides specific to the APP751 isoform allowing comparison of their abundance in AD and control cases. A single APP695 specific tryptic peptide would also be produced but would vary from the KPI domain C-terminal tryptic peptide by just a single amino acid substitution (V:I).

express all three APP isoforms (Burton et al. 2002), and the expression of APP and its proteolysis by BACE1 in astrocytes has been shown to increase following cholesterol exposure (Avila-Munoz and Arias 2015) in a similar manner to that observed in neurons (Marquer et al. 2014). Another important factor to consider is the cell specific expression of BACE1. Early research suggested BACE1 is most highly expressed in human neurons and BACE1 activity within mouse derived astrocytes was shown to be relatively low in comparison to neurons and therefore contribution to Aβ pathology was considered to be relatively minor (Hussain et al. 1999;Zhao et al. 1996). However, astrocyte expression of BACE1 has been shown to increase in reactive astrocytes surrounding amyloid plaques in Tg2576 mice (Rossner et al. 2001) and recent work has shown that at least in mouse models, Aβ is produced from various non-neuronal brain cell types (Veeraraghavalu et al. 2014). Under normal conditions within the brain the relative contribution of glial cells to Aβ generation may be relatively minor, but in the disease state, where inflammation is common, increases in BACE1 expression within glia could significantly contribute to Aβ generation, particularly as glia are more abundant in the brain than neurons (Cole and Vassar 2007). Increased understanding of the spatial and temporal expression profiles of the APP isoforms and BACE1 would contribute significantly to the gap in knowledge surrounding the amyloidogenic potential of the APP isoforms.

6.8 Concluding remarks

Astounding medical progress has been made over the past 100 years across a huge range of diseases, disorders and syndromes, giving a large proportion of the population greater access to medical care and increasing life expectancy significantly. The greatest risk factor for the development of AD is ageing, and thus the probability of developing AD continues to rise alongside life expectancy. Identifying a disease modifying therapeutic should remain an absolute priority for the research community and prevention of the accumulation of Aβ remains a valid target to achieve this goal. The data in this thesis provides novel insights into the production of Aβ and accounts for differences in APP isoforms often not considered in AD research. These data raise interesting questions regarding the function of APP but indicate that the interactome of APP can provide Aβ modulating targets for intervention in AD.

References

Abramov, E., Dolev, I., Fogel, H., Ciccotosto, G. D., Ruff, E. & Slutsky, I. (2009). Amyloid-β as a positive endogenous regulator of release probability at hippocampal synapses. *Nat Neurosci,* 12(12)**,** 1567-1576.

Acx, H., Chavez-Gutierrez, L., Serneels, L., Lismont, S., Benurwar, M., Elad, N. & De Strooper, B. (2014). Signature amyloid beta profiles are produced by different gamma-secretase complexes. *J Biol Chem,* 289(7)**,** 4346-55.

Ahn, K., Shelton, C. C., Tian, Y., Zhang, X., Gilchrist, M. L., Sisodia, S. S. & Li, Y. M. (2010). Activation and intrinsic gamma-secretase activity of presenilin 1. *Proc Natl Acad Sci U S A,* 107(50)**,** 21435-40.

Aisen, P. S., Cummings, J. & Schneider, L. S. (2012). Symptomatic and nonamyloid/tau based pharmacologic treatment for Alzheimer disease. *Cold Spring Harb Perspect Med,* 2(3)**,** a006395.

Akiyama, H., Shin, R. W., Uchida, C., Kitamoto, T. & Uchida, T. (2005). Pin1 promotes production of Alzheimer's amyloid beta from beta-cleaved amyloid precursor protein. *Biochem Biophys Res Commun,* 336(2)**,** 521-9.

Alam, S., Suzuki, H. & Tsukahara, T. (2014). Alternative splicing regulation of APP exon 7 by RBFox proteins. *Neurochem Int,* 78(0)**,** 7-17.

Allinson, T. M., Parkin, E. T., Turner, A. J. & Hooper, N. M. (2003). ADAMs family members as amyloid precursor protein alpha-secretases. *J Neurosci Res,* 74(3)**,** 342-52.

Anandatheerthavarada, H. K., Biswas, G., Robin, M. A. & Avadhani, N. G. (2003). Mitochondrial targeting and a novel transmembrane arrest of Alzheimer's amyloid precursor protein impairs mitochondrial function in neuronal cells. *J Cell Biol,* 161(1)**,** 41-54.

Andersen, O. M., Reiche, J., Schmidt, V., Gotthardt, M., Spoelgen, R., Behlke, J., von Arnim, C. A., Breiderhoff, T., Jansen, P., Wu, X., Bales, K. R., Cappai, R., Masters, C. L., Gliemann, J., Mufson, E. J., Hyman, B. T., Paul, S. M., Nykjaer, A. & Willnow, T. E. (2005). Neuronal sorting protein-related receptor sorLA/LR11 regulates processing of the amyloid precursor protein. *Proc Natl Acad Sci U S A,* 102(38)**,** 13461-6.

Andersen, O. M., Schmidt, V., Spoelgen, R., Gliemann, J., Behlke, J., Galatis, D., McKinstry, W. J., Parker, M. W., Masters, C. L., Hyman, B. T., Cappai, R. & Willnow, T. E. (2006). Molecular Dissection of the Interaction between Amyloid Precursor Protein and Its Neuronal Trafficking Receptor SorLA/LR11†. *Biochemistry,* 45(8)**,** 2618-2628.

Ando, K., Iijima, K. I., Elliott, J. I., Kirino, Y. & Suzuki, T. (2001). Phosphorylation-dependent regulation of the interaction of amyloid precursor protein with Fe65 affects the production of beta-amyloid. *J Biol Chem,* 276(43)**,** 40353-61.

Ankarcrona, M., Mangialasche, F. & Winblad, B. (2010). Rethinking Alzheimer's disease therapy: are mitochondria the key? *J Alzheimers Dis,* 20 Suppl 2(2)**,** S579-90.

Asai, M., Yagishita, S., Iwata, N., Saido, T. C., Ishiura, S. & Maruyama, K. (2011). An alternative metabolic pathway of amyloid precursor protein C-terminal fragments via cathepsin B in a human neuroglioma model. *FASEB J,* 25(10)**,** 3720-30.

Association, A. (2015). 2015 Alzheimer's disease facts and figures. *Alzheimer's & Dementia: The Journal of the Alzheimer's Association,* 11(3)**,** 332-384.

Atwal, J. K., Chen, Y., Chiu, C., Mortensen, D. L., Meilandt, W. J., Liu, Y., Heise, C. E., Hoyte, K., Luk, W., Lu, Y., Peng, K., Wu, P., Rouge, L., Zhang, Y., Lazarus, R. A., Scearce-Levie, K., Wang, W., Wu, Y., Tessier-Lavigne, M. & Watts, R. J. (2011). A therapeutic antibody targeting BACE1 inhibits amyloid-beta production in vivo. *Sci Transl Med,* 3(84)**,** 84-43.

Avila-Munoz, E. & Arias, C. (2015). Cholesterol-induced astrocyte activation is associated with increased amyloid precursor protein expression and processing. *Glia*.

Aydin, D., Weyer, S. W. & Muller, U. C. (2012). Functions of the APP gene family in the nervous system: insights from mouse models. *Experimental Brain Research,* 217(3-4)**,** 423-34.

Bai, B., Hales, C. M., Chen, P. C., Gozal, Y., Dammer, E. B., Fritz, J. J., Wang, X., Xia, Q., Duong, D. M., Street, C., Cantero, G., Cheng, D., Jones, D. R., Wu, Z., Li, Y., Diner, I., Heilman, C. J., Rees, H. D., Wu, H., Lin, L., Szulwach, K. E., Gearing, M., Mufson, E. J., Bennett, D. A., Montine, T. J., Seyfried, N. T., Wingo, T. S., Sun, Y. E., Jin, P., Hanfelt, J., Willcock, D. M., Levey, A., Lah, J. J. & Peng, J. (2013). U1 small nuclear ribonucleoprotein complex and RNA splicing alterations in Alzheimer's disease. *Proc Natl Acad Sci U S A,* 110(41)**,** 16562-7.

Bai, X. C., Yan, C., Yang, G., Lu, P., Ma, D., Sun, L., Zhou, R., Scheres, S. H. & Shi, Y. (2015). An atomic structure of human gamma-secretase. *Nature,* 525(7568)**,** 212-7.

Bai, Y., Markham, K., Chen, F., Weerasekera, R., Watts, J., Horne, P., Wakutani, Y., Bagshaw, R., Mathews, P. M., Fraser, P. E., Westaway, D., St George-Hyslop, P. & Schmitt-Ulms, G. (2008). The in vivo brain interactome of the amyloid precursor protein. *Mol Cell Proteomics,* 7(1)**,** 15-34.

Balklava, Z., Niehage, C., Currinn, H., Mellor, L., Guscott, B., Poulin, G., Hoflack, B. & Wassmer, T. (2015). The Amyloid Precursor Protein Controls PIKfyve Function. *PLoS ONE,* 10(6)**,** e0130485.

Baranger, K., Marchalant, Y., Bonnet, A. E., Crouzin, N., Carrete, A., Paumier, J. M., Py, N. A., Bernard, A., Bauer, C., Charrat, E., Moschke, K., Seiki, M., Vignes, M., Lichtenthaler, S. F., Checler, F., Khrestchatisky, M. & Rivera, S. (2015). MT5-MMP is a new pro-amyloidogenic proteinase that promotes amyloid pathology and cognitive decline in a transgenic mouse model of Alzheimer's disease. *Cell Mol Life Sci***,** 1-20.

Barbagallo, A. P., Weldon, R., Tamayev, R., Zhou, D., Giliberto, L., Foreman, O. & D'Adamio, L. (2010). Tyr(682) in the intracellular domain of APP regulates amyloidogenic APP processing in vivo. *PLoS ONE,* 5(11)**,** e15503.

Barrachina, M., Dalfo, E., Puig, B., Vidal, N., Freixes, M., Castano, E. & Ferrer, I. (2005). Amyloid-beta deposition in the cerebral cortex in Dementia with Lewy bodies is accompanied by a relative increase in AbetaPP mRNA isoforms containing the Kunitz protease inhibitor. *Neurochem Int,* 46(3)**,** 253-60.

Barrett, P. J., Song, Y., Van Horn, W. D., Hustedt, E. J., Schafer, J. M., Hadziselimovic, A., Beel, A. J. & Sanders, C. R. (2012). The amyloid precursor protein has a flexible transmembrane domain and binds cholesterol. *Science,* 336(6085)**,** 1168-71.

Bauereiss, A., Welzel, O., Jung, J., Grosse-Holz, S., Lelental, N., Lewczuk, P., Wenzel, E. M., Kornhuber, J. & Groemer, T. W. (2015). Surface Trafficking of APP and BACE in Live Cells. *Traffic,* 16(6)**,** 655-75.

Beckett, C., Nalivaeva, N. N., Belyaev, N. D. & Turner, A. J. (2012). Nuclear signalling by membrane protein intracellular domains: the AICD enigma. *Cell Signal,* 24(2)**,** 402-9.

Bell, K. F., Zheng, L., Fahrenholz, F. & Cuello, A. C. (2008). ADAM-10 over-expression increases cortical synaptogenesis. *Neurobiol Aging,* 29(4)**,** 554-65.

Belyaev, N. D., Kellett, K. A., Beckett, C., Makova, N. Z., Revett, T. J., Nalivaeva, N. N., Hooper, N. M. & Turner, A. J. (2010). The transcriptionally active amyloid precursor protein (APP) intracellular domain is preferentially produced from the 695 isoform of APP in a β-secretase-dependent pathway. *J Biol Chem,* 285(53)**,** 41443-54.

Ben Khalifa, N., Tyteca, D., Marinangeli, C., Depuydt, M., Collet, J. F., Courtoy, P. J., Renauld, J. C., Constantinescu, S., Octave, J. N. & Kienlen-Campard, P. (2012). Structural features of the KPI domain control APP dimerization, trafficking, and processing. *FASEB J,* 26(2)**,** 855-67.

Benilova, I., Gallardo, R., Ungureanu, A. A., Castillo Cano, V., Snellinx, A., Ramakers, M., Bartic, C., Rousseau, F., Schymkowitz, J. & De Strooper, B. (2014). The Alzheimer disease protective mutation A2T modulates kinetic and thermodynamic properties of amyloid-beta (Abeta) aggregation. *J Biol Chem,* 289(45)**,** 30977-89.

Benilova, I., Karran, E. & De Strooper, B. (2012). The toxic Abeta oligomer and Alzheimer's disease: an emperor in need of clothes. *Nat Neurosci,* 15(3)**,** 349-57.

Bentahir, M., Nyabi, O., Verhamme, J., Tolia, A., Horre, K., Wiltfang, J., Esselmann, H. & De Strooper, B. (2006). Presenilin clinical mutations can affect gamma-secretase activity by different mechanisms. *J Neurochem,* 96(3)**,** 732-42.

Bertram, L., Lange, C., Mullin, K., Parkinson, M., Hsiao, M., Hogan, M. F., Schjeide, B. M., Hooli, B., Divito, J., Ionita, I., Jiang, H., Laird, N., Moscarillo, T., Ohlsen, K. L., Elliott, K., Wang, X., Hu-Lince, D., Ryder, M., Murphy, A., Wagner, S. L., Blacker, D., Becker, K. D. & Tanzi, R. E. (2008). Genome-wide association analysis reveals putative Alzheimer's disease susceptibility loci in addition to APOE. *Am J Hum Genet,* 83(5)**,** 623-32.

Beyreuther, K., Pollwein, P., Multhaup, G., Monning, U., Konig, G., Dyrks, T., Schubert, W. & Masters, C. L. (1993). Regulation and expression of the Alzheimer's beta/A4 amyloid protein precursor in health, disease, and Down's syndrome. *Ann N Y Acad Sci,* 695(1)**,** 91-102.

Bhattacharyya, R., Barren, C. & Kovacs, D. M. (2013). Palmitoylation of amyloid precursor protein regulates amyloidogenic processing in lipid rafts. *J Neurosci,* 33(27)**,** 11169-83.

Bien, J., Jefferson, T., Causevic, M., Jumpertz, T., Munter, L., Multhaup, G., Weggen, S., Becker-Pauly, C. & Pietrzik, C. U. (2012). The metalloprotease meprin beta generates amino terminal-truncated amyloid beta peptide species. *J Biol Chem,* 287(40)**,** 33304-13.

Bieschke, J., Russ, J., Friedrich, R. P., Ehrnhoefer, D. E., Wobst, H., Neugebauer, K. & Wanker, E. E. (2010). EGCG remodels mature alpha-synuclein and amyloid-beta fibrils and reduces cellular toxicity. *Proc Natl Acad Sci U S A,* 107(17)**,** 7710-5.

Bitsikas, V., Riento, K., Howe, J., Barry, N. & Nichols, B. (2014). The role of flotillins in regulating Aβ production, investigated using flotillin 1-/-, flotillin 2-/- double knockout mice. *PLoS ONE,* 9(1)**,** e85217.

Bittner, T., Fuhrmann, M., Burgold, S., Jung, C. K., Volbracht, C., Steiner, H., Mitteregger, G., Kretzschmar, H. A., Haass, C. & Herms, J. (2009). Gamma-secretase inhibition reduces spine density in vivo via an amyloid precursor protein-dependent pathway. *J Neurosci,* 29(33)**,** 10405-9.

Blaskovic, S., Blanc, M. & van der Goot, F. G. (2013). What does S-palmitoylation do to membrane proteins? *FEBS J,* 280(12)**,** 2766-74.

Boddapati, S., Levites, Y. & Sierks, M. R. (2011). Inhibiting beta-secretase activity in Alzheimer's disease cell models with single-chain antibodies specifically targeting APP. *J Mol Biol,* 405(2)**,** 436-47.

Bordji, K., Becerril-Ortega, J., Nicole, O. & Buisson, A. (2010). Activation of extrasynaptic, but not synaptic, NMDA receptors modifies amyloid precursor protein expression pattern and increases amyloid-ss production. *J Neurosci,* 30(47)**,** 15927-42.

Brodeur, J., Theriault, C., Lessard-Beaudoin, M., Marcil, T., Dahan, S. & Lavoie, C. (2012). LDLR-related protein 10 (LRP10) regulates amyloid precusor protein (APP) trafficking and processing: evidence for a role in Alzheimer's disease. *Mol Neurodegener,* 7(31).

Brou, C., Logeat, F., Gupta, N., Bessia, C., LeBail, O., Doedens, J. R., Cumano, A., Roux, P., Black, R. A. & Israel, A. (2000). A novel proteolytic cleavage involved in Notch signaling: the role of the disintegrin-metalloprotease TACE. *Mol Cell,* 5(2)**,** 207-16.

Bucci, C., Thomsen, P., Nicoziani, P., McCarthy, J. & van Deurs, B. (2000). Rab7: a key to lysosome biogenesis. *Mol Biol Cell,* 11(2)**,** 467-80.

Buggia-Prevot, V., Fernandez, C. G., Riordan, S., Vetrivel, K. S., Roseman, J., Waters, J., Bindokas, V. P., Vassar, R. & Thinakaran, G. (2014). Axonal BACE1 dynamics and targeting in hippocampal neurons: a role for Rab11 GTPase. *Mol Neurodegener,* 9(1)**,** 1.

Buggia-Prevot, V. & Thinakaran, G. (2015). Significance of transcytosis in Alzheimer's disease: BACE1 takes the scenic route to axons. *Bioessays,* 37(8)**,** 888-98.

Burd, C. & Cullen, P. J. (2014). Retromer: a master conductor of endosome sorting. *Cold Spring Harb Perspect Biol,* 6(2).

Burgos, P. V., Mardones, G. A., Rojas, A. L., daSilva, L. L., Prabhu, Y., Hurley, J. H. & Bonifacino, J. S. (2010). Sorting of the Alzheimer's disease amyloid precursor protein mediated by the AP-4 complex. *Dev Cell,* 18(3)**,** 425-36.

Burton, T., Liang, B., Dibrov, A. & Amara, F. (2002). Transcriptional activation and increase in expression of Alzheimer's β-amyloid precursor protein gene is mediated by TGF-β in normal human astrocytes. *Biochemical and Biophysical Research Communications,* 295(3)**,** 702-712.

Cabrol, C., Huzarska, M. A., Dinolfo, C., Rodriguez, M. C., Reinstatler, L., Ni, J., Yeh, L. A., Cuny, G. D., Stein, R. L., Selkoe, D. J. & Leissring, M. A. (2009). Small-molecule activators of insulin-degrading enzyme discovered through high-throughput compound screening. *PLoS ONE,* 4(4)**,** e5274.

Cai, D., Netzer, W. J., Zhong, M., Lin, Y., Du, G., Frohman, M., Foster, D. A., Sisodia, S. S., Xu, H., Gorelick, F. S. & Greengard, P. (2006). Presenilin-1 uses phospholipase D1 as a negative regulator of beta-amyloid formation. *Proc Natl Acad Sci U S A,* 103(6)**,** 1941-6.

Cam, J. A., Zerbinatti, C. V., Knisely, J. M., Hecimovic, S., Li, Y. & Bu, G. (2004). The low density lipoprotein receptor-related protein 1B retains beta-amyloid precursor protein at the cell surface and reduces amyloid-beta peptide production. *J Biol Chem,* 279(28)**,** 29639-46.

Cam, J. A., Zerbinatti, C. V., Li, Y. & Bu, G. (2005). Rapid endocytosis of the low density lipoprotein receptor-related protein modulates cell surface distribution and processing of the beta-amyloid precursor protein. *J Biol Chem,* 280(15)**,** 15464-70.

Cao, X. & Sudhof, T. C. (2001). A transcriptionally [correction of transcriptively] active complex of APP with Fe65 and histone acetyltransferase Tip60. *Science,* 293(5527)**,** 115-20.

Caster, A. H. & Kahn, R. A. (2013). Recruitment of the Mint3 adaptor is necessary for export of the amyloid precursor protein (APP) from the Golgi complex. *J Biol Chem,* 288(40)**,** 28567-80.

Castillo-Carranza, D. L., Guerrero-Munoz, M. J., Sengupta, U., Hernandez, C., Barrett, A. D., Dineley, K. & Kayed, R. (2015). Tau immunotherapy modulates both pathological tau and upstream amyloid pathology in an Alzheimer's disease mouse model. *J Neurosci,* 35(12)**,** 4857-68.

Cataldo, A. M., Barnett, J. L., Pieroni, C. & Nixon, R. A. (1997). Increased neuronal endocytosis and protease delivery to early endosomes in sporadic Alzheimer's disease: neuropathologic evidence for a mechanism of increased beta-amyloidogenesis. *J Neurosci,* 17(16)**,** 6142-51.

Chaput, D., Kirouac, L. H., Bell-Temin, H., Stevens, S. M., Jr. & Padmanabhan, J. (2012). SILAC-based proteomic analysis to investigate the impact of amyloid precursor protein expression in neuronal-like B103 cells. *ELECTROPHORESIS,* 33(24)**,** 3728-37.

Chasseigneaux, S. & Allinquant, B. (2012). Functions of Abeta, sAPPalpha and sAPPbeta : similarities and differences. *J Neurochem,* 120 Suppl 1**,** 99-108.

Chavez-Gutierrez, L., Tolia, A., Maes, E., Li, T., Wong, P. C. & de Strooper, B. (2008). Glu(332) in the Nicastrin ectodomain is essential for gamma-secretase complex maturation but not for its activity. *J Biol Chem,* 283(29)**,** 20096-105.

Chen, F., Yang, D. S., Petanceska, S., Yang, A., Tandon, A., Yu, G., Rozmahel, R., Ghiso, J., Nishimura, M., Zhang, D. M., Kawarai, T., Levesque, G., Mills, J., Levesque, L., Song, Y. Q., Rogaeva, E., Westaway, D., Mount, H., Gandy, S., St George-Hyslop, P. & Fraser, P. E. (2000). Carboxyl-terminal fragments of Alzheimer beta-amyloid precursor protein accumulate in restricted and unpredicted intracellular compartments in presenilin 1-deficient cells. *J Biol Chem,* 275(47)**,** 36794-802.

Chen, T. Y., Liu, P. H., Ruan, C. T., Chiu, L. & Kung, F. L. (2006). The intracellular domain of amyloid precursor protein interacts with flotillin-1, a lipid raft protein. *Biochem Biophys Res Commun,* 342(1)**,** 266-72.

Chen, W. T., Hong, C. J., Lin, Y. T., Chang, W. H., Huang, H. T., Liao, J. Y., Chang, Y. J., Hsieh, Y. F., Cheng, C. Y., Liu, H. C., Chen, Y. R. & Cheng, I. H. (2012). Amyloid-beta (Abeta) D7H mutation increases oligomeric Abeta42 and alters properties of Abeta-zinc/copper assemblies. *PLoS ONE,* 7(4)**,** e35807.

Cheng, H., Vetrivel, K. S., Drisdel, R. C., Meckler, X., Gong, P., Leem, J. Y., Li, T., Carter, M., Chen, Y., Nguyen, P., Iwatsubo, T., Tomita, T., Wong, P. C., Green, W. N., Kounnas, M. Z. & Thinakaran, G. (2009). S-palmitoylation of gamma-secretase subunits nicastrin and APH-1. *J Biol Chem,* 284(3)**,** 1373-84.

Chin, J., Palop, J. J., Puolivali, J., Massaro, C., Bien-Ly, N., Gerstein, H., Scearce-Levie, K., Masliah, E. & Mucke, L. (2005). Fyn kinase induces synaptic and cognitive impairments in a transgenic mouse model of Alzheimer's disease. *J Neurosci,* 25(42)**,** 9694-703.

Choi, S. H., Kim, Y. H., Hebisch, M., Sliwinski, C., Lee, S., D'Avanzo, C., Chen, H., Hooli, B., Asselin, C., Muffat, J., Klee, J. B., Zhang, C., Wainger, B. J., Peitz, M., Kovacs, D. M., Woolf, C. J., Wagner, S. L., Tanzi, R. E. & Kim, D. Y. (2014). A three-dimensional human neural cell culture model of Alzheimer's disease. *Nature,* 515(7526)**,** 274-8.

Choy, R. W., Cheng, Z. & Schekman, R. (2012). Amyloid precursor protein (APP) traffics from the cell surface via endosomes for amyloid beta (Abeta) production in the trans-Golgi network. *Proc Natl Acad Sci U S A,* 109(30)**,** E2077-82.

Chua, L. M., Lim, M. L. & Wong, B. S. (2013). The Kunitz-protease inhibitor domain in amyloid precursor protein reduces cellular mitochondrial enzymes expression and function. *Biochem Biophys Res Commun,* 437(4)**,** 642-7.

Chun, Y. S., Park, Y., Oh, H. G., Kim, T. W., Yang, H. O., Park, M. K. & Chung, S. (2015). O-GlcNAcylation promotes non-amyloidogenic processing of amyloid-beta protein precursor via inhibition of endocytosis from the plasma membrane. *J Alzheimers Dis,* 44(1)**,** 261-75.

Cirrito, J. R., Deane, R., Fagan, A. M., Spinner, M. L., Parsadanian, M., Finn, M. B., Jiang, H., Prior, J. L., Sagare, A., Bales, K. R., Paul, S. M., Zlokovic, B. V., Piwnica-Worms, D. & Holtzman, D. M. (2005). P-glycoprotein deficiency at the blood-brain barrier increases amyloid-beta deposition in an Alzheimer disease mouse model. *J Clin Invest,* 115(11)**,** 3285-90.

Cirrito, J. R., Kang, J. E., Lee, J., Stewart, F. R., Verges, D. K., Silverio, L. M., Bu, G., Mennerick, S. & Holtzman, D. M. (2008). Endocytosis is required for synaptic activity-dependent release of amyloid-beta in vivo. *Neuron,* 58(1)**,** 42-51.

Citron, M., Oltersdorf, T., Haass, C., McConlogue, L., Hung, A. Y., Seubert, P., Vigo-Pelfrey, C., Lieberburg, I. & Selkoe, D. J. (1992). Mutation of the beta-amyloid precursor protein in familial Alzheimer's disease increases beta-protein production. *Nature,* 360(6405)**,** 672-4.

Cleary, J. P., Walsh, D. M., Hofmeister, J. J., Shankar, G. M., Kuskowski, M. A., Selkoe, D. J. & Ashe, K. H. (2005). Natural oligomers of the amyloid-beta protein specifically disrupt cognitive function. *Nat Neurosci,* 8(1)**,** 79-84.

Cole, S. L. & Vassar, R. (2007). The Basic Biology of BACE1: A Key Therapeutic Target for Alzheimer's Disease. *Curr Genomics,* 8(8)**,** 509-30.

Colombo, A., Wang, H., Kuhn, P. H., Page, R., Kremmer, E., Dempsey, P. J., Crawford, H. C. & Lichtenthaler, S. F. (2013). Constitutive alpha- and beta-secretase cleavages of the amyloid precursor protein are partially coupled in neurons, but not in frequently used cell lines. *Neurobiol Dis,* 49**,** 137-47.

Copanaki, E., Chang, S., Vlachos, A., Tschape, J. A., Muller, U. C., Kogel, D. & Deller, T. (2010). sAPPalpha antagonizes dendritic degeneration and neuron death triggered by proteasomal stress. *Mol Cell Neurosci,* 44(4)**,** 386-93.

Cordy, J. M., Hussain, I., Dingwall, C., Hooper, N. M. & Turner, A. J. (2003). Exclusively targeting beta-secretase to lipid rafts by GPI-anchor addition up-regulates beta-site processing of the amyloid precursor protein. *Proc Natl Acad Sci U S A,* 100(20)**,** 11735-40.

Corrigan, F., Vink, R., Blumbergs, P. C., Masters, C. L., Cappai, R. & van den Heuvel, C. (2012a). Evaluation of the effects of treatment with sAPPalpha on functional and histological outcome following controlled cortical impact injury in mice. *Neurosci Lett,* 515(1)**,** 50-4.

Corrigan, F., Vink, R., Blumbergs, P. C., Masters, C. L., Cappai, R. & van den Heuvel, C. (2012b). sAPPalpha rescues deficits in amyloid precursor protein knockout mice following focal traumatic brain injury. *J Neurochem,* 122(1)**,** 208-20.

Cossec, J. C., Simon, A., Marquer, C., Moldrich, R. X., Leterrier, C., Rossier, J., Duyckaerts, C., Lenkei, Z. & Potier, M. C. (2010). Clathrin-dependent APP endocytosis and Abeta secretion are highly sensitive to the level of plasma membrane cholesterol. *Biochim Biophys Acta,* 1801(8)**,** 846-52.

Cottrell, B. A., Galvan, V., Banwait, S., Gorostiza, O., Lombardo, C. R., Williams, T., Schilling, B., Peel, A., Gibson, B., Koo, E. H., Link, C. D. & Bredesen, D. E. (2005). A pilot proteomic study of amyloid precursor interactors in Alzheimer's disease. *Ann Neurol,* 58(2)**,** 277-89.

Cousins, S. L., Hoey, S. E., Anne Stephenson, F. & Perkinton, M. S. (2009). Amyloid precursor protein 695 associates with assembled NR2A- and NR2B-containing NMDA receptors to result in the enhancement of their cell surface delivery. *J Neurochem,* 111(6)**,** 1501-13.

Cramer, P. E., Cirrito, J. R., Wesson, D. W., Lee, C. Y., Karlo, J. C., Zinn, A. E., Casali, B. T., Restivo, J. L., Goebel, W. D., James, M. J., Brunden, K. R., Wilson, D. A. & Landreth, G. E. (2012). ApoE-directed therapeutics rapidly clear beta-amyloid and reverse deficits in AD mouse models. *Science,* 335(6075)**,** 1503-6.

Creemers, J. W., Ines Dominguez, D., Plets, E., Serneels, L., Taylor, N. A., Multhaup, G., Craessaerts, K., Annaert, W. & De Strooper, B. (2001). Processing of beta-secretase by furin and other members of the proprotein convertase family. *J Biol Chem,* 276(6)**,** 4211-7.

Crump, C. J., Johnson, D. S. & Li, Y. M. (2013). Development and mechanism of gamma-secretase modulators for Alzheimer's disease. *Biochemistry,* 52(19)**,** 3197-216.

Das, U., Scott, D. A., Ganguly, A., Koo, E. H., Tang, Y. & Roy, S. (2013). Activity-induced convergence of APP and BACE-1 in acidic microdomains via an endocytosis-dependent pathway. *Neuron,* 79(3)**,** 447-60.

Dawkins, E., Gasperini, R., Hu, Y., Cui, H., Vincent, A. J., Bolos, M., Young, K. M., Foa, L. & Small, D. H. (2014). The N-terminal fragment of the beta-amyloid precursor protein of Alzheimer's disease (N-APP) binds to phosphoinositide-rich domains on the surface of hippocampal neurons. *J Neurosci Res,* 92(11)**,** 1478-89.

Dawson, G. R., Seabrook, G. R., Zheng, H., Smith, D. W., Graham, S., O'Dowd, G., Bowery, B. J., Boyce, S., Trumbauer, M. E., Chen, H. Y., Van der Ploeg, L. H. & Sirinathsinghji, D. J. (1999). Age-related cognitive deficits, impaired long-term potentiation and reduction in synaptic marker density in mice lacking the beta-amyloid precursor protein. *Neuroscience,* 90(1)**,** 1-13.

De Strooper, B. (2014). Lessons from a failed gamma-secretase Alzheimer trial. *Cell,* 159(4)**,** 721-6.

De Strooper, B., Annaert, W., Cupers, P., Saftig, P., Craessaerts, K., Mumm, J. S., Schroeter, E. H., Schrijvers, V., Wolfe, M. S., Ray, W. J., Goate, A. & Kopan, R. (1999). A presenilin-1-dependent gamma-secretase-like protease mediates release of Notch intracellular domain. *Nature,* 398(6727)**,** 518-22.

De Strooper, B., Iwatsubo, T. & Wolfe, M. S. (2012). Presenilins and gamma-secretase: structure, function, and role in Alzheimer Disease. *Cold Spring Harb Perspect Med,* 2(1)**,** a006304.

De Strooper, B., Vassar, R. & Golde, T. (2010). The secretases: enzymes with therapeutic potential in Alzheimer disease. *Nat Rev Neurol,* 6(2)**,** 99-107.

DeBoer, S. R., Dolios, G., Wang, R. & Sisodia, S. S. (2014). Differential release of beta-amyloid from dendrite- versus axon-targeted APP. *J Neurosci,* 34(37)**,** 12313-27.

Deng, Y., Wang, Z., Wang, R., Zhang, X., Zhang, S., Wu, Y., Staufenbiel, M., Cai, F. & Song, W. (2013). Amyloid-beta protein (Abeta) Glu11 is the major beta-secretase site of beta-site amyloid-beta precursor protein-cleaving enzyme 1(BACE1), and shifting the cleavage site to Abeta Asp1 contributes to Alzheimer pathogenesis. *Eur J Neurosci,* 37(12)**,** 1962-9.

Deshpande, A., Mina, E., Glabe, C. & Busciglio, J. (2006). Different conformations of amyloid beta induce neurotoxicity by distinct mechanisms in human cortical neurons. *J Neurosci,* 26(22)**,** 6011-8.

Devi, L., Prabhu, B. M., Galati, D. F., Avadhani, N. G. & Anandatheerthavarada, H. K. (2006). Accumulation of amyloid precursor protein in the mitochondrial import channels of

human Alzheimer's disease brain is associated with mitochondrial dysfunction. *J Neurosci,* 26(35)**,** 9057-68.

Di Fede, G., Catania, M., Morbin, M., Rossi, G., Suardi, S., Mazzoleni, G., Merlin, M., Giovagnoli, A. R., Prioni, S., Erbetta, A., Falcone, C., Gobbi, M., Colombo, L., Bastone, A., Beeg, M., Manzoni, C., Francescucci, B., Spagnoli, A., Cantu, L., Del Favero, E., Levy, E., Salmona, M. & Tagliavini, F. (2009). A recessive mutation in the APP gene with dominant-negative effect on amyloidogenesis. *Science,* 323(5920)**,** 1473-7.

Dislich, B., Wohlrab, F., Bachhuber, T., Mueller, S., Kuhn, P. H., Hogl, S., Meyer-Luehmann, M. & Lichtenthaler, S. F. (2015). Label-free quantitative proteomics of mouse cerebrospinal fluid detects BACE1 protease substrates in vivo. *Mol Cell Proteomics*.

Doig, A. J. & Derreumaux, P. (2015). Inhibition of protein aggregation and amyloid formation by small molecules. *Curr Opin Struct Biol,* 30**,** 50-6.

Domert, J., Rao, S. B., Agholme, L., Brorsson, A. C., Marcusson, J., Hallbeck, M. & Nath, S. (2014). Spreading of amyloid-beta peptides via neuritic cell-to-cell transfer is dependent on insufficient cellular clearance. *Neurobiol Dis,* 65(0)**,** 82-92.

Dominguez, D., Tournoy, J., Hartmann, D., Huth, T., Cryns, K., Deforce, S., Serneels, L., Camacho, I. E., Marjaux, E., Craessaerts, K., Roebroek, A. J., Schwake, M., D'Hooge, R., Bach, P., Kalinke, U., Moechars, D., Alzheimer, C., Reiss, K., Saftig, P. & De Strooper, B. (2005). Phenotypic and biochemical analyses of BACE1- and BACE2-deficient mice. *J Biol Chem,* 280(35)**,** 30797-806.

Doody, R. S., Raman, R., Farlow, M., Iwatsubo, T., Vellas, B., Joffe, S., Kieburtz, K., He, F., Sun, X., Thomas, R. G., Aisen, P. S., Alzheimer's Disease Cooperative Study Steering, C., Siemers, E., Sethuraman, G., Mohs, R. & Semagacestat Study, G. (2013). A phase 3 trial of semagacestat for treatment of Alzheimer's disease. *N Engl J Med,* 369(4)**,** 341-50.

Doody, R. S., Thomas, R. G., Farlow, M., Iwatsubo, T., Vellas, B., Joffe, S., Kieburtz, K., Raman, R., Sun, X., Aisen, P. S., Siemers, E., Liu-Seifert, H., Mohs, R., Alzheimer's Disease Cooperative Study Steering, C. & Solanezumab Study, G. (2014). Phase 3 trials of solanezumab for mild-to-moderate Alzheimer's disease. *N Engl J Med,* 370(4)**,** 311-21.

Duce, J. A., Tsatsanis, A., Cater, M. A., James, S. A., Robb, E., Wikhe, K., Leong, S. L., Perez, K., Johanssen, T., Greenough, M. A., Cho, H. H., Galatis, D., Moir, R. D., Masters, C. L., McLean, C., Tanzi, R. E., Cappai, R., Barnham, K. J., Ciccotosto, G. D., Rogers, J. T. & Bush, A. I. (2010). Iron-export ferroxidase activity of beta-amyloid precursor protein is inhibited by zinc in Alzheimer's disease. *Cell,* 142(6)**,** 857-67.

Dulin, F., Leveille, F., Ortega, J. B., Mornon, J. P., Buisson, A., Callebaut, I. & Colloc'h, N. (2008). P3 peptide, a truncated form of A beta devoid of synaptotoxic effect, does not assemble into soluble oligomers. *FEBS Lett,* 582(13)**,** 1865-70.

Edbauer, D., Willem, M., Lammich, S., Steiner, H. & Haass, C. (2002). Insulin-degrading enzyme rapidly removes the beta-amyloid precursor protein intracellular domain (AICD). *J Biol Chem,* 277(16)**,** 13389-93.

Ehehalt, R., Keller, P., Haass, C., Thiele, C. & Simons, K. (2003). Amyloidogenic processing of the Alzheimer beta-amyloid precursor protein depends on lipid rafts. *J Cell Biol,* 160(1)**,** 113-23.

Eisele, Y. S., Monteiro, C., Fearns, C., Encalada, S. E., Wiseman, R. L., Powers, E. T. & Kelly, J. W. (2015). Targeting protein aggregation for the treatment of degenerative diseases. *Nat Rev Drug Discov,* advance online publication.

Emmott, E., Munday, D., Bickerton, E., Britton, P., Rodgers, M. A., Whitehouse, A., Zhou, E. M. & Hiscox, J. A. (2013). The cellular interactome of the coronavirus infectious bronchitis virus nucleocapsid protein and functional implications for virus biology. *J Virol,* 87(17)**,** 9486-500.

Endres, K. & Fahrenholz, F. (2010). Upregulation of the alpha-secretase ADAM10--risk or reason for hope? *FEBS J,* 277(7)**,** 1585-96.

Endres, K., Fahrenholz, F., Lotz, J., Hiemke, C., Teipel, S., Lieb, K., Tuscher, O. & Fellgiebel, A. (2014). Increased CSF APPs-alpha levels in patients with Alzheimer disease treated with acitretin. *Neurology,* 83(21)**,** 1930-5.

Feher, A., Juhasz, A., Pakaski, M., Kalman, J. & Janka, Z. (2014). ABCB1 C3435T polymorphism influences the risk for Alzheimer's disease. *J Mol Neurosci,* 54(4)**,** 826-9.

Fernandez-Echevarria, C., Diaz, M., Ferrer, I., Canerina-Amaro, A. & Marin, R. (2014). Abeta promotes VDAC1 channel dephosphorylation in neuronal lipid rafts. Relevance to the mechanisms of neurotoxicity in Alzheimer's disease. *Neuroscience,* 278(0)**,** 354-66.

Frandemiche, M. L., De Seranno, S., Rush, T., Borel, E., Elie, A., Arnal, I., Lante, F. & Buisson, A. (2014). Activity-dependent tau protein translocation to excitatory synapse is disrupted by exposure to amyloid-beta oligomers. *J Neurosci,* 34(17)**,** 6084-97.

Freude, K. K., Penjwini, M., Davis, J. L., LaFerla, F. M. & Blurton-Jones, M. (2011). Soluble amyloid precursor protein induces rapid neural differentiation of human embryonic stem cells. *J Biol Chem,* 286(27)**,** 24264-74.

Frick, M., Bright, N. A., Riento, K., Bray, A., Merrified, C. & Nichols, B. J. (2007). Coassembly of flotillins induces formation of membrane microdomains, membrane curvature, and vesicle budding. *Curr Biol,* 17(13)**,** 1151-6.

Frost, B., Gotz, J. & Feany, M. B. (2015). Connecting the dots between tau dysfunction and neurodegeneration. *Trends Cell Biol,* 25(1)**,** 46-53.

Frost, J. L., Liu, B., Kleinschmidt, M., Schilling, S., Demuth, H. U. & Lemere, C. A. (2012). Passive immunization against pyroglutamate-3 amyloid-beta reduces plaque burden in Alzheimer-like transgenic mice: a pilot study. *Neurodegener Dis,* 10(1-4)**,** 265-70.

Fu, M. M. & Holzbaur, E. L. (2013). JIP1 regulates the directionality of APP axonal transport by coordinating kinesin and dynein motors. *J Cell Biol,* 202(3)**,** 495-508.

Fukumori, A., Fluhrer, R., Steiner, H. & Haass, C. (2010). Three-amino acid spacing of presenilin endoproteolysis suggests a general stepwise cleavage of gamma-secretase-mediated intramembrane proteolysis. *J Neurosci,* 30(23)**,** 7853-62.

Fukumori, A., Okochi, M., Tagami, S., Jiang, J., Itoh, N., Nakayama, T., Yanagida, K., Ishizuka-Katsura, Y., Morihara, T., Kamino, K., Tanaka, T., Kudo, T., Tanii, H., Ikuta, A., Haass, C. & Takeda, M. (2006). Presenilin-dependent gamma-secretase on plasma membrane and endosomes is functionally distinct. *Biochemistry,* 45(15)**,** 4907-14.

Furukawa, K., Sopher, B. L., Rydel, R. E., Begley, J. G., Pham, D. G., Martin, G. M., Fox, M. & Mattson, M. P. (1996). Increased activity-regulating and neuroprotective efficacy of alpha-secretase-derived secreted amyloid precursor protein conferred by a C-terminal heparin-binding domain. *J Neurochem,* 67(5)**,** 1882-96.

Galvan, V., Gorostiza, O. F., Banwait, S., Ataie, M., Logvinova, A. V., Sitaraman, S., Carlson, E., Sagi, S. A., Chevallier, N., Jin, K., Greenberg, D. A. & Bredesen, D. E. (2006). Reversal of Alzheimer's-like pathology and behavior in human APP transgenic mice by mutation of Asp664. *Proc Natl Acad Sci U S A,* 103(18)**,** 7130-5.

Gautam, V., D'Avanzo, C., Berezovska, O., Tanzi, R. E. & Kovacs, D. M. (2015). Synaptotagmins interact with APP and promote Abeta generation. *Mol Neurodegener,* 10(1)**,** 31.

Gauthier-Kemper, A., Igaev, M., Sundermann, F., Janning, D., Bruhmann, J., Moschner, K., Reyher, H. J., Junge, W., Glebov, K., Walter, J., Bakota, L. & Brandt, R. (2014). Interplay between phosphorylation and palmitoylation mediates plasma membrane targeting and sorting of GAP43. *Mol Biol Cell,* 25(21)**,** 3284-99.

Gersbacher, M., Goodger, Z., Trutzel, A., Bundschuh, D., Nitsch, R. & Konietzko, U. (2013). Turnover of amyloid precursor preotein family members determines their nuclear signaling capacity. *PLoS ONE,* 8(7).

Ghosal, K., Vogt, D. L., Liang, M., Shen, Y., Lamb, B. T. & Pimplikar, S. W. (2009). Alzheimer's disease-like pathological features in transgenic mice expressing the APP intracellular domain. *Proc Natl Acad Sci U S A,* 106(43)**,** 18367-72.

Giliberto, L., d'Abramo, C., Acker, C. M., Davies, P. & D'Adamio, L. (2010). Transgenic expression of the amyloid-beta precursor protein-intracellular domain does not induce Alzheimer's Disease-like traits in vivo. *PLoS ONE,* 5(7)**,** e11609.

Giuffrida, M. L., Caraci, F., Pignataro, B., Cataldo, S., De Bona, P., Bruno, V., Molinaro, G., Pappalardo, G., Messina, A., Palmigiano, A., Garozzo, D., Nicoletti, F., Rizzarelli, E. & Copani, A. (2009). Beta-amyloid monomers are neuroprotective. *J Neurosci,* 29(34)**,** 10582-7.

Glenner, G. G. & Wong, C. W. (1984). Alzheimer's disease: initial report of the purification and characterization of a novel cerebrovascular amyloid protein. *Biochem Biophys Res Commun,* 120(3)**,** 885-90.

Goedert, M. & Spillantini, M. G. (2006). A century of Alzheimer's disease. *Science,* 314(5800)**,** 777-81.

Golde, T. E., Estus, S., Usiak, M., Younkin, L. H. & Younkin, S. G. (1990). Expression of β amyloid protein precursor mRNAs: Recognition of a novel alternatively spliced form and quantitation in alzheimer's disease using PCR. *Neuron,* 4(2)**,** 253-267.

Golde, T. E., Koo, E. H., Felsenstein, K. M., Osborne, B. A. & Miele, L. (2013). gamma-Secretase inhibitors and modulators. *Biochim Biophys Acta,* 1828(12)**,** 2898-907.

Goodger, Z. V., Rajendran, L., Trutzel, A., Kohli, B. M., Nitsch, R. M. & Konietzko, U. (2009). Nuclear signaling by the APP intracellular domain occurs predominantly through the amyloidogenic processing pathway. *J Cell Sci,* 122(Pt 20)**,** 3703-14.

Gotz, J., Chen, F., van Dorpe, J. & Nitsch, R. M. (2001). Formation of neurofibrillary tangles in P301l tau transgenic mice induced by Abeta 42 fibrils. *Science,* 293(5534)**,** 1491-5.

Gowing, E., Roher, A. E., Woods, A. S., Cotter, R. J., Chaney, M., Little, S. P. & Ball, M. J. (1994). Chemical characterization of A beta 17-42 peptide, a component of diffuse amyloid deposits of Alzheimer disease. *J Biol Chem,* 269(15)**,** 10987-90.

Green, R. C., Schneider, L. S., Amato, D. A., Beelen, A. P., Wilcock, G., Swabb, E. A., Zavitz, K. H. & Tarenflurbil Phase 3 Study, G. (2009). Effect of tarenflurbil on cognitive decline and activities of daily living in patients with mild Alzheimer disease: a randomized controlled trial. *JAMA,* 302(23)**,** 2557-64.

Grimm, M. O., Mett, J., Stahlmann, C. P., Grosgen, S., Haupenthal, V. J., Blumel, T., Hundsdorfer, B., Zimmer, V. C., Mylonas, N. T., Tanila, H., Muller, U., Grimm, H. S. & Hartmann, T. (2015). APP intracellular domain derived from amyloidogenic beta- and gamma-secretase cleavage regulates neprilysin expression. *Front Aging Neurosci,* 7**,** 77.

Guerreiro, R., Bras, J. & Hardy, J. (2013). SnapShot: genetics of Alzheimer's disease. *Cell,* 155(4)**,** 968-968 e1.

Gustafsen, C., Glerup, S., Pallesen, L. T., Olsen, D., Andersen, O. M., Nykjaer, A., Madsen, P. & Petersen, C. M. (2013). Sortilin and SorLA display distinct roles in processing and trafficking of amyloid precursor protein. *J Neurosci,* 33(1)**,** 64-71.

Haapasalo, A. & Kovacs, D. M. (2011). The many substrates of presenilin/gamma-secretase. *J Alzheimers Dis,* 25(1)**,** 3-28.

Haass, C., Kaether, C., Thinakaran, G. & Sisodia, S. (2012). Trafficking and proteolytic processing of APP. *Cold Spring Harb Perspect Med,* 2(5)**,** a006270.

Haass, C., Lemere, C. A., Capell, A., Citron, M., Seubert, P., Schenk, D., Lannfelt, L. & Selkoe, D. J. (1995). The Swedish mutation causes early-onset Alzheimer's disease by β-secretase cleavage within the secretory pathway. *Nat Med,* 1(12)**,** 1291-1296.

Haass, C. & Mandelkow, E. (2010). Fyn-tau-amyloid: a toxic triad. *Cell,* 142(3)**,** 356-8.

Haass, C. & Selkoe, D. J. (2007). Soluble protein oligomers in neurodegeneration: lessons from the Alzheimer's amyloid beta-peptide. *Nat Rev Mol Cell Biol,* 8(2)**,** 101-12.

Hardy, J. (2006). Has The Amyloid Cascade Hypothesis for Alzheimer's Disease Been Prooved? *Current Alzheimer Research,* 3**,** 71-73.

Hardy, J. (2009). The amyloid hypothesis for Alzheimer's disease: a critical reappraisal. *J Neurochem,* 110(4)**,** 1129-34.

Hardy, J. (2012). CSF biomarking for diagnosis and treatment assessment in neurodegeneration. *J Neurochem,* 123(3)**,** 339-41.

Hardy, J. & Allsop, D. (1991). Amyloid deposition as the central event in the aetiology of Alzheimer's disease. *Trends in pharmacological sciences,* 12**,** 383-388.

Hardy, J. & Selkoe, D. J. (2002). The amyloid hypothesis of Alzheimer's disease: progress and problems on the road to therapeutics. *Science,* 297(5580)**,** 353-6.

Hartl, D., Klatt, S., Roch, M., Konthur, Z., Klose, J., Willnow, T. E. & Rohe, M. (2013). Soluble Alpha-APP (sAPPalpha) Regulates CDK5 Expression and Activity in Neurons. *PLoS ONE,* 8(6)**,** e65920.

Hartmann, T., Bergsdorf, C., Sandbrink, R., Tienari, P. J., Multhaup, G., Ida, N., Bieger, S., Dyrks, T., Weidemann, A., Masters, C. L. & Beyreuther, K. (1996). Alzheimer's disease betaA4 protein release and amyloid precursor protein sorting are regulated by alternative splicing. *J Biol Chem,* 271(22)**,** 13208-14.

Hattori, C., Asai, M., Onishi, H., Sasagawa, N., Hashimoto, Y., Saido, T. C., Maruyama, K., Mizutani, S. & Ishiura, S. (2006). BACE1 interacts with lipid raft proteins. *J Neurosci Res,* 84(4)**,** 912-7.

Hauptmann, S., Scherping, I., Drose, S., Brandt, U., Schulz, K. L., Jendrach, M., Leuner, K., Eckert, A. & Muller, W. E. (2009). Mitochondrial dysfunction: an early event in Alzheimer pathology accumulates with age in AD transgenic mice. *Neurobiol Aging,* 30(10)**,** 1574-86.

He, W., Lu, Y., Qahwash, I., Hu, X. Y., Chang, A. & Yan, R. (2004). Reticulon family members modulate BACE1 activity and amyloid-beta peptide generation. *Nat Med,* 10(9)**,** 959-65.

Heber, S., Herms, J., Gajic, V., Hainfellner, J., Aguzzi, A., Rulicke, T., von Kretzschmar, H., von Koch, C., Sisodia, S., Tremml, P., Lipp, H. P., Wolfer, D. P. & Muller, U. (2000). Mice with combined gene knock-outs reveal essential and partially redundant functions of amyloid precursor protein family members. *J Neurosci,* 20(21)**,** 7951-63.

Hedskog, L., Pinho, C. M., Filadi, R., Ronnback, A., Hertwig, L., Wiehager, B., Larssen, P., Gellhaar, S., Sandebring, A., Westerlund, M., Graff, C., Winblad, B., Galter, D., Behbahani, H., Pizzo, P., Glaser, E. & Ankarcrona, M. (2013). Modulation of the endoplasmic reticulum-mitochondria interface in Alzheimer's disease and related models. *Proc Natl Acad Sci U S A,* 110(19)**,** 7916-21.

Henriksen, K., O'Bryant, S. E., Hampel, H., Trojanowski, J. Q., Montine, T. J., Jeromin, A., Blennow, K., Lonneborg, A., Wyss-Coray, T., Soares, H., Bazenet, C., Sjogren, M., Hu, W., Lovestone, S., Karsdal, M. A., Weiner, M. W. & Blood-Based Biomarker Interest, G. (2014). The future of blood-based biomarkers for Alzheimer's disease. *Alzheimers Dement,* 10(1)**,** 115-31.

Herrup, K. (2015). The case for rejecting the amyloid cascade hypothesis. *Nat Neurosci,* 18(6)**,** 794-9.

Ho, A., Liu, X. & Sudhof, T. C. (2008). Deletion of Mint proteins decreases amyloid production in transgenic mouse models of Alzheimer's disease. *J Neurosci,* 28(53)**,** 14392-400.

Ho, A. & Sudhof, T. C. (2004). Binding of F-spondin to amyloid- precursor protein: A candidate amyloid- precursor protein ligand that modulates amyloid- precursor protein cleavage. *Proc Natl Acad Sci U S A,* 101(8)**,** 2548-2553.

Ho, L., Fukuchi, K. & Younkin, S. G. (1996). The alternatively spliced Kunitz protease inhibitor domain alters amyloid beta protein precursor processing and amyloid beta protein production in cultured cells. *J Biol Chem,* 271(48)**,** 30929-34.

Hoe, H. S., Lee, K. J., Carney, R. S., Lee, J., Markova, A., Lee, J. Y., Howell, B. W., Hyman, B. T., Pak, D. T., Bu, G. & Rebeck, G. W. (2009). Interaction of reelin with amyloid precursor protein promotes neurite outgrowth. *J Neurosci,* 29(23)**,** 7459-73.

Holmes, C., Boche, D., Wilkinson, D., Yadegarfar, G., Hopkins, V., Bayer, A., Jones, R. W., Bullock, R., Love, S., Neal, J. W., Zotova, E. & Nicoll, J. A. (2008). Long-term effects of Abeta42 immunisation in Alzheimer's disease: follow-up of a randomised, placebo-controlled phase I trial. *Lancet,* 372(9634)**,** 216-23.

Hook, G., Yu, J., Toneff, T., Kindy, M. & Hook, V. (2014). Brain pyroglutamate amyloid-beta is produced by cathepsin B and is reduced by the cysteine protease inhibitor E64d, representing a potential Alzheimer's disease therapeutic. *J Alzheimers Dis,* 41(1)**,** 129-49.

Hook, V., Schechter, I., Demuth, H. U. & Hook, G. (2008). Alternative pathways for production of beta-amyloid peptides of Alzheimer's disease. *Biol Chem,* 389(8)**,** 993-1006.

Hosp, F., Vossfeldt, H., Heinig, M., Vasiljevic, D., Arumughan, A., Wyler, E., Genetic, Environmental Risk for Alzheimer's Disease, G. C., Landthaler, M., Hubner, N., Wanker, E. E., Lannfelt, L., Ingelsson, M., Lalowski, M., Voigt, A. & Selbach, M. (2015). Quantitative interaction proteomics of neurodegenerative disease proteins. *Cell Rep,* 11(7)**,** 1134-46.

Hu, X., Hicks, C. W., He, W., Wong, P., Macklin, W. B., Trapp, B. D. & Yan, R. (2006). BACE1 modulates myelination in the central and peripheral nervous system. *Nat Neurosci,* 9(12)**,** 1520-5.

Huang, D. W., Sherman, B. T. & Lempicki, R. A. (2008). Systematic and integrative analysis of large gene lists using DAVID bioinformatics resources. *Nat. Protocols,* 4(1)**,** 44-57.

Huang, W. D., Sherman, B. T. & Lempicki, R. A. (2009). Bioinformatics enrichment tools: paths toward the comprehensive functional analysis of large gene lists. *Nucleic Acids Res,* 37(1)**,** 1-13.

Hur, J. Y., Teranishi, Y., Kihara, T., Yamamoto, N. G., Inoue, M., Hosia, W., Hashimoto, M., Winblad, B., Frykman, S. & Tjernberg, L. O. (2012). Identification of novel gamma-secretase-associated proteins in detergent-resistant membranes from brain. *J Biol Chem,* 287(15)**,** 11991-2005.

Hussain, I., Powell, D., Howlett, D. R., Tew, D. G., Meek, T. D., Chapman, C., Gloger, I. S., Murphy, K. E., Southan, C. D., Ryan, D. M., Smith, T. S., Simmons, D. L., Walsh, F. S., Dingwall, C. & Christie, G. (1999). Identification of a novel aspartic protease (Asp 2) as beta-secretase. *Mol Cell Neurosci,* 14(6)**,** 419-27.

Hyman, B. T., Phelps, C. H., Beach, T. G., Bigio, E. H., Cairns, N. J., Carrillo, M. C., Dickson, D. W., Duyckaerts, C., Frosch, M. P., Masliah, E., Mirra, S. S., Nelson, P. T., Schneider, J. A., Thal, D. R., Thies, B., Trojanowski, J. Q., Vinters, H. V. & Montine, T. J. (2012). National Institute on Aging-Alzheimer's Association guidelines for the neuropathologic assessment of Alzheimer's disease. *Alzheimers Dement,* 8(1)**,** 1-13.

Ikeuchi, T. & Sisodia, S. S. (2003). The Notch ligands, Delta1 and Jagged2, are substrates for presenilin-dependent "gamma-secretase" cleavage. *J Biol Chem,* 278(10)**,** 7751-4.

Inoue, M., Hur, J. Y., Kihara, T., Teranishi, Y., Yamamoto, N. G., Ishikawa, T., Wiehager, B., Winblad, B., Tjernberg, L. O. & Schedin-Weiss, S. (2015). Human brain proteins showing neuron-specific interactions with gamma-secretase. *FEBS J,* 282(14)**,** 2587-99.

Irwin, D. J., Abrams, J. Y., Schonberger, L. B., Leschek, E. W., Mills, J. L., Lee, V. M. & Trojanowski, J. Q. (2013). Evaluation of potential infectivity of Alzheimer and Parkinson disease proteins in recipients of cadaver-derived human growth hormone. *JAMA Neurol,* 70(4)**,** 462-8.

Ittner, L. M., Ke, Y. D., Delerue, F., Bi, M., Gladbach, A., van Eersel, J., Wolfing, H., Chieng, B. C., Christie, M. J., Napier, I. A., Eckert, A., Staufenbiel, M., Hardeman, E. & Gotz, J. (2010). Dendritic function of tau mediates amyloid-beta toxicity in Alzheimer's disease mouse models. *Cell,* 142(3)**,** 387-97.

Jack, C. R., Jr. & Holtzman, D. M. (2013). Biomarker modeling of Alzheimer's disease. *Neuron,* 80(6)**,** 1347-58.

Jackle, F., Schmidt, F., Wichert, R., Arnold, P., Prox, J., Mangold, M., Ohler, A., Pietrzik, C. U., Koudelka, T., Tholey, A., Gutschow, M., Stirnberg, M. & Becker-Pauly, C. (2015). Metalloprotease meprin beta is activated by transmembrane serine protease matriptase-2 at the cell surface thereby enhancing APP shedding. *Biochem J,* 470(1)**,** 91-103.

Jacobsen, K. T. & Iverfeldt, K. (2011). O-GlcNAcylation increases non-amyloidogenic processing of the amyloid-beta precursor protein (APP). *Biochem Biophys Res Commun,* 404(3)**,** 882-6.

Jager, S., Leuchtenberger, S., Martin, A., Czirr, E., Wesselowski, J., Dieckmann, M., Waldron, E., Korth, C., Koo, E. H., Heneka, M., Weggen, S. & Pietrzik, C. U. (2009). alpha-secretase mediated conversion of the amyloid precursor protein derived membrane stub C99 to C83 limits Abeta generation. *J Neurochem,* 111(6)**,** 1369-82.

Jaunmuktane, Z., Mead, S., Ellis, M., Wadsworth, J. D. F., Nicoll, A. J., Kenny, J., Launchbury, F., Linehan, J., Richard-Loendt, A., Walker, A. S., Rudge, P., Collinge, J. & Brandner, S. (2015). Evidence for human transmission of amyloid-β pathology and cerebral amyloid angiopathy. *Nature,* 525(7568)**,** 247-250.

Jefferson, T., Causevic, M., auf dem Keller, U., Schilling, O., Isbert, S., Geyer, R., Maier, W., Tschickardt, S., Jumpertz, T., Weggen, S., Bond, J. S., Overall, C. M., Pietrzik, C. U. & Becker-Pauly, C. (2011). Metalloprotease meprin beta generates nontoxic N-terminal amyloid precursor protein fragments in vivo. *J Biol Chem,* 286(31)**,** 27741-50.

Jiang, S., Li, Y., Zhang, X., Bu, G., Xu, H. & Zhang, Y. W. (2014). Trafficking regulation of proteins in Alzheimer's disease. *Mol Neurodegener,* 9(1)**,** 6.

Jin, M., Shepardson, N., Yang, T., Chen, G., Walsh, D. & Selkoe, D. J. (2011). Soluble amyloid beta-protein dimers isolated from Alzheimer cortex directly induce Tau hyperphosphorylation and neuritic degeneration. *Proc Natl Acad Sci U S A,* 108(14)**,** 5819-24.

Johnson, K. A., Fox, N. C., Sperling, R. A. & Klunk, W. E. (2012). Brain imaging in Alzheimer disease. *Cold Spring Harb Perspect Med,* 2(4)**,** a006213.

Johnson, S. A., McNeill, T., Cordell, B. & Finch, C. E. (1990). Relation of neuronal APP-751/APP-695 mRNA ratio and neuritic plaque density in Alzheimer's disease. *Science,* 248(4957)**,** 854-7.

Johnston, J. A., Norgren, S., Ravid, R., Wasco, W., Winblad, B., Lannfelt, L. & Cowburn, R. F. (1996). Quantification of APP and APLP2 mRNA in APOE genotyped Alzheimer's disease brains. *Brain Res Mol Brain Res,* 43(1-2)**,** 85-95.

Jones, L., Holmans, P. A., Hamshere, M. L., Harold, D., Moskvina, V., Ivanov, D., Pocklington, A., Abraham, R., Hollingworth, P., Sims, R., Gerrish, A., Pahwa, J. S., Jones, N., Stretton, A., Morgan, A. R., Lovestone, S., Powell, J., Proitsi, P., Lupton, M. K., Brayne, C., Rubinsztein, D. C., Gill, M., Lawlor, B., Lynch, A., Morgan, K., Brown, K. S., Passmore, P. A., Craig, D., McGuinness, B., Todd, S., Holmes, C., Mann, D., Smith, A. D., Love, S., Kehoe, P. G., Mead, S., Fox, N., Rossor, M., Collinge, J., Maier, W., Jessen, F., Schurmann, B., Heun, R., Kolsch, H., van den Bussche, H., Heuser, I., Peters, O., Kornhuber, J., Wiltfang, J., Dichgans, M., Frolich, L., Hampel, H., Hull, M., Rujescu, D., Goate, A. M., Kauwe, J. S., Cruchaga, C., Nowotny, P., Morris, J. C., Mayo, K., Livingston, G., Bass, N. J., Gurling, H., McQuillin, A., Gwilliam, R., Deloukas, P., Al-Chalabi, A., Shaw, C. E., Singleton, A. B., Guerreiro, R., Muhleisen, T. W., Nothen, M. M., Moebus, S., Jockel, K. H., Klopp, N., Wichmann, H. E., Ruther, E., Carrasquillo, M. M., Pankratz, V. S., Younkin, S. G., Hardy, J., O'Donovan, M. C., Owen, M. J. & Williams, J. (2010). Genetic evidence implicates the immune system and cholesterol metabolism in the aetiology of Alzheimer's disease. *PLoS ONE,* 5(11)**,** e13950.

Jonsson, T., Atwal, J. K., Steinberg, S., Snaedal, J., Jonsson, P. V., Bjornsson, S., Stefansson, H., Sulem, P., Gudbjartsson, D., Maloney, J., Hoyte, K., Gustafson, A., Liu, Y., Lu, Y., Bhangale, T., Graham, R. R., Huttenlocher, J., Bjornsdottir, G., Andreassen, O. A., Jonsson, E. G., Palotie, A., Behrens, T. W., Magnusson, O. T., Kong, A., Thorsteinsdottir, U., Watts, R. J. & Stefansson, K. (2012). A mutation in APP protects against Alzheimer's disease and age-related cognitive decline. *Nature,* 488(7409)**,** 96-9.

Jorissen, E., Prox, J., Bernreuther, C., Weber, S., Schwanbeck, R., Serneels, L., Snellinx, A., Craessaerts, K., Thathiah, A., Tesseur, I., Bartsch, U., Weskamp, G., Blobel, C. P., Glatzel,

M., De Strooper, B. & Saftig, P. (2010). The disintegrin/metalloproteinase ADAM10 is essential for the establishment of the brain cortex. *J Neurosci,* 30(14)**,** 4833-44.

Jucker, M. & Walker, L. C. (2013). Self-propagation of pathogenic protein aggregates in neurodegenerative diseases. *Nature,* 501(7465)**,** 45-51.

Jucker, M. & Walker, L. C. (2015). Neurodegeneration: Amyloid-beta pathology induced in humans. *Nature,* 525(7568)**,** 193-4.

Jung, E. S., Hong, H., Kim, C. & Mook-Jung, I. (2015). Acute ER stress regulates amyloid precursor protein processing through ubiquitin-dependent degradation. *Scientific reports,* 5.

Kaden, D., Voigt, P., Munter, L. M., Bobowski, K. D., Schaefer, M. & Multhaup, G. (2009). Subcellular localization and dimerization of APLP1 are strikingly different from APP and APLP2. *J Cell Sci,* 122(Pt 3)**,** 368-77.

Kaether, C., Skehel, P. & Dotti, C. G. (2000). Axonal membrane proteins are transported in distinct carriers: a two-color video microscopy study in cultured hippocampal neurons. *Mol Biol Cell,* 11(4)**,** 1213-24.

Kamenetz, F., Tomita, T., Hsieh, H., Seabrook, G., Borchelt, D., Iwatsubo, T., Sisodia, S. & Malinow, R. (2003). APP processing and synaptic function. *Neuron,* 37(6)**,** 925-37.

Kanatsu, K., Morohashi, Y., Suzuki, M., Kuroda, H., Watanabe, T., Tomita, T. & Iwatsubo, T. (2014). Decreased CALM expression reduces Abeta42 to total Abeta ratio through clathrin-mediated endocytosis of gamma-secretase. *Nat Commun,* 5**,** 3386.

Kang, J., Lemaire, H. G., Unterbeck, A., Salbaum, J. M., Masters, C. L., Grzeschik, K. H., Multhaup, G., Beyreuther, K. & Muller-Hill, B. (1987). The precursor of Alzheimer's disease amyloid A4 protein resembles a cell-surface receptor. *Nature,* 325(6106)**,** 733-6.

Karran, E. & Hardy, J. (2014a). Antiamyloid therapy for Alzheimer's disease--are we on the right road? *N Engl J Med,* 370(4)**,** 377-8.

Karran, E. & Hardy, J. (2014b). A critique of the drug discovery and phase 3 clinical programs targeting the amyloid hypothesis for Alzheimer disease. *Ann Neurol,* 76(2)**,** 185-205.

Kerridge, C., Belyaev, N. D., Nalivaeva, N. N. & Turner, A. J. (2014). The Abeta-clearance protein transthyretin, like neprilysin, is epigenetically regulated by the amyloid precursor protein intracellular domain. *J Neurochem,* 130(3)**,** 419-31.

Kim, H. S., Kim, E. M., Lee, J. P., Park, C. H., Kim, S., Seo, J. H., Chang, K. A., Yu, E., Jeong, S. J., Chong, Y. H. & Suh, Y. H. (2003). C-terminal fragments of amyloid precursor protein exert neurotoxicity by inducing glycogen synthase kinase-3beta expression. *FASEB J,* 17(13)**,** 1951-3.

Kinoshita, A., Fukumoto, H., Shah, T., Whelan, C. M., Irizarry, M. C. & Hyman, B. T. (2003). Demonstration by FRET of BACE interaction with the amyloid precursor protein at the cell surface and in early endosomes. *J Cell Sci,* 116(Pt 16)**,** 3339-46.

Kitaguchi, N., Takahashi, Y., Tokushima, Y., Shiojiri, S. & Ito, H. (1988). Novel precursor of Alzheimer's disease amyloid protein shows protease inhibitory activity. *Nature,* 331(6156)**,** 530-532.

Kohli, B. M., Pflieger, D., Mueller, L. N., Carbonetti, G., Aebersold, R., Nitsch, R. M. & Konietzko, U. (2012). Interactome of the amyloid precursor protein APP in brain reveals a protein network involved in synaptic vesicle turnover and a close association with Synaptotagmin-1. *J Proteome Res,* 11(8)**,** 4075-90.

Koo, E. H., Sisodia, S. S., Cork, L. C., Unterbeck, A., Bayney, R. M. & Price, D. L. (1990). Differential expression of amyloid precursor protein mRNAs in cases of Alzheimer's disease and in aged nonhuman primates. *Neuron,* 4(1)**,** 97-104.

Koo, E. H. & Squazzo, S. L. (1994). Evidence That Production and Release of Amyloid Beta-Protein Involves the Endocytic Pathway. *J Biol Chem,* 269(26)**,** 17386-17389.

Kounnas, M. Z., Moir, R. D., Rebeck, G. W., Bush, A. I., Argraves, W. S., Tanzi, R. E., Hyman, B. T. & Strickland, D. K. (1995). LDL receptor-related protein, a multifunctional ApoE receptor, binds secreted beta-amyloid precursor protein and mediates its degradation. *Cell,* 82(2)**,** 331-40.

Kuhn, P. H., Koroniak, K., Hogl, S., Colombo, A., Zeitschel, U., Willem, M., Volbracht, C., Schepers, U., Imhof, A., Hoffmeister, A., Haass, C., Rossner, S., Brase, S. & Lichtenthaler, S. F. (2012). Secretome protein enrichment identifies physiological BACE1 protease substrates in neurons. *EMBO J,* 31(14)**,** 3157-68.

Kuhn, P. H., Wang, H., Dislich, B., Colombo, A., Zeitschel, U., Ellwart, J. W., Kremmer, E., Rossner, S. & Lichtenthaler, S. F. (2010). ADAM10 is the physiologically relevant, constitutive alpha-secretase of the amyloid precursor protein in primary neurons. *EMBO J,* 29(17)**,** 3020-32.

Kuhnke, D., Jedlitschky, G., Grube, M., Krohn, M., Jucker, M., Mosyagin, I., Cascorbi, I., Walker, L. C., Kroemer, H. K., Warzok, R. W. & Vogelgesang, S. (2007). MDR1-P-Glycoprotein (ABCB1) Mediates Transport of Alzheimer's amyloid-beta peptides--implications for the mechanisms of Abeta clearance at the blood-brain barrier. *Brain Pathol,* 17(4)**,** 347-53.

Kumar, S., Rezaei-Ghaleh, N., Terwel, D., Thal, D. R., Richard, M., Hoch, M., Mc Donald, J. M., Wullner, U., Glebov, K., Heneka, M. T., Walsh, D. M., Zweckstetter, M. & Walter, J. (2011). Extracellular phosphorylation of the amyloid beta-peptide promotes formation of toxic aggregates during the pathogenesis of Alzheimer's disease. *EMBO J,* 30(11)**,** 2255-65.

Lane, R. F., Steele, J. W., Cai, D., Ehrlich, M. E., Attie, A. D. & Gandy, S. (2013). Protein sorting motifs in the cytoplasmic tail of SorCS1 control generation of Alzheimer's amyloid-beta peptide. *J Neurosci,* 33(16)**,** 7099-107.

Larson, M. E. & Lesne, S. E. (2012). Soluble Abeta oligomer production and toxicity. *J Neurochem,* 120 Suppl 1**,** 125-39.

Lauren, J., Gimbel, D. A., Nygaard, H. B., Gilbert, J. W. & Strittmatter, S. M. (2009). Cellular prion protein mediates impairment of synaptic plasticity by amyloid-beta oligomers. *Nature,* 457(7233)**,** 1128-1132.

Laurent, S. A., Hoffmann, F. S., Kuhn, P. H., Cheng, Q., Chu, Y., Schmidt-Supprian, M., Hauck, S. M., Schuh, E., Krumbholz, M., Rubsamen, H., Wanngren, J., Khademi, M., Olsson, T., Alexander, T., Hiepe, F., Pfister, H. W., Weber, F., Jenne, D., Wekerle, H., Hohlfeld, R., Lichtenthaler, S. F. & Meinl, E. (2015). gamma-Secretase directly sheds the survival receptor BCMA from plasma cells. *Nat Commun,* 6**,** 7333.

Lauritzen, I., Pardossi-Piquard, R., Bauer, C., Brigham, E., Abraham, J. D., Ranaldi, S., Fraser, P., St-George-Hyslop, P., Le Thuc, O., Espin, V., Chami, L., Dunys, J. & Checler, F. (2012). The beta-secretase-derived C-terminal fragment of betaAPP, C99, but not Abeta, is a key contributor to early intraneuronal lesions in triple-transgenic mouse hippocampus. *J Neurosci,* 32(46)**,** 16243-55a.

LaVoie, M. J. & Selkoe, D. J. (2003). The Notch ligands, Jagged and Delta, are sequentially processed by alpha-secretase and presenilin/gamma-secretase and release signaling fragments. *J Biol Chem,* 278(36)**,** 34427-37.

Lee, G., Thangavel, R., Sharma, V. M., Litersky, J. M., Bhaskar, K., Fang, S. M., Do, L. H., Andreadis, A., Van Hoesen, G. & Ksiezak-Reding, H. (2004). Phosphorylation of tau by fyn: implications for Alzheimer's disease. *J Neurosci,* 24(9)**,** 2304-12.

Lee, H. G., Castellani, R. J., Zhu, X., Perry, G. & Smith, M. A. (2005). Amyloid-beta in Alzheimer's disease: the horse or the cart? Pathogenic or protective? *Int J Exp Pathol,* 86(3)**,** 133-8.

Lee, J., Retamal, C., Cuitino, L., Caruano-Yzermans, A., Shin, J. E., van Kerkhof, P., Marzolo, M. P. & Bu, G. (2008). Adaptor protein sorting nexin 17 regulates amyloid precursor protein trafficking and processing in the early endosomes. *J Biol Chem,* 283(17)**,** 11501-8.

Lee, K. J., Moussa, C. E., Lee, Y., Sung, Y., Howell, B. W., Turner, R. S., Pak, D. T. & Hoe, H. S. (2010). Beta amyloid-independent role of amyloid precursor protein in generation and maintenance of dendritic spines. *Neuroscience,* 169(1)**,** 344-56.

Lee, M. S., Kao, S. C., Lemere, C. A., Xia, W., Tseng, H. C., Zhou, Y., Neve, R., Ahlijanian, M. K. & Tsai, L. H. (2003). APP processing is regulated by cytoplasmic phosphorylation. *J Cell Biol,* 163(1)**,** 83-95.

Leissring, M. A., Farris, W., Chang, A. Y., Walsh, D. M., Wu, X., Sun, X., Frosch, M. P. & Selkoe, D. J. (2003). Enhanced proteolysis of beta-amyloid in APP transgenic mice prevents plaque formation, secondary pathology, and premature death. *Neuron,* 40(6)**,** 1087-93.

Lesne, S., Ali, C., Gabriel, C., Croci, N., MacKenzie, E. T., Glabe, C. G., Plotkine, M., Marchand-Verrecchia, C., Vivien, D. & Buisson, A. (2005). NMDA receptor activation inhibits alpha-secretase and promotes neuronal amyloid-beta production. *J Neurosci,* 25(41)**,** 9367-77.

Lesne, S., Kotilinek, L. & Ashe, K. H. (2008). Plaque-bearing mice with reduced levels of oligomeric amyloid-beta assemblies have intact memory function. *Neuroscience,* 151(3)**,** 745-9.

Lewis, J., Dickson, D. W., Lin, W. L., Chisholm, L., Corral, A., Jones, G., Yen, S. H., Sahara, N., Skipper, L., Yager, D., Eckman, C., Hardy, J., Hutton, M. & McGowan, E. (2001). Enhanced neurofibrillary degeneration in transgenic mice expressing mutant tau and APP. *Science,* 293(5534)**,** 1487-91.

Li, H., Wang, B., Wang, Z., Guo, Q., Tabuchi, K., Hammer, R. E., Sudhof, T. C. & Zheng, H. (2010). Soluble amyloid precursor protein (APP) regulates transthyretin and Klotho gene expression without rescuing the essential function of APP. *Proc Natl Acad Sci U S A,* 107(40)**,** 17362-7.

Li, S., Hong, S., Shepardson, N. E., Walsh, D. M., Shankar, G. M. & Selkoe, D. (2009). Soluble oligomers of amyloid Beta protein facilitate hippocampal long-term depression by disrupting neuronal glutamate uptake. *Neuron,* 62(6)**,** 788-801.

Li, S., Hou, H., Mori, T., Sawmiller, D., Smith, A., Tian, J., Wang, Y., Giunta, B., Sanberg, P. R., Zhang, S. & Tan, J. (2015). Swedish mutant APP-based BACE1 binding site peptide reduces APP beta-cleavage and cerebral Abeta levels in Alzheimer's mice. *Sci Rep,* 5**,** 11322.

Li, S., Jin, M., Koeglsperger, T., Shepardson, N. E., Shankar, G. M. & Selkoe, D. J. (2011). Soluble Abeta oligomers inhibit long-term potentiation through a mechanism involving excessive activation of extrasynaptic NR2B-containing NMDA receptors. *J Neurosci,* 31(18)**,** 6627-38.

Lichtenthaler, S. F. (2011). alpha-secretase in Alzheimer's disease: molecular identity, regulation and therapeutic potential. *J Neurochem,* 116(1)**,** 10-21.

Little, S. P., Dixon, E. P., Norris, F., Buckley, W., Becker, G. W., Johnson, M., Dobbins, J. R., Wyrick, T., Miller, J. R., MacKellar, W., Hepburn, D., Corvalan, J., McClure, D., Liu, X., Stephenson, D., Clemens, J. & Johnstone, E. M. (1997). Zyme, a novel and potentially amyloidogenic enzyme cDNA isolated from Alzheimer's disease brain. *J Biol Chem,* 272(40)**,** 25135-42.

Liu, C., Tan, F. C., Xiao, Z. C. & Dawe, G. S. (2015a). Amyloid precursor protein enhances Nav1.6 sodium channel cell surface expression. *J Biol Chem,* 290(19)**,** 12048-57.

Liu, E., Schmidt, M. E., Margolin, R., Sperling, R., Koeppe, R., Mason, N. S., Klunk, W. E., Mathis, C. A., Salloway, S., Fox, N. C., Hill, D. L., Les, A. S., Collins, P., Gregg, K. M., Di, J., Lu, Y., Tudor, I. C., Wyman, B. T., Booth, K., Broome, S., Yuen, E., Grundman, M., Brashear, H. R., Bapineuzumab & Clinical Trial, I. (2015b). Amyloid-beta 11C-PiB-PET imaging results from 2 randomized bapineuzumab phase 3 AD trials. *Neurology,* 85(8)**,** 692-700.

Lorenzen, A., Samosh, J., Vandewark, K., Anborgh, P. H., Seah, C., Magalhaes, A. C., Cregan, S. P., Ferguson, S. S. & Pasternak, S. H. (2010). Rapid and direct transport of cell surface APP to the lysosome defines a novel selective pathway. *Mol Brain,* 3(11)**,** 11.

Lu, D. C., Rabizadeh, S., Chandra, S., Shayya, R. F., Ellerby, L. M., Ye, X., Salvesen, G. S., Koo, E. H. & Bredesen, D. E. (2000). A second cytotoxic proteolytic peptide derived from amyloid beta-protein precursor. *Nat Med,* 6(4)**,** 397-404.

Luo, Y., Bolon, B., Kahn, S., Bennett, B. D., Babu-Khan, S., Denis, P., Fan, W., Kha, H., Zhang, J. H., Gong, Y. H., Martin, L., Louis, J. C., Yan, Q., Richards, W. G., Citron, M. & Vassar, R. (2001). Mice deficient in BACE1, the Alzheimer's beta-secretase, have normal phenotype and abolished beta-amyloid generation. *Nature Neuroscience,* 4(3)**,** 231-232.

Maloney, J. A., Bainbridge, T., Gustafson, A., Zhang, S., Kyauk, R., Steiner, P., van der Brug, M., Liu, Y., Ernst, J. A., Watts, R. J. & Atwal, J. K. (2014). Molecular mechanisms of Alzheimer disease protection by the A673T allele of amyloid precursor protein. *J Biol Chem,* 289(45)**,** 30990-1000.

Mandelkow, E. M. & Mandelkow, E. (2012). Biochemistry and cell biology of tau protein in neurofibrillary degeneration. *Cold Spring Harb Perspect Med,* 2(7)**,** a006247.

Mann, M. (2006). Functional and quantitative proteomics using SILAC. *Nat Rev Mol Cell Biol,* 7(12)**,** 952-8.

Marcello, E., Epis, R., Saraceno, C., Gardoni, F., Borroni, B., Cattabeni, F., Padovani, A. & Di Luca, M. (2012). SAP97-mediated local trafficking is altered in Alzheimer disease patients' hippocampus. *Neurobiol Aging,* 33(2)**,** 422 e1-10.

Marquer, C., Laine, J., Dauphinot, L., Hanbouch, L., Lemercier-Neuillet, C., Pierrot, N., Bossers, K., Le, M., Corlier, F., Benstaali, C., Saudou, F., Thinakaran, G., Cartier, N., Octave, J. N., Duyckaerts, C. & Potier, M. C. (2014). Increasing membrane cholesterol of neurons in culture recapitulates Alzheimer's disease early phenotypes. *Mol Neurodegener,* 9(1)**,** 60.

Marz, P., Probst, A., Lang, S., Schwager, M., Rose-John, S., Otten, U. & Ozbek, S. (2004). Ataxin-10, the spinocerebellar ataxia type 10 neurodegenerative disorder protein, is essential for survival of cerebellar neurons. *J Biol Chem,* 279(34)**,** 35542-50.

Masliah, E., Mallory, M., Ge, N. F. & Saitoh, T. (1992a). Amyloid Precursor Protein Is Localized in Growing Neurites of Neonatal Rat-Brain. *Brain Research,* 593(2)**,** 323-328.

Masliah, E., Mallory, M., Hansen, L., Alford, M., DeTeresa, R., Terry, R., Baudier, J. & Saitoh, T. (1992b). Localization of amyloid precursor protein in GAP43-immunoreactive aberrant sprouting neurites in Alzheimer's disease. *Brain Res,* 574(1-2)**,** 312-6.

Masters, C. L. & Selkoe, D. J. (2012). Biochemistry of amyloid beta-protein and amyloid deposits in Alzheimer disease. *Cold Spring Harb Perspect Med,* 2(6)**,** a006262.

Masters, C. L., Simms, G., Weinman, N. A., Multhaup, G., McDonald, B. L. & Beyreuther, K. (1985). Amyloid plaque core protein in Alzheimer disease and Down syndrome. *Proc Natl Acad Sci U S A,* 82(12)**,** 4245-9.

Matsuda, S., Giliberto, L., Matsuda, Y., Davies, P., McGowan, E., Pickford, F., Ghiso, J., Frangione, B. & D'Adamio, L. (2005). The familial dementia BRI2 gene binds the Alzheimer gene amyloid-beta precursor protein and inhibits amyloid-beta production. *J Biol Chem,* 280(32)**,** 28912-6.

Matsuda, S., Giliberto, L., Matsuda, Y., McGowan, E. M. & D'Adamio, L. (2008). BRI2 inhibits amyloid beta-peptide precursor protein processing by interfering with the docking of secretases to the substrate. *J Neurosci,* 28(35)**,** 8668-76.

Matsuda, S., Matsuda, Y. & D'Adamio, L. (2009a). BRI3 inhibits amyloid precursor protein processing in a mechanistically distinct manner from its homologue dementia gene BRI2. *J Biol Chem,* 284(23)**,** 15815-25.

Matsuda, S., Matsuda, Y. & D'Adamio, L. (2009b). CD74 interacts with APP and suppresses the production of Abeta. *Molecular Neurodegeneration,* 4(1)**,** 41.

Matsui, T., Ingelsson, M., Fukumoto, H., Ramasamy, K., Kowa, H., Frosch, M. P., Irizarry, M. C. & Hyman, B. T. (2007). Expression of APP pathway mRNAs and proteins in Alzheimer's disease. *Brain Res,* 1161(0)**,** 116-23.

Mattson, M. P., Cheng, B., Culwell, A. R., Esch, F. S., Lieberburg, I. & Rydel, R. E. (1993). Evidence for excitoprotective and intraneuronal calcium-regulating roles for secreted forms of the beta-amyloid precursor protein. *Neuron,* 10(2)**,** 243-54.

Mayeux, R. & Stern, Y. (2012). Epidemiology of Alzheimer disease. *Cold Spring Harb Perspect Med,* 2(8).

McLean, C. A., Cherny, R. A., Fraser, F. W., Fuller, S. J., Smith, M. J., Konrad, V., Bush, A. I. & Masters, C. L. (1999). Soluble pool of Aβ amyloid as a determinant of severity of neurodegeneration in Alzheimer's disease. *Annals of Neurology,* 46(6)**,** 860-866.

McLoughlin, D. M. & Miller, C. C. (1996). The intracellular cytoplasmic domain of the Alzheimer's disease amyloid precursor protein interacts with phosphotyrosine-binding domain proteins in the yeast two-hybrid system. *FEBS Lett,* 397(2-3)**,** 197-200.

McLoughlin, D. M. & Miller, C. C. (2008). The FE65 proteins and Alzheimer's disease. *J Neurosci Res,* 86(4)**,** 744-54.

Mecozzi, V. J., Berman, D. E., Simoes, S., Vetanovetz, C., Awal, M. R., Patel, V. M., Schneider, R. T., Petsko, G. A., Ringe, D. & Small, S. A. (2014). Pharmacological chaperones stabilize retromer to limit APP processing. *Nat Chem Biol,* 10(6)**,** 443-9.

Messa, M., Colombo, L., del Favero, E., Cantu, L., Stoilova, T., Cagnotto, A., Rossi, A., Morbin, M., Di Fede, G., Tagliavini, F. & Salmona, M. (2014). The peculiar role of the A2V mutation in amyloid-beta (Abeta) 1-42 molecular assembly. *J Biol Chem,* 289(35)**,** 24143-52.

Milosch, N., Tanriover, G., Kundu, A., Rami, A., Francois, J. C., Baumkotter, F., Weyer, S. W., Samanta, A., Jaschke, A., Brod, F., Buchholz, C. J., Kins, S., Behl, C., Muller, U. C. & Kogel, D. (2014). Holo-APP and G-protein-mediated signaling are required for sAPPalpha-induced activation of the Akt survival pathway. *Cell Death Dis,* 5**,** e1391.

Mitani, Y., Yarimizu, J., Saita, K., Uchino, H., Akashiba, H., Shitaka, Y., Ni, K. & Matsuoka, N. (2012). Differential effects between gamma-secretase inhibitors and modulators on cognitive function in amyloid precursor protein-transgenic and nontransgenic mice. *J Neurosci,* 32(6)**,** 2037-50.

Moir, R. D., Lynch, T., Bush, A. I., Whyte, S., Henry, A., Portbury, S., Multhaup, G., Small, D. H., Tanzi, R. E., Beyreuther, K. & Masters, C. L. (1998). Relative increase in Alzheimer's disease of soluble forms of cerebral Abeta amyloid protein precursor containing the Kunitz protease inhibitory domain. *J Biol Chem,* 273(9)**,** 5013-9.

Moore, S., Evans, L. D., Andersson, T., Portelius, E., Smith, J., Dias, T. B., Saurat, N., McGlade, A., Kirwan, P., Blennow, K., Hardy, J., Zetterberg, H. & Livesey, F. J. (2015). APP metabolism regulates tau proteostasis in human cerebral cortex neurons. *Cell Rep,* 11(5)**,** 689-96.

Morris, J. C., Heyman, A., Mohs, R. C., Hughes, J. P., van Belle, G., Fillenbaum, G., Mellits, E. D. & Clark, C. (1989). The Consortium to Establish a Registry for Alzheimer's Disease (CERAD). Part I. Clinical and neuropsychological assessment of Alzheimer's disease. *Neurology,* 39(9)**,** 1159-65.

Morris, M., Knudsen, G. M., Maeda, S., Trinidad, J. C., Ioanoviciu, A., Burlingame, A. L. & Mucke, L. (2015). Tau post-translational modifications in wild-type and human amyloid precursor protein transgenic mice. *Nat Neurosci,* 18(8)**,** 1183-9.

Mucke, L. & Selkoe, D. J. (2012). Neurotoxicity of amyloid beta-protein: synaptic and network dysfunction. *Cold Spring Harb Perspect Med,* 2(7)**,** a006338.

Muller-Hill, B. & Beyreuther, K. (1989). Molecular biology of Alzheimer's disease. *Annu Rev Biochem,* 58(1)**,** 287-307.

Munday, D. C., Surtees, R., Emmott, E., Dove, B. K., Digard, P., Barr, J. N., Whitehouse, A., Matthews, D. & Hiscox, J. A. (2012). Using SILAC and quantitative proteomics to investigate the interactions between viral and host proteomes. *PROTEOMICS,* 12(4-5)**,** 666-72.

Musardo, S., Saraceno, C., Pelucchi, S. & Marcello, E. (2013). Trafficking in neurons: searching for new targets for Alzheimer's disease future therapies. *Eur J Pharmacol,* 719(1-3)**,** 84-106.

Musiek, E. S. & Holtzman, D. M. (2015). Three dimensions of the amyloid hypothesis: time, space and 'wingmen'. *Nat Neurosci,* 18(6)**,** 800-6.

Nalivaeva, N. N., Belyaev, N. D., Kerridge, C. & Turner, A. J. (2014). Amyloid-clearing proteins and their epigenetic regulation as a therapeutic target in Alzheimer's disease. *Front Aging Neurosci,* 6**,** 235.

Nalivaeva, N. N., Belyaev, N. D. & Turner, A. J. (2015). New Insights into Epigenetic and Pharmacological Regulation of Amyloid-Degrading Enzymes. *Neurochemical Research***,** 1-11.

Nalivaeva, N. N. & Turner, A. J. (2013). The amyloid precursor protein: a biochemical enigma in brain development, function and disease. *FEBS Lett,* 587(13)**,** 2046-54.

Neumann-Giesen, C., Falkenbach, B., Beicht, P., Claasen, S., Luers, G., Stuermer, C. A., Herzog, V. & Tikkanen, R. (2004). Membrane and raft association of reggie-1/flotillin-2: role of myristoylation, palmitoylation and oligomerization and induction of filopodia by overexpression. *Biochem J,* 378(Pt 2)**,** 509-18.

Nhan, H. S., Chiang, K. & Koo, E. H. (2015). The multifaceted nature of amyloid precursor protein and its proteolytic fragments: friends and foes. *Acta Neuropathologica,* 129(1)**,** 1-19.

Nicoll, A. J., Panico, S., Freir, D. B., Wright, D., Terry, C., Risse, E., Herron, C. E., O'Malley, T., Wadsworth, J. D., Farrow, M. A., Walsh, D. M., Saibil, H. R. & Collinge, J. (2013). Amyloid-beta nanotubes are associated with prion protein-dependent synaptotoxicity. *Nat Commun,* 4**,** 2416.

Nikolaev, A., McLaughlin, T., O'Leary, D. D. & Tessier-Lavigne, M. (2009). APP binds DR6 to trigger axon pruning and neuron death via distinct caspases. *Nature,* 457(7232)**,** 981-9.

Noble, W., Hanger, D. P., Miller, C. C. & Lovestone, S. (2013). The importance of tau phosphorylation for neurodegenerative diseases. *Front Neurol,* 4**,** 83.

Nostrand, W. E. V., Wagner, S. L., Suzuki, M., Choi, B. H., Farrow, J. S., Geddes, J. W., Cotman, C. W. & Cunningham, D. D. (1989). Protease nexin-II, a potent anti-chymotrypsin, shows identity to amyloid β-protein precursor. *Nature,* 341(6242)**,** 546-549.

Nussbaum, J. M., Schilling, S., Cynis, H., Silva, A., Swanson, E., Wangsanut, T., Tayler, K., Wiltgen, B., Hatami, A., Ronicke, R., Reymann, K., Hutter-Paier, B., Alexandru, A., Jagla, W., Graubner, S., Glabe, C. G., Demuth, H.-U. & Bloom, G. S. (2012). Prion-like behaviour and tau-dependent cytotoxicity of pyroglutamylated amyloid-β. *Nature,* 485(7400)**,** 651-655.

Obregon, D., Hou, H., Deng, J., Giunta, B., Tian, J., Darlington, D., Shahaduzzaman, M., Zhu, Y., Mori, T., Mattson, M. P. & Tan, J. (2012). Soluble amyloid precursor protein-alpha modulates beta-secretase activity and amyloid-beta generation. *Nat Commun,* 3**,** 777.

Octave, J. N., Pierrot, N., Ferao Santos, S., Nalivaeva, N. N. & Turner, A. J. (2013). From synaptic spines to nuclear signaling: nuclear and synaptic actions of the amyloid precursor protein. *J Neurochem,* 126(2)**,** 183-90.

Okada, H., Zhang, W., Peterhoff, C., Hwang, J. C., Nixon, R. A., Ryu, S. H. & Kim, T. W. (2010). Proteomic identification of sorting nexin 6 as a negative regulator of BACE1-mediated APP processing. *FASEB J,* 24(8)**,** 2783-94.

Olsen, O., Kallop, D. Y., McLaughlin, T., Huntwork-Rodriguez, S., Wu, Z., Duggan, C. D., Simon, D. J., Lu, Y., Easley-Neal, C., Takeda, K., Hass, P. E., Jaworski, A., O'Leary, D. D., Weimer, R. M. & Tessier-Lavigne, M. (2014). Genetic analysis reveals that amyloid precursor protein and death receptor 6 function in the same pathway to control axonal pruning independent of beta-secretase. *J Neurosci,* 34(19)**,** 6438-47.

Palmert, M., Golde, T., Cohen, M., Kovacs, D., Tanzi, R., Gusella, J., Usiak, M., Younkin, L. & Younkin, S. (1988). Amyloid protein precursor messenger RNAs: differential expression in Alzheimer's disease. *Science,* 241(4869)**,** 1080-1084.

Pardossi-Piquard, R., Yang, S. P., Kanemoto, S., Gu, Y., Chen, F., Bohm, C., Sevalle, J., Li, T., Wong, P. C., Checler, F., Schmitt-Ulms, G., St George-Hyslop, P. & Fraser, P. E. (2009). APH1 polar transmembrane residues regulate the assembly and activity of presenilin complexes. *J Biol Chem,* 284(24)**,** 16298-307.

Park, J. H., Gimbel, D. A., GrandPre, T., Lee, J. K., Kim, J. E., Li, W., Lee, D. H. & Strittmatter, S. M. (2006). Alzheimer precursor protein interaction with the Nogo-66 receptor reduces amyloid-beta plaque deposition. *J Neurosci,* 26(5)**,** 1386-95.

Parvathy, S., Hussain, I., Karran, E. H., Turner, A. J. & Hooper, N. M. (1999). Cleavage of Alzheimer's amyloid precursor protein by alpha-secretase occurs at the surface of neuronal cells. *Biochemistry,* 38(30)**,** 9728-34.

Pastorino, L., Kondo, A., Zhou, X. Z. & Lu, K. P. (2013). *Pin1 Protects Against Alzheimer's Disease: One Goal, Multiple Mechanisms*.

Pastorino, L., Sun, A., Lu, P.-J., Zhou, X. Z., Balastik, M., Finn, G., Wulf, G., Lim, J., Li, S.-H., Li, X., Xia, W., Nicholson, L. K. & Lu, K. P. (2006). The prolyl isomerase Pin1 regulates amyloid

precursor protein processing and amyloid-[beta] production. *Nature,* 440(7083)**,** 528-534.

Pavlov, P. F., Hansson Petersen, C., Glaser, E. & Ankarcrona, M. (2009). Mitochondrial accumulation of APP and Abeta: significance for Alzheimer disease pathogenesis. *J Cell Mol Med,* 13(10)**,** 4137-45.

Pavlov, P. F., Wiehager, B., Sakai, J., Frykman, S., Behbahani, H., Winblad, B. & Ankarcrona, M. (2011). Mitochondrial gamma-secretase participates in the metabolism of mitochondria-associated amyloid precursor protein. *FASEB J,* 25(1)**,** 78-88.

Pawlik, M., Otero, D. A., Park, M., Fischer, W. H., Levy, E. & Saitoh, T. (2007). Proteins that bind to the RERMS region of beta amyloid precursor protein. *Biochem Biophys Res Commun,* 355(4)**,** 907-12.

Perreau, V. M., Orchard, S., Adlard, P. A., Bellingham, S. A., Cappai, R., Ciccotosto, G. D., Cowie, T. F., Crouch, P. J., Duce, J. A., Evin, G., Faux, N. G., Hill, A. F., Hung, Y. H., James, S. A., Li, Q. X., Mok, S. S., Tew, D. J., White, A. R., Bush, A. I., Hermjakob, H. & Masters, C. L. (2010). A domain level interaction network of amyloid precursor protein and Abeta of Alzheimer's disease. *PROTEOMICS,* 10(12)**,** 2377-95.

Pierrot, N., Tyteca, D., D'Auria, L., Dewachter, I., Gailly, P., Hendrickx, A., Tasiaux, B., Haylani, L. E., Muls, N., N'Kuli, F., Laquerriere, A., Demoulin, J. B., Campion, D., Brion, J. P., Courtoy, P. J., Kienlen-Campard, P. & Octave, J. N. (2013). Amyloid precursor protein controls cholesterol turnover needed for neuronal activity. *EMBO Mol Med,* 5(4)**,** 608-25.

Pimplikar, S. W. (2009). Reassessing the amyloid cascade hypothesis of Alzheimer's disease. *Int J Biochem Cell Biol,* 41(6)**,** 1261-8.

Pimplikar, S. W., Nixon, R. A., Robakis, N. K., Shen, J. & Tsai, L. H. (2010). Amyloid-independent mechanisms in Alzheimer's disease pathogenesis. *J Neurosci,* 30(45)**,** 14946-54.

Poleev, A., Hartmann, A. & Stamm, S. (2000). A trans-acting factor, isolated by the three-hybrid system, that influences alternative splicing of the amyloid precursor protein minigene. *European Journal of Biochemistry,* 267(13)**,** 4002-4010.

Portelius, E., Brinkmalm, G., Tran, A., Andreasson, U., Zetterberg, H., Westman-Brinkmalm, A., Blennow, K. & Ohrfelt, A. (2010). Identification of novel N-terminal fragments of amyloid precursor protein in cerebrospinal fluid. *Exp Neurol,* 223(2)**,** 351-8.

Portelius, E., Dean, R. A., Andreasson, U., Mattson, N., Westerlund, A., Olsson, M., Demattos, R. B., Racke, M. M., Zetterberg, H., May, P. C. & Blennow, K. (2014). β-site Amyloid Precursor Protein-Cleaving enzyme 1 (BACE1) inhibitor treatment induces Aβ5-X Peptides Through Alternative Amyloid Precursor Protein Cleavage. *Alzheimer's Research and Therapy,* 6(75)**,** doi:10.1186/s13195-014-0075-0.

Portelius, E., Lashley, T., Westerlund, A., Persson, R., Fox, N. C., Blennow, K., Revesz, T. & Zetterberg, H. (2015). Brain amyloid-beta fragment signatures in pathological ageing and Alzheimer's disease by hybrid immunoprecipitation mass spectrometry. *Neurodegener Dis,* 15(1)**,** 50-7.

Priller, C., Bauer, T., Mitteregger, G., Krebs, B., Kretzschmar, H. A. & Herms, J. (2006). Synapse formation and function is modulated by the amyloid precursor protein. *J Neurosci,* 26(27)**,** 7212-21.

Prokop, S., Shirotani, K., Edbauer, D., Haass, C. & Steiner, H. (2004). Requirement of PEN-2 for stabilization of the presenilin N-/C-terminal fragment heterodimer within the gamma-secretase complex. *J Biol Chem,* 279(22)**,** 23255-61.

Querfurth, H. W. & LaFerla, F. M. (2010). Alzheimer's disease. *N Engl J Med,* 362(4)**,** 329-44.

Radde, R., Bolmont, T., Kaeser, S. A., Coomaraswamy, J., Lindau, D., Stoltze, L., Calhoun, M. E., Jaggi, F., Wolburg, H., Gengler, S., Haass, C., Ghetti, B., Czech, C., Holscher, C., Mathews, P. M. & Jucker, M. (2006). Abeta42-driven cerebral amyloidosis in transgenic mice reveals early and robust pathology. *EMBO Rep,* 7(9)**,** 940-6.

Rajan, K. B., Wilson, R. S., Weuve, J., Barnes, L. L. & Evans, D. A. (2015). Cognitive impairment 18 years before clinical diagnosis of Alzheimer disease dementia. *Neurology,* 85(10)**,** 898-904.

Rajendran, L. & Annaert, W. (2012). Membrane trafficking pathways in Alzheimer's disease. *Traffic,* 13(6)**,** 759-70.

Rajendran, L., Honsho, M., Zahn, T. R., Keller, P., Geiger, K. D., Verkade, P. & Simons, K. (2006). Alzheimer's disease beta-amyloid peptides are released in association with exosomes. *Proc Natl Acad Sci U S A,* 103(30)**,** 11172-7.

Rajendran, L., Schneider, A., Schlechtingen, G., Weidlich, S., Ries, J., Braxmeier, T., Schwille, P., Schulz, J. B., Schroeder, C., Simons, M., Jennings, G., Knolker, H. J. & Simons, K. (2008). Efficient inhibition of the Alzheimer's disease beta-secretase by membrane targeting. *Science,* 320(5875)**,** 520-3.

Reddy, P. H. (2013). Is the mitochondrial outermembrane protein VDAC1 therapeutic target for Alzheimer's disease? *Biochim Biophys Acta,* 1832(1)**,** 67-75.

Reinhard, C., Hebert, S. S. & De Strooper, B. (2005). The amyloid-beta precursor protein: integrating structure with biological function. *EMBO J,* 24(23)**,** 3996-4006.

Reitz, C. (2012). Alzheimer's disease and the amyloid cascade hypothesis: a critical review. *Int J Alzheimers Dis,* 2012(Article ID 369808)**,** 369808.

Reitz, C., Tokuhiro, S., Clark, L. N., Conrad, C., Vonsattel, J. P., Hazrati, L. N., Palotas, A., Lantigua, R., Medrano, M., I, Z. J.-V., Vardarajan, B., Simkin, I., Haines, J. L., Pericak-Vance, M. A., Farrer, L. A., Lee, J. H., Rogaeva, E., George-Hyslop, P. S. & Mayeux, R. (2011). SORCS1 alters amyloid precursor protein processing and variants may increase Alzheimer's disease risk. *Ann Neurol,* 69(1)**,** 47-64.

Rezai-Zadeh, K., Arendash, G. W., Hou, H., Fernandez, F., Jensen, M., Runfeldt, M., Shytle, R. D. & Tan, J. (2008). Green tea epigallocatechin-3-gallate (EGCG) reduces beta-amyloid mediated cognitive impairment and modulates tau pathology in Alzheimer transgenic mice. *Brain Res,* 1214**,** 177-87.

Rice, H. C., Townsend, M., Bai, J., Suth, S., Cavanaugh, W., Selkoe, D. J. & Young-Pearse, T. L. (2012). Pancortins interact with amyloid precursor protein and modulate cortical cell migration. *Development,* 139(21)**,** 3986-96.

Rice, H. C., Young-Pearse, T. L. & Selkoe, D. J. (2013). Systematic evaluation of candidate ligands regulating ectodomain shedding of amyloid precursor protein. *Biochemistry,* 52(19)**,** 3264-77.

Riddell, D. R., Christie, G., Hussain, I. & Dingwall, C. (2001). Compartmentalization of β-secretase (Asp2) into low-buoyant density, noncaveolar lipid rafts. *Current Biology,* 11(16)**,** 1288-1293.

Ring, S., Weyer, S. W., Kilian, S. B., Waldron, E., Pietrzik, C. U., Filippov, M. A., Herms, J., Buchholz, C., Eckman, C. B., Korte, M., Wolfer, D. P. & Muller, U. C. (2007). The secreted beta-amyloid precursor protein ectodomain APPs alpha is sufficient to rescue the anatomical, behavioral, and electrophysiological abnormalities of APP-deficient mice. *J Neurosci,* 27(29)**,** 7817-26.

Roberson, E. D., Halabisky, B., Yoo, J. W., Yao, J., Chin, J., Yan, F., Wu, T., Hamto, P., Devidze, N., Yu, G. Q., Palop, J. J., Noebels, J. L. & Mucke, L. (2011). Amyloid-beta/Fyn-induced synaptic, network, and cognitive impairments depend on tau levels in multiple mouse models of Alzheimer's disease. *J Neurosci,* 31(2)**,** 700-11.

Roberson, E. D. & Mucke, L. (2006). 100 years and counting: prospects for defeating Alzheimer's disease. *Science,* 314(5800)**,** 781-4.

Roberson, E. D., Scearce-Levie, K., Palop, J. J., Yan, F., Cheng, I. H., Wu, T., Gerstein, H., Yu, G. Q. & Mucke, L. (2007). Reducing endogenous tau ameliorates amyloid beta-induced deficits in an Alzheimer's disease mouse model. *Science,* 316(5825)**,** 750-4.

Rockenstein, E. M., McConlogue, L., Tan, H., Power, M., Masliah, E. & Mucke, L. (1995). Levels and alternative splicing of amyloid beta protein precursor (APP) transcripts in brains of APP transgenic mice and humans with Alzheimer's disease. *J Biol Chem,* 270(47)**,** 28257-67.

Rogaeva, E., Meng, Y., Lee, J. H., Gu, Y., Kawarai, T., Zou, F., Katayama, T., Baldwin, C. T., Cheng, R., Hasegawa, H., Chen, F., Shibata, N., Lunetta, K. L., Pardossi-Piquard, R., Bohm, C.,

Wakutani, Y., Cupples, L. A., Cuenco, K. T., Green, R. C., Pinessi, L., Rainero, I., Sorbi, S., Bruni, A., Duara, R., Friedland, R. P., Inzelberg, R., Hampe, W., Bujo, H., Song, Y. Q., Andersen, O. M., Willnow, T. E., Graff-Radford, N., Petersen, R. C., Dickson, D., Der, S. D., Fraser, P. E., Schmitt-Ulms, G., Younkin, S., Mayeux, R., Farrer, L. A. & St George-Hyslop, P. (2007). The neuronal sortilin-related receptor SORL1 is genetically associated with Alzheimer disease. *Nat Genet,* 39(2)**,** 168-77.

Rohan de Silva, H. A., Jen, A., Wickenden, C., Jen, L. S., Wilkinson, S. L. & Patel, A. J. (1997). Cell-specific expression of beta-amyloid precursor protein isoform mRNAs and proteins in neurons and astrocytes. *Brain Res Mol Brain Res,* 47(1-2)**,** 147-56.

Romero, K., Ito, K., Rogers, J. A., Polhamus, D., Qiu, R., Stephenson, D., Mohs, R., Lalonde, R., Sinha, V., Wang, Y., Brown, D., Isaac, M., Vamvakas, S., Hemmings, R., Pani, L., Bain, L. J., Corrigan, B., Alzheimer's Disease Neuroimaging, I. & Coalition Against Major, D. (2015). The future is now: model-based clinical trial design for Alzheimer's disease. *Clin Pharmacol Ther,* 97(3)**,** 210-4.

Rossner, S., Apelt, J., Schliebs, R., Perez-Polo, J. R. & Bigl, V. (2001). Neuronal and glial beta-secretase (BACE) protein expression in transgenic Tg2576 mice with amyloid plaque pathology. *J Neurosci Res,* 64(5)**,** 437-46.

Rovelet-Lecrux, A., Legallic, S., Wallon, D., Flaman, J. M., Martinaud, O., Bombois, S., Rollin-Sillaire, A., Michon, A., Le Ber, I., Pariente, J., Puel, M., Paquet, C., Croisile, B., Thomas-Anterion, C., Vercelletto, M., Levy, R., Frebourg, T., Hannequin, D., Campion, D. & Investigators of the, G. p. (2012). A genome-wide study reveals rare CNVs exclusive to extreme phenotypes of Alzheimer disease. *Eur J Hum Genet,* 20(6)**,** 613-7.

Rushworth, J. V., Griffiths, H. H., Watt, N. T. & Hooper, N. M. (2013). Prion protein-mediated toxicity of amyloid-beta oligomers requires lipid rafts and the transmembrane LRP1. *J Biol Chem,* 288(13)**,** 8935-51.

Rushworth, J. V. & Hooper, N. M. (2010). Lipid Rafts: Linking Alzheimer's Amyloid-beta Production, Aggregation, and Toxicity at Neuronal Membranes. *Int J Alzheimers Dis,* 2011**,** 603052.

Sabo, S. L., Lanier, L. M., Ikin, A. F., Khorkova, O., Sahasrabudhe, S., Greengard, P. & Buxbaum, J. D. (1999). Regulation of beta-amyloid secretion by FE65, an amyloid protein precursor-binding protein. *J Biol Chem,* 274(12)**,** 7952-7.

Saido, T. C., Iwatsubo, T., Mann, D. M. A., Shimada, H., Ihara, Y. & Kawashima, S. (1995). Dominant and differential deposition of distinct β-amyloid peptide species, AβN3(pE), in senile plaques. *Neuron,* 14(2)**,** 457-466.

Saito, T., Iwata, N., Tsubuki, S., Takaki, Y., Takano, J., Huang, S. M., Suemoto, T., Higuchi, M. & Saido, T. C. (2005). Somatostatin regulates brain amyloid beta peptide A beta(42) through modulation of proteolytic degradation. *Nature Medicine,* 11(4)**,** 434-439.

Saitoh, T., Sundsmo, M., Roch, J.-M., Kimura, N., Cole, G., Schubert, D., Oltersdorf, T. & Schenk, D. B. (1989). Secreted form of amyloid β protein precursor is involved in the growth regulation of fibroblasts. *Cell,* 58(4)**,** 615-622.

Salloway, S., Sperling, R., Gilman, S., Fox, N. C., Blennow, K., Raskind, M., Sabbagh, M., Honig, L. S., Doody, R., van Dyck, C. H., Mulnard, R., Barakos, J., Gregg, K. M., Liu, E., Lieberburg, I., Schenk, D., Black, R., Grundman, M. & Bapineuzumab 201 Clinical Trial, I. (2009). A phase 2 multiple ascending dose trial of bapineuzumab in mild to moderate Alzheimer disease. *Neurology,* 73(24)**,** 2061-70.

Sandbrink, R., Masters, C. L. & Beyreuther, K. (1996). APP gene family. Alternative splicing generates functionally related isoforms. *Ann N Y Acad Sci,* 777(1)**,** 281-7.

Sannerud, R., Declerck, I., Peric, A., Raemaekers, T., Menendez, G., Zhou, L., Veerle, B., Coen, K., Munck, S., De Strooper, B., Schiavo, G. & Annaert, W. (2011). ADP ribosylation factor 6 (ARF6) controls amyloid precursor protein (APP) processing by mediating the endosomal sorting of BACE1. *Proc Natl Acad Sci U S A,* 108(34)**,** E559-68.

Sano, Y., Nakaya, T., Pedrini, S., Takeda, S., Iijima-Ando, K., Iijima, K., Mathews, P. M., Itohara, S., Gandy, S. & Suzuki, T. (2006). Physiological mouse brain Abeta levels are not related to the phosphorylation state of threonine-668 of Alzheimer's APP. *PLoS ONE,* 1(1)**,** e51.

Savva, G. M., Wharton, S. B., Ince, P. G., Forster, G., Matthews, F. E., Brayne, C., Medical Research Council Cognitive, F. & Ageing, S. (2009). Age, neuropathology, and dementia. *N Engl J Med,* 360(22)**,** 2302-9.

Schenk, D., Barbour, R., Dunn, W., Gordon, G., Grajeda, H., Guido, T., Hu, K., Huang, J., Johnson-Wood, K., Khan, K., Kholodenko, D., Lee, M., Liao, Z., Lieberburg, I., Motter, R., Mutter, L., Soriano, F., Shopp, G., Vasquez, N., Vandevert, C., Walker, S., Wogulis, M., Yednock, T., Games, D. & Seubert, P. (1999). Immunization with amyloid-beta attenuates Alzheimer-disease-like pathology in the PDAPP mouse. *Nature,* 400(6740)**,** 173-7.

Scheuner, D., Eckman, C., Jensen, M., Song, X., Citron, M., Suzuki, N., Bird, T. D., Hardy, J., Hutton, M., Kukull, W., Larson, E., Levy-Lahad, L., Viitanen, M., Peskind, E., Poorkaj, P., Schellenberg, G., Tanzi, R., Wasco, W., Lannfelt, L., Selkoe, D. & Younkin, S. (1996). Secreted amyloid β-protein similar to that in the senile plaques of Alzheimer's disease is increased in vivo by the presenilin 1 and 2 and APP mutations linked to familial Alzheimer's disease. *Nat Med,* 2(8)**,** 864-870.

Schilling, S., Lauber, T., Schaupp, M., Manhart, S., Scheel, E., Bohm, G. & Demuth, H. U. (2006). On the seeding and oligomerization of pGlu-amyloid peptides (in vitro). *Biochemistry,* 45(41)**,** 12393-9.

Schilling, S., Zeitschel, U., Hoffmann, T., Heiser, U., Francke, M., Kehlen, A., Holzer, M., Hutter-Paier, B., Prokesch, M., Windisch, M., Jagla, W., Schlenzig, D., Lindner, C., Rudolph, T., Reuter, G., Cynis, H., Montag, D., Demuth, H. U. & Rossner, S. (2008). Glutaminyl cyclase inhibition attenuates pyroglutamate Abeta and Alzheimer's disease-like pathology. *Nat Med,* 14(10)**,** 1106-11.

Schlenzig, D., Ronicke, R., Cynis, H., Ludwig, H. H., Scheel, E., Reymann, K., Saido, T., Hause, G., Schilling, S. & Demuth, H. U. (2012). N-Terminal pyroglutamate formation of Abeta38 and Abeta40 enforces oligomer formation and potency to disrupt hippocampal long-term potentiation. *J Neurochem,* 121(5)**,** 774-84.

Schmidt, V., Sporbert, A., Rohe, M., Reimer, T., Rehm, A., Andersen, O. M. & Willnow, T. E. (2007). SorLA/LR11 regulates processing of amyloid precursor protein via interaction with adaptors GGA and PACS-1. *J Biol Chem,* 282(45)**,** 32956-64.

Schneider-Poetsch, T., Ju, J., Eyler, D. E., Dang, Y., Bhat, S., Merrick, W. C., Green, R., Shen, B. & Liu, J. O. (2010). Inhibition of eukaryotic translation elongation by cycloheximide and lactimidomycin. *Nat Chem Biol,* 6(3)**,** 209-217.

Schneider, A., Rajendran, L., Honsho, M., Gralle, M., Donnert, G., Wouters, F., Hell, S. W. & Simons, M. (2008). Flotillin-dependent clustering of the amyloid precursor protein regulates its endocytosis and amyloidogenic processing in neurons. *J Neurosci,* 28(11)**,** 2874-82.

Schon, E. A. & Area-Gomez, E. (2013). Mitochondria-associated ER membranes in Alzheimer disease. *Mol Cell Neurosci,* 55(0)**,** 26-36.

Schreiner, B., Hedskog, L., Wiehager, B. & Ankarcrona, M. (2015). Amyloid-beta peptides are generated in mitochondria-associated endoplasmic reticulum membranes. *J Alzheimers Dis,* 43(2)**,** 369-74.

Schubert, D., Jin, L. W., Saitoh, T. & Cole, G. (1989). The regulation of amyloid beta protein precursor secretion and its modulatory role in cell adhesion. *Neuron,* 3(6)**,** 689-94.

Seabrook, G. R., Smith, D. W., Bowery, B. J., Easter, A., Reynolds, T., Fitzjohn, S. M., Morton, R. A., Zheng, H., Dawson, G. R., Sirinathsinghji, D. J., Davies, C. H., Collingridge, G. L. & Hill, R. G. (1999). Mechanisms contributing to the deficits in hippocampal synaptic plasticity in mice lacking amyloid precursor protein. *Neuropharmacology,* 38(3)**,** 349-59.

Selkoe, D. J. (1991). The molecular pathology of Alzheimer's disease. *Neuron,* 6(4)**,** 487-98.

Selkoe, D. J. (2000). Toward a Comprehensive Theory for Alzheimer's Disease. Hypothesis: Alzheimer's Disease Is Caused by the Cerebral Accumulation and Cytotoxicity of Amyloid β-Protein. *Annals of the New York Academy of Sciences,* 924(1)**,** 17-25.

Selkoe, D. J. (2011). Resolving controversies on the path to Alzheimer's therapeutics. *Nat Med,* 17(9)**,** 1060-5.

Serrano-Pozo, A., Frosch, M. P., Masliah, E. & Hyman, B. T. (2011). Neuropathological alterations in Alzheimer disease. *Cold Spring Harb Perspect Med,* 1(1)**,** a006189.

Shah, S., Lee, S. F., Tabuchi, K., Hao, Y. H., Yu, C., LaPlant, Q., Ball, H., Dann, C. E., 3rd, Sudhof, T. & Yu, G. (2005). Nicastrin functions as a gamma-secretase-substrate receptor. *Cell,* 122(3)**,** 435-47.

Shariati, S. A. & De Strooper, B. (2013). Redundancy and divergence in the amyloid precursor protein family. *FEBS Lett,* 587(13)**,** 2036-45.

Shen, J. & Kelleher, R. J., 3rd (2007). The presenilin hypothesis of Alzheimer's disease: evidence for a loss-of-function pathogenic mechanism. *Proc Natl Acad Sci U S A,* 104(2)**,** 403-9.

Shipton, O. A., Leitz, J. R., Dworzak, J., Acton, C. E., Tunbridge, E. M., Denk, F., Dawson, H. N., Vitek, M. P., Wade-Martins, R., Paulsen, O. & Vargas-Caballero, M. (2011). Tau protein is required for amyloid beta-induced impairment of hippocampal long-term potentiation. *J Neurosci,* 31(5)**,** 1688-92.

Shirotani, K., Edbauer, D., Kostka, M., Steiner, H. & Haass, C. (2004). Immature nicastrin stabilizes APH-1 independent of PEN-2 and presenilin: identification of nicastrin mutants that selectively interact with APH-1. *J Neurochem,* 89(6)**,** 1520-7.

Siemers, E. R., Sundell, K. L., Carlson, C., Case, M., Sethuraman, G., Liu-Seifert, H., Dowsett, S. A., Pontecorvo, M. J., Dean, R. A. & Demattos, R. (2015). Phase 3 solanezumab trials: Secondary outcomes in mild Alzheimer's disease patients. *Alzheimers Dement*.

Small, S. A., Kent, K., Pierce, A., Leung, C., Kang, M. S., Okada, H., Honig, L., Vonsattel, J. P. & Kim, T. W. (2005). Model-guided microarray implicates the retromer complex in Alzheimer's disease. *Ann Neurol,* 58(6)**,** 909-19.

Small, S. A. & Petsko, G. A. (2015). Retromer in Alzheimer disease, Parkinson disease and other neurological disorders. *Nat Rev Neurosci,* 16(3)**,** 126-32.

Smith, P., Al Hashimi, A., Girard, J., Delay, C. & Hebert, S. S. (2011). In vivo regulation of amyloid precursor protein neuronal splicing by microRNAs. *J Neurochem,* 116(2)**,** 240-7.

So, P. P., Zeldich, E., Seyb, K. I., Huang, M. M., Concannon, J. B., King, G. D., Chen, C. D., Cuny, G. D., Glicksman, M. A. & Abraham, C. R. (2012). Lowering of amyloid beta peptide production with a small molecule inhibitor of amyloid-beta precursor protein dimerization. *Am J Neurodegener Dis,* 1(1)**,** 75-87.

Soba, P., Eggert, S., Wagner, K., Zentgraf, H., Siehl, K., Kreger, S., Lower, A., Langer, A., Merdes, G., Paro, R., Masters, C. L., Muller, U., Kins, S. & Beyreuther, K. (2005). Homo- and heterodimerization of APP family members promotes intercellular adhesion. *EMBO J,* 24(20)**,** 3624-34.

Sperling, R., Salloway, S., Brooks, D. J., Tampieri, D., Barakos, J., Fox, N. C., Raskind, M., Sabbagh, M., Honig, L. S., Porsteinsson, A. P., Lieberburg, I., Arrighi, H. M., Morris, K. A., Lu, Y., Liu, E., Gregg, K. M., Brashear, H. R., Kinney, G. G., Black, R. & Grundman, M. (2012). Amyloid-related imaging abnormalities in patients with Alzheimer's disease treated with bapineuzumab: a retrospective analysis. *Lancet Neurol,* 11(3)**,** 241-9.

Spillantini, M. G., Hunt, S. P., Ulrich, J. & Goedert, M. (1989). Expression and cellular localization of amyloid beta-protein precursor transcripts in normal human brain and in Alzheimer's disease. *Brain Res Mol Brain Res,* 6(2-3)**,** 143-50.

Spires-Jones, T. L. & Hyman, B. T. (2014). The intersection of amyloid beta and tau at synapses in Alzheimer's disease. *Neuron,* 82(4)**,** 756-71.

Stenmark, H. (2009). Rab GTPases as coordinators of vesicle traffic. *Nature Reviews Molecular Cell Biology,* 10(8)**,** 513-525.

Suh, J., Choi, S. H., Romano, D. M., Gannon, M. A., Lesinski, A. N., Kim, D. Y. & Tanzi, R. E. (2013). ADAM10 missense mutations potentiate beta-amyloid accumulation by impairing prodomain chaperone function. *Neuron,* 80(2)**,** 385-401.

Suh, J., Lyckman, A., Wang, L., Eckman, E. A. & Guenette, S. Y. (2011). FE65 proteins regulate NMDA receptor activation-induced amyloid precursor protein processing. *J Neurochem,* 119(2)**,** 377-88.

Sullivan, S. E., Dillon, G. M., Sullivan, J. M. & Ho, A. (2014). Mint proteins are required for synaptic activity-dependent amyloid precursor protein (APP) trafficking and amyloid beta generation. *J Biol Chem,* 289(22)**,** 15374-83.

Tai, H. C., Serrano-Pozo, A., Hashimoto, T., Frosch, M. P., Spires-Jones, T. L. & Hyman, B. T. (2012). The synaptic accumulation of hyperphosphorylated tau oligomers in Alzheimer disease is associated with dysfunction of the ubiquitin-proteasome system. *Am J Pathol,* 181(4)**,** 1426-35.

Takami, M. & Funamoto, S. (2012). gamma-Secretase-Dependent Proteolysis of Transmembrane Domain of Amyloid Precursor Protein: Successive Tri- and Tetrapeptide Release in Amyloid beta-Protein Production. *Int J Alzheimers Dis,* 2012**,** 591392.

Takami, M., Nagashima, Y., Sano, Y., Ishihara, S., Morishima-Kawashima, M., Funamoto, S. & Ihara, Y. (2009). gamma-Secretase: successive tripeptide and tetrapeptide release from the transmembrane domain of beta-carboxyl terminal fragment. *J Neurosci,* 29(41)**,** 13042-52.

Tam, J. H. K., Seah, C. & Pasternak, S. H. (2014). The Amyloid Precursor Protein is rapidly transported from the Golgi apparatus to the lysosome and where it is processed into beta-amyloid. *Molecular Brain,* 7(54)**,** doi:10.1186/s13041-014-0054-1.

Tamayev, R., Matsuda, S., Arancio, O. & D'Adamio, L. (2012). beta- but not gamma-secretase proteolysis of APP causes synaptic and memory deficits in a mouse model of dementia. *EMBO Mol Med,* 4(3)**,** 171-9.

Tan, J. & Evin, G. (2012). Beta-site APP-cleaving enzyme 1 trafficking and Alzheimer's disease pathogenesis. *J Neurochem,* 120(6)**,** 869-80.

Tanaka, S., Shiojiri, S., Takahashi, Y., Kitaguchi, N., Ito, H., Kameyama, M., Kimura, J., Nakamura, S. & Ueda, K. (1989). Tissue-specific expression of three types of beta-protein precursor mRNA: enhancement of protease inhibitor-harboring types in Alzheimer's disease brain. *Biochem Biophys Res Commun,* 165(3)**,** 1406-14.

Tang, W., Tam, J. H., Seah, C., Chiu, J., Tyrer, A., Cregan, S. P., Meakin, S. O. & Pasternak, S. H. (2015). Arf6 controls beta-amyloid production by regulating macropinocytosis of the Amyloid Precursor Protein to lysosomes. *Mol Brain,* 8(41)**,** 41.

Tanzi, R. E. (2012). The genetics of Alzheimer disease. *Cold Spring Harb Perspect Med,* 2(10).

Taylor, C. J., Ireland, D. R., Ballagh, I., Bourne, K., Marechal, N. M., Turner, P. R., Bilkey, D. K., Tate, W. P. & Abraham, W. C. (2008). Endogenous secreted amyloid precursor protein-alpha regulates hippocampal NMDA receptor function, long-term potentiation and spatial memory. *Neurobiol Dis,* 31(2)**,** 250-60.

Tesco, G., Koh, Y. H., Kang, E. L., Cameron, A. N., Das, S., Sena-Esteves, M., Hiltunen, M., Yang, S. H., Zhong, Z., Shen, Y., Simpkins, J. W. & Tanzi, R. E. (2007). Depletion of GGA3 stabilizes BACE and enhances beta-secretase activity. *Neuron,* 54(5)**,** 721-37.

Tharp, W. G., Lee, Y. H., Greene, S. M., Vincellete, E., Beach, T. G. & Pratley, R. E. (2012). Measurement of altered AbetaPP isoform expression in frontal cortex of patients with Alzheimer's disease by absolute quantification real-time PCR. *J Alzheimers Dis,* 29(2)**,** 449-57.

Thathiah, A., Horre, K., Snellinx, A., Vandewyer, E., Huang, Y., Ciesielska, M., De Kloe, G., Munck, S. & De Strooper, B. (2013). beta-arrestin 2 regulates Abeta generation and gamma-secretase activity in Alzheimer's disease. *Nat Med,* 19(1)**,** 43-9.

Thinakaran, G., Borchelt, D. R., Lee, M. K., Slunt, H. H., Spitzer, L., Kim, G., Ratovitsky, T., Davenport, F., Nordstedt, C., Seeger, M., Hardy, J., Levey, A. I., Gandy, S. E., Jenkins, N.

A., Copeland, N. G., Price, D. L. & Sisodia, S. S. (1996a). Endoproteolysis of presenilin 1 and accumulation of processed derivatives in vivo. *Neuron,* 17(1)**,** 181-90.

Thinakaran, G. & Koo, E. H. (2008). Amyloid precursor protein trafficking, processing, and function. *J Biol Chem,* 283(44)**,** 29615-9.

Thinakaran, G., Teplow, D. B., Siman, R., Greenberg, B. & Sisodia, S. S. (1996b). Metabolism of the ''Swedish'' amyloid precursor protein variant in neuro2a (N2a) cells - Evidence that cleavage at the ''beta-secretase'' site occurs in the Golgi apparatus. *J Biol Chem,* 271(16)**,** 9390-9397.

Tian, J., Tian, C., Ding, Y. H., Li, Z., Geng, Q. Z., Xiahou, Z. K., Wang, J., Hou, W. Y., Liao, J., Dong, M. Q., Xu, X. Z. & Li, J. (2015). Aurora B-dependent phosphorylation of Ataxin-10 promotes the interaction between Ataxin-10 and Plk1 in cytokinesis. *Scientific reports,* 5.

Tian, Y., Crump, C. J. & Li, Y. M. (2010). Dual role of alpha-secretase cleavage in the regulation of gamma-secretase activity for amyloid production. *J Biol Chem,* 285(42)**,** 32549-56.

Toledo, J. B., Zetterberg, H., van Harten, A. C., Glodzik, L., Martinez-Lage, P., Bocchio-Chiavetto, L., Rami, L., Hansson, O., Sperling, R., Engelborghs, S., Osorio, R. S., Vanderstichele, H., Vandijck, M., Hampel, H., Teipl, S., Moghekar, A., Albert, M., Hu, W. T., Monge Argiles, J. A., Gorostidi, A., Teunissen, C. E., De Deyn, P. P., Hyman, B. T., Molinuevo, J. L., Frisoni, G. B., Linazasoro, G., de Leon, M. J., van der Flier, W. M., Scheltens, P., Blennow, K., Shaw, L. M., Trojanowski, J. Q. & Alzheimer's Disease Neuroimaging, I. (2015). Alzheimer's disease cerebrospinal fluid biomarker in cognitively normal subjects. *Brain,* 138(Pt 9)**,** 2701-15.

Tomic, J. L., Pensalfini, A., Head, E. & Glabe, C. G. (2009). Soluble fibrillar oligomer levels are elevated in Alzheimer's disease brain and correlate with cognitive dysfunction. *Neurobiol Dis,* 35(3)**,** 352-8.

Tyler, S. J., Dawbarn, D., Wilcock, G. K. & Allen, S. J. (2002). alpha- and beta-secretase: profound changes in Alzheimer's disease. *Biochem Biophys Res Commun,* 299(3)**,** 373-6.

Udayar, V., Buggia-Prevot, V., Guerreiro, R. L., Siegel, G., Rambabu, N., Soohoo, A. L., Ponnusamy, M., Siegenthaler, B., Bali, J., Aesg, Simons, M., Ries, J., Puthenveedu, M. A., Hardy, J., Thinakaran, G. & Rajendran, L. (2013). A paired RNAi and RabGAP overexpression screen identifies Rab11 as a regulator of beta-amyloid production. *Cell Rep,* 5(6)**,** 1536-51.

Ulery, P. G., Beers, J., Mikhailenko, I., Tanzi, R. E., Rebeck, G. W., Hyman, B. T. & Strickland, D. K. (2000). Modulation of β-Amyloid Precursor Protein Processing by the Low Density Lipoprotein Receptor-related Protein (LRP): EVIDENCE THAT LRP CONTRIBUTES TO THE PATHOGENESIS OF ALZHEIMER'S DISEASE. *Journal of Biological Chemistry,* 275(10)**,** 7410-7415.

Um, J. W., Kaufman, A. C., Kostylev, M., Heiss, J. K., Stagi, M., Takahashi, H., Kerrisk, M. E., Vortmeyer, A., Wisniewski, T., Koleske, A. J., Gunther, E. C., Nygaard, H. B. & Strittmatter, S. M. (2013). Metabotropic glutamate receptor 5 is a coreceptor for Alzheimer abeta oligomer bound to cellular prion protein. *Neuron,* 79(5)**,** 887-902.

Um, J. W., Nygaard, H. B., Heiss, J. K., Kostylev, M. A., Stagi, M., Vortmeyer, A., Wisniewski, T., Gunther, E. C. & Strittmatter, S. M. (2012). Alzheimer amyloid-beta oligomer bound to postsynaptic prion protein activates Fyn to impair neurons. *Nat Neurosci,* 15(9)**,** 1227-35.

Underwood, E. (2015). NEUROSCIENCE. Alzheimer's amyloid theory gets modest boost. *Science,* 349(6247)**,** 464.

Van Cauwenberghe, C., Van Broeckhoven, C. & Sleegers, K. (2015). The genetic landscape of Alzheimer disease: clinical implications and perspectives. *Genet Med*.

van der Kant, R. & Goldstein, L. S. (2015). Cellular functions of the amyloid precursor protein from development to dementia. *Dev Cell,* 32(4)**,** 502-15.

Vassar, R. (2004). BACE1: The β-Secretase Enzyme in Alzheimer's Disease. *Journal of Molecular Neuroscience,* 23(1-2)**,** 105-114.

Vassar, R. (2014). BACE1 inhibitor drugs in clinical trials for Alzheimer's disease. *Alzheimers Res Ther,* 6(9)**,** 89.

Vassar, R., Bennett, B. D., Babu-Khan, S., Kahn, S., Mendiaz, E. A., Denis, P., Teplow, D. B., Ross, S., Amarante, P., Loeloff, R., Luo, Y., Fisher, S., Fuller, J., Edenson, S., Lile, J., Jarosinski, M. A., Biere, A. L., Curran, E., Burgess, T., Louis, J. C., Collins, F., Treanor, J., Rogers, G. & Citron, M. (1999). Beta-secretase cleavage of Alzheimer's amyloid precursor protein by the transmembrane aspartic protease BACE. *Science,* 286(5440)**,** 735-41.

Vassar, R., Kovacs, D. M., Yan, R. & Wong, P. C. (2009). The beta-secretase enzyme BACE in health and Alzheimer's disease: regulation, cell biology, function, and therapeutic potential. *J Neurosci,* 29(41)**,** 12787-94.

Vassar, R., Kuhn, P. H., Haass, C., Kennedy, M. E., Rajendran, L., Wong, P. C. & Lichtenthaler, S. F. (2014). Function, therapeutic potential and cell biology of BACE proteases: current status and future prospects. *J Neurochem,* 130(1)**,** 4-28.

Veeraraghavalu, K., Zhang, C., Zhang, X., Tanzi, R. E. & Sisodia, S. S. (2014). Age-dependent, non-cell-autonomous deposition of amyloid from synthesis of beta-amyloid by cells other than excitatory neurons. *J Neurosci,* 34(10)**,** 3668-73.

Vella, L. J. & Cappai, R. (2012). Identification of a novel amyloid precursor protein processing pathway that generates secreted N-terminal fragments. *FASEB J,* 26(7)**,** 2930-40.

Verghese, P. B., Castellano, J. M. & Holtzman, D. M. (2011). Apolipoprotein E in Alzheimer's disease and other neurological disorders. *Lancet Neurol,* 10(3)**,** 241-52.

Vetrivel, K. S., Barman, A., Chen, Y., Nguyen, P. D., Wagner, S. L., Prabhakar, R. & Thinakaran, G. (2011). Loss of cleavage at beta'-site contributes to apparent increase in beta-amyloid peptide (Abeta) secretion by beta-secretase (BACE1)-glycosylphosphatidylinositol (GPI) processing of amyloid precursor protein. *J Biol Chem,* 286(29)**,** 26166-77.

Vetrivel, K. S., Meckler, X., Chen, Y., Nguyen, P. D., Seidah, N. G., Vassar, R., Wong, P. C., Fukata, M., Kounnas, M. Z. & Thinakaran, G. (2009). Alzheimer disease Abeta production in the absence of S-palmitoylation-dependent targeting of BACE1 to lipid rafts. *J Biol Chem,* 284(6)**,** 3793-803.

Vieira, S. I., Rebelo, S., Esselmann, H., Wiltfang, J., Lah, J., Lane, R., Small, S. A., Gandy, S., da Cruz, E. S. E. F. & da Cruz, E. S. O. A. (2010). Retrieval of the Alzheimer's amyloid precursor protein from the endosome to the TGN is S655 phosphorylation state-dependent and retromer-mediated. *Mol Neurodegener,* 5(1)**,** 40.

Villegas, C., Muresan, V. & Ladescu Muresan, Z. (2014). Dual-tagged amyloid-beta precursor protein reveals distinct transport pathways of its N- and C-terminal fragments. *Hum Mol Genet,* 23(6)**,** 1631-43.

Vincent, B., Paitel, E., Saftig, P., Frobert, Y., Hartmann, D., De Strooper, B., Grassi, J., Lopez-Perez, E. & Checler, F. (2001). The disintegrins ADAM10 and TACE contribute to the constitutive and phorbol ester-regulated normal cleavage of the cellular prion protein. *J Biol Chem,* 276(41)**,** 37743-6.

von Einem, B., Wahler, A., Schips, T., Serrano-Pozo, A., Proepper, C., Boeckers, T. M., Rueck, A., Wirth, T., Hyman, B. T., Danzer, K. M., Thal, D. R. & von Arnim, C. A. (2015). The Golgi-Localized gamma-Ear-Containing ARF-Binding (GGA) Proteins Alter Amyloid-beta Precursor Protein (APP) Processing through Interaction of Their GAE Domain with the Beta-Site APP Cleaving Enzyme 1 (BACE1). *PLoS ONE,* 10(6)**,** e0129047.

von Rotz, R. C., Kohli, B. M., Bosset, J., Meier, M., Suzuki, T., Nitsch, R. M. & Konietzko, U. (2004). The APP intracellular domain forms nuclear multiprotein complexes and regulates the transcription of its own precursor. *J Cell Sci,* 117(Pt 19)**,** 4435-48.

Wahle, T., Prager, K., Raffler, N., Haass, C., Famulok, M. & Walter, J. (2005). GGA proteins regulate retrograde transport of BACE1 from endosomes to the trans-Golgi network. *Mol Cell Neurosci,* 29(3)**,** 453-61.

Wakabayashi, T., Craessaerts, K., Bammens, L., Bentahir, M., Borgions, F., Herdewijn, P., Staes, A., Timmerman, E., Vandekerckhove, J., Rubinstein, E., Boucheix, C., Gevaert, K. & De

Strooper, B. (2009). Analysis of the gamma-secretase interactome and validation of its association with tetraspanin-enriched microdomains. *Nat Cell Biol,* 11(11)**,** 1340-6.

Wang, H., Wang, R., Xu, S. & Lakshmana, M. K. (2014). RanBP9 overexpression accelerates loss of pre and postsynaptic proteins in the APDeltaE9 transgenic mouse brain. *PLoS ONE,* 9(1)**,** e85484.

Wang, Z., Wang, B., Yang, L., Guo, Q., Aithmitti, N., Songyang, Z. & Zheng, H. (2009). Presynaptic and postsynaptic interaction of the amyloid precursor protein promotes peripheral and central synaptogenesis. *J Neurosci,* 29(35)**,** 10788-801.

Welzel, A. T., Maggio, J. E., Shankar, G. M., Walker, D. E., Ostaszewski, B. L., Li, S., Klyubin, I., Rowan, M. J., Seubert, P., Walsh, D. M. & Selkoe, D. J. (2014). Secreted amyloid beta-proteins in a cell culture model include N-terminally extended peptides that impair synaptic plasticity. *Biochemistry,* 53(24)**,** 3908-21.

Whitehouse, I. J., Jackson, C., Turner, A. J. & Hooper, N. M. (2010). Prion Protein is Reduced in Aging and in Sporadic but not in Familial Alzheimer's Disease. *Journal of Alzheimers Disease,* 22(3)**,** 1023-1031.

Wildsmith, K. R., Schauer, S. P., Smith, A. M., Arnott, D., Zhu, Y., Haznedar, J., Kaur, S., Mathews, W. R. & Honigberg, L. A. (2014). Identification of longitudinally dynamic biomarkers in Alzheimer's disease cerebrospinal fluid by targeted proteomics. *Mol Neurodegener,* 9(1)**,** 22.

Wiley, J. C., Smith, E. A., Hudson, M. P., Ladiges, W. C. & Bothwell, M. (2007). Fe65 stimulates proteolytic liberation of the beta-amyloid precursor protein intracellular domain. *J Biol Chem,* 282(46)**,** 33313-25.

Willem, M., Garratt, A. N., Novak, B., Citron, M., Kaufmann, S., Rittger, A., De Strooper, B., Saftig, P., Birchmeier, C. & Haass, C. (2006). Control of peripheral nerve myelination by the beta-secretase BACE1. *Science,* 314(5799)**,** 664-6.

Willem, M., Tahirovic, S., Busche, M. A., Ovsepian, S. V., Chafai, M., Kootar, S., Hornburg, D., Evans, L. D., Moore, S., Daria, A., Hampel, H., Muller, V., Giudici, C., Nuscher, B., Wenninger-Weinzierl, A., Kremmer, E., Heneka, M. T., Thal, D. R., Giedraitis, V., Lannfelt, L., Muller, U., Livesey, F. J., Meissner, F., Herms, J., Konnerth, A., Marie, H. & Haass, C. (2015). eta-Secretase processing of APP inhibits neuronal activity in the hippocampus. *Nature,* advance online publication.

Willoughby, D. A., Rozovsky, I., Lo, A. C. & Finch, C. E. (1995). Beta-amyloid precursor protein (APP) and APP-RNA are rapidly affected by glutamate in cultured neurons: selective increase of mRNAs encoding a Kunitz protease inhibitor domain. *J Mol Neurosci,* 6(4)**,** 257-76.

Wisniewski, T. & Goni, F. (2015). Immunotherapeutic approaches for Alzheimer's disease. *Neuron,* 85(6)**,** 1162-76.

Wolfe, M. S., Xia, W., Ostaszewski, B. L., Diehl, T. S., Kimberly, W. T. & Selkoe, D. J. (1999). Two transmembrane aspartates in presenilin-1 required for presenilin endoproteolysis and gamma-secretase activity. *Nature,* 398(6727)**,** 513-7.

Wu, J., Petralia, R. S., Kurushima, H., Patel, H., Jung, M. Y., Volk, L., Chowdhury, S., Shepherd, J. D., Dehoff, M., Li, Y., Kuhl, D., Huganir, R. L., Price, D. L., Scannevin, R., Troncoso, J. C., Wong, P. C. & Worley, P. F. (2011). Arc/Arg3.1 regulates an endosomal pathway essential for activity-dependent beta-amyloid generation. *Cell,* 147(3)**,** 615-28.

Wu, W., Tran, K. C., Teng, M. N., Heesom, K. J., Matthews, D. A., Barr, J. N. & Hiscox, J. A. (2012). The interactome of the human respiratory syncytial virus NS1 protein highlights multiple effects on host cell biology. *J Virol,* 86(15)**,** 7777-89.

Xie, Z., Dong, Y., Maeda, U., Xia, W. & Tanzi, R. E. (2007). RNA interference silencing of the adaptor molecules ShcC and Fe65 differentially affect amyloid precursor protein processing and Abeta generation. *J Biol Chem,* 282(7)**,** 4318-25.

Xu, F., Davis, J., Miao, J., Previti, M. L., Romanov, G., Ziegler, K. & Van Nostrand, W. E. (2005). Protease nexin-2/amyloid beta-protein precursor limits cerebral thrombosis. *Proc Natl Acad Sci U S A,* 102(50)**,** 18135-40.

Xu, F., Previti, M. L., Nieman, M. T., Davis, J., Schmaier, A. H. & Van Nostrand, W. E. (2009). AbetaPP/APLP2 family of Kunitz serine proteinase inhibitors regulate cerebral thrombosis. *J Neurosci,* 29(17)**,** 5666-70.

Yamakawa, H., Yagishita, S., Futai, E. & Ishiura, S. (2010). beta-Secretase inhibitor potency is decreased by aberrant beta-cleavage location of the "Swedish mutant" amyloid precursor protein. *J Biol Chem,* 285(3)**,** 1634-42.

Yang, Y., Turner, R. S. & Gaut, J. R. (1998). The chaperone BiP/GRP78 binds to amyloid precursor protein and decreases Abeta40 and Abeta42 secretion. *J Biol Chem,* 273(40)**,** 25552-5.

Yates, P. A., Desmond, P. M., Phal, P. M., Steward, C., Szoeke, C., Salvado, O., Ellis, K. A., Martins, R. N., Masters, C. L., Ames, D., Villemagne, V. L., Rowe, C. C. & Group, A. R. (2014). Incidence of cerebral microbleeds in preclinical Alzheimer disease. *Neurology,* 82(14)**,** 1266-73.

Ye, X. & Cai, Q. (2014). Snapin-mediated BACE1 retrograde transport is essential for its degradation in lysosomes and regulation of APP processing in neurons. *Cell Rep,* 6(1)**,** 24-31.

Young-Pearse, T. L., Bai, J., Chang, R., Zheng, J. B., LoTurco, J. J. & Selkoe, D. J. (2007). A critical function for beta-amyloid precursor protein in neuronal migration revealed by in utero RNA interference. *J Neurosci,* 27(52)**,** 14459-69.

Young-Pearse, T. L., Chen, A. C., Chang, R., Marquez, C. & Selkoe, D. (2008). Secreted APP regulates the function of full-length APP in neurite outgrowth thorugh interaction with integrin beta1. *Neural Dev,* 3(15).

Yu, J. T., Tan, L. & Hardy, J. (2014). Apolipoprotein E in Alzheimer's disease: an update. *Annu Rev Neurosci,* 37(1)**,** 79-100.

Yu, Y. J., Zhang, Y., Kenrick, M., Hoyte, K., Luk, W., Lu, Y., Atwal, J., Elliott, J. M., Prabhu, S., Watts, R. J. & Dennis, M. S. (2011). Boosting brain uptake of a therapeutic antibody by reducing its affinity for a transcytosis target. *Sci Transl Med,* 3(84)**,** 84ra44.

Zhan, S. S., Kamphorst, W., Van Nostrand, W. E. & Eikelenboom, P. (1995). Distribution of neuronal growth-promoting factors and cytoskeletal proteins in altered neurites in Alzheimer's disease and non-demented elderly. *Acta Neuropathologica,* 89(4)**,** 356-62.

Zhang, C., Browne, A., Child, D., Divito, J. R., Stevenson, J. A. & Tanzi, R. E. (2010). Loss of function of ATXN1 increases amyloid beta-protein levels by potentiating beta-secretase processing of beta-amyloid precursor protein. *J Biol Chem,* 285(12)**,** 8515-26.

Zhang, X., Li, Y., Xu, H. & Zhang, Y. W. (2014). The gamma-secretase complex: from structure to function. *Front Cell Neurosci,* 8**,** 427.

Zhao, J., Paganini, L., Mucke, L., Gordon, M., Refolo, L., Carman, M., Sinha, S., Oltersdorf, T., Lieberburg, I. & McConlogue, L. (1996). beta-secretase processing of the beta-amyloid precursor protein in transgenic mice is efficient in neurons but inefficient in astrocytes. *J Biol Chem,* 271(49)**,** 31407-31411.

Zhao, Y. & Zhao, B. (2013). Oxidative stress and the pathogenesis of Alzheimer's disease. *Oxid Med Cell Longev,* 2013**,** 316523.

Zheng, L., Cedazo-Minguez, A., Hallbeck, M., Jerhammar, F., Marcusson, J. & Terman, A. (2012). Intracellular distribution of amyloid beta peptide and its relationship to the lysosomal system. *Transl Neurodegener,* 1(1)**,** 19.

Zhou, X., Hu, X., He, W., Tang, X., Shi, Q., Zhang, Z. & Yan, R. (2011). Interaction between amyloid precursor protein and Nogo receptors regulates amyloid deposition. *FASEB J,* 25(9)**,** 3146-56.

Zhu, L., Su, M., Lucast, L., Liu, L., Netzer, W. J., Gandy, S. E. & Cai, D. (2012). Dynamin 1 regulates amyloid generation through modulation of BACE-1. *PLoS ONE,* 7(9)**,** e45033.